SECTION 2.6.1—INTRODUCTION

BICTEGRAVIR/EMTRICITABINE/TENOFOVIR ALAFENAMIDE FIXED-DOSE COMBINATION (B/F/TAF FDC)

Gilead Sciences

[redacted] **20**

TABLE OF CONTENTS

GLOSSARY OF ABBREVIATIONS AND DEFINITION OF TERMS

B/F/TAF	bictegravir/emtricitabine/tenofovir alafenamide (coformulated)
BIC, B	bictegravir
COBI, C	cobicistat (Tybost®)
DNA	deoxyribonucleic acid
DTG	dolutegravir
E/C/F/TAF	elvitegravir/cobicistat/emtricitabine/tenofovir alafenamide (coformulated; Genvoya®)
EVG	elvitegravir (JTK-303; Vitekta®)
FDC	fixed-dose combination
F/TAF	emtricitabine/tenofovir alafenamide (coformulated; Descovy®)
FTC, F	emtricitabine (Emtriva®)
FTC/RPV/TAF	emtricitabine/rilpivirine/tenofovir alafenamide (coformulated; Odefsey®)
FTC-TP	emtricitabine triphosphate
HBV	hepatitis B virus
HIV-1	human immunodeficiency virus type 1
NNRTI	non-nucleoside reverse transcriptase inhibitor
NRTI	nucleoside reverse transcriptase inhibitor
NtRTI	nucleotide reverse transcriptase inhibitor
PBMC	peripheral blood mononuclear cell
RAL	raltegravir
RPV	rilpivirine
TAF	tenofovir alafenamide (Vemlidy®)
TDF	tenofovir disoproxil fumarate (Viread®)
TFV	tenofovir (PMPA; (*R*)-9-(2-Phosphonoylmethoxypropyl)adenine)

1. NONCLINICAL SUMMARY

1.1. Introduction

This dossier is being submitted in support of a license application for a fixed-dose combination (FDC) tablet of bictegravir (BIC; B), emtricitabine (FTC; F) and tenofovir alafenamide (TAF) (B/F/TAF; 50/200/25 mg) for the treatment of human immunodeficiency virus, type 1 (HIV-1) infection.

Comprehensive programs of nonclinical studies with BIC, FTC, and TAF as individual agents have been conducted; the nonclinical data are summarized in m2.6 of this submission. To facilitate the evaluation of BIC, FTC, TAF, and the B/F/TAF FDC, nonclinical virology studies with the individual agents and B/F/TAF FDC are discussed in detail in m2.6.2 and summarized together with the clinical virology data in m2.7.2, Section 4.1. Nonclinical study reports are provided in m4 and clinical study reports are provided in m5.

1.1.1. BIC

Bictegravir (2R,5S,13aR)-8-hydroxy-7,9-dioxo-N-(2,4,6-trifluorobenzyl)-2,3,4,5,7,9,13,13a-octahydro-2,5-methanopyrido[1',2':4,5]pyrazino[2,1-b][1,3]oxazepine-10-carboxamide is a novel strand transfer inhibitor of HIV-1 integrase which does not require modification for activity. Bictegravir inhibits HIV integrase by binding to the integrase active site and blocking the strand transfer step of retroviral deoxyribonucleic acid (DNA) integration which is essential for the HIV replication cycle, demonstrating high potency and selectivity in antiviral assays. Bictegravir displays a high resistance barrier and has an improved phenotypic resistance profile compared to dolutegravir (DTG), raltegravir (RAL) and elvitegravir (EVG; E). Bictegravir has a longer dissociation half-life from both wild-type and mutant HIV-1 integrase/DNA complexes compared with DTG, RAL, and EVG.

The chemical structure of BIC is as follows:

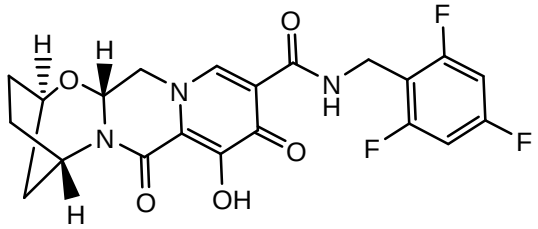

1.1.2. FTC

Emtricitabine (FTC) is a nucleoside reverse transcriptase inhibitor (NRTI). Emtricitabine has been approved for the treatment of HIV-1 infection as a standalone agent (Emtriva®) or in FDC products with the following trade names: Truvada® (FTC/tenofovir disoproxil fumarate [TDF]), Atripla® (efavirenz/FTC/TDF), Complera/Eviplera® (FTC/rilpivirine [RPV]/TDF), Stribild® (EVG/cobicistat [COBI; C]/FTC/TDF), Genvoya® (E/C/F/TAF), Descovy® (F/TAF), and Odefsey® (FTC/RPV/TAF).

Following absorption, FTC is phosphorylated by cellular enzymes to emtricitabine triphosphate (FTC-TP), the active metabolite, an analog of 2'-deoxycytidine triphosphate. Emtricitabine 5'-triphosphate inhibits the activity of HIV-1 reverse transcriptase through high-affinity binding, competing with the natural substrate 2'-deoxycytidine 5'-triphosphate. Emtricitabine 5'-triphosphate is efficiently incorporated into the nascent viral DNA chain by HIV-1 reverse transcriptase resulting in termination of DNA synthesis due to the lack of a hydroxyl group at the 3'- position of the sugar moiety of FTC, which in turn inhibits viral replication. In a clinical study, the intracellular half-life of FTC-TP in peripheral blood mononuclear cells (PBMCs) was 39 hours. Intracellular triphosphate levels increased with dose but reached a plateau at doses of 200 mg or greater. Emtricitabine has activity against retroviruses and hepadnaviruses.

The chemical structure of FTC is as follows:

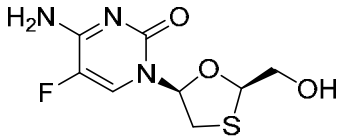

1.1.3. TAF

Tenofovir alafenamide (TAF) is a prodrug of tenofovir (TFV; PMPA), a nucleotide reverse transcriptase inhibitor (NtRTI). TAF is approved for the treatment of HIV-1 infection in FDC products with the following trade names: Genvoya®, Descovy®, and Odefsey®. TAF is also approved for the treatment of chronic hepatitis B (CHB) infection as a standalone agent (Vemlidy®). The other tenofovir prodrug is tenofovir disoproxil fumarate (TDF), the active ingredient in Viread®, which is approved for the treatment of HIV-1 infection and CHB.

Cells are permeable to TAF and, due to increased plasma stability and intracellular activation through hydrolysis by cathepsin A, TAF is more efficient than TDF in loading tenofovir into PBMCs (including lymphocytes and other HIV target cells) and macrophages. Intracellular tenofovir is subsequently phosphorylated to the pharmacologically active metabolite, tenofovir diphosphate. Tenofovir diphosphate inhibits HIV and HBV replication through incorporation into viral DNA by the HIV-1 or HBV reverse transcriptase, which results in DNA chain-termination.

The chemical structure of TAF hemi-fumarate is as follows:

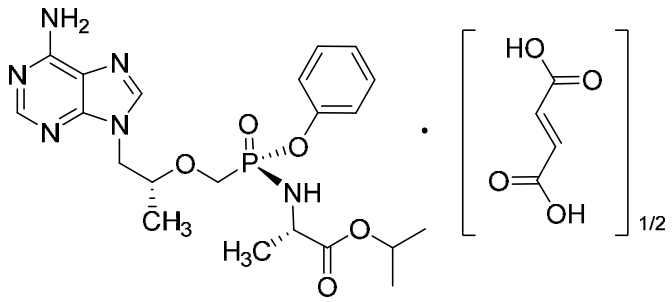

1.1.4. B/F/TAF

Bictegravir, FTC, and TAF are potent and selective inhibitors of HIV-1. All 3 drugs show potent antiretroviral activity against diverse subtypes of HIV-1 in vitro. Emtricitabine and TFV are phosphorylated intracellularly through nonoverlapping pathways; in combination, they show no antagonism for the formation of their active metabolites. The anti-HIV-1 activity of 3-drug combination of BIC, FTC, and TAF was found to be highly synergistic with no evidence of antagonism in vitro, supporting the use of these agents in combination in HIV-1 infected patients. In addition, in vitro combination studies have shown that BIC, FTC, and TFV have additive to synergistic anti-HIV-1 activity with other approved NRTIs, non-nucleoside reverse transcriptase inhibitors (NNRTIs), and protease inhibitors. The resistance profiles of the individual agents BIC, FTC, and TAF are distinct and nonoverlapping.

The toxicity profiles of the 3 agents differ substantially with no clinically significant overlapping toxicity. Because the target organ profiles are different, and there is no evidence of genotoxicity, carcinogenicity, or reproductive toxicity in the absence of maternal toxicity, administration of the B/F/TAF combination product is unlikely to introduce new toxicities or to exacerbate known toxicities of the individual agents.

Overall, the nonclinical data presented in this dossier support the favorable benefit-risk profile for the proposed use of the B/F/TAF FDC in the treatment of HIV-1 infection. All information from nonclinical studies that is relevant to prescribers and patients has been included in the proposed prescribing information.

SECTION 2.6.2—PHARMACOLOGY WRITTEN SUMMARY

BICTEGRAVIR/EMTRICITABINE/TENOFOVIR ALAFENAMIDE

Gilead Sciences

[redacted] 20[redacted]

TABLE OF CONTENTS

LIST OF IN-TEXT TABLES

LIST OF IN-TEXT FIGURES

LIST OF ABBREVIATIONS

Ci	Curie
cm	centimeter
cpm	counts per minute
dpm	disintegrations per minute
g	gram
h	hours
Hz	Hertz
ic	intracutaneous
im	intramuscular
ip	intraperitoneal
iv	intravenous
kg	kilogram
LC50	medial lethal concentration
LD50	medial lethal dose
m	meter
µg	microgram
µl	microliter
µm	micrometer
µM	micromolar
mg	milligram
ml	milliliter
mm	millimeter
mM	millimolar
min	minutes
M	Molar
mol	mole
N	Normal
ng	nanogram
nm	nanometer
po	oral
ppm	parts per million
s	seconds
sc	subcutaneous
SD	standard deviation
SE	standard error
TLV	threshold limit value
X	mean

Abbreviations are in accordance with those accepted by Toxicology and Applied Pharmacology.

2’-FDG	2'-fluoro-2'-deoxyguanosine
3TAM	3 thymidine analog-associated mutation
3TC	lamivudine
3TC-TP	lamivudine 5′-triphosphate
α_1-AGP	α_1-acid glycoprotein
ABC	abacavir
ADV	adefovir dipivoxil
ADV-R	adefovir dipivoxil resistant
AFV	adefovir
ART	antiretroviral therapy
ARV	antiretroviral
ATP	adenosine triphosphate
ATV	atazanavir
B/F/TAF	bictegravir/emtricitabine/tenofovir alafenamide (coformulated)
BIC	bictegravir (GS-9883)
BID	twice daily
BLQ	below the limit of quantitation
BNPP	bis-p-nitrophenyl phosphate
CatA	cathepsin A
CBV-TP	carbovir triphosphate
CC_{50}	concentration that resulted in 50% cytotoxicity
CD	cluster determinant
CD4	cluster determinant 4
CES1	carboxylesterase 1
CHB	chronic hepatitis B
CHMP	Committee for Medicinal Products for Human Use
CHO	Chinese hamster ovary
CI	combination index
C_{max}	maximum observed concentration of drug
CNS	central nervous system
COBI	cobicistat (Tybost®)
COX	cytochrome c oxidase
d4T	stavudine
d4T-TP	stavudine triphosphate
dATP	deoxyadenosine triphosphate
dCTP	deoxycytidine triphosphate
ddATP	dideoxyadenosine triphosphate
ddC	zalcitabine
ddCTP	dideoxycytidine triphosphate
DDDP	DNA-dependent DNA polymerase
ddI	didanosine

dGTP	deoxyguanosine triphosphate
DMSO	dimethylsulfoxide
DNA	deoxyribonucleic acid
dNTP	2′-deoxynucleoside triphosphate
DRV	darunavir
DTG	dolutegravir
EC_{50}	half-maximal response
EC_{95}	95% effective concentration
ECG	electrocardiogram
EFV	efavirenz
ELISA	enzyme-linked immunosorbent assay
EQDS	equilibrium dialysis
ETV	etravirine
EVG	elvitegravir (Vitekta®)
fbe	free base equivalents
FBS	fetal bovine serum
FDA	Food and Drug Administration
FDC	fixed-dose combination
FIAU	fialuridine
FLT	alovudine
FTC	emtricitabine (Emtriva®)
FTC-TP	emtricitabine 5′-triphosphate
GI	gastrointestinal
GLP	Good Laboratory Practice
HBeAg	hepatitis B e antigen
HBsAg	hepatitis B surface antigen
HBV	hepatitis B virus
HCV	hepatitis C virus
hERG	human ether-a-go-go-related gene
HIV	human immunodeficiency virus
HIV-1	human immunodeficiency virus type 1
HIV-2	human immunodeficiency virus type 2
HPLC	high-performance liquid chromatography
HRV	human rhinovirus
HS	human serum
HSA	human serum albumin
HSV	herpes simplex virus
IC_{50}	50% inhibitory concentration
ICH	International Council for Harmonisation (of Technical Requirements for Pharmaceuticals for Human Use)
IDV	indinavir

IN	integrase
INSTI	integrase strand-transfer inhibitor
INSTI-R	integrase strand-transfer inhibitor resistant
K_d	dissociation constant
K_i	kinetic inhibition constant
K_m	Michaelis-Menten constant
k_{pol}	incorporation rate
LAM	lamivudine
LAM-R	lamivudine resistant
LC/MS/MS	liquid chromatography/tandem mass spectrometry
LDH	lactate dehydrogenase
LNMC	lymph node mononuclear cell
LPV	lopinavir
MATE1	multidrug and toxin extrusion 1
MDR	multidrug-resistant
MOI	multiplicity of infection
MRP4	multidrug resistance-associated protein 4
mtDNA	mitochondrial DNA
NA	not applicable
ND	not determined
NFV	nelfinavir
NNRTI	nonnucleoside reverse transcriptase inhibitor
NOEL	no observed effect level
NRTI	nucleoside reverse transcriptase inhibitor
NS3	nonstructural protein 3
NS5B	nonstructural protein 5B
NtRTI	nucleotide reverse transcriptase inhibitor
NVP	nevirapine
OAT	organic anion transporter
OAT1	organic anion transporter 1
OAT3	organic anion transporter 3
OATP	organic anion transporting polypeptide
OCT2	organic cation transporter 2
$PAEC_{95}$	protein-adjusted EC_{95}
PBMC	peripheral blood mononuclear cell
PCR	polymerase chain reaction
PHA	phytohemagglutinin
PI	protease inhibitor
PK	pharmacokinetic(s)
PMPA	tenofovir
PMPAp	tenofovir monophosphate

PMPApp	tenofovir diphosphate
PNP	purine nucleoside phosphorylase
Pol γ	polymerase γ
pol/RT	polymerase/reverse transcriptase
PR interval	electrocardiographic interval occurring between the onset of the P wave and the QRS complex representing time for atrial and ventricular depolarization, respectively
PX	passage X
QD	once daily
QRS	electrocardiographic deflection between the beginning of the Q wave and termination of the S wave, representing time for ventricular depolarization
QT	electrocardiographic interval between the beginning of the Q wave and termination of the T wave, representing the time for both ventricular depolarization and repolarization to occur
QTc	QT interval corrected for heart rate
-R	resistant
RAL	raltegravir
RAM	resistance-associated mutation
RBV	ribavirin
RDDP	RNA-dependent DNA polymerase
RNA	ribonucleic acid
rNTP	ribonucleoside triphosphate
RPV	rilpivirine
RPTEC	renal proximal tubule epithelial cell
RSV	respiratory syncytial virus
RT	reverse transcriptase
RTV	ritonavir
SD	standard deviation
SEM	standard error of the mean
SCID	Severe combined immunodeficiency
SI	selectivity index (ratio of CC_{50} to IC_{50})
SIV	simian immunodeficiency virus
SkMC	skeletal muscle cell
SOF	sofosbuvir (Sovaldi®)
$t_{1/2}$	estimate of the terminal elimination half-life of the drug, calculated by dividing the natural log of 2 by the terminal elimination rate constant (λ_z)
T-20	enfuvirtide
TAF	tenofovir alafenamide (Vemlidy®)
TAM	thymidine analog mutation
TBV	telbivudine
TDF	tenofovir disoproxil fumarate (Viread®)
TFV	tenofovir
TFV-DP	tenofovir diphosphate

TFV-MP	tenofovir monophosphate
TIBO	tetrahydro-imidazo-benzodiazepine-one
T_{max}	time (observed time point) of C_{max}
US	United States
V_{max}	maximal upstroke velocity
vs	versus
VZV	varicella zoster virus
WHsAg	woodchuck hepatitis virus surface antigen
WHV	woodchuck hepatitis virus
WT	wild type
ZDV	zidovudine

1. BRIEF SUMMARY

This pharmacology written summary is being submitted in support of a marketing application for a fixed dose combination (FDC) of bictegravir (BIC, B, GS-9883), emtricitabine (FTC, F, GS-9019) and tenofovir alafenamide (TAF, GS-7340): the B/F/TAF (50/200/25 mg) FDC. Bictegravir is a low molecular weight HIV-1 integrase strand transfer inhibitor (INSTI) active against a broad panel of HIV-1 viral lab strains and clinical isolates and is fully active against a panel of mutant viruses with resistance to nucleoside reverse transcriptase inhibitors (NRTI), non-nucleoside reverse-transcriptase inhibitors (NNRTI) and protease inhibitors (PI). Emtricitabine is a nucleoside reverse transcriptase inhibitor (NRTI) and is approved for the treatment of HIV-1 infection as a single agent (Emtriva®) for use in combination with other antiretrovirals (ARVs) for the treatment of HIV-1 infection, and in the FDC products Truvada® (FTC/tenofovir disoproxil fumarate [TDF]), Atripla® (efavirenz/FTC/TDF), Complera®/ Eviplera® (FTC/rilpivirine [RPV]/TDF), Stribild® (elvitegravir [EVG; E]/cobicistat [COBI; C]/ FTC/TDF), Genvoya® (E/C/F/TAF), Descovy® (F/TAF) and Odefsey® (FTC/RPV/TAF). Tenofovir alafenamide is a prodrug of tenofovir (TFV), a nucleotide reverse transcriptase inhibitor (NtRTI). Tenofovir alafenamide is approved for the treatment of HIV-1 infection in the FDC products Genvoya®, Descovy® and Odefsey®. Tenofovir alafenamide is also approved for the treatment of hepatitis B virus (HBV) infection as a single agent (Vemlidy®). Information from all nonclinical studies with FTC, and TAF/TFV should be considered in the context of their clinical experience within ARV combination therapy for the treatment of HIV-1 infection.

The INSTI BIC and the N[t]RTIs FTC and TAF are potent and selective inhibitors of HIV-1 and HIV-2. FTC and TAF are also potent and selective inhibitors of hepatitis B virus (HBV). All 3 drugs show potent ARV activity against diverse subtypes of HIV-1 in vitro. Emtricitabine and TAF are phosphorylated intracellularly through nonoverlapping pathways, and in combination show no antagonism for the formation of their active metabolites. Bictegravir does not require metabolic modification for activity. Two and 3 drug combinations of BIC, FTC, and TAF consistently show synergistic anti-HIV-1 activity in vitro and no evidence of antagonism or toxicity.

The resistance profiles for the individual agents of BIC, FTC, and TAF have been well characterized. There is no cross-resistance between the NRTI and INSTI classes.

Both FTC and TAF have shown a low potential for mitochondrial toxicity in long-term toxicity studies and there was no evidence of toxicity to mitochondria in vitro and in vivo. Active metabolites of FTC and tenofovir disoproxil fumarate (TDF) have a high selectivity for HIV reverse transcriptase (RT) and are very weak inhibitors of mammalian DNA polymerases α, β, δ, and ε and mitochondrial DNA (mtDNA) polymerase γ. However, as mitochondrial toxicity has not been associated with INSTIs as a class, and as BIC is not anticipated to significantly increase the exposure of FTC or tenofovir (TFV), the potential for exacerbating mitochondrial toxicity is low.

Bictegravir, FTC, and TAF have no pharmacologically significant off-target binding affinity to the receptors tested. Bictegravir, FTC, and TAF have low in vitro cytotoxicity in a variety of human cell types. Bictegravir, FTC, and TAF had no or little effect on vital organ systems in safety pharmacology studies. Although TAF showed some potential to prolong the PR interval in the 39-week dog study (m2.6.7, Section 7.3.5, TOX-120-002), no findings were noted in the cardiovascular (CV) safety pharmacology study in dogs (m2.6.3, Section 4.2.3, D2000006) or in the thorough QT study (GS-US-120-0107).

Overall, the pharmacodynamic and pharmacological assessment of BIC, FTC, and TAF supports the effective and safe use of these 3 agents together in combination therapy for HIV-1 infection.

1.1. Primary Pharmacodynamics

1.1.1. BIC

Bictegravir is a novel strand transfer inhibitor of HIV-1 integrase with high potency and selectivity in antiviral assays and does not require metabolic modification to exert ARV activity (m2.6.3, Section 1.1, PC-141-2032, PC-141-2034, and PC-141-2036). Using lymphoblastoid T-cell lines and primary human T-lymphocytes in HIV-1 antiviral assays, the estimated concentration of drug for a half maximal response (EC_{50}) of BIC ranged from 1.5 to 2.4 nM and the selectivity indices ranged from 1500 to 8800 (m2.6.3, Section 1.1, PC-141-2032 and PC-141-2034). When tested in primary human peripheral blood mononuclear cells (PBMCs) against clinical isolates of all HIV-1 groups (M, N, O), including subtypes A, B, C, D, E, F, and G, BIC displayed similar antiviral activity across all clinical isolates with mean and median EC_{50} values of 0.60 and 0.55 nM, respectively, based on a range of EC_{50} values between < 0.05 and 1.71 nM (m2.6.3, Section 1.1, PC-141-2035 and PC-141-2057). HIV-2 was similarly susceptible to BIC with an EC_{50} value of 1.1 nM (m2.6.3, Section 1.1, PC-141-2035). Bictegravir is a specific inhibitor of HIV with no measurable antiviral activity against non-HIV viruses, including HBV, hepatitis C virus (HCV), influenzas A and B, human rhinovirus, and respiratory syncytial virus (RSV) (m2.6.3, Section 1.4, PC-141-2043).

Bictegravir maintains potent antiviral activity against HIV-1 variants resistant to currently approved ARVs from the NRTI, nonnucleoside reverse transcriptase inhibitor (NNRTI), and protease inhibitor (PI) classes (m2.6.3, Section 1.1, PC-141-2039). Bictegravir displays a resistance profile similar to that of dolutegravir (DTG) and markedly improved compared with that of raltegravir (RAL) and elvitegravir (EVG). Bictegravir retains full susceptibility against clonal isolates from virologic failures treated with Stribild® (STB; E/ cobicistat [COBI; C]/F/TDF) (m2.6.3, Section 1.1, PC-141-2040 and PC-141-2050). Bictegravir has an improved resistance profile compared to EVG, RAL, and DTG in patient isolates, particularly for isolates with high-level INSTI resistance containing combinations of mutations such as E92Q + N155H or G140C/S + Q148R/H/K ± additional INSTI mutations, and may have unmet clinical utility in these patients (m2.6.3, Section 1.1, PC-141-2051). Bictegravir has a longer dissociation half-life from HIV-1 integrase-DNA complexes compared with DTG, RAL, and EVG (m2.6.3, Section 1.1, PC-141-2058).

HIV-1 isolates with reduced susceptibility to BIC have been selected in cell culture (m2.6.3, Section 1.1, PC-141-2041, PC-141-2052, and PC-141-2056). These selections showed that BIC

displayed a comparable barrier to resistance emergence as DTG, and a higher barrier than EVG. Bictegravir selected the M50I + R163K combination and S153F with a transient T66I substitution in HIV-1 integrase. The R263K single mutant and M50I + R263K double mutant viruses had low-level reduced susceptibility to BIC, but the single M50I mutant was fully sensitive to BIC. The M50I + R263K selected variants exhibited low-level cross-resistance to RAL and DTG and intermediate cross-resistance to EVG but remained susceptible to other classes of ARVs. The effect of the T66I and S153F/Y single mutants and the T66I + S153F double mutant in integrase (IN) on BIC susceptibility was minimal.

Similar to a number of other ARV agents, the in vitro activity of BIC was reduced in the presence of human serum due to significant protein binding. Bictegravir exhibited approximately 70-fold increase in the EC_{50} value in the presence of 100% serum relative to its activity in cell culture medium. The EC_{95} calculated from the high density antiviral dose response was used in conjunction with the human serum shift determined by equilibrium dialysis to calculate the protein-adjusted EC_{95} ($PAEC_{95}$) of 361 nM (m2.6.3, Section 1.1, PC-141-2033 and m2.6.5, Section 6.1, AD-141-2287).

1.1.2. FTC

Emtricitabine, an NRTI, is a synthetic analogue of the naturally occurring pyrimidine nucleoside, 2′-deoxycytidine. Intracellularly, FTC is converted through 3 phosphorylation reactions to its active tri-phosphorylated anabolite emtricitabine 5′-triphosphate (FTC-TP) {Paff 1994}, {Furman 1992}. Emtricitabine 5'-triphosphate inhibits the activity of viral polymerases, including HIV-1 RT by direct binding competition with the natural deoxyribonucleotide substrate (deoxycytidine triphosphate [dCTP]) and by being incorporated into nascent viral DNA, which results in chain termination {Wilson 1993}. FTC has activity that is specific to HIV (HIV-1 and HIV-2) and HBV. The EC_{50} of FTC against laboratory adapted strains of HIV-1 ranged from 0.001 to 0.62 μM depending on cell type and virus strain used in the assay {Schinazi 1992}, {Painter 1995}, {Jeong 1993}. With clinical isolates of HIV-1, EC_{50} values ranged from 0.002 to 0.028 μM {Schinazi 1992}. Emtricitabine 5’-triphosphate is a weak inhibitor of mammalian DNA polymerases α, β, and ε and mtDNA polymerase γ {Painter 1995}. There was no evidence of toxicity to mitochondria in vitro and in vivo.

The antiviral activity of FTC against laboratory and clinical isolates of HIV-1 was assessed in lymphoblastoid cell lines, the MAGI-CCR5 cell line, and PBMCs. The EC_{50} values for FTC were in the range of 0.001 to 0.62 μM. FTC displayed antiviral activity in cell culture against HIV-1 clades A, B, C, D, E, F, G, and O (EC_{50} values ranged from 0.007 to 0.140 μM) and showed activity against HIV-2 (EC_{50} values ranged from 0.007 to 1.5 μM).

HIV-1 isolates with reduced susceptibility to FTC have been selected in cell culture. Reduced susceptibility to FTC was associated with M184V/I mutations in HIV-1 RT.

1.1.3. TAF

TAF is a phosphonamidate prodrug of TFV (2’-deoxyadenosine monophosphate analogue). Cells are permeable to TAF, and due to increased plasma stability and intracellular activation through hydrolysis by cathepsin A, TAF is more efficient than TDF in loading TFV into PBMCs,

including T cells and macrophages {Birkus 2008}, {Birkus 2007}. Intracellular TFV is subsequently phosphorylated to the pharmacologically active metabolite tenofovir diphosphate (TFV-DP) {Robbins 1998}. Tenofovir diphosphate inhibits HIV replication through incorporation into viral DNA by the HIV RT, which results in DNA chain-termination {Yokota 1994}, {Cherrington 1995b}. Tenofovir has activity that is specific to human immunodeficiency virus (HIV-1 and HIV-2) and HBV {Lee 2005}, {Kalayjian 2003}, {Delaney 2006}. In vitro studies have shown that both FTC and TFV can be fully phosphorylated when combined in cells (m2.6.3, Section 1.3, PC-164-2001). Tenofovir diphosphate is a weak inhibitor of mammalian DNA polymerases that include mtDNA polymerase γ {Kramata 1998}, {Cherrington 1994}, and there is no evidence of mitochondrial toxicity *in vitro* based on several assays including mtDNA analyses {Birkus 2002}, {Stray 2017}.

The antiviral activity of TAF against laboratory and clinical isolates of HIV-1 subtype B was assessed in lymphoblastoid cell lines, PBMCs, primary monocyte/macrophage cells, and CD4-T lymphocytes. The EC_{50} values for TAF were in the range of 2.0 to 14.7 nM. TAF displayed antiviral activity in cell culture against all HIV-1 groups (M, N, O), including subtypes A, B, C, D, E, F, and G (EC_{50} values ranged from 0.10 to 12.0 nM) and activity against HIV-2 (EC_{50} values ranged from 0.91 to 2.63 nM) (m2.6.3, Section 1.3, PC-120-2004). The antiviral activity of two TAF metabolites, M18 (GS-645552) and M28 (GS-652829), were evaluated in two T-lymphoblastoid cell lines (MT-2 and MT-4) following 5 days of compound exposure (m2.6.3, Section 1.3, PC-120-2021). GS-645552 is also a drug product degradant. Both metabolites/degradants showed weak inhibition of HIV-1 replication with 1723 to 2630-fold lower inhibitory potency relative to TAF (EC_{50} values of 7.41 to 21.04 μM) for metabolite M28 and 121 to 130-fold lower inhibitor potency relative to TAF (EC_{50} values of 0.56 to 0.97 μM) for metabolite M18.

HIV-1 isolates with reduced susceptibility to TAF have been selected in cell culture. HIV-1 isolates selected by TAF expressed a K65R mutation in HIV-1 RT; in addition, a K70E mutation in HIV-1 RT has been transiently observed {Margot 2006b}. HIV-1 isolates with the K65R mutation have low-level reduced susceptibility to abacavir (ABC), FTC, TFV, and lamivudine (LAM) {Kagan 2007}, {Margot 2006b} (m2.6.3, Section 1.3, PC-120-2011). In vitro drug resistance selection studies with TAF have shown no development of high-level resistance after extended time in culture.

Tenofovir has activity that is specific to HBV in addition to HIV-1 and HIV-2. The antiviral activity of TAF against a panel of HBV clinical isolates representing genotypes A-H was assessed in HepG2 cells. The EC_{50} values for TAF ranged from 34.7 to 134.4 nM, with an overall mean EC_{50} of 86.6 nM (m2.6.3, Section 1.3, PC-320-2003). The CC_{50} in HepG2 cells was >44,400 nM (m2.6.3, Section 1.3, PC-320-2003 and PC-120-2007). The combination of TFV and FTC was studied for cytotoxicity in MT-2 cells. No cytotoxicity was observed at the highest concentrations tested, up to 50 μM TFV and 5 μM FTC (m2.6.3, Section 1.12, PC-164-2002). Cytotoxicity studies were also conducted on the combination of TFV and FTC in HepG2 cells and no cytotoxicity was observed (m2.6.3, Section 1.6, TX-104-2001).

The antiviral activity of TAF was evaluated against a panel of HBV isolates containing nucleos(t)ide RT inhibitor mutations in HepG2 cells. HBV isolates expressing the rtV173L,

rtL180M, and rtM204V/I substitutions associated with resistance to LAM remained susceptible to TAF (< 2-fold change in EC_{50}) (m2.6.3, Section 1.3, PC-320-2007). HBV isolates expressing the rtL180M, rtM204V plus rtT184G, rtS202G, or rtM250V substitutions associated with resistance to entecavir (ETV) remained susceptible to TAF. HBV isolates expressing the rtA181T, rtA181V, or rtN236T single substitutions associated with resistance to adefovir remained susceptible to TAF; however, the HBV isolate expressing rtA181V plus rtN236T exhibited reduced susceptibility to TAF (3.7-fold change in EC_{50}). The clinical relevance of these substitutions is not known.

1.1.4. B/F/TAF

Bictegravir, FTC, and TAF are potent and selective inhibitors of HIV-1. All 3 drugs show potent antiretroviral activity against diverse subtypes of HIV-1 in vitro. Emtricitabine and TFV are phosphorylated intracellularly through nonoverlapping pathways, and in combination show no antagonism for the formation of their active metabolites (m2.6.3, Section 1.3, PC-164-2001). Bictegravir does not require metabolic modification for activity. The anti-HIV-1 activity of 3-drug combination of BIC, FTC, and TAF were found to be highly synergistic with no evidence of antagonism in vitro, supporting the use of these agents in combination in HIV-1 infected patients (m2.6.3, Section 1.10, PC-141-2038). In addition, in vitro combination studies have shown that in 2-drug combination studies BIC, FTC, and TFV have additive to synergistic anti-HIV-1 activity with other approved NRTIs, NNRTIs, and PIs {Miller 1999}, {Hill 1997}, {Rimsky 2001}, (m2.6.3, Section 1.10, PC-141-2038). The resistance profiles of the individual agents BIC, TFV, and FTC are distinct and non-overlapping (m2.6.3, Section 1.1, PC-141-2039).

1.2. Secondary Pharmacodynamics

1.2.1. Cytotoxicity

For BIC, the concentration that resulted in 50% cytotoxicity (CC_{50}) in primary CD4+ T-lymphocytes, MT-4, MT-2, resting and activated PBMCs, and monocyte-derived macrophages cells ranged from of 3700 to 29800 nM (m2.6.3, Section 1.1, PC-141-2032 and PC-141-2034).

The cytotoxicity of FTC has been evaluated extensively in vitro. In all the cell lines examined, cell growth was not affected at concentrations of FTC ≥ 100 µM {Schinazi 1994}, {Van Draanen 1994}, {Furman 1992}.

Both TAF and its metabolites M18 and M28 had no cytotoxicity up to the highest tested concentration (57 µM) (m2.6.3, Section 1.3, PC-120-2021).

1.2.2. Off-Target Activity

Bictegravir had no pharmacologically significant binding affinity to a diverse panel of 68 protein targets, including neuroreceptors, ion channels, and nuclear receptors (m2.6.3, Section 3.1, PC-141-2029). Inhibition of transporters, including organic cation transporter 2 (OCT2) and multidrug and toxin extrusion 1 (MATE1) are discussed in m2.6.4, Section 7.1.4.

Emtricitabine had no pharmacologically significant binding affinity to 19 different receptors (m2.6.3, Section 1.5, TPZZ/93/0002), showed little or no direct effect on various isolated muscle preparations (cholinergic, adrenergic, histaminergic, and serotonergic), and had no major inhibitory effects on the contractile responses to acetylcholine, norepinephrine, serotonin, isoproterenol, arachidonic acid, histamine, bradykinin, and angiotensin II (m2.6.3, Section 1.5, TPZZ/92/0055).

Tenofovir showed no significant inhibition of, or increased binding to a series of 111 protein targets (neuroreceptors, ion channels, transporters, and nuclear receptors) (m2.6.3, Section 1.6, V2000020).

1.3. Safety Pharmacology

1.3.1. BIC

Bictegravir was evaluated in safety pharmacology studies of the central nervous system (CNS), respiratory, and cardiovascular systems (m2.6.3, Section 4.2.1, PC-141-2047, PC-141-2048, and PC-141-2046, respectively). At the highest doses tested, BIC had no effects on the central nervous and respiratory systems of rats (300 mg/kg), no effects on the cardiovascular system of monkeys (1000 mg/kg), and no notable inhibition of the human ether-a-go-go-related gene (hERG) potassium channel current at a concentration > 7.1 μM (m2.6.3, Section 1.7, PC-141-2049). Plasma exposures (free [unbound] C_{max}) in the in vivo studies were at least 0.92-fold (rats) and 22-fold (monkeys) of the free BIC C_{max} concentration following clinical administration of the B/F/TAF fixed-dose combination (FDC). In the hERG study, exposures were at least 200-fold above free BIC C_{max} concentration following clinical administration of the B/F/TAF FDC.

1.3.2. FTC

A comprehensive range of safety pharmacology studies revealed no treatment-related adverse effects on any organ system at systemic exposure levels much higher than those anticipated in patients at the recommended clinical dose (10- to more than 50-fold) (m2.6.3, Section 4.2.2, 477, TPZZ/93/0001, TPZZ/93/0119, and TPZZ/92/0057, and m2.6.3, Section 4.1.2, TPZZ/92/0056). No effects on the CV system were reported in anesthetized dogs administered a cumulative dose of 38.5 mg/kg of FTC intravenously over a 1-hour period (m2.6.3, Section 4.2.2, TPZZ/92/0076). In addition, there were no abnormalities reported on the electrocardiogram (ECG) data obtained from the repeated-dose toxicity studies in monkeys, where plasma AUC exposures were up to 26-fold higher than in humans administered the 200-mg dose (m2.6.7, Section 7.2.6, TOX600; Section 7.2.7, TOX627; Section 7.2.8, TOX032).

1.3.3. TAF

Tenofovir alafenamide was evaluated in safety pharmacology studies of the rat central nervous, renal, gastrointestinal (GI), and CV systems. In vivo safety pharmacology experiments were conducted using TAF as the monofumarate form (GS-7340-02) in 50 mM citric acid. The 50% inhibitory concentration (IC_{50}) for the inhibitory effect of TAF on hERG potassium current was estimated to be > 10 μM, far above human plasma exposure (m2.6.3, Section 4.1.3,

PC-120-2005).There were no adverse effects detected in the CNS in rats dosed at 1000 mg/kg (m2.6.3, Section 4.2.3, R990188) or in the renal system in rats administered 1000 mg/kg (m2.6.3, Section 4.2.3, R990186). In the chronic repeat dose dog study (m2.6.7, Section 7.3.5, TOX-120-002), a dose-related prolongation of PR interval was noted at Week 39; however, in the single dose CV safety pharmacology study in dogs (m2.6.3, Section 4.2.3, D2000006) dosed at 100 mg/kg (80 mg free base equivalents/kg), there were no findings. There was reduced gastric emptying in rats dosed at 1000 mg/kg but not at 100 mg/kg (m2.6.3, Section 4.2.3, R990187).

1.3.4. B/F/TAF

A comprehensive safety pharmacology program has been conducted for the 3 individual components of the B/F/TAF regimen. While the designs for these safety studies varied between the agents, the major organ systems were evaluated. Bictegravir had no effect on vital organ systems in safety pharmacology studies. Neither FTC nor TAF had clinically relevant effects on vital organ systems in safety pharmacology studies. Although TAF showed some potential to prolong the PR interval in the 39-week dog study (m2.6.7, Section 7.3.5, TOX-120-002), no PR prolongation or any change in ECG results occurred in the CV safety pharmacology study (m2.6.3, Section 4.2.3, D2000006) or in the thorough QT study (GS-US-120-0107). Neither BIC nor FTC had an effect on PR interval in safety pharmacology studies; therefore, there is no potential for overlapping toxicity. Overall, the pharmacological assessment of BIC, FTC, and TAF supports the effective use of these 3 agents together in combination therapy for HIV-1 infection. Additional safety pharmacology studies on the B/F/TAF combination are considered unwarranted.

1.4. Pharmacodynamic Drug Interactions

The anti-HIV-1 activity of 2-drug and 3-drug combinations of BIC, FTC, and TAF were found to be additive to highly synergistic with no evidence of antagonism in multiple in vitro assay systems, supporting the use of these agents in combination in HIV-infected patients (m2.6.3, Section 1.10, PC-380-2001).

In vitro two-drug combination studies have shown that BIC has additive to synergistic anti-HIV-1 activity with other approved NRTIs, NNRTIs, and PIs, including synergistic activity with TAF, FTC, and darunavir (DRV). No antagonistic antiviral interaction was found between BIC and the tested clinically relevant classes of antiretrovirals (m2.6.3, Section 1.10, PC-141-2038).

In two-drug combination studies of FTC with NRTIs, NNRTIs, PIs, and INSTIs, additive to synergistic effects were observed. No antagonism was observed for these combinations {Hill 1997}, {Rimsky 2001} .

In a study of TAF with a broad panel of representatives from the major classes of approved anti-HIV agents (NRTIs, NNRTIs, INSTIs, and PIs), additive to synergistic effects were observed. No antagonism was observed for these combinations (m2.6.3, Section 1.12, PC-104-2005, PC-104-2006, PC-264-2001, and PC-120-2002).

In cell culture combination antiviral activity studies of TFV with the HBV NRTIs FTC, ETV, LAM, and telbivudine, no antagonistic activity was observed (m2.6.3, Section 1.12, PC-120-2001 and PC-120-2032). The anti-hepatitis C virus (HCV) PIs telaprevir and boceprevir were identified as the only potent inhibitors of cathepsin A (CatA)-mediated hydrolysis of TAF in a biochemical assay. The tested HIV PIs, host serine PIs, and the majority of other HCV PIs exhibit minimal potential to interfere with the intracellular activation of TAF (m2.6.3, Section 1.12, PC-120-2001). These data support the co-administration of the tested therapeutic PIs, with the exception of telaprevir and boceprevir, in combination with TAF, without negatively affecting its clinical pharmacology and intracellular conversion to TFV.

2. PRIMARY PHARMACODYNAMICS

2.1. Primary Pharmacodynamics

2.1.1. BIC

2.1.1.1. Metabolic Activation of BIC

Bictegravir does not require metabolic activation for its activity.

2.1.1.2. Antiviral Activity of BIC

The ability of BIC to inhibit HIV-1 replication in vitro was evaluated in lymphoblastoid T-cell lines MT-2 and MT-4, and in primary human T-lymphocytes and macrophages. The antiviral activity of BIC was also tested against HIV-1 clinical isolates in human PBMCs. The effect of human serum and serum protein components on the antiviral activity of BIC was studied in MT-2 cells.

2.1.1.2.1. Antiviral Activity of BIC Against HIV-1 in T-Cell Lines

The anti-HIV activity and cytotoxicity of BIC were evaluated in 5-day cytopathic assays with acutely infected and uninfected MT-2 and MT-4 cell lines (m2.6.3, Section 1.1, PC-141-2032). BIC is a potent inhibitor of HIV-1 replication in both MT-2 and MT-4 cells with EC_{50} values of 1.5 and 2.4 nM, respectively (Table 1). In both cell lines, BIC showed similar antiretroviral activity as DTG.

Table 1. Antiviral Activity of BIC in T-Cell Lines

Compound	EC_{50} (nM)	
	MT-2 Cells[a]	MT-4 Cells[a]
BIC	1.5 ± 0.2	2.4 ± 0.4
DTG	1.5 ± 0.2	1.5 ± 0.3

a EC_{50} values represent the mean ± SD of at least 4 independent measurements performed in triplicate.
Source: PC-141-2032.

2.1.1.2.2. Antiviral Activity of BIC Against HIV-1 in Primary T-Cells and Macrophages

Antiretroviral activity and cytotoxicity of BIC were determined in freshly isolated and acutely infected primary human CD4 T-cells and monocyte-derived macrophages following a 5-day incubation with the compound (m2.6.3, Section 1.1, PC-141-2034). BIC exhibits an antiviral potency comparable to that in T-cell lines with EC_{50} values of 1.5 ± 0.3 nM and 6.6 ± 4.1 nM for $CD4^+$ T-lymphocytes and monocyte-derived macrophages, respectively (Table 2).

Table 2. Antiviral Activity of BIC in Primary Cells

Compound	EC_{50} (nM)	
	$CD4^+$ T Lymphocytes[a]	Monocyte-derived Macrophages[a]
BIC	1.5 ± 0.3	6.6 ± 4.1
DTG	1.0 ± 0.3	3.1 ± 2.5

a EC_{50} values represent the mean ± SD of 4 independent donor determined in triplicate.
Source: PC-141-2034.

2.1.1.2.3. Antiviral Activity of BIC against HIV Clinical Isolates

The antiretroviral activity of BIC was tested against 18 clinical isolates of HIV-1 and one isolate of HIV-2 in freshly isolated human PBMCs (Table 3) (m2.6.3, Section 1.1, PC-141-2035 and PC-141-2057). BIC displayed similar antiviral activity across all HIV-1 clinical isolates tested with mean and median EC_{50} values of 0.60 nM and 0.55 nM, respectively, and a range of EC_{50} values between <0.05 and 1.71 nM (Table 3 and Table 4). DTG tested in parallel exhibited a similar potency with mean and median EC_{50} values of 0.61 nM and 0.68 nM, respectively, and a range of EC_{50} values from 0.09 to 1.13 nM against the same tested isolates (Table 3 and Table 4). HIV-2 was similarly susceptible to both BIC and DTG with EC_{50} values of 1.1 nM and 2.1 nM, respectively (Table 3).

Table 3. Antiviral Activity of BIC against HIV Clinical Isolates

HIV-1 Subtype	HIV-1 Isolate	Genbank Accession #	EC_{50} (nM)[a]		
			BIC	DTG	ZDV
A	92RW016	AF009409	0.74	0.35	2.61
A	92UG037	AB253428	1.71	0.93	10.9
B	Ba-L	AY713409	0.35	0.29	3.39
B	89BZ_167	AY173956	0.88	1.13	2.65
B	91US001	AY173952	0.87	0.84	5.61
B	91US004	AY173955	0.82	0.94	2.74
C	93IN905	AF067158	0.15	0.15	1.61
C	98US_MSC5016	AY444801	1.4	0.92	10.3
D	98UG_57128	AF484502	0.31	0.67	0.55
D	99UG_A07412M1	AF484477	1.06	0.93	9.99
E	96TH_M02138	AY713424	0.8	0.69	5.79
E	96TH_NI1046	AY713421	0.28	0.3	2.6
F	93BR020	AF005494	1.13	0.37	8.72
G	01CM1475MV	AY371138	< 0.05	0.09	0.98
O	BCF01	AF458283	< 0.08	nd	5.60

HIV-1 Subtype	HIV-1 Isolate	Genbank Accession #	EC_{50} (nM)[a]		
			BIC	DTG	ZDV
O	BCF02	Y14497	0.09	nd	9.28
O	BCF03	AJ133055	< 0.08	nd	7.14
N	HIV-1 YBF30	AJ006022	< 0.08	nd	2.18
HIV-2	CDC 310319	AY965902	1.11	2.1	4.1

nd = no data available; ZDV = zidovudine
a EC_{50} values represent the mean of triplicate measurements in human PBMCs.
Source: PC-141-2035 and PC-141-2057

Table 4. Summary of the Antiviral Activity of BIC against HIV-1 Clinical Isolates

Compound	EC_{50} (nM)		
	Mean	Median	Range
BIC	0.60	0.55	<0.05 – 1.71
DTG	0.61	0.68	0.09 – 1.13
ZDV	5.15	4.50	0.55 – 10.9

Source: PC-141-2035 and PC-141-2057

2.1.1.2.4. Effect of Increasing Multiplicity of Infection on BIC Antiviral Activity

The antiviral activity of BIC in MT-2 cells was determined against the IIIb strain of HIV-1 with different multiplicities of infection (MOI) of 0.009, 0.03, 0.09, and 0.3 in parallel with DTG and other control compounds (m2.6.3, Section 1.1, PC-141-2054). For all drugs tested, EC_{50} values increased as the MOI increased. BIC and DTG had similar antiviral potencies at all MOIs tested with EC_{50} values ranging from 0.44 nM to 2.86 nM for BIC and 0.30 nM to 2.33 nM for DTG. Thus, the EC_{50} values of both BIC and DTG increased approximately 6- to 7-fold across the 30-fold range in virus MOI. The in vitro antiviral activity of BIC decreased as the amount of virus used for infection increased, which is similar to the effect of MOI on antiviral activity observed for other antiretroviral drugs.

2.1.1.3. Effect of Human Serum and Serum Protein Components on the Antiviral Activity of BIC and Determination of the Protein-Adjusted EC_{95}

The EC_{95} value for the inhibition of HIV-1 replication was calculated using a Hill slope determined from the curve fit to a high density dose response in MT-4 cells (Table 5). BIC high density dose response had a mean Hill slope of 2.1 in MT-4 cells, which in turn yielded an EC_{95} value of 8.3 nM. Parallel profiling of DTG resulted in an EC_{95} value close to that determined for BIC. The EC_{95} calculated from the high density antiviral dose response was used in conjunction with the human serum shift determined by equilibrium dialysis to calculate the protein-adjusted EC_{95} ($PAEC_{95}$) (m2.6.3, Section 1.1, PC-141-2032). The calculated $PAEC_{95}$ for BIC was 361 nM. The $PAEC_{95}$ value was subsequently used for the estimation of clinical inhibitory quotient (IQ) based on the projected trough concentration of BIC in humans.

Table 5. Protein-Adjusted EC_{95} of BIC in MT-4 Cells

Compound	MT-4 Cells[a]				
	EC_{50} (nM)	Hill Slope	EC_{95} (nM)	EQDS Shift (Fold-change)[b]	$PAEC_{95}$ (nM)
BIC	1.9 ± 0.6	2.1 ± 0.3	8.3	43.6 ± 7.7	361
DTG	1.7 ± 0.2	2.0 ± 0.3	7.4	27.5	204

$PAEC_{95}$ = protein-adjusted EC_{95}; EQDS = equilibrium dialysis
a EC_{50}, Hill Slope, and EC_{95} values represent the mean ± SD of at least 8 measurements in quadruplicate.
b Values represent mean ± SD of 3 measurements for BIC and mean of two measurements for DTG.
Source: PC-141-2032

The antiviral EC_{50} of BIC was determined in MT-2 cells in the presence of two key human serum components, human serum albumin (HSA) and α_1-acid glycoprotein (α_1-AGP) or in the presence of complete human serum (m2.6.3, Section 1.1, PC-141-2033).

Each of these serum components were tested at their concentrations found in human serum (HSA at 35 mg/ml and α_1-AGP at 1.5 mg/ml) (Table 6). The presence of the two serum components reduced the antiviral activity of BIC by 20-fold, compared to 11-fold reduction of the potency of DTG. These data indicate that the two tested components of human serum are capable of binding BIC as well as DTG (Table 6).

Table 6. Effect of Serum Protein Components on the Antiviral Activity of BIC

Compound	10% FBS[a,b] EC_{50} (nM)	10% FBS + HSA + α_1-AGP[a,b] EC_{50} (nM)	Protein Shift (Fold Change)
BIC	0.9 ± 0.04	18.6 ± 4.6	20.4
DTG	1.1 ± 0.3	11.7 ± 1.4	10.7

FBS = fetal bovine serum; HSA = human serum albumin; α_1-AGP = α_1-acid glycoprotein
a Assays with 10% FBS and 10% FBS + HSA + α_1-AGP were determined in parallel.
b EC_{50} values represent mean ± SD of 3 independent measurements in triplicate.
Source: PC-141-2033

The effect of human serum on the antiretroviral activity of BIC was evaluated by determining the EC_{50} in MT-2 cells in the presence of human serum concentrations ranging from 10% to 50%. The resulting serum dose response of EC_{50} was analyzed by linear regression to extrapolate the EC_{50} at 100% human serum (Table 7). In the presence of human serum, the shift in EC_{50} for both BIC and DTG exhibited similar trends as observed with the serum protein components. The BIC EC_{50} value, extrapolated to 100% human serum, shifted 74-fold and was comparable to the 39-fold shift extrapolated for DTG. The serum shift determined in this antiviral assay is comparable to the fold-shift determined by equilibrium dialysis (m2.6.3, Section 1.1, PC-141-2033) of the compound between complete culture medium and human serum (Table 7).

Table 7. Effect of Human Serum on the Antiviral Activity of BIC

Compound	10% FBS[a] EC_{50} (nM)	100% HS[b] EC_{50} (nM)	HS Shift (Fold Change)	EQDS Shift[c] (Fold Change)
BIC	0.37 ± 0.06	27.4 ± 7	74.0	43.6 ± 7.7
DTG	0.38 ± 0.05	14.7 ± 2	38.5	27.5

EQDS = equilibrium dialysis; FBS = fetal bovine serum; HS = human serum
a EC_{50} values represent mean ± SD of 3 independent measurements in triplicate.
b Determined by linear extrapolation of 10 to 50% human serum dose response of EC_{50} values.
c Values represent mean ± SD of 3 independent measurements for BIC and mean of two independent measurements for DTG.
Source: PC-141-2033 and AD-141-2287

2.1.1.4. Mechanism of Action of BIC

After HIV-1 entry and uncoating in the infected cell, the viral RNA is reverse transcribed by HIV-1 RT into a double stranded linear DNA. This linear viral DNA is associated with HIV-1 integrase, which processes both of its ends by removing a di-nucleotide from each 3'-terminus in a reaction referred to as 3'-processing. While integrase is still associated with the processed ends of viral DNA, the integrase-DNA complex is transported into the nucleus where integrase performs a concerted integration of both viral DNA ends into host chromosomal DNA in a reaction referred to as strand transfer. This integration of viral DNA into host chromosomal DNA is essential for HIV-1 replication, making HIV-1 integrase an attractive target for antiretroviral therapy {Pommier 1997}, {Thomas 1997}.

Inhibition of the enzymatic activity of HIV integrase alone in a biochemical assay is not sufficient to confirm the mechanism of action of integrase inhibitors since certain previously described inhibitors that were active in biochemical assays of HIV IN failed to inhibit integration in infected cells {Pluymers 2000}. Two assays were used to confirm that the BIC mechanism of action is mediated by the inhibition of HIV DNA integration in infected target cells: (1) Circular HIV DNA species containing 1 or 2 long terminal repeats (1-LTR and 2-LTR circles) accumulate when viral integration fails and thus, they serve as surrogates for HIV integration failure {Bukrinsky 1993}; (2) The inhibition of HIV-1 integration in infected cells can be assessed by direct measurement of integration junctions formed by the proviral DNA and the host chromosomal DNA {Butler 2001}.

2.1.1.4.1. Inhibition of HIV-1 Integrase Enzymatic Activity by BIC

The inhibitory activity of BIC was evaluated in biochemical assays that measured the 3'-processing and strand transfer activities of purified recombinant HIV-1 integrase. BIC inhibited the strand transfer activity with an IC_{50} value of 7.5 nM (Table 8) (m2.6.3, Section 1.1, PC-141-2036), an activity comparable to those of EVG and DTG {Shimura 2008}, {Min 2010}. In contrast, inhibition of HIV-1 integrase 3'-processing activity by BIC showed an IC_{50} of 241 nM that was weaker than the inhibition of strand transfer activity. Similar potency profiles in the inhibition of strand transfer and 3'-processing activities were observed for DTG and EVG.

Table 8. Inhibition of HIV-1 Integrase Strand Transfer and 3'-Processing Activities by BIC

Compound	Inhibition of Strand Transfer[a] IC_{50} (nM)	Inhibition of 3'-Processing[b] IC_{50} (nM)
BIC	7.5 ± 0.3	241 ± 51
DTG	7.4 ± 0.6	232 ± 33
EVG	8.4 ± 0.7	556 ± 40

a The data represent the mean ± SD of 3 independent experiments performed in triplicates.
b The data represent the mean ± SD of 5 independent experiments performed in triplicates.
Source: PC-141-2036.

2.1.1.4.2. Inhibition of HIV-1 Integration in MT-2 Cells by BIC

BIC inhibition of HIV-1 DNA integration in cell culture during HIV-1 infection was further evaluated by assessing the quantity of aborted 2-LTR circles, as well as the quantity of authentic HIV-1 integration products in infected MT-2 cells (Table 9) (m2.6.3, Section 1.1, PC-141-2037). BIC enhanced the accumulation of 2-LTR circles, a product of integration failure. In an assessment of the direct effect on the integration products in the chromosomal DNA of infected cells (Alu-LTR), BIC profoundly decreased integration junctions but did not affect viral DNA synthesis as measured by the late reverse transcription products, demonstrating an authentic inhibition of HIV-1 integration (Table 9). As expected, DTG exhibited a similar effect on the integration junctions. In contrast, efavirenz (EFV), a NNRTI, decreased the late reverse transcription products with subsequent downstream effects on both 2-LTR circles and integration products. The PI DRV had no effect on either DNA synthesis or integration.

Table 9. Inhibition of HIV-1 Integration in MT-2 Cells by BIC

Compound	Concentration Used[b] (nM)	Integration Failure	Assessment of Direct Effect on Integration	
		2-LTR Circles[a] (fold-change)[c]	Late Reverse Transcription Product[a] (fold-change)[c]	Alu-LTR[a] (fold-change)[c]
DMSO	—	1.0	1.0	1.0
BIC	28	3.3	0.9	0.01
DTG	31	4.5	0.8	0.02
EFV	17	0.1	0.2	0.08
DRV	57	1.1	0.9	0.8

a The quantitative polymerase chain reaction (PCR) data of HIV target sequences were normalized against the corresponding quantitative PCR data for the globin gene from the same sample and represent the mean of two independent experiments.
b The concentrations used represent ~20 times the respective antiviral EC_{50} of each drug.
c Fold-change is relative to the DMSO control.
Source: PC-141-2037.

2.1.1.4.3. Dissociation Half-Life of BIC from HIV-1 IN/DNA Complexes

The dissociation kinetics of ^{3}H-labelled INSTIs BIC, DTG, RAL, and EVG were measured using wild-type HIV integrase/DNA complexes and a scintillation proximity assay (SPA) as previously described {Hightower 2011}. Single exponential decay functions were used to analyze the competition binding phases yielding dissociation half-lives ($t_{1/2}$) of the INSTIs (Table 10) (m2.6.3, Section 1.1, PC-141-2058). However, the competition binding phases deviated significantly from the single exponential decay function due to the gradual sedimentation of the SPA beads, necessitating modeling of the equilibrium binding with off-rate constants as decreasing functions of time with k_{off} as initial values of each function. By both data analysis methods, BIC had a longer dissociation half-life from HIV-1 integrase/DNA complexes compared to DTG, RAL, and EVG {White 2016}; the long dissociation half-life has been proposed to contribute to a high barrier to resistance.

Table 10. Dissociation Half-life of INSTIs from WT HIV-1 Integrase/DNA Complexes

Compound	Apparent $t_{1/2}$ (h)[a] Exponential Decay Method	$t_{1/2}$ (h)[a] Equilibrium Binding Model
BIC	135 ± 20	39 ± 19
DTG	79 ± 13	16 ± 9
RAL	14 ± 3	5.2 ± 0.6
EVG	3.6 ± 0.7	1.5 ± 0.2

a Mean ± SD from 5 to 7 experiments.
Source: PC-141-2058

2.1.1.5. Viral Resistance to BIC

Viral resistance to BIC was assessed in two types of studies. The first focused on the determination of whether BIC may overcome viral resistance developed against currently approved HIV antiviral drug classes including NRTIs, NNRTIs, PIs, and other INSTIs. The second type of studies aimed to characterize the rate of resistance emergence, as well as genotypic and phenotypic changes occurring in vitro under BIC selective pressure.

2.1.1.5.1. Activity of BIC Against INSTI Resistant Mutants of HIV-1

BIC was tested for antiviral activity against a panel of INSTI-resistant viruses (m2.6.3, Section 1.1, PC-141-2040). A panel of 8 mutant viruses representing the major resistance development pathways against RAL and EVG {Geretti 2012}, {Quashie 2013b}, {Mesplede 2012} containing both single and double mutants in the integrase were used for the profiling of BIC. The set of tested mutations included E92Q, Y143R, Q148R, N155H, E138K/Q148R, G140S/Q148R, E92Q/N155H, and Q148R/N155H. In addition, R263K, an integrase mutation that was selected in vitro with DTG {Quashie 2012} and that has been reported to emerge in rare patient cases following the treatment with DTG (50 mg once daily) in combination with a background NRTI regimen {Pozniak 2013} was also included in the test panel. As expected, all tested mutant variants displayed much less resistance against DTG compared to either RAL or EVG. In a side-by-side comparison with DTG, the same variants displayed comparable or even

lower levels of resistance against BIC (Table 11). Among the tested variants, three double mutants (E138K/Q148K, G140S/Q148R, and N155H/Q148R) showed intermediate (3.5- to 10-fold) levels of resistance to DTG. Similar to DTG, BIC showed no changes in its antiviral potency against any of the single mutants tested. In addition, BIC exhibited similar or slightly lower levels of resistance against the double integrase mutants tested compared to DTG. Collectively, these data indicate that BIC has a potential to be clinically active against the majority of known INSTI-associated resistance mutations. As an NNRTI, EFV was used as a control, which remained active against all the INSTI resistance mutants.

Table 11. Activity of BIC Against INSTI-Resistant HIV-1 Mutants

	EC_{50}[b] (nM)	EC_{50} Fold-Change Relative to WT[b]								
Compounds[a]	WT	E92Q[c]	Y143R[c]	Q148R[c]	N155H[c]	R263K[c]	E138K/ Q148K[c]	G140S/ Q148R[c]	E92Q/ N155H[c]	N155H/ Q148R[c]
BIC	1.6	1.2	1.1	0.7	1.0	1.9	8.8	2.0	1.3	4.5
DTG	1.4	1.3	1.4	0.8	1.8	1.9	10.1	4.8	2.1	3.5
RAL	9.4	4.0	45	45	20	1.1	163	262	67	232
EVG	2.4	36	6.1	154	48	4.4	1520	369	326	921
EFV	1.9	0.8	0.9	0.9	0.9	1.0	1.0	0.8	0.8	1.2

a RAL = raltegravir, EVG = elvitegravir, DTG = dolutegravir, EFV = efavirenz.
b EC_{50} and Fold-Change represent the mean of at least 3 determinations each in triplicate.
c HIV-integrase (IN) mutations.
Fold-change values ≥ 2.5 to < 10 are shown in gray and fold-change values > 10 are shown in black shading.
Source: PC-141-2040.

2.1.1.5.2. Activity of BIC Against Site-Directed Mutant HIV-1 Containing INSTI Resistance Mutations

The antiviral activity of BIC was determined against site-directed mutant viruses containing the T97A IN mutation in the absence of other primary INSTI resistance-associated mutations (RAMs) (m2.6.3, Section 1.1, PC-141-2055). The panel included 49 site-directed HIV-1 IN mutant viruses containing single, double, and multiple mutants of IN with or without the T97A IN mutation and with or without additional secondary IN mutations (M50I, V72I, L74M, S119G/P/R/T, and G163R).

In addition, viruses containing the G118R and F121Y site-directed IN mutations were also included in this virus panel. The G118R IN mutation has been selected in vitro with DTG {Quashie 2013a} and has been reported to emerge rarely in patients treated with DTG (50 mg once daily) {Brenner 2016} and RAL (400 mg twice daily) {Malet 2014}, {Malet 2011}. The F121Y IN mutation has been selected in vitro with EVG {Jones 2007}, {Margot 2012} and S/GSK-364735 {Kobayashi 2008} and has been reported to emerge rarely in patients treated with RAL (400 mg twice daily) with {Cavalcanti 2012} or without T97A {Malet 2014}.

Phenotypic data were available for 41 of 49 IN mutant viruses (Table 12). IN mutant viruses displayed 0.3- to 3.4-fold and 0.5- to 11-fold reduced susceptibility to BIC and DTG, respectively, compared to control wild-type virus. The degree of INSTI resistance to both BIC and DTG was substantially less than that observed with EVG and RAL. In addition, these IN mutant viruses displayed comparable or a lower level of resistance to BIC relative to DTG.

Table 12. Antiviral Susceptibilities of INSTIs Against HIV-1 by Single-cycle Infectivity Assay

Site-Directed Mutant HIV-1	EC_{50}, nM (Fold-Change)[a]				RC, %WT[b]
	Compound				
	BIC	DTG	EVG	RAL	
Single IN Mutants					
T97A	0.83 (0.56)	1.03 (0.64)	6.85 (3.79)	13.21 (1.62)	9.0
T97S	1.21 (0.79)	1.13 (0.72)	4.08 (2.05)	8.99 (1.12)	8.8
T97P	AF	AF	AF	AF	AF
T97I	0.71 (0.46)	0.86 (0.55)	3.48 (1.75)	8.32 (1.03)	11
T97V	0.67 (0.44)	0.99 (0.63)	5.68 (2.85)	11.74 (1.46)	153
M50I	1.55 (0.95)	1.75 (1.13)	2.73 (1.53)	8.72 (1.15)	111
G70R	1.28 (0.87)	1.76 (1.1)	3.62 (2)	9.55 (1.17)	9.1
V72I	1.45 (0.96)	1.61 (0.96)	3.20 (1.81)	10.02 (1.21)	98
L74I	1.40 (0.92)	1.55 (0.98)	3.36 (1.68)	9.18 (1.14)	224
L74M	0.99 (0.67)	1.18 (0.74)	3.09 (1.71)	9.54 (1.17)	93
A91E	0.97 (0.66)	1.17 (0.73)	1.93 (1.07)	6.57 (0.81)	69
G118R	5.18 (3.42)	10.20 (6.07)	8.71 (4.92)	51.09 (6.20)	36
S119G	1.14 (0.75)	1.47 (0.93)	3.01 (1.51)	8.62 (1.07)	166
S119P	1.39 (0.94)	1.42 (0.89)	3.39 (1.88)	8.08 (0.99)	117
S119R	1.57 (1.06)	1.70 (1.06)	3.75 (2.07)	10.41 (1.28)	66
S119T	1.37 (0.90)	1.52 (0.96)	3.22 (1.62)	10.14 (1.26)	215
F121Y	0.64 (0.39)	0.86 (0.55)	28.13 (16.00)	39.85 (5.27)	6.3
T122I	1.45 (0.95)	1.67 (0.99)	2.68 (1.51)	9.25 (1.12)	54
G163R	1.55 (1.05)	1.79 (1.11)	3.27 (1.81)	10.81 (1.33)	74
Double IN Mutants					
T97A+M50I	0.89 (0.61)	1.11 (0.69)	6.3 (3.49)	13.16 (1.61)	14
T97A+G70R	AF	AF	AF	AF	0.03
T97A+V72I	0.82 (0.50)	1.00 (0.65)	6.58 (3.70)	15.03 (1.99)	3.6
T97A+L74I	0.9 (0.60)	1.05 (0.67)	7.42 (3.72)	19.83 (2.47)	AF
T97A+L74M	0.85 (0.52)	1.00 (0.64)	8.77 (4.92)	21.15 (2.8)	66
T97A+A91E	AF	AF	AF	AF	0.01
T97A+G118R	4.62 (2.82)	16.71 (11.00)	15.25 (8.56)	154.23 (20)	4.4
T97A+S119G	0.49 (0.32)	1.07 (0.68)	11.67 (5.85)	19.77 (2.46)	3.0
T97A+S119P	0.80 (0.49)	0.96 (0.62)	16.95 (9.51)	17.04 (2.25)	5.5
T97A+S119R	1.21 (0.74)	1.73 (1.12)	23.07 (13)	26.54 (3.51)	3.7
T97A+S119T	0.64 (0.42)	0.90 (0.57)	10.47 (5.25)	16.11 (2)	8.4
T97A+F121Y	AF	AF	AF	AF	AF
T97A+T122I	AF	AF	AF	AF	0.12
T97A+G163R	1.63 (1.00)	1.85 (1.20)	5.19 (2.92)	16.33 (2.16)	0.9
V72I+L74M	0.89 (0.54)	1.09 (0.71)	4.07 (2.28)	11.82 (1.56)	69
V72I+T122I	1.41 (0.86)	1.73 (1.12)	3.10 (1.74)	11.12 (1.47)	31
S119P+L74M	1.02 (0.62)	1.11 (0.72)	4.35 (2.44)	7.01 (0.93)	80
S119R+L74M	1.21 (0.74)	1.42 (0.92)	4.90 (2.75)	12.56 (1.66)	36

Site-Directed Mutant HIV-1	EC_{50}, nM (Fold-Change)[a]				RC, %WT[b]
	Compound				
	BIC	DTG	EVG	RAL	
S119R+G118R	AF	AF	AF	AF	0.11
S119R+F121Y	1.09 (0.72)	1.69 (1.07)	148.2 (74.0)	111.6 (14.0)	3.3
Multiple IN Mutants					
T97A+S119G+L74M	0.62 (0.41)	0.80 (0.51)	17.73 (8.89)	29.05 (3.61)	AF
T97A+S119P+L74M	0.80 (0.49)	0.95 (0.62)	29.51 (17.00)	33.07 (4.37)	58
T97A+S119R+L74M	1.02 (0.62)	1.22 (0.79)	31.61 (18.00)	31.42 (4.15)	28
T97A+S119R+G118R	0.77 (0.47)	0.96 (0.62)	7.35 (4.13)	19.60 (2.59)	61
T97A+S119T+L74M	0.69 (0.46)	0.79 (0.50)	15.51 (7.78)	25.52 (3.17)	92
T97A+V72I+L74M	0.82 (0.50)	0.92 (0.60)	8.70 (4.88)	24.78 (3.27)	36
T97A+V72I+T122I	AF	AF	AF	AF	0.13
T97A+S119R+V72I+L74M	0.90 (0.55)	1.43 (0.92)	46.57 (26.00)	36.37 (4.81)	22
S119R+V72I+L74M	1.25 (0.76)	1.37 (0.89)	7.13 (4.00)	14.32 (1.89)	31

AF = assay failure; DTG = dolutegravir; EVG = elvitegravir; RAL = raltegravir;
a Data shown represent the results of an independent experiment performed with replicate drug dilutions using the PhenoSense Integrase assay (Monogram Biosciences, South San Francisco, CA). Phenotypic fold change compared with wild-type control. Shaded cells represent a fold-change value ≥ the biological cutoff (EVG = 2.5; RAL = 1.5; BIC = 2.5) or clinical cutoff (DTG = 4.0) of each drug as defined in the Monogram PhenoSense Integrase assay.
b Replication capacity (RC) expressed as % of wild-type control.
Source: PC-141-2055

2.1.1.5.3. Activity of BIC Against Clinical Isolate HIV-1 Clones Containing INSTI Resistance Mutations

An additional study of the antiretroviral activity of BIC was conducted against 18 HIV-1 clonal variants containing integrase sequences from 12 EVG/COBI/FTC/TDF-treated patients from clinical trials GS-US-236-0102 and GS-US-236-0103 who had virologic failure and emergent NRTI and/or INSTI resistance mutations (m2.6.3, Section 1.1, PC-141-2050). Seventeen of 18 clones had INSTI resistance mutations and reduced susceptibility to EVG and RAL (Table 13). All 18 clones remained susceptible (< 2-fold change) to BIC and DTG with mean and median fold-change values of 1.04- and 1.17-fold for BIC, and 1.29- and 1.39-fold for DTG.

Table 13. Antiviral Activity of INSTIs Against HIV-1 IN Clinical Isolate Clones

Patient ID-Clone#	INSTI Resistance Mutations[a]	Susceptibility (Fold-change vs WT)[b]			
		BIC	DTG	RAL	EVG
7332-10	none	0.80	0.87	0.79	0.79
7476-5	T66I, E157Q	0.18	0.25	1.63	22
7476-9	T66I, T97A, E157Q	0.26	0.34	2.45	22
6503-10	E92Q	1.46	1.87	3.88	25
6041-11	E92Q	1.17	1.53	3.67	26
6648-11	E92Q	1.23	1.57	3.97	32
6322-1	N155H, G163R	1.03	1.37	15	35
7562-12	N155H	1.19	1.37	13	35
7425-11	E92Q	0.91	1.29	1.95	37
6545-7	N155H	1.51	1.61	15	41
6648-10	E92Q	1.16	1.60	4.2	42
6322-11	N155H	1.20	1.41	11	42
6648-7	E92Q	1.07	1.46	4.20	43
6667-1	E92Q	1.17	1.21	5.09	57
6101-15	E92Q	1.20	1.26	4.41	57
6101-14	N155H	0.98	1.48	6.56	60
6101-12	Q148R	0.74	0.76	32	123
7299-11	Q148R, G140C	1.52	1.97	24	>208

DTG = dolutegravir; EVG = elvitegravir; RAL = raltegravir

a Primary and other integrase strand transfer inhibitor resistant (INSTI-R) mutations are listed. Primary INSTI-R mutations are T66I/A/K, E92Q/G, T97A, Y143C/H/R, S147G, Q148H/K/R, N155H, and other INSTI-R mutations are H51Y, L68I/V, V72A/N/T, L74M, Q95K/R, F121C/Y, A128T, E138A/K, G140A/C/S, P145S, Q146I/K/L/P/R, V151L/A, S153A/F/Y, E157K/Q, G163K/R, E170A, and R263K in IN.

b Susceptibility was determined as the fold-change values versus NL4-3 wild-type vector by Monogram Biosciences, Inc. The wild-type virus had a mean EC_{50} of 1.55 nM for BIC.

Source: PC-141-2050.

2.1.1.5.4. Activity of BIC Against HIV-1 Clinically-Derived Viruses with INSTI Resistance

The antiretroviral activity of BIC was determined against 47 HIV-1 patient-derived isolates containing INSTI RAMs and phenotypic resistance to at least one approved INSTI. This set represented isolates from multiple patients and spanned single to triple INSTI RAMs. All isolates with INSTI resistance mutations had reduced susceptibility to EVG or RAL, and 24 isolates had reduced susceptibility to DTG (≥ 2.5-fold change versus [vs] wild type [WT]). The EC_{50} values for the wild-type control virus were 1.94 nM for BIC and 2.79 nM, 2.34 nM, and 7.06 nM for DTG, EVG, and RAL, respectively (m2.6.3, Section 1.1, PC-141-2051).

Of the 47 isolates tested, 32 were fully susceptible to BIC, 7 isolates had 2.5- to 5-fold reduced susceptibility, 6 isolates had 5- to 10-fold reduced susceptibility, and 1 isolate had > 10-fold reduced susceptibility to BIC (Table 14). The only isolate with > 10-fold reduced susceptibility to BIC had a 19-fold change for BIC, compared to the 63-fold change for DTG and >143-fold resistance to EVG and RAL. This isolate had a complex INSTI resistance pattern of E138K + G140A + Q148K and, notably, was the only isolate studied with a Q148K substitution. The phenotypic susceptibility of BIC for all isolates tested was statistically significantly improved over DTG (p = 0.042), EVG (p = < 0.001), and RAL (p = < 0.001).

All isolates with reduced susceptibility to DTG (≥ 2.5-fold change vs WT, n = 24) had numerically lower fold-change values for BIC. In these isolates, BIC showed a significantly improved resistance profile compared to DTG (p = 0.033), EVG (p = < 0.001), and RAL (p = < 0.001). The improved resistance profile of BIC compared to DTG was associated with the INSTI mutations at E92Q + N155H or G140C/S + Q148R/H/K ± additional INSTI mutations.

Table 14. Antiviral Activity of BIC and other INSTIs Against HIV-1 Patient-derived Isolates with INSTI Resistance Mutations

INSTI Resistance Mutations[a]	Susceptibility (Fold-change vs. WT)[b]			
	BIC	DTG	EVG	RAL
E92Q,E157E/Q	1.16	1.41	51	4.80
E92Q	1.19	1.58	60	18
E92Q	1.30	1.73	61	6.70
L74M,T97A	0.50	0.64	16	8.48
T97A	0.66	0.88	10	1.78
T97A,F121Y	0.80	1.63	>150	112
L74I,F121Y	0.84	1.05	38	12
N155H,E157E/Q	1.23	1.66	28	19
N155H,G163R	1.70	1.95	31	15
L68V,Y143C	0.54	0.54	1.90	4.06
L68L/V,L74M,Y143R	0.59	0.74	26	>143
Y143R	1.39	1.50	2.26	22
Y143R	1.39	1.40	2.19	16
Y143C	1.49	1.76	4.24	14
Q148R,E138A	1.69	2.17	>150	43
E138K,Q148R	1.80	2.05	>150	54
T97A,Y143R	0.83	1.11	20	>143
T97A,Y143C	1.02	1.35	29	>143
T97A,Y143C	1.60	1.47	42	>143
L74M,N155H	0.90	1.08	103	89
T97A,N155H	0.99	1.51	95	53

INSTI Resistance Mutations[a]	Susceptibility (Fold-change vs. WT)[b]			
	BIC	DTG	EVG	RAL
N155H	1.42	2.07	>150	107
G140A,Q148R	2.03	2.22	>150	88
E92Q,N155H	1.72	3.49	>150	>143
E92Q,N155H,G163R	2.02	4.12	>150	>143
G140S,Q148H	1.99	3.60	>150	>143
G140S,Q148H	2.12	3.44	>150	>143
G140S, Q148H	2.17	4.00	>150	>143
G140S,Q148H	2.46	4.73	>150	>143
G140S,Q148H	2.03	3.52	>150	>143
E138K,G140S,Q148H	2.42	3.59	>150	>143
G140S,Q148H, G163K	2.48	5.68	>150	>143
G140S,Q148H	2.49	5.56	>150	>143
G140S,Q148H	2.92	5.46	>150	>143
G140S,Q148R	3.01	6.15	>150	>143
E138K,G140S,Q148H	2.52	5.34	>150	>143
E138K G140S Q148H	2.62	13	>141	>114
G140S,Q148H	3.81	11	>150	>143
G140S,Q148H	4.37	13	>150	>143
T97A,G140S,Q148H	4.39	15	>150	>143
E138K,G140C,Q148R	5.32	8.58	>150	>143
L74L/M,G140A,Q148R	5.38	8.81	>150	>143
L74M,G140C,Q148R	8.36	9.06	>150	>143
G140S,Q148R	7.05	17	>150	>143
G140S,Q148H,E138A	7.23	10	>150	>143
T97A,G140S,Q148H	7.62	14	>150	>143
E138K,G140A,Q148K	19	63	>150	>143

a Primary and other integrase strand transfer inhibitor resistance (INSTI-R) mutations are listed. Primary INSTI-R mutations are T66I/A/K, E92Q/G, T97A, Y143C/H/R, S147G, Q148H/K/R, N155H, and other INSTI-R mutations are H51Y, L68I/V, V72A/N/T, L74M, Q95K/R, F121C/Y, A128T, E138A/K, G140A/C/S, P145S, Q146I/K/L/P/R, V151L/A, S153A/F/Y, E157K/Q, G163K/R, E170A, and R263K in IN.

b Susceptibility was determined as the fold-change in EC_{50} versus NL4-3 wild-type vector by Monogram Biosciences, Inc. The biological or lower clinical cut-offs for reduced susceptibility in this assay are 4.0 for DTG, 1.5 for RAL, and 2.5 for EVG. No cut-off has been determined for BIC, but 2.5 has been assumed in the absence of clinical data. Fold-change values greater than or equal to the cutoffs have been shaded grey.

Source: PC-141-2051.

2.1.1.5.5. Activity of BIC Against Other Drug Resistant Mutants of HIV-1

The antiviral activity of BIC was also determined against a panel of known HIV-1 mutants conferring resistance to NRTIs, NNRTIs and/or PIs (m2.6.3, Section 1.1, PC-141-2039). Similar to DTG and EVG, BIC is fully active against all tested NRTI, NNRTI and PI resistant mutants (Table 15 – Table 17, inclusively). These results indicate that BIC has a strong potential to be effectively used to treat HIV-1 infections with virus variants resistant to other classes of antiretrovirals.

Table 15. Activity of BIC Against NRTI-Resistant HIV-1 Mutants

	EC_{50} (nM)[b]	EC_{50} Fold-Change Relative to WT[b]		
Compounds[a]	**WT**	**K65R[c]**	**M184V[c]**	**6TAMs[c,d]**
BIC	1.4	1.4	1.4	1.4
DTG	1.0	1.5	1.6	1.5
EVG	2.7	1.7	1.5	1.2
FTC	385	21.5	>300	10.8
TFV	3716	4.6	1.4	7.1

a DTG = dolutegravir, EVG = elvitegravir, FTC = emtricitabine, TFV = tenofovir.
b The data represent the mean of 3 independent experiments performed in triplicate.
c HIV-1 reverse transcriptase (RT) mutations.
d 6TAMs = Six thymidine associated mutations: M41L, D67N, K70R, L210W, T215F, K219Q.
Fold-change values ≥ 2.5 to < 10 are shown in gray and fold-change values > 10 are shown in black shading.
Source: PC-141-2039.

Table 16. Activity of BIC Against NNRTI-Resistant HIV-1 Mutants

	EC_{50} (nM)[b]	EC_{50} Fold-Change Relative to WT[b]				
Compound[a]	**WT**	**K103N[c]**	**Y181C[c]**	**Y188L[c]**	**L100I/K103N[c]**	**K103N/Y181C[c]**
BIC	1.8	0.8	1.2	0.9	1.0	1.2
DTG	1.7	0.8	1.4	0.9	1.1	1.4
EVG	2.0	1.2	1.2	1.3	1.1	1.1
RPV	0.8	1.5	5.6	24.5	21.9	9.1
EFV	1.2	46	3.6	>83	>83	>83

a DTG = dolutegravir, EVG = elvitegravir, RPV = rilpivirine, EFV = efavirenz.
b The data represent the mean of 3 independent experiments performed in triplicate.
c HIV-1 reverse transcriptase (RT) mutations.
Fold-change values ≥ 2.5 to < 10 are shown in gray and fold-change values > 10 are shown in black shading.
Source: PC-141-2039.

Table 17. Activity of BIC Against PI-Resistant HIV-1 Mutants

Compound[a]	EC_{50} (nM)[b]	EC_{50} Fold-Change Relative to WT[b]			
	WT	I50V[c]	I84V/L90M[c]	I54V/V82S[c]	G48V/V82A/L90M[c]
BIC	1.9	1.9	1.5	1.1	1.3
DTG	2.2	1.4	1.2	1.0	1.0
EVG	2.7	1.4	1.0	0.9	1.0
DRV	3.5	40	3.1	0.4	0.5
ATV	1.6	4.9	114	55	30

a DTG = dolutegravir, EVG = elvitegravir, DRV = darunavir, ATV = atazanavir.
b The data represent the mean of 3 independent experiments performed in triplicate.
c HIV-1 protease (PR) mutations.
Fold-change values ≥ 2.5 to < 10 are shown in gray and fold-change values > 10 are shown in black shading.
Source: PC-141-2039.

2.1.1.5.6. Viral Resistance Selection Studies with BIC

HIV-1 resistance breakthrough and dose escalation resistance selections for BIC were conducted. Overall, BIC and DTG had high barriers to resistance, both of which were higher than EVG. Two pathways for resistance to BIC were observed: 1) M50I and R263K IN substitutions with a 2.9-fold reduced susceptibility to BIC, and 2) T66I and S153F IN substitutions with 0.4 and 1.9-fold reduced susceptibility to BIC, respectively.

Resistant virus breakthrough experiments with BIC were performed in both MT-2 cells and primary human $CD4_+$ T-cells, with HIV-1 IIIb and BaL respectively, and showed no viral breakthrough over a period of up to 35 days in the presence of the estimated tissue culture equivalent of the BIC clinical C_{min} concentration of 138 nM (m2.6.3, Section 1.1, PC-141-2052). FTC, EVG and DTG served as experimental comparative controls (Figure 1) and similar results were obtained with DTG. In contrast, HIV-1 started breaking through in the presence of FTC (used at 50 × EC_{95}) and EVG (used at 5 × EC_{95}) as early as Days 7 and 22 post-infection, respectively, and included known resistance mutations. This comparative analysis suggests that BIC has a barrier to resistance emergence *in vitro* similar to DTG but has a higher barrier to *in vitro* resistance emergence relative to either FTC or EVG.

Figure 1. BIC Breakthrough Resistance Selection with HIV-1-(IIIb in MT-2 Cells)

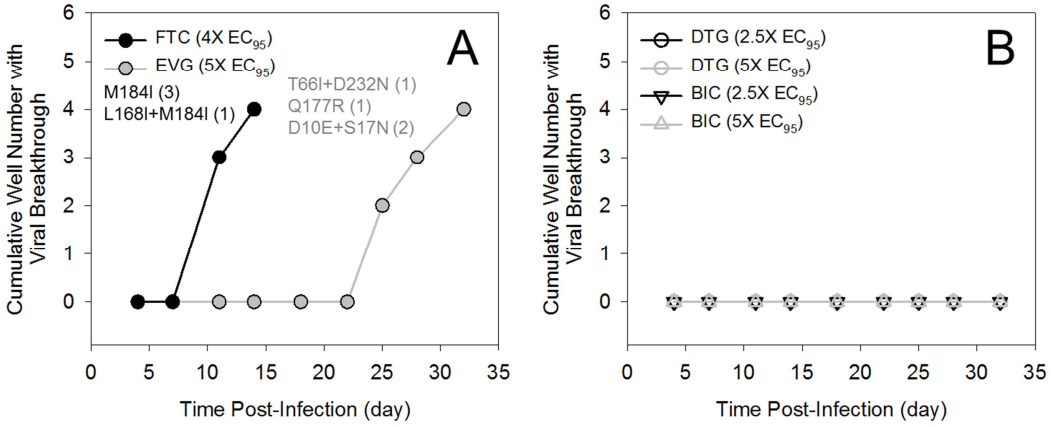

In vitro resistance selections for BIC were also performed using the dose escalation method in the MT-2 T cell line infected with HIV-1 (IIIb and xxLAI). Comparative parallel selections were conducted with other INSTIs under the same conditions (m2.6.3, Section 1.1, PC-141-2041, PC-141-2052, and PC-141-2056). Resistance selections in the presence of BIC progressed at rates that were similar to DTG and considerably slower than that of EVG or RAL, suggesting that BIC has a higher genetic barrier to resistance emergence than EVG and RAL (Figure 2 and Figure 3).

Figure 2. Progress of BIC Resistance Selection with HIV-1 (IIIb)

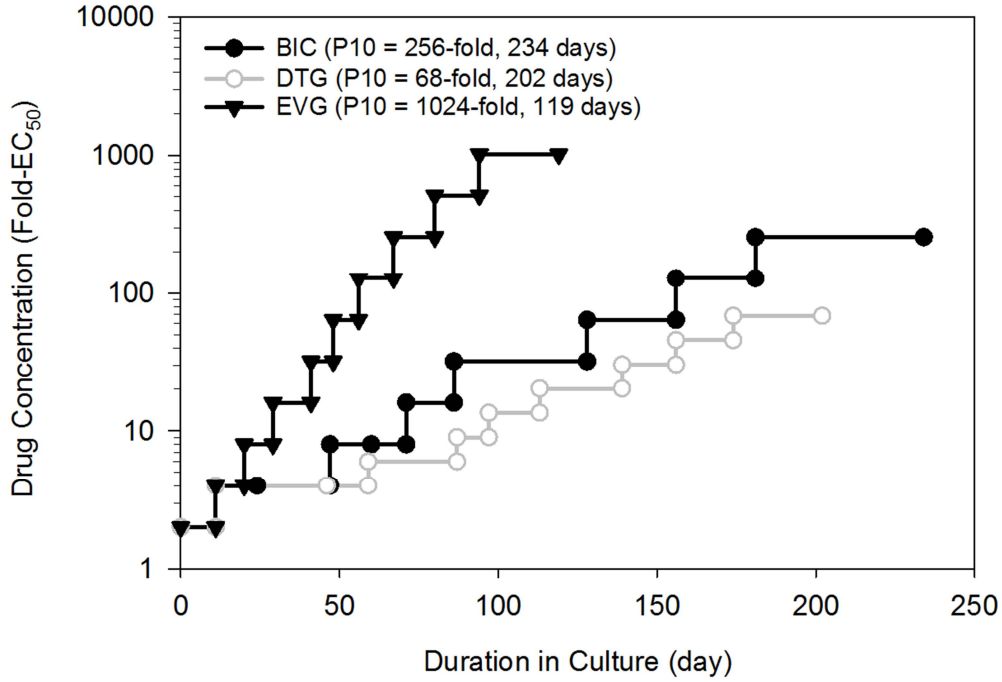

Source: PC-141-2052

Figure 3. Progress of BIC Resistance Selection with HIV-1 (xxLAI)

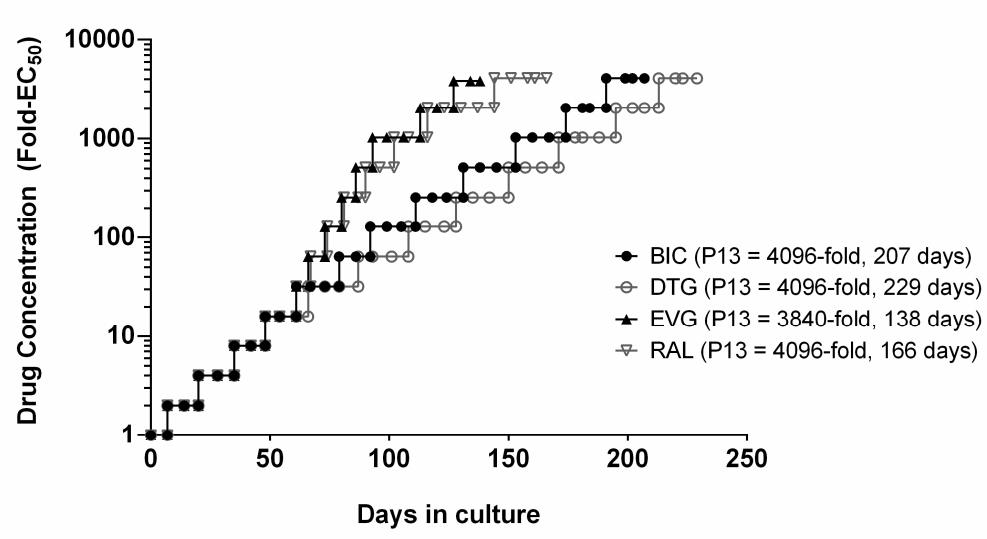

Source: PC-141-2056

The HIV-1 IIIb selections were analyzed by population sequencing and the xxLAI selections were analyzed by population and more sensitive next generation sequencing (deep sequencing) (Table 18). The HIV-1 IIIb selection with BIC resulted in IN mutations R263K and M50I that successively emerged at passage 5 (P5) and P8, respectively. For the BIC HIV-1 xxLAI selection, a transient T66I and S153F developed at P6, with the final variant exhibiting exclusively S153F at P13. The R263K mutation is a natural polymorphism of HIV-1 integrase {Lataillade 2007} that was first reported to be enriched during *in vitro* selection with EVG {Margot 2012}. It was also selected *in vitro* using DTG, conferring low-level of reduced susceptibility to DTG {Quashie 2012}. The R263K frequency in treatment-naive HIV-infected patients is extremely low, only reaching approximately 0.4% of the analyzed patient population {Lataillade 2007}. The M50I mutation is also a natural polymorphism of HIV-1 integrase {Lataillade 2007} and emerged after R263K in previous *in vitro* selection with DTG {Quashie 2012} but has not been observed in patients treated with the first-line regimen containing DTG. T66I is a primary INSTI resistance substitution selected in vitro and in vivo by EVG {McColl 2010}. S153F and S153Y are secondary INSTI resistance substitutions that are not usually observed clinically but have previously emerged in vitro under DTG and EVG or EVG-metabolite selective pressure {Kobayashi 2011}, {Margot 2012}.

The selection experiments with EVG resulted in the successive emergence of R263K and T66I in P4 and P7, respectively, for IIIb and T66I at P4 followed by T66I, Q146L, Q148R, and Q148K at P10 to P13 for xxLAI. These EVG selected mutations are all consistent with previously published studies {Margot 2012}. The RAL selection resulted in T66K at P4 followed by T66K and Q148K, with the final passage containing exclusively Q148K. These RAL selected mutations are all consistent with previously published studies {McColl 2010}. The DTG selection had no substitutions at P4, S153Y and R263K at P6 through the final passage P13.

Table 18. Genotypic Profile of BIC and other INSTI Selected Viral Passages

Selected Virus	IN Mutations[a]	Note[b]
HIV-1 IIIB Selection		
No Drug P8	None	
No Drug P16	None	
BIC P3	R263R/K	Mixture of R and K present at position 263
BIC P5	R263K	R263K is a natural polymorphism associated with INSTI resistance occurring at a frequency of 0.4%. M50I is a natural polymorphism occurring at a frequency of 6.2%
BIC P6	R263K	
BIC P8	R263K, M50I	
BIC P9	R263K, M50I	
BIC P10	R263K, M50I	
DTG P3 low	None	S153Y is a natural integrase polymorphism at a frequency of 0.4% associated with integrase resistance
DTG P4	S153Y, R263R/K	Mixture of R and K at position 263
DTG P5	S153S/Y, R263K	Mixture of S and Y at position 153
DTG P7	S153S/Y, R263R/K	Mixture of S and Y at position 153 and mixture of R and K at position 263
DTG P9	S119R, R263R/K	S119R is a natural integrase polymorphism at a frequency of 6.2% associated with T97A conferring reduced susceptibility to EVG and RAL but not DTG
DTG P10	M50I, S119R, R263K	M50I is a natural polymorphism occurring at a frequency of 6.2%
EVG P2	D10D/E, S17S/N, R263R/K	Mixture of (D and E), (S and N) and (R and K) present at positions 10, 17 and 263, respectively.
EVG P4	D10E, S17N, R263K	R263K is a natural polymorphism associated with INSTI resistance occurring at a frequency of 0.4% D10E (89%) and S17N (21%) are natural polymorphisms
EVG P6	D10E, S17N, T66T/I, R263K	Mixture of T and I present at position 66.
EVG P7	D10E, S17N, T66I, R263K	R263K is a natural polymorphism associated with INSTI resistance D10E (89%) and S17N (21%) are natural polymorphisms
EVG P9	D10E, S17N, T66I, R263K	
EVG P10	D10E, S17N, T66I, R263K	
HIV-1 xxLAI Selection[c]		
No Drug P34	(V31I, A21T, V151I, M154I, G163E)	V31I, A21T, V151I, M154I, and G163E are natural polymorphisms
BIC P4	None	
BIC P6	T66I, S153F	T66I is a primary INSTI resistance substitution S153F and Y have been selected in vitro by DTG
BIC P8-P9	T66I, S153F (E152K, M154I, E157K)	T66I is a primary INSTI resistance substitution S153F and Y have been selected in vitro by DTG E152K and M154I are natural polymorphisms E157K is a secondary INSTI resistance substitution
BIC P10-P12	S153F (S24G, M154I, E157K)	S24G is a natural polymorphism
BIC P13	S153F (S24G, M154I)	S153F and Y have been selected in vitro by DTG
DTG P4	None	
DTG P6	S153Y (A124T)	A124T is a natural polymorphism

Selected Virus	IN Mutations[a]	Note[b]
DTG P8-P12	S153Y (L234F, M154I)	S153F and Y have been selected in vitro by DTG are natural polymorphisms
DTG P13	S153Y (L234F, M154I, G237R, M275I)	S153F and Y have been selected in vitro by DTG M154I, L234F, G237R, and M275I are natural polymorphisms
EVG P4-P6	T66I	T66I is a primary INSTI resistance substitution
EVG P8-P9	T66I, Q146L, Q148R (E92V)	T66I is a primary INSTI resistance substitution E92V reduced susceptibility EVG Q146L is a secondary INSTI resistance substitution Q148R is a primary INSTI resistance substitution
EVG P10-P13	T66I, Q146L, Q148R (E92V, E138K)	T66I is a primary INSTI resistance substitution E92V reduced susceptibility EVG E138K is a secondary INSTI resistance substitution Q146L is a secondary INSTI resistance substitution Q148R is a primary INSTI resistance substitution
RAL P4	T66K	T66K is a primary INSTI resistance substitution
RAL P6-P9	T66K, Q148K	T66K is a primary INSTI resistance substitution
RAL P10-P12	Q148K	Q148K is a primary INSTI resistance substitution
RAL P13	Q148K (E138K, G118D, I84T, M154I, D235E)	Q148K is a primary INSTI resistance substitution E138K is a secondary INSTI resistance substitution

PX = passage X
a Relative to HIV-1 IIIb or xxLAI consensus sequence corresponding to the starting HIV-1 strain used
b Natural polymorphism frequencies are calculated from {Lataillade 2007}.
c Primary INSTI mutations are listed with secondary mutations or other substitutions shown in parentheses
Source: PC-141-2041 and PC-141-2056

The viruses selected with BIC from IIIb P3 to P9 displayed gradually increasing resistance to BIC with the final isolated variant exhibiting a 9.2-fold reduced susceptibility (Table 19). The variants isolated during the selection with BIC exhibited similarly low- to medium-level cross-resistance to RAL and DTG (up to 9.2-fold), but somewhat higher level of cross-resistance to EVG (up to 34.3-fold). All BIC selected HIV-1 variants remained fully sensitive to EFV. In contrast, the viruses selected with EVG displayed a much greater and faster increase in resistance against EVG from P2 to P10, reaching up to 123-fold resistance at the end of the selection (Table 19). Notably, variants with high-level resistance to EVG (123- to 131-fold) were only mildly cross-resistant to BIC and DTG (1.4 – 4.3-fold).

Table 19. Phenotypic Profile of BIC and other INSTI Selected Viral Passages from the HIV-1 IIIb selections

Selected Virus	Duration of Selection (days)	Drug Conc. Reached (nM)	EC_{50} (nM) (Fold-Resistance Change Relative to WT)[a]				
			BIC	DTG	EVG	RAL	EFV
HIV-1 IIIb	—	—	2.3 (1)	2.6 (1)	2.1 (1)	9.1 (1)	1.8 (1)
BIC P3	47	6	4.4 (1.9)	3.6 (1.4)	6.1 (2.9)	23.2 (2.6)	1.8 (1.0)
BIC P5	71	12	6.6 (2.8)	6.5 (2.5)	8.3 (3.9)	21.8 (2.4)	1.6 (0.9)
BIC P6	86	24	8.4 (3.6)	8.2 (3.2)	7.3 (3.4)	27.4 (3.0)	1.7 (1.0)
BIC P8	156	96	14.3 (6.1)	14.0 (5.4)	45.0 (21.2)	36.5 (4.0)	2.0 (1.1)
BIC P9	181	192	21.3 (9.2)	22.4 (8.6)	72.9 (34.3)	49.9 (5.5)	3.6 (2.0)
EVG P2	20	7.2	6.8 (2.9)	6.0 (2.3)	20.4 (9.6)	26.7 (2.9)	3.4 (1.9)
EVG P4	41	28.8	6.2 (2.7)	6.9 (2.7)	30.8 (14.5)	30.7 (3.4)	3.2 (1.8)
EVG P6	56	115	7.4 (3.2)	7.8 (3.0)	66.6 (31.3)	24.8 (2.7)	3.0 (1.7)
EVG P7	67	230	10.0 (4.3)	8.6 (3.3)	264 (124)	33.7 (3.7)	4.7 (2.6)
EVG P9	94	922	7.6 (3.3)	7.2 (2.8)	280 (131)	55.2 (6.1)	3.7 (2.1)
EVG P10	119	1843	3.2 (1.4)	3.6 (1.4)	262 (123)	19.8 (2.2)	2.4 (1.3)

a The fold-change is calculated from the ratio of EC_{50} of the selected virus over the EC_{50} of HIV-1 IIIb. The values represent the mean of at least two experiments performed in triplicate.

Source: PC-141-2041

The susceptibility of the IN mutations selected in IIIb and xxLAI were evaluated as recombinant site-directed mutants (Table 20 and Table 21). BIC selected IIIb virus with M50I and R263K. The R263K substitution alone shifted the BIC and DTG EC_{50} values by only ~2-fold, and similarly shifted the EVG EC_{50} by 3.8-fold, but did not alter the susceptibility to RAL. The M50I substitution alone does not confer any resistance to BIC or the other INSTIs tested. Virus with the double mutations M50I+R263K was slightly less susceptible to BIC and EVG (2.9-fold and 5.1-fold, respectively) and showed about 2-fold reduced susceptibility to DTG but not RAL.

The S153F and S153Y substitutions, selected by BIC and DTG, respectively, caused 1.6- to 2.5-fold increases in the EC_{50} values of BIC, DTG, and EVG but no change in RAL susceptibility. The T66I substitution, identified transiently in the BIC selection and as a predominant subpopulation in the EVG selection, shifted only the EVG EC_{50} value higher (9.2-fold) and was fully sensitive to BIC and DTG (EC_{50} value changes of 0.4-fold). The T66I/S153F double mutant was also fully susceptible to BIC and DTG (EC_{50} value changes of 0.5-fold). In contrast, the T66I/S153F mutant showed increased resistance to EVG (33-fold) relative to T66I alone (9.2-fold) or S153F alone (2.1-fold). The T66I and S153F substitutions, alone or in combination, did not alter the EC_{50} to RAL (1.0- to 1.3-fold shifts). The addition of L234F to S153Y, representing the final genotype from the DTG selection, did not significantly affect the EC_{50} values for BIC, DTG, RAL, or EVG (1.2- to 3.8- fold shifts). The L234F substitution alone was fully susceptible to all INSTIs tested. The E138K substitution, which developed late in the EVG and RAL selections, alone did not confer resistance to any of the

INSTIs tested. The Q148K and Q148R substitutions, observed as predominant variants in the EVG and RAL selections, each greatly reduce susceptibility to EVG (76- and 92-fold, respectively) and RAL (38- and 28-fold, respectively) but did not affect susceptibility to BIC and DTG. The virus with a combination of T66I, E138K, and Q148K substitutions, potentially present together in the final population from the EVG selection, had high level resistance to all INSTIs (≥26-fold). The EVG-selected triple mutant T66I + E138K + Q148K showed high-level resistance to all INSTIs, with 44-fold change in EC_{50} to BIC. The genotype/phenotype of this mutant was consistent with data from the patient-derived isolate study where E138K + G140A + Q148K showed 19-fold change in EC_{50} to BIC.

Table 20. Phenotypic Profile of Selected IN Mutations from the IIIb Selections to BIC

Virus Genotype	Selection Observed	EC_{50} (nM) (Fold-Resistance Change Relative to WT)[a]			
		BIC	DTG	EVG	RAL
WT	—	1.44 (1.0)	1.70 (1.0)	1.43 (1.0)	6.70 (1.0)
M50I	BIC	1.92 (1.3)	1.99 (1.2)	1.99 (1.4)	7.26 (1.1)
R263K	BIC	3.1 (2.1)	3.62 (2.1)	5.37 (3.8)	7.64 (1.2)
M50I + R263K	BIC	4.12 (2.9)	3.55 (2.1)	7.34 (5.1)	7.55 (1.2)

a EC_{50} and fold-change in EC_{50} represents the mean of at least 3 independent determination in triplicate. Color coding: grey = FC ≥2.5,.
Source: PC-141-2052

Table 21. Phenotypic Profile of Selected IN Mutations from the xxLAI Selections to BIC

Virus Genotype	Selection Observed	EC_{50} (nM) (Fold-Resistance Change Relative to WT)[a]			
		BIC	DTG	EVG	RAL
T66I	BIC, EVG	1.34 (0.4)	1.42 (0.4)	26 (9.2)	6.98 (1.3)
S153F	BIC	3.85 (1.9)	2.93 (1.6)	6.83 (2.1)	12.9 (1.0)
T66I + S153F	BIC	1.66 (0.5)	1.62 (0.5)	92 (33)	5.39 (1.2)
S513Y	DTG	6.47 (1.9)	5.19 (1.7)	6.92 (2.5)	7.23 (1.3)
L234F	DTG	3.30 (1.0)	3.20 (1.0)	4.12 (1.5)	5.85 (1.0)
S153Y + L234F	DTG	6.22 (1.9)	5.37 (1.6)	10.8 (3.8)	6.95 (1.2)
E138K	EVG, RAL	1.88 (0.9)	1.66 (0.9)	2.88 (0.9)	9.25 (0.7)
Q148K	EVG, RAL	2.24 (0.7)	1.89 (0.6)	214 (76)	213 (38)
T66I + E138K + Q148K	EVG	144 (44)	87 (26)	>350 (>125)	>1000 (>179)
Q148R	EVG	1.39 (0.7)	1.21 (0.6)	308 (92)	375 (28)

a Data from single-cycle HIV-1 assay (PhenoSense IN, Monogram Biosciences) using resistance test vectors with HXB2 IN from site-directed mutants cloned into the NL4-3 plasmid. Fold-change values are calculated from the intra-assay EC_{50} values of the HXB2 wild-type IN tested in parallel. Average wild-type EC_{50} values were 2.67 nM for BIC, 2.58 nM for DTG, 3.07 nM for EVG, and 9.49 nM for RAL. Color coding: grey = FC ≥2.5 to 10.0, black = FC >10.0.
Source: PC-141-2052 and PC-141-2056

2.1.2. FTC

Emtricitabine is a synthetic analogue of the naturally occurring pyrimidine nucleoside, 2′-deoxycytidine. Intracellularly, FTC is converted through 3 phosphorylation reactions to its active tri-phosphorylated anabolite FTC-TP {Paff 1994}, {Furman 1992}. Emtricitabine triphosphate inhibits viral polymerases by direct binding competition with the natural deoxyribonucleotide substrate (dCTP), and after incorporation into DNA, by DNA chain termination {Wilson 1993}. The EC_{50} of FTC against laboratory adapted strains of HIV-1 ranged from 0.001 to 0.62 µM depending on cell type and virus strain used in the assay {Schinazi 1992}, {Painter 1995}, {Jeong 1993}. With clinical isolates of HIV-1, EC_{50} values ranged from 0.002 to 0.028 µM {Schinazi 1992}.

2.1.2.1. Intracellular Metabolism of FTC

In Vitro

FTC is efficiently phosphorylated in HepG2 cells to the corresponding 5′-monophosphate, 5′-diphosphate, and 5′-triphosphate. A time course showed that the 5’-phosphorylated metabolites of FTC were formed rapidly and reached a steady-state intracellular concentration by 3 to 6 hours {Paff 1994}. The intracellular concentrations of the 5′-phosphorylated forms produced as a function of the extracellular FTC concentration are presented in Figure 4. The concentrations of these derivatives increase in a linear manner indicating that the anabolic pathway is not saturated over the concentration range tested. The concentration of FTC 5′-diphosphate was somewhat higher than those of the 5′-monophosphate and 5′-triphosphate derivatives {Furman 1992}, {Paff 1994}.

In studies to determine which enzymes were responsible for phosphorylating FTC to the 5′-triphosphate, 2′-deoxycytidine kinase was identified as the enzyme that catalyzes the phosphorylation of FTC to the corresponding 5′-monophosphate. An apparent Michaelis-Menton constant (K_m) value of 11.8 µM and an apparent relative maximum velocity (V_{max}) of 9.3 $nmol \cdot mL^{-1} \cdot h^{-1}$ was determined when uridine triphosphate (UTP) was the phosphate donor. When adenosine triphosphate (ATP) was the phosphate donor, an apparent K_m value of 7.4 µM and an apparent relative V_{max} of 3.8 $nmol \cdot mL^{-1} \cdot h^{-1}$ was obtained {Shewach 1993}. Using calf thymus 2′-deoxycytidine kinase, the relative rate of phosphorylation was 3.4% of that measured for 2′-deoxyguanosine and 40% of that observed for 2′-deoxycytidine (m2.6.3, Section 1.2, TESF/91/0014 and TESF/92/0002). Phosphorylation of the 5′-monophosphate was catalyzed by 2′-deoxycytidine monophosphate kinase {Furman 1992}, {Furman 1995}. The efficiency with which the enzyme purified from calf thymus phosphorylated the 5′-monophosphate of FTC was approximately 32% of that observed when using the natural substrate, 2′-deoxycytidine 5′-monophosphate (m2.6.3, Section 1.2, TEIT/92/0005). FTC 5′-monophosphate can also be phosphorylated by nucleoside monophosphate kinase purified from beef liver. However, the phosphorylation catalyzed by this enzyme is relatively inefficient. The formation of the 5′-triphosphate of FTC from the 5′-diphosphate has been proposed to be catalyzed by nucleoside diphosphate kinase {Furman 1992}, a cytosolic enzyme with a broad specificity for nucleoside 5′-diphosphates (m2.6.3, Section 1.2, TGZZ/93/0025). However, Cheng and colleagues have suggested that L-nucleoside 5′-diphosphates cannot be utilized as substrates by nucleoside diphosphate kinases and are selectively phosphorylated by 3-phosphoglyceride kinase {Cheng 2001}.

The metabolism of FTC was studied in HepG2.2.2.15 human hepatocellular carcinoma cells (m2.6.3, Section 1.2, TEZA/92/0062) and CEM human T-lymphoblasts (m2.6.3, Section 1.2, TEZA/92/0103). Both cell lines anabolize FTC to the 5'triphsophate, the intracellular form of the compound having antiviral activity. The intracellular $t_{1/2}$ of the triphosphate in these cells ranged from 2 to 5 hours.

The anabolism of FTC was evaluated as a function of time and drug concentration in HepG2.2.2.15 and CEM cells. The intracellular concentrations of the monophosphate, diphosphate, and triphosphate of FTC increased in a concentration-dependent manner and reached their maximum levels by 4 hours postdose (Figure 4) (m2.6.3, Section 1.2, TEZA/92/0062). Two other metabolites were observed, although at much lower concentrations than the monophosphate, diphosphate, and triphosphate. A study was performed to determine the intracellular metabolism of FTC in normal HepG2 cells and to compare it to that in HBV-infected HepG2.2.2.15 and P5A cells (m2.6.3, Section 1.2, TEZA/92/0111). The metabolites were identified as FTC-diphosphoethanolamine and FTC-diphosphocholine.

Figure 4. Intracellular Levels of FTC-TP as a Function of Extracellular FTC Concentration in HepG2 Cells

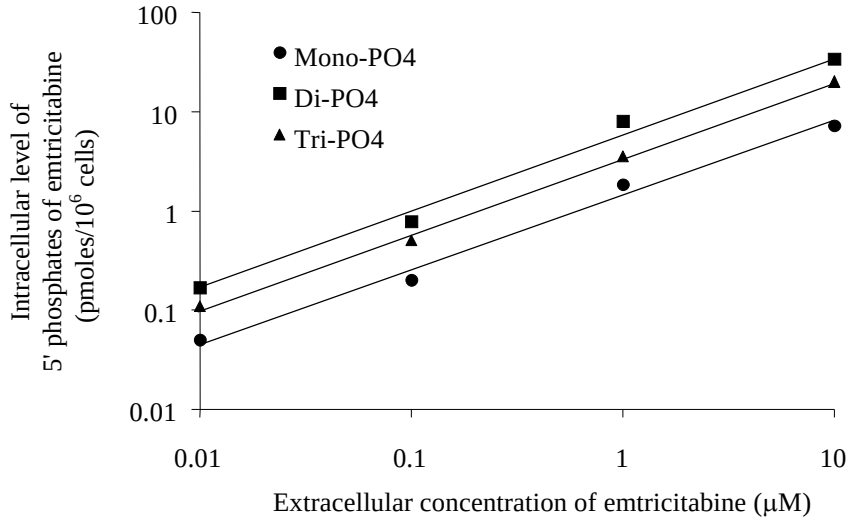

FTC-TP = emtricitabine 5′-triphosphate; PO_4 = phosphate
Source: {Paff 1994}

In Vivo

The $t_{1/2}$ for FTC-TP has been determined directly in PBMCs, taken from healthy subjects dosed orally with 200 mg of FTC once daily. The in vivo $t_{1/2}$ value was found to be approximately 39 hours (FTC-106). The long intracellular $t_{1/2}$ supports once daily dosing.

2.1.2.2. Antiviral Activity of FTC

2.1.2.2.1. Antiviral Activity of FTC in T-Cell Lines and Primary Cells

The ability of FTC to inhibit replication of HIV-1 and HIV-2 in cell culture has been studied extensively using various human T-lymphoid cell lines (MT-2, MT-4, CEM, and HT4-6C) and PBMCs infected with laboratory-adapted strains of HIV-1 (IIIB, LAI, or LAV) and HIV-2 (ZY, ROD2). The results are summarized in Table 22. Several investigators have compared directly the anti-HIV activity of FTC with that of lamivudine (3TC) in the same assay. The results are summarized in Table 23. Although different laboratory strains of virus, different cell types, and different assay methods were used, FTC consistently showed greater activity than 3TC with the activity advantage ranging from 3- to 11-fold.

Table 22. Inhibitory Effect of FTC on the Replication of Laboratory Strains of HIV-1 and HIV-2

Virus	Cell Type	Assay	EC_{50} (μM)
$HIV\text{-}1_{IIIB}$	CEM	RT	0.1[a,b]
	MT-4	cytoprotection	0.5[a,b]
	PBMC	RT	0.01[b]
$HIV\text{-}1_{LAV}$	CEM	RT	0.009[a]
	HT4-6C	RT	0.02[a]
	PBMC	p24	0.009[b]
	PBMC	RT	0.001[d]
$HIV\text{-}1_{LAI}$	CEM	cytoprotection	0.04[c]
	MT-2	cytoprotection	0.62[c]
	PBMC	p24	0.03[c]
	PBMC	p24	0.0014[e]
$HIV\text{-}2_{ZY}$	MT-4	RT	1.5[a]
	CEM	RT	0.1[a]
$HIV\text{-}2_{ROD2}$	PBMC	p24	0.007[b]

EC_{50} = concentration inhibiting viral replication by 50%; PBMC = peripheral blood mononuclear cell; RT = reverse transcriptase
a Source: {Schinazi 1992}
b Source: {Painter 1995}
c Source: TPI 462 v2
d Source: {Jeong 1993}
e Source: TPI 10498 v2

Table 23. Comparison of the Antiviral Activities of FTC and 3TC Against Various Laboratory Strains of HIV-1

HIV-1 Strain	Cell Line	EC_{50} (μM)		Activity Ratio[d]
		FTC	3TC	
LAI[a]	PBMC	0.018	0.19	11
IIIB[b]	PBMC	0.01	0.07	7
IIIB[b]	MT-4	0.5	3.2	6
LAI[a]	MT-2	0.3	1.6	5
HXB2[b]	MT-4	0.09	0.24	3
LAI[c]	CD4+ HeLa	0.06	0.18	4

a Source: TPI 10498 v2
b Source: {Schinazi 1992}
c Source: {Tisdale 1993}
d Ratio of 3TC to FTC EC_{50} values

The potency of FTC has also been determined using a coculture assay of PBMCs from HIV-1 positive donors and HIV-1 negative freshly isolated PBMCs {Mathez 1993} and compared directly to the potencies of 3TC, zalcitabine (ddC), didanosine (ddI), zidovudine (ZDV), and the NNRTI tetrahydro-imidazo-benzodiazepine-one (TIBO) compound R82913. At the end of the coculture period, viral replication was estimated by HIV-1 p24 enzyme-linked immunosorbent assay (ELISA). Results from this study expressed as mean EC_{50}, EC_{90}, and EC_{99} values are given in Table 24. A potency ranking (based on EC_{90} values) showed FTC to be the most potent compound. The low potency ranking for ZDV compared with that observed in laboratory strains may be the result of inclusion of PBMCs from ZDV-experienced patients in the coculture.

Table 24. Comparative Potency of RT Inhibitors in HIV-1 Infected PBMCs Using a Coculture Method

Inhibitor	EC_{50} (μM)	EC_{90} (μM)	EC_{99} (μM)
FTC	0.0085	0.055	0.43
3TC	0.11	0.3	0.85
ddC	0.011	0.074	0.6
ddI	0.76	6.4	65.8
ZDV	0.055	0.53	6.4
TIBO R82913	0.17	0.67	2.95

Source: {Mathez 1993}

2.1.2.2.2. Antiviral Activity of FTC Against HIV Clinical Isolates

Schinazi and colleagues tested 2 low passage HIV-1 clinical isolates, J6 and 2:DR2, in phytohemagglutinin (PHA)-stimulated PBMCs isolated from uninfected donors for FTC activity {Schinazi 1992}. The EC_{50} values were similar to those determined using laboratory strains of

virus in PBMCs (Table 25). The sensitivities to FTC reported for 2 additional wild-type clinical isolates, WT-pre-ZDV and WT-MKC09-day 29, were similar to those determined against J6 and 2:DR2 (m2.6.3, Section 1.2, TPI 462 v2). In the single experiment in which a direct comparison was made between the activity of FTC and 3TC, FTC demonstrated the same 5-fold potency advantage observed using laboratory strains of virus.

Table 25. Inhibition of HIV-1 Clinical Isolates by FTC

Virus	EC_{50} (µM)	
	FTC	3TC
J6[a]	0.002	0.01
2:DR2[a]	0.002	ND
WT – pre-ZDV[b]	0.008	ND
WT – MKC09-day 29[b]	0.02	ND

a Source: {Schinazi 1992}
b Source: TPI 462 v2

The activity of FTC on non-B subtypes of HIV-1 clinical isolates (group M subtypes A, C, D, E, F, and G, and group O) was evaluated. The EC_{50} values were determined in MAGI-CCR5 cells and PBMCs. Within each model, EC_{50} values were comparable for all subtypes of HIV-1. Results are presented in Table 26. FTC was more active than 3TC and ddI, and had activity comparable with that of ZDV for all subtypes of HIV-1 tested. Overall, the EC_{50} values of FTC against various HIV-1 subtypes were 2- to 5-fold higher in MAGI-CCR5 cells than in PBMCs (m2.6.3, Section 1.2, TPI 10498 v2 and TPI 11419 v2).

Table 26. EC_{50} Values of NRTIs Against HIV-1 Group M and Group O Isolates in PBMCs and MAGI-CCR5 Cells

Isolate	Subtype	Host Cell	ZDV (µM)	3TC (µM)	ddI (µM)	FTC (µM)
Group M						
RW/92/008	A	PBMCs[a]	0.008	0.054	0.26	0.012
		MAGI-CCR5[b]	0.085	0.20	3.0	0.055
BR/92/025	C	PBMCs[a]	0.035	0.027	0.49	0.017
		MAGI-CCR5[b]	0.033	0.17	0.95	0.032
UG/92/024	D	PBMCs[a]	0.003	0.026	0.21	0.007
		MAGI-CCR5[b]	0.035	0.11	1.70	0.030
Tha/92/019	E	PBMCs[a]	0.039	0.069	0.5	0.028
		MAGI-CCR5[b]	0.080	0.15	1.50	0.065
Br/930/20	F	PBMCs[a]	0.003	0.022	0.34	0.009
		MAGI-CCR5[b]	0.045	0.15	1.50	0.050
RU570	G	PBMCs[a]	0.008	0.090	0.34	0.030
		MAGI-CCR5[b]	0.150	0.18	2.50	0.075

Isolate	Subtype	Host Cell	ZDV (μM)	3TC (μM)	ddI (μM)	FTC (μM)
Group O						
BCF02 O		MAGI-CCR5[b]	0.09	0.20	2.20	0.065
		PBMCs[a]	0.028	0.25	4.75	0.14

a Source: TPI 10498 v2
b Source: TPI 11419 v2

2.1.2.2.3. Effect of Increasing Multiplicity of Infection on FTC Antiviral Activity

The effect of MOI on the antiviral activity of FTC was assessed in 2 cell lines using 2 different assay methods and was found to be minimal. In MAGI-CCR5 cells (Figure 5), an increase of 5.7-fold in infectious titer resulted in no change in EC_{50} (m2.6.3, Section 1.2, 10518 v2). In PBMCs (Figure 6), using p24 ELISA, increasing the MOI from 0.01 to 0.1 caused approximately a 10-fold shift in apparent EC_{50} (m2.6.3, Section 1.2, 11773). Increasing the MOI above 0.1 produced no further change in apparent EC_{50}.

Figure 5. Effect of Multiplicity of Infection on the EC_{50} of FTC in MAGI-CCR5 Cells

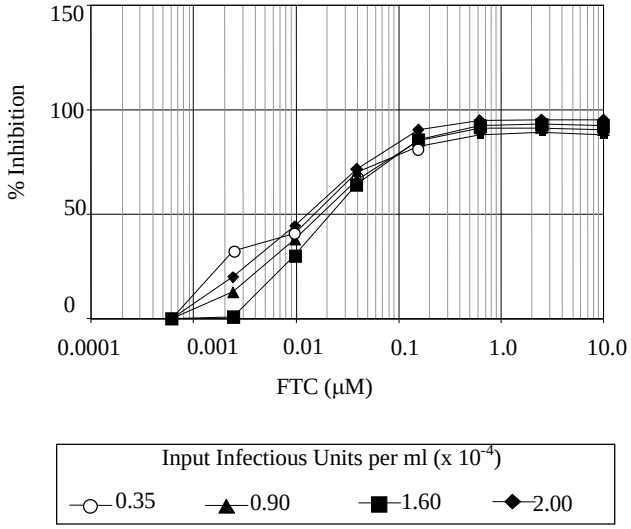

Source: 10518 v2

Figure 6. Effect of Multiplicity of Infection on the EC_{50} of FTC in PBMCs

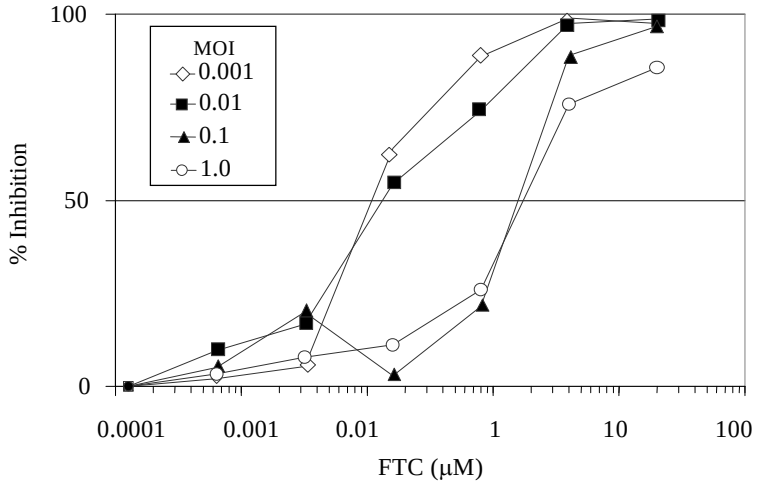

Source: 11773

2.1.2.2.4. Effect of Time of Addition on FTC Antiviral Activity

Various concentrations of FTC were added to MAGI-CCR5 cells infected with HIV-1_{LAI} (m2.6.3, Section 1.2, 10247), and EC_{50} values were determined at −1, 0, +1, +2, +4, +6, and +8 hours postinfection. Results of the study are presented in Figure 7 as fold change in EC_{50} over time of addition. FTC maintained maximal antiviral activity when added as late as 6 hours postinfection. However, adding FTC 8 hours postinfection resulted in a decrease in antiviral activity consistent with the mechanism of action of an NRTI.

Figure 7. Fold Change in FTC EC_{50} as a Function of Time of Addition

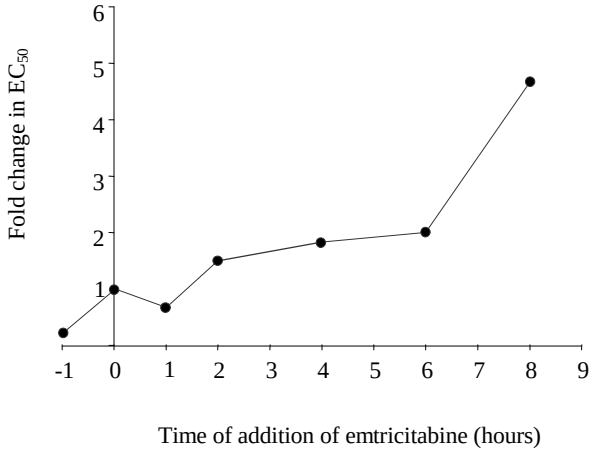

Source: 10247

2.1.2.3. Effect of Serum Proteins and Serum Protein Components on the Antiviral Activity of FTC

The potential effect of protein binding on the antiviral activity of FTC was evaluated in CEM cells. Cells were infected with HIV-1_{LAI} and maintained in culture in the presence of various concentrations of FTC in standard 10% fetal bovine serum-containing media, or in modified media where fetal bovine serum was replaced with 25% HSA or 25% HSA plus 1-mg/mL α1-AGP. Neither the medium containing 25% HSA alone or in combination with 1-mg/mL α_1-AGP affected the antiviral activity of FTC (m2.6.3, Section 1.2, 463), indicating that FTC activity is not affected by binding to serum proteins.

2.1.2.4. Inhibition of HIV-1 Reverse Transcriptase Enzymatic Activity by FTC Triphosphate

FTC-TP serves as an alternative substrate inhibitor of HIV-1 RT and is incorporated into nascent chain viral DNA. Incorporation results in the obligate termination of DNA synthesis due to the lack of a hydroxyl group in the 3′-position of the sugar moiety of FTC, which in turn inhibits viral replication. The kinetic inhibition constant (K_i) values for FTC-TP inhibition of HIV RT-catalyzed RNA-dependent DNA synthesis and DNA-dependent DNA synthesis were calculated to be 0.6 μM and 0.43 μM, respectively {Wilson 1996}. In comparison, the K_i values for lamivudine triphosphate (3TC-TP) inhibition of HIV RT-catalyzed RNA-dependent and DNA-dependent DNA synthesis were comparable at 0.97 μM and 0.7 μM, respectively. In separate experiments in which calf thymus DNA was used as the template primer, a K_i value of 0.17 μM was obtained for FTC-TP against HIV-1 RT {Painter 1995}.

Using rapid quench techniques, Feng and colleagues compared the pre-steady state kinetics of single nucleotide incorporation of dCTP, 3TC-TP, and FTC-TP opposite a template guanosine in RNA-dependent DNA synthesis catalyzed by HIV-1 RT {Feng 1999}. The results are presented in Table 27. The overall incorporation rate (k_{pol}) values of FTC-TP and 3TC-TP are significantly slower than that observed for the natural substrate dCTP. However the equilibrium binding or affinity constant (K_d) values reveal that FTC-TP and 3TC-TP bind much tighter to the active site of the enzyme-DNA complex than the natural substrate, with the K_d values of the analogues being approximately 6- to 30-fold lower than those of the natural substrate. The K_d and k_{pol} values both indicate that FTC-TP is a better overall substrate for the enzyme than 3TC-TP. This efficiency advantage may account in part for the higher activity seen for FTC compared with 3TC in cell culture.

Table 27. Kinetic Constants for the Incorporation of dCTP, FTC-TP, and 3TC-TP into an RNA/DNA Template/Primer by HIV-1 RT

Compound	Template/Primer	k_{pol} (s^{-1})	K_d (μM)	k_{pol}/K_d ($\mu M^{-1}s^{-1}$)
dCTP	r44/d23	9 ± 2	16 ± 5	0.56
	R45/D23	22.9 ± 0.7	30 ± 4	0.76
FTC-TP	r44/d23	0.240 ± 0.02	1.7 ± 0.3	0.14
	R45/D23	0.082 ± 0.005	1.4 ± 0.4	0.06
3TC-TP	R45/D23	0.033 ± 0.002	5.0 ± 0.8	0.0067

3TC-TP = lamivudine 5′-triphosphate; dCTP = deoxycytidine triphosphate; FTC-TP = emtricitabine 5′-triphosphate; k_{pol} = incorporation rate; K_d = equilibrium binding or affinity constant
Source: {Feng 1999}

2.1.2.5. Activity of FTC Against NRTI-Resistant Mutants of HIV-1

FTC activity has been evaluated extensively against a panel of clinical isolates (m2.6.3, Section 1.2, TPI 11148) and {Balzarini 1998} The panel consists of a series of recombinant wild-type clinical isolates and recombinant isolates containing anywhere from 1 to 12 mutations. Consistent with earlier passaging experiments, a high level of resistance is imparted by introduction of the M184V mutation onto any mutation background. Moderate resistance to FTC is seen for the highly mutated isolate (M41L, E44D, D67N, T69D, L74I, K101E, V108I, V118I, Y181C, G190A, L210W, T215Y), which contains 2 mutations associated with moderate resistance to 3TC (E44D, V118I) {Hertogs 2000}. In addition, moderate resistance was observed for both FTC and 3TC, with isolates harboring the K65R mutation or a multidrug resistance genotype containing the T69S(SS) insertion as previously described for 3TC {Hertogs 2000}, {Gu 1994b}, {Gu 1994a}. The antiviral activity of FTC against HIV-1 containing K65R, Q151M, and K65R+Q151M showed reduced susceptibility (8.4-, 2.3-, and > 20-fold, respectively) in cell culture. Evaluation of the mutant RT enzymes suggested that resistance was mainly due to a significant decrease in the rate of incorporation of FTC using presteady-state kinetics studies in vitro. Similar levels of virus resistance and incorporation defects were measured for FTC and 3TC in this study {Feng 2006}.

Table 28. Susceptibility of a Panel of Recombinant Mutant Viruses to FTC, 3TC, and ZDV

Genotype	EC_{50} (μM)		
	FTC	3TC	ZDV
Wild-Type ($HIV\text{-}1_{HXB2}$)[a]	0.053	0.3235	0.0305
K65R, F116Y, Q151M, V106I[a]	2.607	3.327	0.696
M41L, D67N, K70R, A98S, Y181C, M184V[a], G190A, K219E, T215Y[a]	> 5	> 31.25	0.53
V75I, M184V[a]	> 125	> 31.25	0.029
A62V, T69S(SS), K70R, T215Y[a]	0.893	2.566	0.965
K103N, V108I/V, P225H[a]	0.123	0.618	0.0358
G190A, K238T[a]	< 0.122	0.541	0.05
V106A, G190A[a]	0.292	2.16	> 1.25
$HIV\text{-}1_{IIIB}$[b]	0.01	0.02	0.01
V106A[b]	0.03	0.03	0.014
V106A, F227L[b]	0.003	0.007	0.003
V106A, F227L, K101I, Y181C[b]	0.01	0.03	0.01

a Source: TPI 11148
b Source: {Balzarini 1998}

Table 29. Susceptibility to FTC, 3TC, and ZDV of Recombinant HIV-1 Viruses Generated from Clinical Isolates

Genotype	EC_{50} (μM)[a]		
	FTC	3TC	ZDV
Wild-Type (LAI)	0.619[b]	2.567[b]	0.487[b]
Wild-Type (n = 16)	0.64[c]	2.998[c]	0.917[c]
L100I (A)	0.176	2.125	0.037
L100I (B)	0.595	2.350	0.160
G190A	0.220	0.900	0.205
G333E	1.350	1.265	0.260
M184V	> 20	> 50	0.140
K103T	0.330	1.100	0.140
V108I	0.205	0.650	0.135
K103N (A)	0.825	3.150	0.595
K103N (B)	0.680	4.000	0.250
K103N, M184V (A)	> 20	> 50	0.185

Genotype	EC_{50} (μM)[a]		
	FTC	3TC	ZDV
K103N, M184V (B)	> 20	> 20	3.02
E138K, M184V (A)	> 20	> 50	0.145
E138K, M184V (B)	> 20	> 50	0.130
E13Q, M184V	> 20	> 50	0.890
A98S, M184V	> 20	> 50	0.120
L74V, K103N	2.34	> 2.26	1.87
K101Q, E138K	1.38	1.94	0.54
K103R, Y188C	1.13	1.16	0.72
K103N, Y181C	0.55	1.17	0.29
K70R, L74V, M184V	> 20	> 20	0.90
K103T, V106I, M184V	> 20	> 20	0.36
K101Q, E138K, K103N	0.55	0.48	0.67
K103N, V108I, M184V	> 20	> 20	0.31
T215Y, K103N, L210W	0.73	1.05	> 2
M41L, K101R, M184V, T215Y	> 20	> 20	> 2
A98S, F116Y, Q151M, T215Y	1.45	0.55	> 2
T69N, K70R, M184V, K219Q	> 20	> 20	1.23
D67N, K70R, M184V, G190A	> 20	> 50	0.35
D67N, T69D, K103R, T219Q	2.58	2.92	5.75
A62V, A98S, K101D, K102Q, M184V	> 20	> 50	0.35
M41L, D67N, M184V, L210W, T215Y	> 20	> 20	> 2
D67N, K70R, E138A, M184V, T215Y, K219E	> 20	> 20	> 2
M41L, D67N, Y181C, M184V, L210W, T215Y	> 25	> 20	> 2
M41L, D67N, T69D, V108I, M184V, T215Y	> 20	> 20	> 2
A62V, V75M, K103N, F116Y, Q151M, M184V	> 20	> 20	> 2
D67N, T69D, K70R, K103N, M184V, T215Y, K219Q	> 20	> 20	> 2
M41L, D67N, A98G, K101E, K103N, M184V, G190A, L210W, T215Y, G333E	> 20	> 20	> 2
M41L, E44D, D67N, T69D, L74I, K101E, V108I, V118I, Y181C, G190A, L210W, T215Y	7.27	6.63	1.85

a EC_{50} values are expressed as the median value of at least 3 replicates unless otherwise noted.
b EC_{50} is the average value of at least 10 replicates.
c EC_{50} values are the average of replicates from 16 different recombinants displaying a wild-type genotype.

2.1.2.6. Viral Resistance Selection Studies with FTC

The development of resistance to FTC was examined by passaging virus in vitro in the presence of drug. In a study reported by Tisdale and colleagues, the wild-type virus HIV-1_{HXB2} or the ZDV-resistant mutant virus HIV-1_{RTMC} (containing D67N, K70R, T215Y, and K219Q RT mutations) was passaged in MT-4 cells in the presence of increasing concentrations of FTC or 3TC {Tisdale 1993}. Rapid emergence of resistance occurred with both compounds. By the fourth passage of HIV-1_{HXB2} and the second passage of HIV-1_{RTMC}, EC_{50} values exceeded 50 μM and by passage 6, EC_{50} values were in excess of 250 μM. These FTC-induced variants were highly cross-resistant to 3TC but showed no cross-resistance to ZDV, ddI, or nevirapine (NVP). DNA sequence analysis showed a change in RT of M184V. Passaging virus in the presence of increasing concentrations of FTC and 50 μM ZDV was able to delay appreciably, but not prevent, the emergence of FTC-resistant virus.

In experiments performed by Schinazi and colleagues, the relative potential for HIV-1 to develop resistance to 3TC and FTC was evaluated by serial passage of the virus in human PBMCs in the presence of increasing drug concentrations {Schinazi 1993}. Results presented in Figure 8 show that after 2 weeks of infection, 0.1 μM 3TC was no longer able to inhibit virus replication and drug-resistant variants dominated the replicating virus population. In contrast, FTC remained highly active under identical conditions, reducing virus replication by 80%. FTC was still able to inhibit virus replication by 50% at Week 3. At Week 5, the concentration of 3TC was increased 100-fold to 10 μM and the concentration of FTC was increased 10-fold to 1 μM to produce the same level of inhibition. FTC retained up to a 10-fold potency advantage over 3TC after 5 weeks of passaging. These data suggest that, due to greater potency, FTC may delay the breakthrough of M184V resistant viruses longer than 3TC.

DNA sequence analysis of the RT gene amplified from resistant viruses generated in these passaging experiments consistently identified mutations at M184V/I. Resistant variants were cross-resistant to both FTC and 3TC, but remained sensitive to ddC, ddI, ZDV, phosphonoformic acid, 3′-fluoro-3′-deoxythymidine, and 2 NNRTIs, the TIBO compound R82150, and the bis(heteroaryl) piperazine (BHAP) derivative U-87201E {Schinazi 1993}.

Figure 8. HIV-1 Breakthrough in the Presence of FTC and 3TC

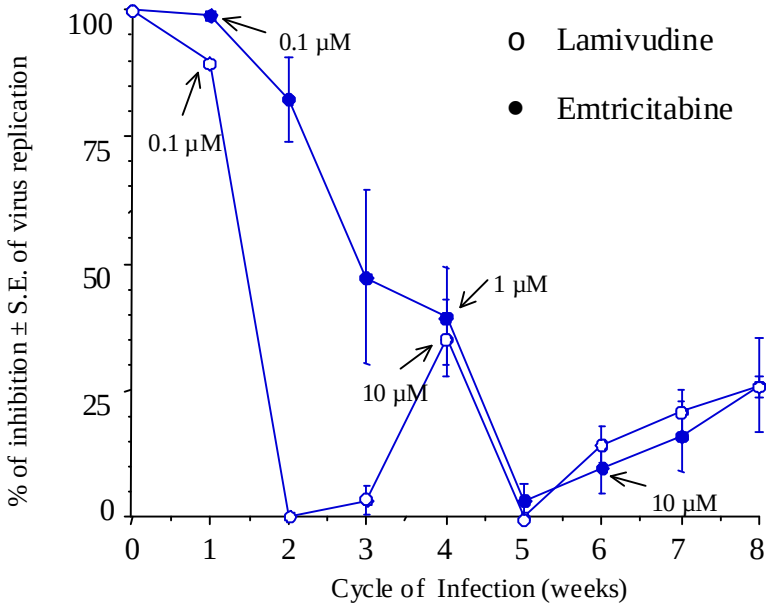

Source: {Schinazi 1993}

2.1.2.7. Mechanisms of Resistance

Biochemical studies were performed to quantify the change in susceptibility of HIV-1 RT derived from virus resistant to FTC-TP, 3TC-TP, and ddC 5′-triphosphate {Schinazi 1993}. Virus particle-derived RT was obtained from the supernatant of human PBMCs that were infected with M184V mutant virus. The mutated enzyme was 15-fold less sensitive to inhibition by FTC-TP or 3TC-TP than was wild-type (LAI) HIV-1 RT. However, only a 3-fold decrease in susceptibility was noted for ddC 5′-triphosphate. Similar results were reported using a highly purified cloned RT containing the M184V mutation for which the K_i values of FTC-TP and 3TC-TP were increased 320- and 80-fold, respectively, compared with wild-type HIV-1 RT {Feng 1999}. Using steady-state and pre-steady state kinetic analysis, Wilson and colleagues examined the effect of the M184V mutation on HIV-1 RT catalytic function {Wilson 1993}. These kinetic studies showed that the M184V mutation did not alter either the K_m or the enzyme catalytic constant (k_{cat}) values for the natural substrates, but did cause a 300-fold increase in the K_i for FTC-TP.

The M184V mutant HIV-1 is also associated with a decrease in replication capacity of HIV-1 expressing this mutation. This has been observed previously for a site-directed mutant expressing the M184V mutation {White 2002}, and is shown in Table 29 for a panel of clinical isolates expressing the M184V mutation that were obtained from a random set of plasma samples submitted to Monogram Biosciences for phenotypic analyses {Miller 2003} (m2.6.3, Section 1.3, PC-104-2004). The combination of K65R with M184V showed the greatest reduction in replication capacity {Deval 2004}. Decreases in natural substrate binding (M184V), incorporation (K65R), and reduced initiation of minus-strand single-stranded DNA synthesis (K65R+M184V) {Frankel 2007} are likely responsible for these observed additive decreases in viral replication capacity.

2.1.2.8. FTC: In Vivo Efficacy Against Retroviruses in an Animal Model

The anti-HIV activity of FTC has been tested in severe combined immunodeficiency (SCID) mice. Mice were reconstituted with human PBMCs and, after 2 weeks, infected with HIV-1_{A018} {Ussery 1998} (m2.6.3, Section 1.2, TPI 11985). Drug therapy was initiated 1 day before infection. Test compounds were administered intraperitoneally at 30 mg/kg twice daily. Viral inhibition was measured by quantitative cocultures for infectious HIV-1, and quantitative RNA viral load was measured on peritoneal wash cells, lymph nodes, spleen cells, and plasma. At the concentration used in this study, FTC completely inhibited viral infection.

Black and Furman evaluated the anti–HIV-1 activity of orally administered FTC and 3TC side-by-side in the HuPBMC-SCID mouse model (TPI 11985). Groups of 12 or 15 female C.B-17 SCID mice were reconstituted by the intraperitoneal injection of 1.3×10^8 human PBMCs. Two weeks later, the mice were infected intraperitoneally with 2000 tissue culture infectious doses of HIV-1_{A018}. Drugs were then administered in drinking water, which contained 0.3 mg/mL of FTC or 3TC. Seven days after infection, viral load in plasma was measured using a real-time reverse transcription polymerase chain reaction (RT-PCR). Both FTC and 3TC were well tolerated during the 7 days of the study with no evident toxicity. The average daily doses of the 2 drugs were similar, about 60 mg/kg. In the control group, the geometric mean viral load was 2.5×10^4 copies/mL. FTC reduced plasma viral loads to below 50 copies/mL in all 12 treated mice, and 3TC reduced plasma viral loads to below the limit of detection in 11 of the 12 treated mice. The reductions in viral loads in both treatment groups were statistically significant ($p < 10^{-5}$) compared with control, but did not differ significantly from each other.

2.1.3. TAF

2.1.3.1. Metabolic Activation of TAF

TAF and TDF, both prodrugs of TFV, are metabolized into the pharmacologically active metabolite TFV-DP {Robbins 1998}, {Delaney 2006}, {Lee 2005}. TFV-DP is a competitive inhibitor of HIV-1 RT and HBV polymerase/reverse transcriptase (pol/RT) that terminates the elongation of the viral DNA chain {Yokota 1994}, {Cherrington 1995a}, {Delaney 2006}. Compared to TDF, TAF has been synthesized to permit enhanced delivery of the parent nucleotide TFV into target cells and tissues, resulting in higher intracellular levels of TFV-DP, and lower circulating levels of TFV {Markowitz 2011}. TAF has antiviral activity against HIV and HBV. Herein, the metabolism of activation of TAF in lymphocytes and hepatocytes, antiviral activity against HIV and HBV, cross-resistance profile, and resistance selections are described.

After TAF penetrates cells, the prodrug carboxylester bond is cleaved by a hydrolase (ie, carboxylesterase 1 [CES1], CatA, etc), releasing an intermediate metabolite TFV-alanine (TFV-Ala), which is further hydrolyzed to parent TFV and sequentially phosphorylated by adenylate kinase and nucleoside diphosphate kinase to form the active metabolite TFV-DP {Eisenberg 2001}, {Birkus 2007}, {Murakami 2015}.

2.1.3.1.1. Cellular Uptake

TFV has limited cellular permeability due to the presence of 2 negative charges, which preclude oral administration due to low intestinal absorption. In contrast, TAF contains a lipophilic group masking the charged phosphonate moiety that allows for high permeability and efficient delivery of TFV into target cells and tissues.

Transport studies were conducted to determine the mechanism(s) by which TAF is delivered to target cells and tissues. A study was conducted in wild-type and transfected Chinese hamster ovary (CHO) cells to determine whether TAF is a substrate for hepatic uptake transporters organic anion transporting polypeptide (OATP) 1B1 and 1B3 (m2.6.3, Section 1.3, AD-120-2022; {Murakami 2015}).

TAF was taken up by wild-type CHO cells at a rate of 9.0 pmol/min/10^6 cells, indicating that TAF has high-passive permeability. The rate of TAF uptake increased by 30% and 168% in cells transfected with OATP1B1 (CHO-OATP1B1) and OATP1B3 (CHO-OATP1B3), respectively, compared with wild-type cells (m2.6.3, Section 1.3, AD-120-2022; {Murakami 2015}). The rate of TAF uptake decreased by 48% in CHO-OATP1B1 cells and 76% in CHO-OATP1B3 cells, respectively, in the presence of the OATP inhibitor rifampicin. These results demonstrate that TAF has high permeability but also is a substrate for hepatic uptake transporters OATP1B1 and OATP1B3. The effect of rifampicin on TAF uptake into primary human hepatocytes was assessed in vitro and the results from 4 different hepatocyte donors suggested that OATP-mediated transport makes a small contribution to TAF uptake (m2.6.5, Section 14.3.5, AD-120-2042).

2.1.3.1.2. Intracellular Metabolism of TAF in Lymphoid Cells

In Vitro

The lysosomal carboxypeptidase CatA plays an essential role in the intracellular activation of TAF in lymphoid cells and tissues (Figure 9). Cathepsin A levels and the intracellular activation of TAF-were evaluated in primary CD4+ T lymphocytes and monocyte-derived macrophages (MDMs) isolated from PBMCs from 13 donors of variable gender, age, and ethnicity (m2.6.3, Section 1.3, PC-120-2017). Cathepsin A activity was determined by measuring the rate of conversion of TAF to TFV-alanine in extracts prepared from quiescent and PHA/interleukin-2 (IL-2) activated CD4+ T cells and MDMs from each donor. For both primary cell types, the level of active CatA was similar across the donors. The mean (± standard deviation [SD]) rate of TFV-alanine formation was similar between quiescent and activated CD4+ T cells extracts (2.7 ± 0.9 vs 3.0 ± 0.6 pmol/min•µg, respectively), with ≤ 3-fold differences between donors. Cathepsin A activity was approximately 2-fold greater in MDMs compared with CD4+ T cells. The mean (± SD) rate of TFV-alanine formation was 7.1 ± 3.3 pmol/min•µg in MDMs (range: 3.1 to 13.9 pmol/min•µg across the donors). In both primary cell types, the intracellular accumulation of TAF metabolites and conversion of TAF to TFV-DP were consistent across the 8 demographically diverse donors (Figure 10).

Figure 9. Intracellular Activation of TAF in Lymphoid Cells and Tissues

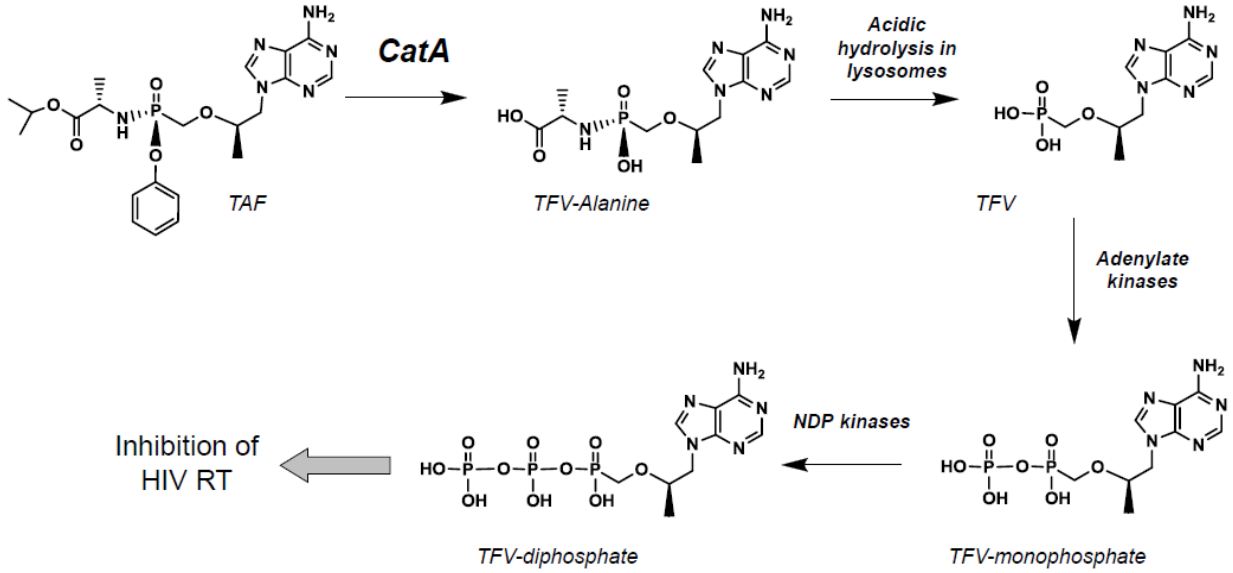

Cat A = cathepsin A; NDP = nucleoside diphosphate; RT = reverse transcriptase; TAF = tenofovir alafenamide; TFV = tenofovir
Source: Figure copied from {Bam 2014a}; Report PC-120-2017

Figure 10. Intracellular TAF Metabolites in CD4+ T cells and Monocyte-derived Macrophages from Different Donors

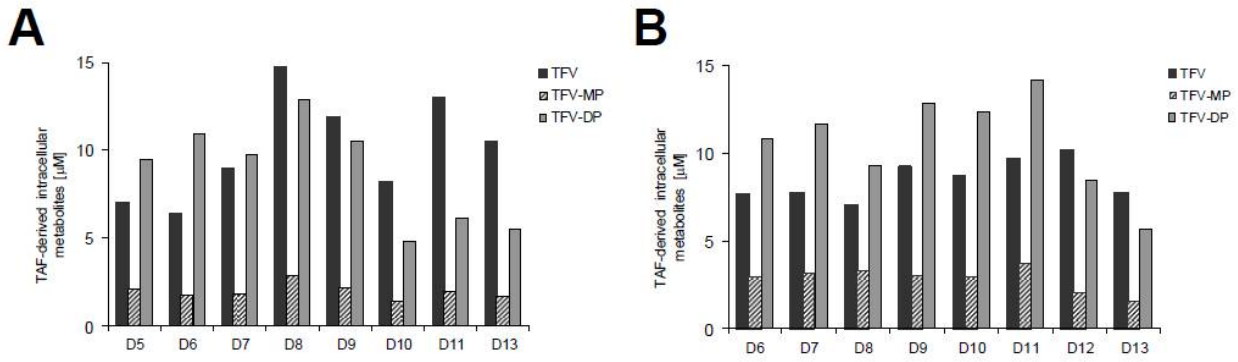

D= Donor; TAF = tenofovir alafenamide; TFV = tenofovir; TFV-MP = tenofovir monophosphate; TFV-DP = tenofovir diphosphate
Following incubation for 4 hours with 1µM TAF, the formation and quantity of intracellular TAF metabolites in CD4+ T cells (A) and MDMs (B) were determined by HPLC combined with mass spectrometry.
Source: Figure copied from {Bam 2014a}; Report PC-120-2017

TFV is a nucleotide analog (ie, a nucleoside deoxyadenosine monophosphate analog) and, therefore, does not require the activation step to a nucleoside monophosphate metabolite by intracellular nucleoside kinase activity. In some cells, intracellular concentrations of nucleoside kinases are cell-cycle dependent. The cellular enzymes responsible for TFV metabolism to the phosphorylated forms are adenylate kinase (AK) {Robbins 1995} and nucleotide diphosphate kinase, which are highly active and ubiquitous. Adenylate kinase exists as 2 isoenzymes, AK1 and AK2, with the phosphorylation of TFV mediated more efficiently by AK2.

The intracellular metabolism of TFV was studied in PBMCs {Robbins 1998}. The intracellular $t_{1/2}$ of TFV and the phosphorylated metabolites TFV monophosphate (TFV-MP, previously abbreviated PMPAp) and TFV-DP differs in resting cells versus activated PBMCs, as presented in Figure 11. In resting human PBMCs, the $t_{1/2}$ of TFV-DP was found to be approximately 50 hours, whereas the $t_{1/2}$ in PHA-stimulated PBMCs was found to be approximately 10 hours. This long intracellular $t_{1/2}$ supports once-daily dosing.

Figure 11. TFV Intracellular Metabolism in Human PBMCs

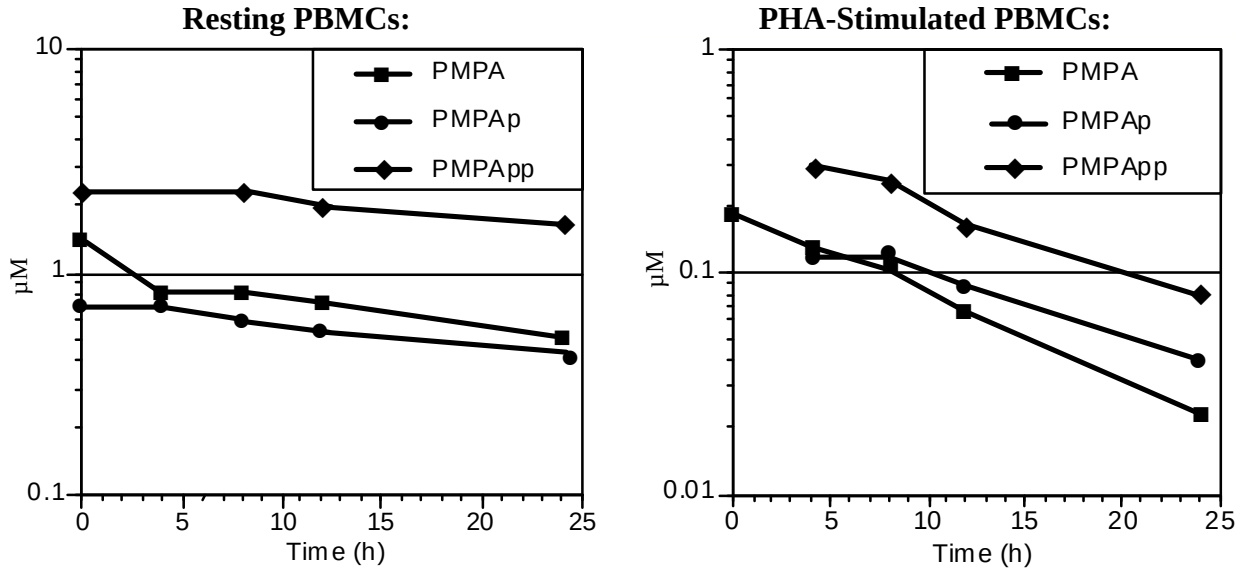

PMPA = tenofovir; PMPAp = tenofovir monophosphate; PMPApp = tenofovir diphosphate
Source: {Robbins 1998}

In Vivo

The kinetics of intracellular TFV metabolism were studied in monkeys that received a single dose of 30 mg/kg [^{14}C]TFV subcutaneously. After dosing, serial blood samples were obtained and analyzed. Plasma TFV levels and PBMC intracellular TFV and TFV metabolite concentrations were determined (m2.6.3, Section 1.3, P2001025). The TFV concentration in plasma reached a maximum of approximately 50 μM and declined with a $t_{1/2}$ of 5 to 7 hours. Consistent with the in vitro studies, TFV is efficiently taken up by PBMCs and is metabolized to TFV-DP, with the intracellular concentrations of the active metabolite TFV-DP reaching 0.9 μM. The $t_{1/2}$ of TFV-DP in this experiment was > 50 hours (Figure 12).

Figure 12. Plasma TFV Concentrations and Concentrations of TFV, TFV-MP, and TFV-DP in PBMCs After Administration of a Single Dose of [^{14}C]TFV to Monkeys

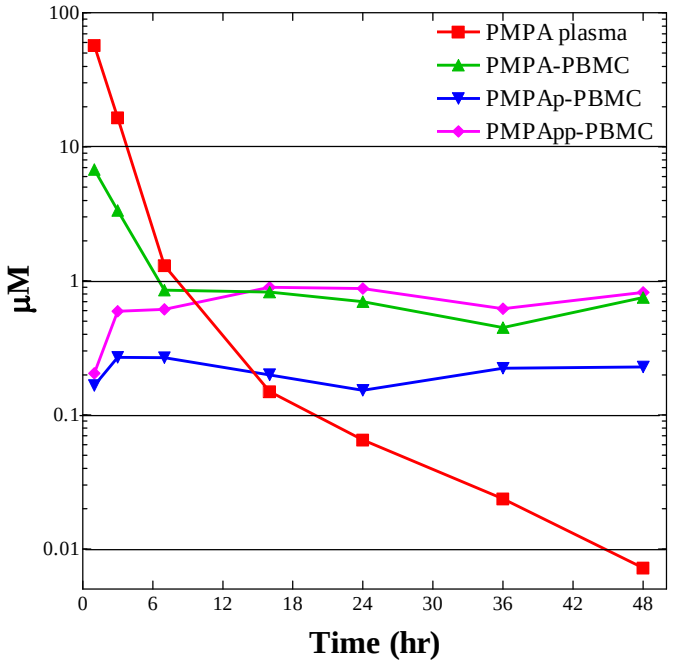

PMPA = tenofovir; PMPAp = tenofovir monophosphate; PMPApp = tenofovir diphosphate
Source: P2001025

To assess the metabolism of TFV in lymph nodes, axillary, inguinal, and mesenteric lymph nodes were obtained at 48 hours after dosing of [^{14}C]TFV in the monkey. As observed in PBMCs, significant intracellular concentrations of TFV and its metabolites were observed in lymph node mononuclear cells from all 3 sites (Table 30).

Table 30. TFV and Metabolites in Selected Lymph Nodes of a Monkey 48 Hours After Administration of a Single Dose of [^{14}C]TFV

	Intracellular Concentration (µM)		
Node	**TFV**	**TFV-MP**	**TFV-DP**
Axillary	0.37	0.26	0.27
Inguinal	1.3	0.65	ND
Mesenteric	5.2	0.17	0.13

Source: P2001025

2.1.3.1.3. TAF (and TFV) Intracellular Metabolism in Rhesus Monkey

The plasma pharmacokinetic profile of TAF (and TFV) and intracellular TAF metabolism in PBMCs were studied in rhesus monkeys that received a single oral dose of GS-7340-02 at 5.0 or 50 mg/kg (m2.6.3, Section 1.3, P2000087). In monkeys dosed with GS-7340-02 at 50 mg/kg,

TAF and TFV levels in the plasma increased rapidly with T_{max} values of 0.5 and 1 hour, respectively. In these same monkeys, TAF and TFV levels in the plasma decreased with $t_{1/2}$ values of 0.40 and 17.33 hours, respectively. In PBMCs, TFV levels persisted up to 96 hours with an apparently slower decline than in plasma (Table 31). The TFV levels were significantly higher in the samples treated with acid phosphatase, suggesting that a significant proportion of TFV-related material in PBMCs was in phosphorylated forms.

Table 31. Intracellular TFV Levels Detected in PBMCs from Rhesus Monkeys Dosed Once Orally with GS-7340-02

GS-7340-02 Dose (mg/kg)	TFV Concentration (ng/10^6 Cells)					
	Single Oral Dose					
	Without Acid Phosphatase Treatment			With Acid Phosphatase Treatment		
	2 hours	24 hours	96 hours	2 hours	24 hours	96 hours
5	0.47	0.06	BLQ	0.73	0.62	0.18
50	17.0	6.82	3.03	34.2	20.1	8.68

BLQ = below limit of quantitation; GS-7340-02 = tenofovir alafenamide (TAF) monofumarate; TFV = tenofovir
Phosphorylated metabolites of TAF were converted to TFV by treatment with acid phosphatase for 30 min at 4°C. Data were mean values obtained from 6 rhesus monkeys.
Source: P2000087

In a separate study, the plasma PK profile of TFV and intracellular TFV metabolism in PBMCs and lymph node mononuclear cells (LNMCs) were studied in rhesus monkeys that received a single subcutaneous dose of [^{14}C]TFV at 15, 30, or 60 mg/kg (m2.6.3, Section 1.3, P2001025). TFV and TFV metabolite concentrations were determined by high-performance liquid chromatography (HPLC).

Consistent with the in vitro studies, TFV was efficiently taken up by PBMCs in rhesus monkeys and metabolized to TFV-DP, with the intracellular concentrations of the active metabolite TFV-DP reaching 0.9 µM (30-mg/kg dose group). The $t_{1/2}$ of TFV-DP in PBMCs was > 50 hours. Significant levels of TFV and its metabolites were also observed in LNMCs from axillary, inguinal, and mesenteric lymph node sites 48 hours after dosing.

2.1.3.1.4. TAF Intracellular Metabolism in Dogs

The plasma and liver PK profiles were determined following a single oral dose of TAF 10 mg/kg to male beagle dogs (m2.6.3, Section 1.3, AD-120-2034). TAF was rapidly absorbed and eliminated with observed plasma T_{max} of 0.08 hours and $t_{1/2}$ of 0.24 hours. Tenofovir was the major metabolite found in plasma with a C_{max} value of 2.23 µM. TFV-DP was the major metabolite in liver, achieving a C_{max} of 126 µM at 4.0 hours postdose.

In a separate study, plasma and liver PK profiles were determined on Days 1 and 7 following daily oral administration of TAF 8.29 mg/kg to male beagle dogs (m2.6.3, Section 1.3, AD-120-2033). TAF was rapidly absorbed and exhibited a short $t_{1/2}$ of 0.3 hours in plasma on both Days 1 and 7. The rapid disappearance of TAF was accompanied by an increase in TFV.

Tenofovir was the major metabolite detected in plasma, achieving C_{max} levels of 1.47 and 2.12 µM on Days 1 and 7, respectively. TFV-DP was the major metabolite in liver, achieving C_{max} levels of 242 and 153 µM at 4.0 and 24 hours postdose on Day 7, respectively.

2.1.3.1.5. TAF (and TFV) Intracellular Metabolism in Humans

In the Phase 1 Study GS-US-120-0104, a 10-day monotherapy study, TAF 25 mg once daily resulted in approximately 90% lower TFV plasma levels and approximately 5-fold higher TFV-DP levels in PBMCs compared with TDF 300 mg. Subjects dosed with TAF 25 mg once daily achieved a mean TFV-DP concentration in PBMCs of 0.677 µM predose at Day 10, with a slight 2-fold increase by 12 hours postdose to 1.493 µM. The mean TAF plasma C_{max} observed at steady state was 0.484 µM {Ruane 2013}.

In vitro TAF intracellular metabolism studies in PBMCs were undertaken to determine the TAF concentrations that result in TFV-DP levels comparable with those observed in vivo (m2.6.3, Section 1.3, PC-120-2008; {Liu 2013}). TAF exposure conditions included a 48-hour continuous incubation and 2-hour pulse incubation with washout. The continuous incubation was evaluated as a comparator, while the 2-hour pulse incubation with washout best mimicked the limited in vivo TAF plasma exposure (T_{max} = 38 minutes, $t_{1/2}$ = 25 minutes) observed at steady state in Study GS-US-120-0104 {Ruane 2013}. TFV-DP levels were measured at 6, 24, and 48 hours by LC/MS/MS.

The results indicate that TFV-DP levels were dose proportional for both continuous incubation and 2-hour pulse experiments (Table 32). After 6 hours of continuous incubation with 13.7 to 124 nM TAF, the target TFV-DP concentration of 0.677 to 1.493 µM was achieved. For the 2-hour pulse incubation with washout, the target TFV-DP concentration of 0.677 to 1.493 µM was achieved with 124 to 370 nM TAF, which was in alignment with the mean TAF plasma C_{max} of 0.484 µM observed at steady state in Study GS-US-120-0104 {Ruane 2013}.

Table 32. Intracellular TFV-DP Levels Detected in PBMCs Incubated with TAF

	TFV-DP Concentration (µM)					
	Continuous Incubation			2-Hour Pulse Incubation		
TAF (nM)	6 hours	24 hours	48 hours	6 hours	24 hours	48 hours
13.7	0.56	1.18	2.12	BLQ	BLQ	BLQ
41.2	0.82	3.35	6.00	BLQ	BLQ	BLQ
124	2.89	10.3	19.4	BLQ	BLQ	BLQ
370	5.93	25.4	49.9	1.89	1.35	0.95
1111	20.2	69.0	128	7.05	4.01	3.17
3333	59.5	204	357	19.9	13.5	7.03
10000	176	453	840	73.5	46.7	24.5

BLQ = below limit of quantitation (limit of TFV-DP quantitation: 0.5 µM); TAF = tenofovir alafenamide; TFV-DP = tenofovir diphosphate
Formation of TFV-DP in PBMCs was determined by LC/MS/MS. Data were mean values performed in duplicate.
Source: PC-120-2008; {Liu 2013}

In a separate study, TFV-DP persistence in resting and PHA-stimulated human PBMCs was evaluated by HPLC at different time intervals after drug removal, following a 24-hour incubation with 10 µM TFV {Robbins 1998}. In resting PBMCs, the $t_{1/2}$ of TFV-DP was approximately 49 hours, whereas the $t_{1/2}$ of TFV-DP in PHA-stimulated PBMCs was approximately 11 hours.

2.1.3.1.6. TAF Intracellular Metabolism in Primary Human CD4$^+$ T Cell Subsets

TFV-DP levels were evaluated in primary human CD4$^+$ T cell subsets loaded with a clinically relevant concentration of TAF (m2.6.3, Section 1.3, PC-120-2023). Four CD4$^+$ T cell subsets (naive, effector, central memory, and effector memory) based on CD3, CD4, CD45RA, and chemokine receptor 7 expression as well as total CD4$^+$ T cells from 3 healthy human donors were isolated by cell sorting. Based on data generated in PBMCs, TAF loading was evaluated in CD4$^+$ T cell subsets using a 2-hour pulse with 400 nM TAF followed by a 22-hour washout with drug-free media. TFV-DP levels were measured at 2 and 24 hours posttreatment by LC/MS/MS.

TAF intracellular metabolism achieved similar intracellular TFV-DP levels in each CD4$^+$ T cell subset compared with the total CD4$^+$ T cells from the same donor, with minimal variation between donors. Mean TFV-DP levels after the 22-hour washout were comparable with TFV-DP levels after the 2-hour TAF pulse across each CD4$^+$ T cell population, with a trend toward higher TFV-DP levels in the central memory subset after the 22-hour washout (Table 33).

These results indicate that TFV-DP has a uniformly long intracellular half-life in all CD4$^+$ T cell subsets evaluated, consistent with the half-life of TFV-DP in PBMCs from Study GS-US-120-0104 in subjects dosed with TAF 25 mg once daily {Ruane 2013}.

Similar results have been correlated with 58.7% persistent inhibition of anti-HIV activity at 24 hours in primary CD4$^+$ T lymphocytes after incubation with TFV {Ledford 2006}.

Table 33. Intracellular TFV-DP Levels Detected in CD4$^+$ T Cell Subsets Pulse Loaded with 400 nM TAF

	TFV-DP Concentration (µM)		
	2-Hour Pulse Incubation with 400 nM TAF		
CD4$^+$ T Cell Population	2 hours	24 hours	24-hour/2-hour Ratio
Total	1.68	1.96	1.1
Naive	1.01	1.35	1.3
Effector	1.21	1.66	1.3
Central Memory	1.82	3.25	1.7
Effector Memory	2.12	2.92	1.3

TFV-DP = tenofovir diphosphate
Formation of TFV-DP in CD4$^+$ T cells was determined by LC/MS/MS. Data were mean values from 3 donors performed in duplicate.
Source: PC-120-2023

2.1.3.1.7. TAF (and TFV) Intracellular Metabolism in Primary Human Hepatocytes

The metabolism of TAF was compared with the prodrug TDF and the parent TFV in primary human hepatocytes by LC/MS/MS (m2.6.3, Section 1.3, AD-120-2017; {Murakami 2015}). A time course showed that the active metabolite, TFV-DP, increased over 24 hours. Continuous incubation with 5 µM of TFV, TDF, or TAF resulted in TFV-DP levels of 12.1, 302, and 1470 pmol/10^6 cells after 24 hours, respectively (Figure 13). Based on these results, incubation with TAF resulted in approximately 120- or 5-fold higher levels of intracellular TFV-DP compared with TFV or TDF, respectively.

Figure 13. In Vitro Metabolism in Primary Human Hepatocytes

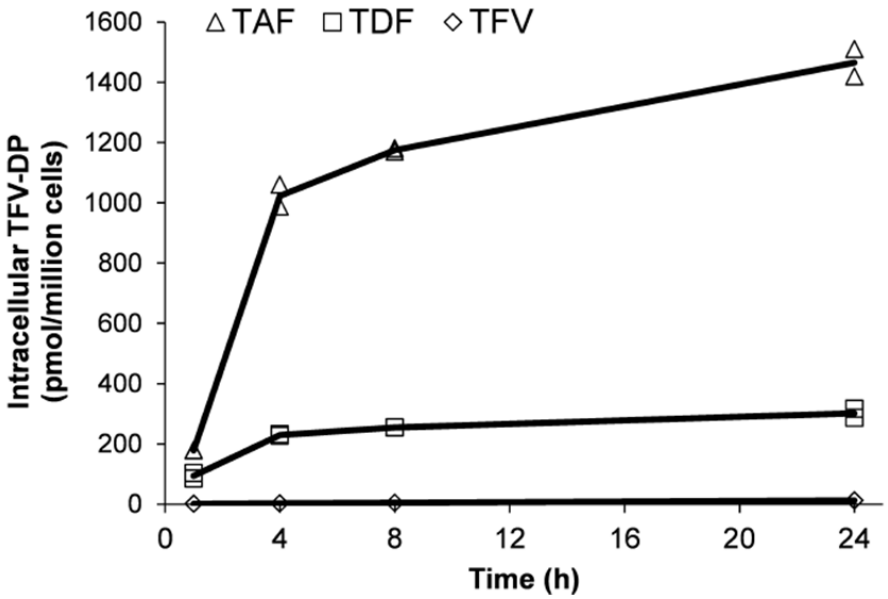

TAF = tenofovir alafenamide; TDF = tenofovir disoproxil fumarate; TFV = tenofovir
Data were mean values performed in duplicate.
Source: AD-120-2017; {Murakami 2015}

In order to assess TFV-DP persistence in primary human hepatocytes, TAF loading was evaluated using a 2-hour pulse with 5 µM TAF followed by a washout with drug-free media for 22 hours {Murakami 2015}. As shown in Figure 14, TFV-DP levels reached approximately 700 pmol/10^6 cells at 3 hours and only decreased slightly over the 24-hour time course. In a separate study that evaluated later time points in primary human hepatocytes following incubation with TFV, the half-life ($t_{1/2}$) of TFV-DP of approximately 95 hours supported once-daily dosing {Delaney 2006}. These results correlated with persistent inhibition of anti-HBV activity > 24 hours in HepG2 cells after a short incubation with TFV {Ying 2000}.

Figure 14. Half-Life of TFV-DP in Primary Human Hepatocytes Loaded with 5 µM TAF

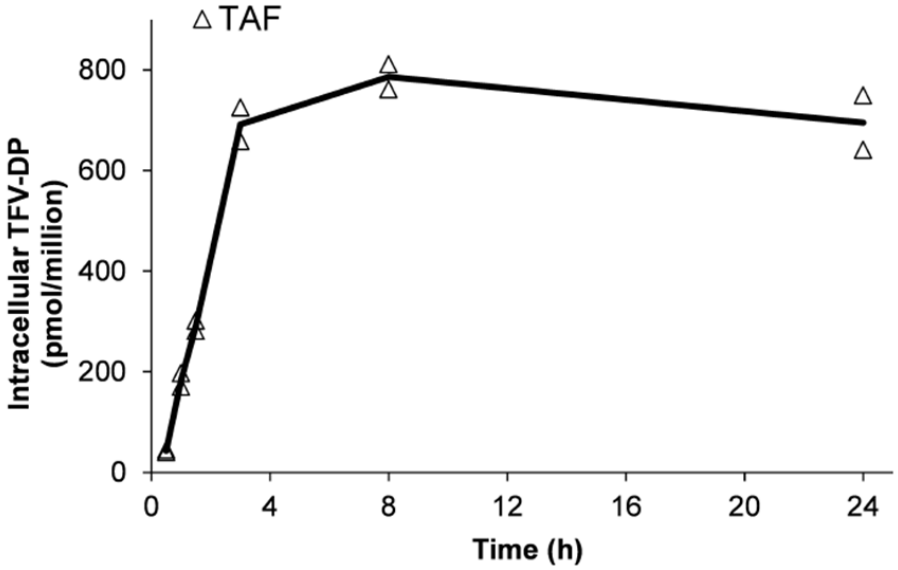

TAF = tenofovir alafenamide
Data were mean values performed in duplicate.
Source: {Murakami 2015}

2.1.3.1.8. Intracellular Metabolism of TAF in Hepatic Cell Lines

Due to their critical enzymatic role in TAF metabolism, differences in CES1 and/or CatA cellular levels may affect the antiviral activity of TAF. The expression levels of CES1 and CatA and their contribution to intracellular metabolism of TAF were assessed in two hepatic cell lines commonly used for antiviral assays (HepG2 and HepAD38) (m2.6.3, Section 1.12, PC-320-2006).

The expression level of CES1 in both hepatic cell extracts was 17- to 43-fold less than in pooled human liver S9 fractions (Table 34). By comparison, the expression of CatA in both hepatic cell extracts was 2.4- to 4.8-fold greater than in pooled human liver S9 fractions. One possible explanation for this difference is that suppression of CES1 expression levels may be common in hepatic cell lines {Murakami 2013}, {Yang 2007}, {Murakami 2010}.

Table 34. Expression of CES1 and CatA in Hepatic Cell Lines

	Relative Concentration (ng/µg Total Protein)[a]	
Cells	**CES1**	**CatA**
HepG2	0.9	2.9
HepAD38	2.3	5.7
Pooled Human Liver S9 Fraction	39.0	1.2
Pooled Human Intestinal S9 Fraction	< 0.1	1.4

a Data shown represent the mean values of three independent experiments.
Source: Report PC-320-2006

Hydrolytic activation of TAF in extracts of HepG2 and HepAD38 cells was also evaluated in the presence or absence of inhibitors of CES1 (bis-p-nitrophenyl phosphate [BNPP]) and/or CatA (telaprevir). BNPP showed no impact on TAF hydrolysis in either HepG2 or HepAD38 cells up to the highest concentration tested (50 µM). In contrast, telaprevir was a potent inhibitor of TAF hydrolysis to TFV-Ala in both HepG2 and HepAD38 cells with similar IC_{50} values of 0.2 and 0.1 µM, respectively (Table 35).

Table 35. Effect of CES1 or CatA or Inhibitors on Intracellular Hydrolysis of 100 µM TAF in HepG2 and HepAD38 Cells

Cell Type	Target (Inhibitor Class)	Compound	IC_{50} (µM)
HepG2	CES1 (N/A)	BNPP	> 50
	CatA (HCV PI)	telaprevir	0.2
HepAD38	CES1 (N/A)	BNPP	> 50
	CatA (HCV PI)	telaprevir	0.1

BNPP = bis-p-nitrophenyl phosphate; CatA = cathepsin A, CES1 = carboxylesterase 1; IC_{50} = 50% inhibitory concentration; PI = protease inhibitor
Source: Report PC-320-2006

In addition, following incubation of HepAD38 cells with 0.5 µM of TAF, telaprevir significantly inhibited metabolism of TAF to TFV-DP by 2.2-fold, while the effect of BNPP was negligible (1.2-fold) (Figure 15). When both telaprevir and BNPP were combined, a 3.7-fold greater inhibition of TFV-DP formation was observed, relative to telaprevir alone.

Figure 15. Effect of CES1 and/or CatA Inhibitors on Metabolism of 0.5 µM TAF in HepAD38 Cells

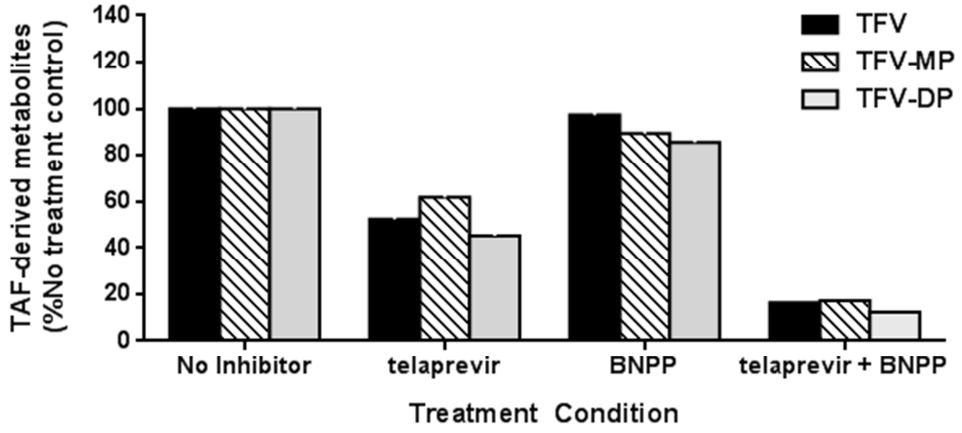

BNPP = bis-p-nitrophenyl phosphate; TAF = tenofovir alafenamide; TFV = tenofovir; TFV-MP = tenofovir monophosphate; TFV-DP = tenofovir diphosphate
HepAD38 cells continuously incubated with 0.5 µM TAF for 24 hours in the presence of inhibitors.
Data represent mean from a single experiment performed in duplicate.
Source: Report PC-320-2006

These results indicate that CatA is the major hydrolyzing enzyme of TAF in hepatic cell lines, while CES1 has a modest contribution. While the level of contribution to TAF metabolism from CatA and CES1 are different in HepAD38 and primary human hepatocytes (m2.6.5, Section 9.3.8, AD-120-2031, {Murakami 2015}), both enzymes are responsible for hydrolysis of TAF in both cell types.

2.1.3.2. Antiviral Activity of TAF

2.1.3.2.1. Antiviral Activity of TAF in T-Cell Lines and Primary Cells

TAF, TFV, and TDF were evaluated in vitro for antiviral activity against HIV-1 (EC_{50}) and cytotoxicity (CC_{50}) in MT-2 cells, MT-4 cells, and PBMCs (m2.6.3, Section 1.3, PC-120-2004, PC-120-2007, and PC-120-2009). Other ARV drugs, including NRTI, NNRTI, INSTI, and PI classes, were also evaluated in MT-2 and MT-4 cells (PC-120-2007). Quiescent and PHA-activated PBMCs, MT-2, and MT-4 cells were incubated with serially diluted drug concentrations for 5 days and then evaluated for cytotoxicity (PC-120-2007 and PC-120-2009). The maximum concentrations of drugs used were 100, 50, and 2000 µM, for TAF, TDF, and TFV, respectively. MT-2 and MT-4 cells were also infected with the HIV-1_{IIIB} strain, incubated with serially diluted drug concentrations for 5 days, and then evaluated for antiviral activity (reduction of viral cytopathic effect) (PC-120-2007). The antiviral activity of TAF was evaluated against a panel of HIV-1 clinical isolates in PHA-activated PBMCs, as described in Section 2.1.3.2.1.

Based on the results of these experiments, the selectivity index ($SI = CC_{50}/EC_{50}$) for TAF was 1997 and > 3607 in the T-lymphoblastoid cell lines and 1889 in dividing PBMCs (Table 36). Due to its increased cellular permeability, the anti-HIV activity of TAF was increased by 228- and 1232-fold over TFV in MT-2 and MT-4 cells, respectively; in comparison, the anti-HIV activity of TDF was increased over TFV by 55- and 729-fold (Table 36; PC-120-2007). The SIs for TAF were also higher compared with TFV and TDF in all cell types tested (Table 36; PC-120-2007 and PC-120-2009). In the MT-2 and MT-4 lymphoblastoid cell lines, TAF ranked first in SI among all the NRTIs tested, followed by TDF and TFV. Among all ARV drugs tested, TAF ranked fourth in SIs, following an NNRTI (EFV), an INSTI (RAL), and a PI (atazanavir [ATV]). The SI values in the MT-2 cells in the current study (PC-120-2007) were within 1.7- to 2.2-fold agreement with previously reported values for TAF (8000), TFV (1250), and TDF (1000) {Lee 2005}; the differences may reflect minor differences in kinetic cell loading.

The ARV activity of TAF and TFV was also assessed in monocyte-derived macrophages (MDMs) obtained from a demographically diverse group of donors. The MDMs were infected with the HIV-1_{BaL} strain, incubated with serially diluted drug concentrations for 14 days, and then evaluated for virus production (m2.6.3, Section 1.3, PC-120-2017). ZDV and EFV were included as positive controls. The relative range of TAF antiviral activity across all tested donors was higher than that for TFV and comparable with that of the other HIV-1 RT inhibitors tested, with a mean EC_{50} value of 9.7 nM compared with 799, 15.3, and 0.9 nM for TFV, ZDV, and EFV, respectively (Table 36; PC-120-2017).

Table 36. Anti-HIV Activity (EC_{50}) and Cytotoxicity (CC_{50}) of TAF, TFV, and TDF

Drug	Cells/Virus									
	MT-2/HIV-1_{IIIB}			MT-4/HIV-1_{IIIB}			PBMC[b]/HIV-1_{IIIB}[c]			Macrophage-Monocytes/ HIV-1_{BaL}
	EC_{50} (µM)	CC_{50} (µM)	SI[a]	EC_{50} (µM)	CC_{50} (µM)	SI[a]	EC_{50} (µM)	CC_{50} (µM)	SI[a]	EC_{50} (µM)
TAF	0.0147	> 53.0	> 3607	0.0116	23.2	1997	0.0036	6.8	1889	0.0097
TFV	3.35	7605	2265	14.3	6264	438	1.9	2150	> 1100	0.799
TDF	0.0614	37.1	604	0.0196	22.9	1167	0.015	19.6	> 1300	ND

CC_{50} = concentration that resulted in 50% cytotoxicity; EC_{50} = concentration inhibiting viral replication by 50%; ND = not determined; PBMC = peripheral blood mononuclear cell; SI = selectivity index; TDF = tenofovir disoproxil fumarate; TFV = tenofovir

a Ratio of CC_{50} to EC_{50}.

b Data is shown for dividing PBMCs.

c EC_{50} for TAF is mean of EC_{50} values for 26 primary HIV-1 isolates.

Source: PC-120-2004, PC-120-2007, PC-120-2009, and PC-120-2017

TFV was investigated in a novel antiviral persistence assay to assess the ability of the intracellular drug to maintain antiviral suppression over extended periods of time {Ledford 2006}. TFV demonstrated long-term antiviral persistence through 24 hours in primary CD4 T cells (58.7% persistence at 24 hours), whereas ABC was much less persistent (< 0.5% persistence at 4 hours) in comparison. Consistent with the sustained antiviral persistence of TFV, the calculated in vitro $t_{1/2}$ of TFV-DP in primary CD4 T cells was ~21 hours compared with ~5 hours for the active metabolite of ABC, carbovir triphosphate (CBV-TP).

Both TFV and FTC have been tested in parallel for their anti-HIV activity (m2.6.3, Section 1.12, PC-164-2002). Two HIV-1 isolates were used in these analyses, the laboratory-adapted LAI strain and a recombinant HIV-1 strain containing a wild-type patient-derived RT and protease sequence (MM-317). The infections were carried out at 2 different MOIs (0.03 and 0.1), and the results were calculated as EC_{50} and EC_{90} values for each drug (Table 37). Overall, there was some effect of MOI observed, with increased EC_{50} and EC_{90} values noted for FTC with both viruses and increased values for TFV with the MM-317 virus. The drug susceptibility values derived from the laboratory strain and the patient recombinant virus were similar for both drugs. The EC_{90} values were approximately 3-fold greater than the EC_{50} values. The combined effects of TFV and FTC together on HIV-1 replication are described in the pharmacodynamic drug interactions section (Section 5.4.1).

Table 37. Mean EC_{50} and EC_{90} Values for TFV and FTC Against HIV-1_{LAI} and HIV-1_{MM-317} Strains

Viral Isolate	MOI	TFV EC_{50} (µM)	TFV EC_{90} (µM)	FTC EC_{50} (µM)	FTC EC_{90} (µM)
LAI	0.03	5.1 ± 1.8	19.1 ± 5.8	0.132 ± 0.039	0.440 ± 0.128
LAI	0.1	5.1 ± 0.9	17.0 ± 6.0	0.222 ± 0.065	0.721 ± 0.128
MM-317	0.03	6.2 ± 1.4	20.5 ± 4.8	0.127 ± 0.025	0.421 ± 0.084
MM-317	0.1	11.2 ± 0.9	37.0 ± 3.3	0.217 ± 0.038	0.721 ± 0.128

Source: PC-164-2002

2.1.3.2.2. Antiviral Activity of TAF Against HIV Clinical Isolates

The antiviral activity of TAF was assessed in fresh human PBMCs against a panel of 26 wild-type HIV-1 clinical isolates representing all HIV-1 groups (M, N, O), including M subtypes A to G (m2.6.3, Section 1.3, PC-120-2004). Virus and activated PBMCs were mixed in the presence of TAF and incubated for 7 days before antiviral effect (based on RT activity measurements) and cytotoxicity were assessed. In this in vitro experiment, PBMC viability remained high throughout the incubation period; thus virus-infected cells were used for the assessment of both antiviral activity and cytotoxicity. ZDV was included as a positive control drug.

Overall, TAF showed potent antiviral activity against the HIV-1 groups/subtypes evaluated (Table 38). The EC_{50} values for the 26 isolates ranged from 0.10 to 12.0 nM, with an overall mean EC_{50} of 3.6 nM. No significant differences were observed between the mean TAF EC_{50} values for any of the HIV-1 subtypes/groups evaluated. No cytotoxicity was observed with TAF or ZDV at the concentrations evaluated (concentration that results in 50% cytotoxicity [CC_{50}] > 500 and > 1000 nM, respectively).

Table 38. TAF Antiviral Activity Against Primary HIV-1 Isolates

Primary HIV-1 Isolates				EC_{50} (nM)[a]	
Type	**Group**	**Subtype**	**Isolate**	**TAF**	**ZDV**
HIV-1	M	A	92UG029	8.75	26.4
			92UG037	0.69	2.12
			92RW016	0.71	1.53
		B	93BR021	9.69	48.0
			JR-CSF	1.05	1.95
			90US873	3.87	6.03
		C	92BR025	4.16	9.00
			98BR004	1.75	7.56
			93IN101	1.50	5.49
		D	92UG001	3.79	11.3
			92UG046	0.99	3.33
			92UG024	6.27	7.21
		E	93TH073	1.18	3.54
			CMU06	1.36	4.09
			CMU08	5.88	13.1
		F	93BR019	0.73	4.87
			92BR024	5.97	17.1
			93BR029	0.14	1.28
			93BR020	2.22	7.41
		G	G3	5.34	14.0
			RU570	12.0	66.4
			JV1083	9.85	27.4
	N	NA	YBF30	1.98	5.23
	O	NA	BCF02	1.30	1.23
			BCF03	3.01	7.20
			BCF07	0.10	3.81

NA = Not applicable
a Data are from single experiments performed in triplicate.
Source: PC-120-2004

The antiviral activity of TAF was assessed in fresh human PBMC against 3 wild-type HIV-2 clinical isolates (m2.6.3, Section 1.3, PC-120-2004). Virus and activated PBMCs were mixed in the presence of TAF and incubated for 7 days before antiviral effect (ie, inhibition of RT activity) and cytotoxicity were assessed. In this in vitro experiment, PBMC viability remains high throughout the incubation period; thus, virus-infected cells were used for the assessment of both antiviral activity and cytotoxicity. ZDV was included as a positive control drug.

Overall, TAF showed potent antiviral activity against the 3 HIV-2 isolates evaluated (Table 39). TAF EC_{50} values ranged from 0.91 to 2.63 nM. No significant differences were observed between the TAF EC_{50} values for any of the isolates evaluated. No cytotoxicity was observed with TAF or ZDV at the concentrations evaluated (CC_{50} > 500 and > 1000 nM, respectively).

Table 39. TAF Antiviral Activity Against Primary HIV-2 Isolates

Primary HIV-2 Isolates				**EC_{50} (nM)[a]**	
Type	Group	Subtype	Isolate	TAF	ZDV
HIV-2	NA	NA	CDC310319	2.63	15.6
			CDC310342	1.96	1.39
			CBL-20	0.91	2.18

a Data are from single experiments performed in triplicate.
Source: PC-120-2004

2.1.3.3. Effect of Serum Proteins on the Antiviral Activity of TAF

The protein binding of TAF was moderate in human plasma, with 20% unbound based on multiple human ex vivo studies; the mean percentage of unbound TAF ranged from 14% to 23% in all subjects (GS-US-120-0108 and GS-US-120-0114). The protein binding of TFV was studied in the presence or absence of human plasma and human serum (m2.6.3, Section 1.3, P0504-00039.1). The percentages of TFV that remained unbound in human plasma and human serum were 99.3% and 92.8%, respectively.

2.1.3.4. Inhibition of HIV-1 Reverse Transcriptase Enzymatic Activity by the TAF Active Metabolite

Inside the cells, TAF is converted to its active metabolite TFV-DP that efficiently inhibits both RNA- and DNA-directed HIV-1 RT DNA polymerization. It competes with deoxyadenosine triphosphate (dATP) for incorporation into DNA and, since it lacks a 3′-hydroxyl group, causes premature termination of DNA synthesis upon its incorporation into the nascent DNA chain {White 2004}. The K_i for TFV-DP against HIV-1 RT were determined using both RNA and DNA templates (Table 40). The K_i values for reverse transcription (RNA-dependent DNA synthesis) and the second strand DNA synthesis (DNA-dependent DNA synthesis) are 0.02 and 1.6 μM, respectively {Cherrington 1995a}. The removal of incorporated TFV can occur by wild-type RT and RT with mutations that enhance excision (notably T215F/Y or T69SSS) by both pyrophosphorolysis and ATP-mediated excision mechanisms; however, TFV-terminated primers are efficiently translocated, which can result in partial protection from the excision process {White 2005}, {Marchand 2007}.

Table 40. Kinetic Inhibition Constants of TFV-DP Against HIV-1 Reverse Transcriptase

Template	K_i (μM)	K_m dATP (μM)	K_i/K_m
RNA Template	0.02	0.05	0.40
DNA Template	1.6	4.6	0.35

Source: {Cherrington 1995a}

2.1.3.5. Activity of TAF Against NRTI Resistant Mutants of HIV-1

Resistance analyses of the parent compound, TFV, are relevant to the TAF in vitro resistance profile since TAF is a prodrug of TFV.

Site-directed recombinant virus expressing the K65R mutation showed 3-fold reduced susceptibility to TFV, 3- to 12-fold reduced susceptibility to ABC, ddI, FTC, 3TC, ddC, and stavudine (d4T), but full susceptibility to ZDV (m2.6.3, Section 1.2, TPI 15883). The K65R mutation has also been selected in vitro by ddC, d4T, and ABC; and in vivo by ddI, ddC, and ABC {Gu 1994b}, {Zhang 1994}, {Tisdale 1997}, {De Antoni 1997}, {Garcia-Lerma 2003}. However, in clinical studies, the K65R mutation is infrequently observed to develop with these ARV drugs and is observed in the plasma HIV of 2% to 4% of antiretroviral therapy (ART)-experienced patients {Bloor 2000}, {Winston 2002}, {McColl 2008}.

The activity of TFV against drug-resistant HIV-1 has been extensively studied in vitro. As shown in Table 41, TFV remains active (within 2-fold of wild type) against recombinant mutant molecular clones of HIV-1 expressing ddI resistance (L74V), ddC resistance (T69D), ZDV resistance (D67N + K70R, D67N + K70R + K219Q, or T215Y), or multinucleoside drug resistance (Q151M complex) mutations in HIV-1 RT {Wainberg 1999}, {Srinivas 1998}, {Miller 2001}, {Shirasaka 1995}, {Tisdale 1997}. TFV was fully active against recombinant HIV-1 expressing the K70E mutation that was observed to develop in 2 patients treated with adefovir dipivoxil {Wainberg 1999}, {Mulato 1998}. However, biochemical studies of the K70E mutant RT have suggested low-level reduced susceptibility of this mutant to TFV {Sluis-Cremer 2007}. The M184V substitution is commonly observed in HIV-1 isolates from 3TC- and FTC-treated patients and is associated with high-level resistance to FTC and 3TC and low-level resistance to ABC. TFV shows slightly increased activity against HIV-1 expressing the ABC/3TC/FTC resistance mutation M184V or the combination of the high-level ZDV resistance mutation T215Y and M184V {Wainberg 1999}, {Miller 1999}.

Table 41. Antiviral Susceptibilities of Molecular Clones of HIV-1 Expressing Nucleoside-Associated Resistance Mutations in Reverse Transcriptase

RT Mutation	EC_{50} Fold Increase Above Wild-Type (HXB2D or IIIB)						
	TFV	ZDV	d4T	ddI	3TC	ddC	ABC
D67N + K70R	0.7	5.7	ND	ND	ND	ND	1.7
D67N + K70R + K219Q	1.8	23	ND	ND	3.1	ND	1.2
T69D	2	1.7	4	ND	19	4.3	ND
K70E	1.3	0.6	1.1	1	3.8	0.7	ND
L74V	1	2	1.1	2.8	2.4	3.9	3.7
Q151M[a]	0.8	39	69	42	1.9	7.3	ND
M184V	0.2–0.9	0.7	1.5	2.8	> 50	1.8	4.9
T215Y	1.8	6.9	1.6	2.2	1.1	1.3	2.2
T215Y + M184V	0.5	0.7	1.1	2	< 50	1.7	7

a Site-directed recombinant also includes A62V, V75I, F77L, and F116Y RT mutations.
Source: {Wainberg 1999}, {Miller 2001}, {Shirasaka 1995}, {Tisdale 1997}, {Srinivas 1998}

TAF and TFV Antiviral Activity Against Recombinant HIV-1 Clinical Isolates

The susceptibility results with molecular clones of HIV-1 were confirmed and extended with phenotypic analyses of a panel of recombinant HIV-1 clinical isolates from ART-experienced patients (m2.6.3, Section 1.3, PC-120-2014). The potencies of TAF and TFV were determined for 24 patient-derived recombinant HIV-1 variants selected based on their genotypic resistance to multiple NRTIs, spanning a wide range of NRTI resistance. The choice of the mutants present in the panel was meant to capture the diversity of fold changes observed for TFV, from hypersusceptible to highly resistant, and is not representative of their incidence in the HIV-infected population. The activity of TAF and TFV against the tested viruses was determined by Monogram Biosciences (South San Francisco, CA, USA) using the single-cycle PhenoSense® assay {Petropoulos 2000} and expressed as the fold change in the calculated EC_{50} relative to that of the wild-type reference strain HIV-1_{NL4-3}. In the PhenoSense assay, clinical susceptibility cutoffs for TDF have been established at 1.4 (lower cutoff) and 4 (higher cutoff) {Miller 2004}. TFV fold change from wild-type < 1.4, ≥ 1.4 to ≤ 4, and > 4 indicate sensitivity, reduced sensitivity, and resistance, respectively, to TFV.

In terms of fold change compared with wild-type virus, susceptibility to TAF for this panel of HIV-1 mutants was almost identical to TFV, ranging from 0.34- to 23-fold of the EC_{50} (Table 42). Tenofovir and TAF profiles were similar against the tested viruses, with the exception of virus 18 that was categorized differently for TAF compared with TFV, based on the established cutoffs for TDF resistance. Susceptibility cutoffs for TAF have not been established. As a result, there was a strong correlation between the fold change for TFV and TAF with a coefficient of determination (R^2) value of 0.97, as shown in Figure 16, indicating that TAF and TFV show the same resistance profile against NRTI-resistant HIV-1 mutants in this assay.

Table 42. Phenotypic Susceptibilities of 24 Recombinant HIV-1 Isolates with NRTI Mutations Against TAF and TFV

Virus ID	EC_{50} FC[a]		Mutation Category	NRTI Mutations
	TAF	TFV		
13	0.34	0.41	NRTI	L74V
16	0.40	0.47	NRTI + M184V	L74V Y115F M184V*
5	0.50	0.48	M184V	M184V
14	0.43	0.50	NRTI	L74V
22	0.56	0.53	Q151M + M184V	Q151M M184V*
15	0.50	0.59	NRTI + M184V	L74V Y115F M184V*
6	0.67	0.65	M184V	M184V*
21	0.82	0.82	Q151M + M184V	A62V V75V/I F116Y Q151M M184V*
20	0.91	0.93	Q151M	F116Y Q151M*
11	0.78	0.98	K65R + M184V	A62A/V K65R M184V*
12	1.09	1.18	K65R + M184V	K65R M184V*
9	1.68	1.48	K65R	K65R*
10	1.91	1.71	K65R	K65R*
17	1.62	1.81	3 TAMs	M41L L74V L210W T215Y
3	2.11	2.27	6 TAMs + M184V	M41L D67N K70R M184V L210W T215Y K219E
19	3.43	2.82	Q151M Complex	A62V V75I F77L Y115F F116Y Q151M*
1	3.62	3.48	6 TAMs	M41L D67N K70R L210W T215F K219Q*
18	8.80	3.80	5 TAMs	M41L D67N T69D L74V L210W T215Y K219R*
2	4.77	4.01	6 TAMs	M41L D67N K70R L210W T215Y K219E*
4	9.16	6.11	6 TAMs + M184V	M41L D67N K70R M184V L210W T215Y K219E*
24	9.07	9.60	Q151M Complex + K65R	A62V K65R K70K/R V75I F77L F116Y Q151M*
8	20.0	18.0	T69 Insertion	M41L T69ins L74V L210W T215Y*
23	22.0	19.0	T69 Insertion	M41L A62V T69ins L210W T215Y*
7	23.0	20.0	T69 Insertion	A62V T69ins V75I*

FC = fold-change
a Susceptibilities are expressed as FCs in EC_{50} from wild-type control. Wild-type EC_{50} for TAF and TFV was 10 nM and 0.6 µM, respectively.
* Indicates the presence of NNRTI RAMs (not shown).
Source: PC-120-2014

Figure 16. Resistance Profile Comparison Between TAF and TFV in the Monogram PhenoSense Assay

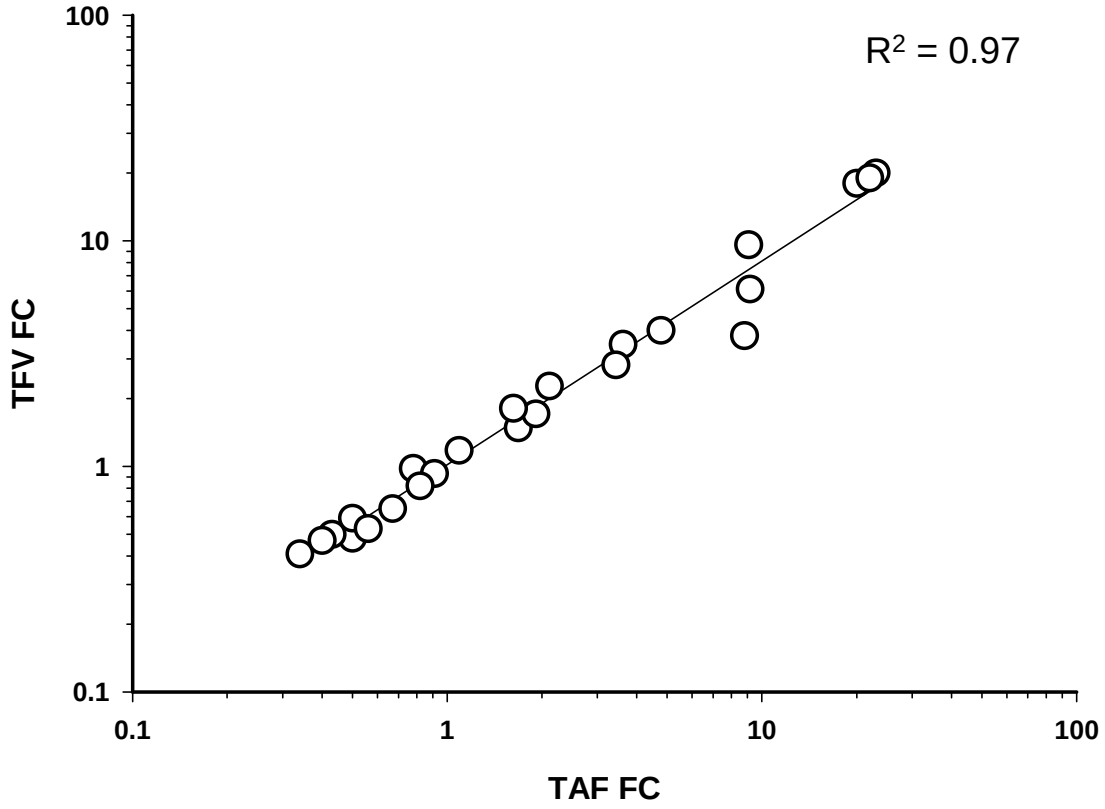

FCs for the panel of 24 recombinant HIV-1 isolates (Table 42) for TAF and TFV were plotted. Linear regression was calculated using SigmaPlot.
Source: PC-120-2014

The panel of recombinant mutants showed TFV fold changes from wild-type ranging from 0.41 to 20, with 11 isolates showing full sensitivity to TFV, 7 isolates showing reduced susceptibility to TFV, and 6 isolates showing full resistance to TFV (Table 42). Most isolates sensitive to TFV had the M184V mutation (8 of 11) plus few additional NRTI resistance mutations, including 2 isolates with K65R + M184V, and no thymidine analog mutations (TAMs; M41L, D67N, K70R, L210W, T215Y/F, K219Q/E/N/R). Isolates with reduced susceptibility to TFV rarely had the M184V mutation (1 of 7 only) and had an increasingly complex resistance pattern, with either ≥ 3 TAMs, K65R alone, or the Q151M MDR complex. Isolates resistant to TFV had either 6 TAMs, Q151M complex + K65R, or double insertions at T69 + other NRTI mutations and/or TAMs. The highest level of resistance to TFV was observed for isolates with T69 double insertions.

TFV Antiviral Activity Against Primary HIV-1 Isolates in PBMC

The activity of TFV was also evaluated against primary PBMC-derived HIV-1 isolates directly in donor PBMCs {Palmer 2001}. The 10 primary HIV-1 isolates in this study were derived from nucleoside-experienced patients, and all isolates expressed one or more nucleoside-associated RT mutations. The drug susceptibility results, as well as the resistance genotype for each isolate,

are presented Table 43 in order of increasing ZDV resistance. Nine of these primary isolates demonstrated high-level 3TC resistance as a result of the M184V RT mutation. The mean fold change in TFV susceptibility of all 10 primary HIV-1 isolates was unchanged from the wild-type reference (range: 0.4 to 2.2). In contrast, these primary HIV-1 isolates showed a mean resistance to ZDV, ABC, and 3TC of 20.4-fold, 11.9-fold, and > 45-fold, respectively.

Table 43. Drug Susceptibilities of Nucleoside-Resistant Primary HIV-1 Isolates

Virus ID	Nucleoside-Associated RT Mutations[b]	Drug Susceptibility (Fold Change from Wild Type[a])			
		TFV	ZDV	ABC	3TC
1-MLS	M184V	0.5	0.3	1.7	> 50
2-JMG	M184V	0.4	0.6	1.9	> 50
3-OT	K70R M184V	0.5	0.7	1.8	> 50
4-RJN	T69N K70R	0.7	1.4	0.8	0.4
5-AB	M41L M184V T215Y	0.4	2.8	8.3	> 50
6-EDM	M41L M184V L210W T215Y	1.0	3.1	6.8	> 50
7-WK	M41L D67N M184V T215F K219Q	1.0	15	4.6	> 50
8-RON	M41L M184V T215Y	1.3	16	26	> 50
9-EMS	D67N K70R M184V T215F K219E	1.5	50	43	> 50
10-GGR	M41L D67N T69D M184V L210W T215Y	2.2	> 100	21	> 50
	Mean (n = 10):	1.0	20.4	11.9	> 45
	Range	0.4 to 2.2	0.3 to > 100	0.8 to 43	0.4 to > 50

a Wild-type HIV_{IIIB} EC_{50} values for ZDV, TFV, ABC, and 3TC were 0.012, 1.7, 0.09, and 0.27 μM, respectively, for these experiments. The fold change from these wild-type EC_{50} values was calculated as the mean of 2 to 3 independent experiments for each nucleoside-resistant primary isolate analyzed.

b NRTI RAMs are any of the following amino acid changes in RT: M41L, A62V, K65R, D67N, T69N/D, K70R, L74V/I, V75T, F77L, Y115F, F116Y, Q151M, M184V/I, L210W, T215Y/F or K219Q/E.

Source: {Palmer 2001}

TFV Antiviral Activity Against NRTI-resistant Recombinant Patient-derived HIV-1 Isolates

The distribution of TFV susceptibility in over 1000 ART-naive, HIV-infected individuals worldwide was determined using the Virco® Antivirogram® assay. In addition, phenotypic susceptibility to TFV and other RT inhibitors was determined in a panel of nearly 5000 recombinant HIV-1 clinical isolates from predominantly ART-experienced patients analyzed as a part of routine drug resistance testing.

Greater than 97.5% of isolates from ART-naive patients had TFV susceptibility < 3-fold above the wild-type controls using the Antivirogram. The clinically derived panel of 5000 samples exhibited a broad range of ARV drug susceptibilities, including 69%, 43%, and 16% having > 10-fold decreased susceptibility to at least 1, 2, and 3 ARV drug classes, respectively. Greater than 88% of these 5000 clinical isolates were within the 3-fold susceptibility range for TFV, and > 99% exhibited < 10-fold reduced susceptibility to TFV.

The results suggest that the majority of ART-naive and ART-experienced individuals are infected with HIV-1 that remains within the normal range of TFV susceptibility and may be susceptible to TDF or TAF therapy {Harrigan 2002}.

A retrospective analysis was undertaken to look for patterns of resistance among TFV-naive, ART-experienced patients that can result in a reduction in TFV susceptibility {Wolf 2003}. In this study, 321 samples from 294 patients that had been sent to the German National Reference Centre for Retroviruses for drug resistance testing between January 1998 and July 2002 were analyzed. When the susceptibility of viruses to TFV was examined, viruses with insertion mutations (n = 6) were highly resistant. Viruses with Q151M could be divided into 2 subsets of susceptible (n = 12) and highly resistant (n = 8), where 7 of 8 viruses in the resistant set also contained K65R. A clonal analysis of viruses containing TAMs (M41L, D67N, L210W, T215F/Y, and K219Q/E/N) showed that when present as single mutations, resistance to TFV could be ranked as increasing for mutations at position 41 > 215 > 70. Additionally, viral clones with M184V or M184I exhibited slightly increased susceptibilities to TFV (0.7-fold), and almost all clones with TAM-induced resistance were resensitized when M184V was present. However, accumulation of at least 2 TAMs resulted in more than 2.0-fold reduced susceptibility to TFV, irrespective of the presence of M184V. Overall, a total of 40.4%, 34.3%, and 25.3% of the viruses had < 1.5-fold, 1.5- to 4.0-fold, and > 4.0-fold reduced susceptibilities to TFV, respectively.

Two studies have confirmed the resensitizing effect of the M184V/I mutation on TFV susceptibility with recombinant clinical isolates using the Monogram Biosciences PhenoSense assay {Ross 2004}, {McColl 2008}. The effect appears across all genotypic backgrounds, including K65R, L74V, and TAMs. For viruses with TAMs (n = 3805), the resensitization effect for viruses containing M184V/I resulted in 19% of isolates showing reduced susceptibility to TFV above the clinical cutoff of 1.4-fold versus 52% of isolates in the absence of M184V/I. The resistance mechanisms of HIV-1 RT with K65R+M184V mutations suggest that the increased susceptibility conferred by M184V to TFV is mediated by decreased incorporation of the competing natural substrate dATP relative to TFV compared with the K65R mutant {Ly 2008}, {Deval 2004}.

Using clonal sequencing analyses of viral populations, recent studies demonstrated that K65R can be found on the same genome as L74V or T215Y, although they do not often occur together {Henry 2006}. A set of studies describe that K65R and TAMs were antagonistic both for their prevalence in database searches of patient isolates, as well as for their resistance profiles and mechanisms of resistance {White 2006}, {Parikh 2006a}, {Parikh 2006b}, {Parikh 2007}. Genotypic and molecular antagonism was also found between the RT mutations K65R and K70E using clonal sequencing of virus from patients, which was primarily explained by the dramatically reduced replication capacity of the constructed double mutant {Kagan 2007}.

TFV Antiviral Activity Against NRTI-resistant HIV-2 Clinical Isolates

In a previous analysis, a panel of HIV-2 clinical isolates with pre- and post-Q151M mutation development and laboratory strain HIV-2_{ROD} was evaluated for drug susceptibilities in a PBMC-based assay {Damond 2005}. The specific components of the ART used that led to the development of Q151M were not described. Prior to the development of the Q151M mutation,

the EC_{50} value for TFV for HIV-2_{ROD} was 0.3 µM, and the clinical isolates had EC_{50} values that ranged from 0.14 to 0.52 µM (n = 4). Of the HIV-2 isolates that showed development of the Q151M mutation in their RT, 2 of 4 patients showed no change in susceptibility to TFV, while the remaining 2 showed 8.6- and 29-fold reductions in TFV susceptibility as compared with pre-Q151M HIV-2. The patients with phenotypic changes also developed either a V111I or a K65R mutation in addition to Q151M. For comparison, all 4 patients had developed reductions in susceptibility to d4T and ABC associated solely with Q151M.

TAF Activity Against HIV-1 with NNRTI, PI, and INSTI Resistance Associated Mutations

The antiviral activity of TAF was assessed against a panel of 7 drug-resistant HIV-1 clinical isolates, including NRTI-R, NNRTI-R, PI-R, and INSTI-R viruses (m2.6.3, Section 1.3, PC-120-2004). Five of the 7 isolates were single class resistant mutants, including 1 NNRTI-R mutant, 2 PI-R mutants, and 2 INSTI-R mutants. The 2 remaining isolates had either NRTI-R + NNRTI-R or NRTI-R + NNRTI-R + PI-R mutants (Table 44).

Virus and activated human PBMCs were mixed in the presence of TAF and incubated for 7 days before antiviral effect (ie, inhibition of RT activity) and cytotoxicity were assessed. In this in vitro experiment, PBMC viability remains high throughout the incubation period; thus, virus-infected cells were used for the assessment of both antiviral activity and cytotoxicity. Various other ARV drugs were included as positive controls, depending on the drug-resistance isolate tested: ZDV for all isolates, NVP and enfuvirtide (T-20) for NRTI-R and NNRTI-R isolates, indinavir and T-20 for PI-R isolates, and RAL and EVG for INSTI-R isolates.

Overall, TAF showed potent antiviral activity against HIV-1 isolates resistant to other ARV drug classes (Table 44). TAF demonstrated antiviral activity against the NNRTI-R, PI-R, and INSTI-R mutants. For the 2 viruses that contained NRTI-R mutations, TAF showed a 2.1- and 5.4-fold reduced susceptibility associated with the presence of the following resistance mutations: 3 TAMs + M184V (D67N, K70R, M184V, and K219E) in the first isolate (5705-72), and MDR Q151M mutation complex (A62V, V75I, F116Y, Q151M) + K65R + TAMs (M41L, K65R, D67N, L210W, and T215Y) in the second isolate (MDR 769). No cytotoxicity was observed with TAF or the other drugs at the concentrations evaluated.

Table 44. TAF Antiviral Activity Against Drug-Resistant Primary HIV-1 Isolates

Isolate ID	Resistance Class	Resistance Mutations	Drug Susceptibility (Fold Change from Wild Type[a])						
			TAF	ZDV	NVP	IDV	T-20	RAL	EVG
A-17	NNRTI-R	RT: K103N Y181C	1.7	0.7	> 380		0.2	—	—
1064-52	PI-R	RT: D67N PR: I54V V82F L90M	0.5	1.0	—	39.3	0.4	—	—
52-52	PI-R	PR: M46I I54V V82T	0.4	0.4	—	15.2	0.2	—	—
8070_1	INSTI-R	IN: G140S Y143H Q148H	0.2	0.2	—	—	—	250	222
4736_4	INSTI-R	IN: E92Q N155H	0.1	0.2	—	—	—	18.9	101
5705-72	NRTI-R, NNRTI-R	RT: D67N K70R K103N M184V K219E	2.1	33.1	279	—	0.6	—	—
MDR 769	NRTI-R, NNRTI-R, PI-R	RT: M41L A62V K65R D67N V75I F116Y Q151M L210W T215Y Y181I PR: M46L I54V V82A I84V L90M	5.4	> 89	—	210	0.7	—	—

— = not tested
a Fold change calculated from the average EC_{50} across wild-type isolates: 3.4 nM (TAF), 11.2 nM (ZDV), 25.1 nM (NVP), 12.0 nM (IDV), 39.4 nM (T-20), 3.1 nM (RAL), 1.0 nM (EVG)
Source: PC-120-2004

2.1.3.6. Viral Resistance Selection Studies with TAF

The resistance profile of TAF was studied in parallel with that of the parent drug TFV in a series of dose-escalation resistance selection experiments in MT-2 cells (m2.6.3, Section 1.3, PC-120-2011). The effect of the increasing selective pressure on the wild-type HIV-1_{IIIB} from TAF and TFV was assessed by analyzing the genotypic and phenotypic changes in the virus over time.

Successive passage of wild-type HIV-1_{IIIB} in increasing concentrations of TAF or TFV led to the emergence of the K65R mutation in RT at drug concentrations between 4- and 15-times EC_{50}, independent of the drug used. Importantly, attempts to increase the drug concentrations beyond 16 times the EC_{50} of each drug (to 24-times EC_{50} [336 nM] for TAF and 24-times EC_{50} [84 µM] for TFV) over > 5 weeks did not yield additional resistance or viable virus. The K65R mutation was accompanied by an S68N mutation in 3 of 4 selections performed, either as a full mutation or mixture. The development of the S68N mutation alongside K65R has been observed previously in TDF/TFV clinical and in vitro studies {Margot 2006b}, {Margot 2006a} where it is likely playing a role in partially restoring reduced replication capacity induced by the K65R mutation {Svarovskaia 2008}. A transient K70E mutation as a mixture with wild-type virus was also observed along with a K65R mutation as a mixture with wild-type virus in the second experiment with TAF, but was not detected at subsequent time points. A transient K70E mutation has been observed previously in clinical studies of TDF and is associated with minor decreases in TFV susceptibility in phenotypic assays {Kagan 2007}, {Margot 2006a}.

The phenotypic resistance of HIV to TAF was also similar to TFV in analyses conducted using the final mutant viruses obtained, with TAF activity reduced 6.5-fold from wild-type for both selected viruses and TFV activity reduced 5.5- and 5.1-fold from wild-type virus for the TAF- and TFV-selected viruses, respectively (Table 45). These minimal differences between TAF and TFV in fold change from wild-type virus for each of the selected viruses were not statistically significant (Student t-test, p-values of 0.17 and 0.25 for TAF- and TFV-selected viruses, respectively). Reduced FTC susceptibility was also observed at similar levels between the 2 selected viruses (8.5- and 6.7-fold from wild-type virus), while susceptibility to the control drugs EFV (NNRTI) and EVG (INSTI) was near wild-type levels, with fold changes of < 2-fold of the wild-type control.

Overall, TAF showed a nearly identical resistance profile to TFV in these experiments, with no development of high-level resistance after extended culture.

Table 45. Characteristics and Drug Susceptibilities of TAF- and TFV-Selected Viruses

Selected Viruses				Drug Susceptibility (Fold Change from Wild Type[a])				
Drug	**Final Concentration (FC over EC_{50})**	**Time Point**	**Genotype**	**TAF**	**TFV**	**FTC**	**EFV**	**EVG**
TAF	224 nM (16×)	Day 148	K65R	6.5[b]	5.5[b]	8.5[b]	1.4	1.7
TFV	56 µM (16×)	Day 154	K65R S68S/N/R/K	6.5[b]	5.1[b]	6.7[b]	1.5	1.4

a EC_{50} values against HIV-1_{IIIB} in MT-2 standard assay were 10 nM, 2.9 µM, 1.2 nM, 0.77 µM, and 1.5 nM for TAF, TFV, EVG, FTC, and EFV, respectively. Fold changes of the average EC_{50} were obtained from 5 independent experiments.
b Student t-test p-value < 0.05 as compared with WT control.
Source: PC-120-2011

2.1.3.6.1. In Vitro Selection of Resistant HIV-1 with TFV and FTC

In vitro resistance selection experiments were performed with the wild-type HIV-1_{IIIB} in the immortalized MT-2 cell line with the combination of TFV and FTC (m2.6.3, Section 1.3, PC-164-2005). In parallel, resistance selections were performed with each drug separately. The concentrations of drugs used to initiate the selection experiments were at the EC_{50} values for each individual drug for the 1-drug selections and one-half the EC_{50} values for the 2-drug selections to allow for adequate virus replication. As summarized in Table 46, FTC-resistant virus was selected in both cultures containing FTC when the concentration of FTC had reached 1.6 µM or 2-fold the EC_{50} value. The genotype of this virus showed an M184I mutation in RT as the dominant mutation, with some evidence of M184V but no other genotypic changes in the first 250 amino acids of RT. Resistant virus continued to grow in the FTC-alone culture at an FTC concentration of 230 µM (> 200-fold resistance to FTC), with further evolution to dominance of the M184V mutation. Previous resistance selection experiments have also resulted in the M184I mutation, which later converted to an M184V mutation upon further in vitro passage {Schinazi 1993}.

Table 46. In Vitro Selection of TFV and FTC Resistant HIV-1

Selecting Drugs	Starting Drug Concentration	Ending Conditions		Days in Culture	HIV RT Genotype
		Drug Concentration	Fold Above EC_{50}		
TFV	3.5 μM	112 μM	32	99	K65R (at 56 μM TFV; Day 56)
FTC	0.8 μM	230 μM	287	48	M184I/V (at 1.6 μM FTC; Day 17) M184V/I (at 230 μM FTC; Day 44)
FTC+TFV	0.4 μM FTC	19.2 μM	24	155	M184I L214F (at 1.6 μM FTC, 7 μM TFV; Day 24)
	1.8 μM TFV	84 μM	24		K65R (at 12.8 μM FTC, 56 μM TFV; Day 114)

Source: PC-164-2005

In the TFV-alone culture, resistance to TFV was observed with the K65R mutation in RT at Day 56 at a TFV concentration of 56 μM, 16-fold above the TFV EC_{50} value. In the FTC-alone culture, resistance to FTC was observed with the M184V/I mutations in RT at Day 17 at an FTC concentration of 1.6 μM. In the combination culture, an M184I mutation was detected at Day 24 in culture and at an FTC concentration of 1.6 μM, and a K65R mutation was observed later at Day 114 at a TFV concentration of 56 μM. The M184I mutation was not observed at this time point; however, the M184V mutation was observed upon subsequent increases in the FTC concentration to 25.6 μM. Attempts to increase the TFV concentration have resulted in a loss of HIV-1 growth in both cultures. The results obtained show that resistance development to FTC occurs much more readily and quickly than resistance development to TFV in vitro. These in vitro results suggest that under conditions of continued viral replication in vivo, the combination of TFV and FTC would initially select for the M184V/I mutation, and then potentially for TFV resistance in the form of the K65R mutation.

2.1.3.6.2. In Vitro Evaluation of TAF Resistance Barrier

The resistance profile for TAF was the same as that for TFV in in vitro drug resistance selection studies with wild-type or NRTI-resistant HIV-1 isolates (Sections 2.1.3.6 and 2.1.3.6.3). However, the in vivo resistance profile may differ between the 2 drugs since the level of TFV-DP achieved in vivo upon loading with TAF is significantly higher (≥ 5 times) than that with TDF (GS-US-120-0104). Therefore, viral breakthrough experiments were conducted using previously defined TDF-resistant HIV-1 isolates (Table 47) in MT-2 cells to model the impact on antiviral efficacy of the 5-to 7-times higher TFV-DP concentration observed in vivo with TAF treatment compared with TDF treatment (m2.6.3, Section 1.3, PC-120-2013). These experiments were conducted at a higher MOI than in the typical EC_{50} assays; the EC_{50} values for TAF and TFV were 0.02 and 5 μM, respectively. The cells were incubated in the presence of TAF or TFV followed by HIV-1 infection. TAF and TFV concentrations were equivalent to the EC_{95} (estimated at 10 × EC_{50}) for each drug, with a 5-fold increase for TAF to take into account the 5-times increase in TFV-DP concentration in vivo. After 4 or 5 days of incubation, cultures were scored for viral breakthrough (ie, presence of virus-induced cytopathic effect). The procedure was repeated every 4 to 5 days for up to 4 weeks.

Table 47. Genotypic and Phenotypic Characteristics of the Viral Isolates for Breakthrough Experiments

Isolate ID	Mutant Category[a]	RT Sequence[b]	FC (EC_{50} Fold Change from WT Control)		
			MT-2 Assay[c]		Monogram Assay[d]
			TAF	TFV	TFV
PD9	3TAMs	D67N K70R M184V K219Q	4.3	3.7	1.9
PD6	3TAMs	M41L L210W T215Y	3.0	3.1	1.8
PD20	3TAMs	M41L L210W T215Y	10.3	7.2	2.9
K65R	K65R	K65R	3.3	3.3	NA
PD11	K65R	K65R M184V	3.3	3.1	2
PD15	Q151M/K65R	M41L A62V K65R T69I K70T L74V V75I Y115F F116Y Q151M M184V	5.9	4.1	2.4
PD25	4TAMs	D67N K70R T215F K219Q	6.1	5.1	3.3
PD30	T69ins	D67E T69SSG	10.1	10.1	4.5
PD31	5TAMs	M41L D67N T69D L210W T215Y K219R	25.5	21.9	4.5
PD34	5TAMs	M41L D67N L210W T215Y K219R	14.8	14.7	5.8

a TAMs: M41L, D67N, K70R, L210W, T215Y/F, K219E/N/Q/R.
b NAMs at positions: 41, 62, 65, 67, 69, 70, 74, 75, 77, 115, 116, 151, 184, 210, 215, and 219.
c Wild-type (LAI) EC_{50} in the MT-2 assay was 0.014, and 3.4 µM for TAF and TFV, respectively.
d Wild-type EC_{50} in the Monogram PhenoSense GT assay was 1 µM for TFV.
Source: PC-120-2013 and PC-120-2015

The results of this experiment (Table 48) showed that physiologically relevant concentrations of TAF inhibited viral breakthrough for the duration of the experiment for 9 to 11 viruses, including viruses with 3 TAMs, K65R, Q151M complex, 4 TAMs, or T69 insertion. In contrast, viral breakthrough was only inhibited for 2 of 11 viruses in the presence of TFV. For viruses with the highest resistance (5 TAMs, fold change > 14), neither TAF nor TFV could achieve inhibition of viral breakthrough. These results are in agreement with the higher activity of TAF compared with TDF observed in vivo and suggest that treatment with TAF may lead to antiviral efficacy against previously defined TDF-resistant viruses.

Table 48. Time to Viral Breakthrough

Isolate ID	Mutant Category[a]	Time to Viral Breakthrough (days)	
		TAF[b]	TFV[b]
LAI	WT	> 28	> 28
PD9	3TAMs	> 28	> 28
PD6	3TAMs	> 28	13
PD20	3TAMs	> 28	4
K65R	K65R	> 28	18
PD11	K65R	> 28	4
PD15	Q151M/K65R	> 28	8
PD25	4TAMs	> 28	8
PD30	T69ins	> 28	4
PD31	5TAMs	8	4
PD34	5TAMs	8	4

a TAMs: M41L, D67N, K70R, L210W, T215Y/F, K219E/N/Q/R
b Drug concentrations were 1× the EC_{95}.
Source: PC-120-2013

2.1.3.6.3. Viral Resistance Selection with TAF and NRTI Resistant Mutants of HIV-1

Resistance selection experiments using HIV-1 isolates with preexisting TFV-resistance (K65R, 3 thymidine analog-associated mutations [3TAMs], and Q151M complex) were carried out with TAF, TFV, and the INSTI comparator RAL to investigate the potential for additional resistance development in the presence of TAF or TFV (m2.6.3, Section 1.3, PC-120-2012). Lymphoid (MT-2) T cells infected with wild-type (HIV-1_{LAI}) and TFV-resistant (HIV-$1_{LAI\ -K65R}$, HIV-$1_{LAI\text{-}3TAM}$, and HIV-$1_{LAI\text{-}Q151M}$) viral isolates were incubated with escalating doses of TAF, TFV, or RAL, with a starting concentration of twice the EC_{50} for each drug (Table 49). Final viral supernatants were sequenced (population sequencing) and phenotyped in a 5-day multicycle antiviral assay in MT-2 cells with TAF, TFV, RAL, ZDV, or EFV.

Table 49. Initial Drug Concentrations Used in Selection Experiments

Viral Isolate	Starting Concentration (2 × EC_{50})		
	TAF (nM)	TFV (µM)	RAL (nM)
HIV-1_{LAI}	30	7	20
HIV-$1_{LAI\text{-}K65R}$	90	21	20
HIV-$1_{LAI\text{-}3TAM}$	90	21	20
HIV-$1_{LAI\text{-}Q151M}$	390	91	20

Source: PC-120-2012

After 6 months of selection with the wild-type isolate HIV-1_{LAI}, the maximum viable TAF or TFV concentration supporting virus growth was 4 times the starting concentration for each drug. The selected viruses acquired the K65R mutation with TAF and the K65R+S68N mutation with TFV (Table 50). Phenotypic analyses of the resulting mutant viruses showed 3.5- and 3.7-fold

decreased susceptibility to TAF and TFV, respectively, for the TAF-selected K65R virus, and 5.2- to 5.4-fold decreased susceptibility to TAF and TFV, respectively, for the TFV-selected K65R+S68N virus.

With the mutant isolate HIV-$1_{LAI-K65R}$, the maximum viable TAF or TFV concentration supporting virus growth was 3 times the starting concentration for TAF and 2 times the starting concentration for TFV (18- and 12-fold increase based on wild-type EC_{50}, respectively). The selected viruses acquired the S68N mutation. Phenotypic analyses of the 3 resulting mutant viruses showed 5.9- to 6.8-fold decreased susceptibility to TAF and similarly reduced susceptibility to TFV (5.9- to 6.3-fold above wild type). These phenotypic fold changes for viruses with K65R+S68N are consistent with the fold changes observed in the wild-type selections.

The maximum viable TAF or TFV concentration still allowing for virus growth when starting with the mutant isolate HIV-$1_{LAI-3TAM}$ (M41L, L210W, T215Y) was 3 times the starting concentration for either drug (18-fold increase based on wild-type EC_{50}). The selected viruses acquired the RT mutation L429I, which is located in the RT connection domain {Champoux 2009}. This mutation has not been previously seen or characterized, as it lies beyond the range of standard genotypic assays (residues 1-400). Phenotypic characterization was obtained for only 3 of the 4 viruses selected with TAF or TFV, due to very weak infectivity of 1 viral isolate. A modest, approximately 2-to 3-fold change increase for both TAF and TFV was observed for all 3 selected viruses compared with the HIV-$1_{LAI-3TAM}$ starting material.

For the heavily mutated HIV-$1_{LAI-Q151M}$ isolate (A62V, K65R, S68G, V75I, F77L, F116Y, and Q151M), the maximum TAF or TFV concentration still allowing for virus growth was 1.5 times the starting concentration for either drug (39-fold increase based on wild-type EC_{50}). The selected viruses acquired the uncharacterized RT mutation T69I. Phenotypic susceptibilities to TAF and TFV for the 2 selected viruses were very similar for the 2 drugs, ranging from 22.1- to 34.5-fold above wild-type virus, and were within 2-fold of the value for the starting material that was determined concurrently. This suggests a very limited impact on resistance, if any, for the emerging T69I mutation in that isolate.

In contrast to TAF and TFV, growth of wild-type and TFV-resistant virus isolates was sustained at much higher concentrations of the control compound RAL (64 times wild-type EC_{50} for each isolate), where the viruses acquired INSTI-resistance mutations with > 13-fold (wild-type isolate) or > 200-fold (TFV-resistant isolates) decreases in RAL susceptibility. This result demonstrates that high levels of resistance can be achieved in this experimental model and, when compared with the relatively low maximal dose for TAF and TFV, suggests a lack of alternative resistance/survival pathways for these viruses under TAF- or TFV-selective pressure. Notably, the K65R mutation reverted to the wild-type residue in the absence of TFV selective pressure (no drug control and RAL control), consistent with the known reduced replication fitness of the K65R virus {Svarovskaia 2008}. Phenotypic susceptibilities to RAL were near wild-type levels for all selected viruses, except those selected with RAL (noted above). Phenotypic susceptibilities of all selected viruses to EFV and ZDV were as expected, with the exception of a low fold change in susceptibility for ZDV with the K65R + S68N mutation.

Overall, the results of this study show limited viral evolution and phenotypic changes after 6 months of resistance selection with TAF or TFV in viruses harboring NRTI−resistance-associated mutation (RAMs).

Table 50. Characteristics and Drug Susceptibilities of Selected Viruses

Virus Name	Selecting Drug	Drug Concentration (FC from WT EC_{50})[a]	Genotype (RT, IN)[b]	EC_{50} and FC from WT Control ($HIV\text{-}1_{LAI}$)[c]				
				TAF	TFV	RAL	ZDV	EFV
$HIV\text{-}1_{LAI}$			RT: WT	0.014	2.6	0.003	0.17	0.002
WT-A3	TAF	120 nM (8×)	RT: **K65R**	3.5*	3.7*	1.0	0.7	0.6
WT-F3	TFV	28 µM (8×)	RT: **K65R**, **S68N**	5.2*	5.4*	1.6	1.2	0.6
WT-R6	RAL	640 nM (64×)	RT: WT IN: **E92Q**, **V151I**	0.9	1.0	13.4*	1.0	0.7
WT-ND	None	NA	RT: WT	1.0	1.1	1.9	0.7	1.0
$HIV\text{-}1_{LAI\text{-}K65R}$			RT: K65R	4.4*	4.9*	1.4	0.9	0.9
K65R-A2	TAF	180 nM (12×)	RT: K65R, **S68N**	5.9*	6.3*	1.9	2.8*	1.3
K65R-A2.5	TAF	270 nM (18×)	RT: K65R, **S68N**	6.8*	6.3*	1.5	2.3*	1.0
K65R-F2	TFV	42 µM (12×)	RT: K65R, **S68N**	6.1*	5.9*	1.2	2.2	1.4
K65R-R6	RAL	640 nM (64×)	RT: **WT** (loss of K65R) IN: **E138K**, **Q148R**, **V151I**	0.8	1.0	>200*	0.9	0.7
K65R-ND	None	NA	RT: **WT** (loss of K65R)	1.0	1.1	2.2	0.9	1.1
$HIV\text{-}1_{LAI\text{-}3TAM}$			RT: M41L, Y181C, G190A, L210W, T215Y (“3TAM”) IN: WT	3.8*	3.7*	1.1	> 90*	> 54*
3TAM-A2	TAF	180 nM (12×)	RT: “3TAM” + **L429I**	8.5*	6.1*	2.2*	> 90*	> 54*
3TAM-A2.5	TAF	270 nM (18×)	RT: “3TAM” + **L429I**	8.6*	6.1*	1.9	> 90*	> 54*
3TAM-F2	TFV	42 µM (12×)	RT: “3TAM” + **L429I**	9*	6.1*	1.7	> 90*	> 54*
3TAM-F2.5	TFV	63 µM (18×)	RT: “3TAM” + **L429I**	ND	ND	ND	ND	ND
3TAM-R6	RAL	640 nM (64×)	RT: “3TAM” IN: **Q148R, D232N**	4.8*	4.9*	> 204*	> 90*	> 54*
3TAM-ND	None	NA	RT: “3TAM”	3.5*	4.2*	2.1*	> 57*	> 54*
$HIV\text{-}1_{LAI\text{-}Q151M}$			RT: A62V, K65R, S68G, V75I, F77L, F116Y, Q151M (“Q151M”) IN: WT	18.6*	19*	1.7	> 90*	3.3*
Q151M-A1.5	TAF	585 nM (39×)	RT: “Q151M” + **T69I**	26.1*	22.1*	1.5	> 90*	3.4*
Q151M-F1.5	TFV	137 µM (39×)	RT: “Q151M” + **T69I**	32.5*	34.5*	2.2*	> 90*	2.7*
Q151M-R6	RAL	640 nM (64×)	RT: “ Q151M” IN: **L74M, Q148R, S230R**	19.3*	15.7*	>264*	> 90*	3.0*
Q151M-ND	None	NA	RT: “Q151M”	15.3*	15.2*	2.0	> 90*	2.4*

a Concentrations based on previously defined EC_{50} values against $HIV\text{-}1_{LAI}$ in MT-2 assay of 0.015, 3.5, and 0.010 µM for TAF, TFV, and RAL, respectively.
b Boldface font indicates changes from starting material. WT IN sequences not shown.
c Fold changes calculated from EC_{50} values for $HIV\text{-}1_{LAI}$ shown in first row (shaded). Data averaged from at least 4 independent experiments.
* p-value < 0.01 (student t-test comparing mutant EC_{50} values with wild-type EC_{50} values)
Source: PC-120-2012

2.1.3.7. Mechanisms of Resistance to TAF

The molecular mechanisms of HIV resistance to TAF should reflect those of TFV since TAF, a prodrug of TFV, is predominantly hydrolyzed to TFV by CatA in target lymphoid cells {Birkus 2008}, {Birkus 2007}.

Reduced susceptibility to TFV associated with the K65R mutation is mediated by a decrease in the incorporation of the active metabolite of TFV, TFV-DP, relative to the natural substrate dATP. This can be enzymatically observed as an increase in K_i in steady-state kinetics experiments and as a decrease in the k_{pol} in presteady-state enzyme kinetics experiments with the K65R mutant RT {Deval 2004}, {White 2005}, {White 2002}. Similarly, presteady-state kinetics showed an approximate 5-fold decrease in incorporation (decreased k_{pol}) for both FTC-TP and 3TC 5′-triphosphate (3TC-TP) for the K65R mutant RT in accordance with the observed decreased susceptibility of the K65R mutant HIV for these drugs (m2.6.3, Section 1.2, TPI 15883). Significant decreases in the incorporation of natural substrates, most notably the purines dATP and deoxyguanosine triphosphate (dGTP), were also observed in this enzymatic analysis. The K65R mutant RT also showed decreased ATP-mediated excision of incorporated NRTIs that resulted in increased stability of the chain-termination activity of NRTIs. The combined effects of altered NRTI incorporation and excision provide explanation for the susceptibility profile of K65R, which showed low-level decreased susceptibility to all NRTIs with the exception of ZDV (which remained fully active due to the strongly decreased excision caused by the mutation) {White 2005}, {Marchand 2007}.

The addition of the M184V mutation to a virus expressing K65R results in an increase in TFV susceptibility to near wild-type values. The mechanism by which this occurs appears to be through a reduction in the affinity of the natural substrate dATP that is associated with the M184V mutation and results in an increase in the incorporation of TFV-DP relative to dATP and, thus, improved TFV susceptibility for the double mutant virus (TPI 15883) {Deval 2004}.

The K65R mutant HIV-1 is also associated with a decrease in replication capacity for HIV-1 expressing this mutation. This has been observed previously for a site-directed mutant expressing the K65R mutation {White 2002} and is shown in Table 51 for a panel of clinical isolates expressing the K65R mutation that were obtained from a random set of plasma samples submitted to Monogram Biosciences for phenotypic analyses {Miller 2003} (m2.6.3, Section 1.3, PC-104-2004). Reduced replication capacity of K65R mutant HIV-1 was also found in macrophages {Perez-Bercoff 2007}. Interestingly, A62V and S68G are 2 mutations in RT that can occur with K65R and can act as partial compensatory mutations to increase the fitness of K65R-containing viruses without significantly altering the resistance to TFV {Svarovskaia 2008}. The M184V mutation is also associated with reduced replication capacity, and the combination of mutations (K65R+M184V) showed the greatest reduction in replication capacity {Deval 2004}. Decreases in natural substrate binding (M184V) and incorporation (K65R) and reduced initiation of minus strand single-stranded DNA synthesis (K65R+M184V) {Frankel 2007} for these HIV mutants are likely responsible for these observed additive decreases in viral replication capacity.

Table 51. Replication Capacity of Primary HIV-1 Isolates with NRTI Resistance Mutations

	N	Replication Capacity			p-value[a]
		Mean	Median	SD	
No NRTI-Associated Mutations	1307	94.9	92.7	45.7	—
M184V/I Alone	291	65.4	60.8	41.5	< 0.0001
K65R Alone	17	57.6	58.7	38.6	0.0008
K65R + M184V/I	12	37.7	27.5	29.3	< 0.0001

a p-value from Student's unpaired t-test.
Source: PC-104-2004

The removal of NRTIs by HIV-1 RT using a pyrophosphate acceptor molecule or a similar mechanism using ATP as an acceptor has been proposed as mechanisms of NRTI resistance {Meyer 1998}. Removal of the inhibitors by these mechanisms frees the HIV-1 RT to incorporate the natural nucleotide substrate and resume/rescue HIV-1 replication. The excision of TFV from TFV chain-terminated primers was originally not detected {Naeger 2000}. However, newer methodology has demonstrated that TFV can be efficiently excised by pyrophosphorolysis and ATP-mediated excision mechanisms {Marchand 2007}, {White 2005}, {White 2006}. The excision of NRTIs occurs only when the nucleotide exists in its pretranslocational state. The binding of the next complementary nucleotide causes the formation of a stable dead-end complex in the posttranslocational state, which blocks the excision reaction. The excision of TFV was highly sensitive to dead-end complex formation, allowing greater chain termination stability. Thus, the rate of excision of TFV is partially neutralized by the facile switch to the posttranslocational state and by dead-end complex formation {Marchand 2007}.

Drug-resistant HIV-1 RT with mutations that are known to cause high-level NRTI excision, such as TAMs either with or without a T69S Ins mutation, also excise TFV at high rates to contribute to resistance {Marchand 2007}, {White 2003}. These mutants also show greater phenotypic changes to TFV in vitro. The greater levels of resistance associated with the M41L-L210W-T215Y pattern of TAM resistance have also been shown to be clinically significant in terms of reduced responses to TDF therapy {Miller 2004}.

2.1.3.8. Antiviral Activity and Cytotoxicity of TAF Metabolites

Two TAF metabolites, M18 and M28, were identified as intermediates during intracellular conversion of TAF to TFV and were also identified as degradation products of TAF during drug product manufacturing (Figure 17). The antiviral activity and cytotoxicity of these metabolites was evaluated in 2 T-lymphoblastoid cell lines (MT-2 and MT-4) following 5 days of compound exposure (m2.6.3, Section 1.3, PC-120-2021). Both metabolites showed weak inhibition of HIV-1 replication; relative to TAF, the inhibitory potency of M18 was 121- to 130-fold lower (EC_{50} values of 0.56 to 0.97 µM) and the inhibitory potency of M28 was 1723- to 2630-fold lower (EC_{50} values of 7.41 to 21.04 µM). Both metabolites had no cytotoxicity up to the highest tested concentration (57 µM).

Figure 17. Structures of TAF and Its Metabolites M18 and M28

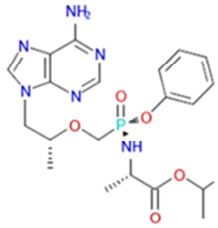

TAF
(GS-7340)

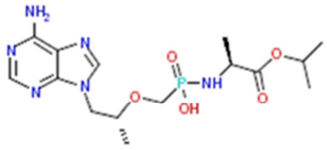

Metabolite M18
(GS-645552)

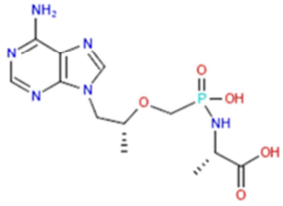

Metabolite M28
(GS-652829)

Source: PC-120-2021

2.1.3.9. Antiviral Activity of TAF Against Hepatitis B Virus

TFV is a potent and selective inhibitor of HBV. TFV inhibits HBV production in HepG2 2.2.15 and HB611 cells with EC_{50} values of 1.1 and 2.5 µM, respectively, and corresponding CC_{50} values of > 100 and 260 µM, respectively (m2.6.3, Section 1.3, P4331-00038) {Yokota 1994}. As observed with anti-HIV activity, TDF showed increased in vitro potency against HBV in comparison with TFV (EC_{50} = 0.018 µM in HEPG2 2.2.15 cells). TFV activity against 4 laboratory strains of HBV with up to three 3TC-associated HBV polymerase mutations was shown to be within 2.2-fold of the wild-type EC_{50} {Yang 2005}. A range of 0.7- to 3.3-fold reductions in TFV susceptibility was observed for 3TC-resistant HBV clinical isolates with multiple mutations in HBV polymerase {Lacombe 2006}, {Brunelle 2007}, {Lada 2004}. In contrast, 3TC demonstrated > 200-fold reduced activity against these HBV mutants. The rtA194T HBV mutant, either alone or in the presence of two 3TC-resistance mutations, showed < 2.4-fold change in TFV susceptibility (m2.6.3, Section 1.3, PC-104-2012). Laboratory strains of HBV expressing adefovir dipivoxil-associated HBV mutations (rtN236T, rtA181V/T) showed reductions in TFV susceptibility ranging from 1.5- to 10-fold as compared with wild type {Qi 2007}. A panel of ETV-associated HBV mutations showed reductions in TFV susceptibility ranging from 0.6- to 6.9-fold as compared with wild type (m2.6.3, Section 1.3, PC-174-2003). TFV has also been shown to inhibit the replication of duck HBV in primary duck hepatocytes with an EC_{50} of 0.11 µM {Heijtink 1994}.

TAF was evaluated in vitro for antiviral activity against HBV (EC_{50}) and cytotoxicity (concentration that results in 50% cytotoxicity [CC_{50}]) in HepG2 cells (m2.6.3, Section 1.3, PC-320-2003 and PC-120-2007). TAF exhibited potent antiviral activity against all tested HBV genotypes (A to H), with an overall mean EC_{50} of 86.6 nM. In addition, TAF had no observed cellular cytotoxicity up to the highest tested concentration (44400 nM). Based on these results, the selectivity (therapeutic) index (SI) for TAF was > 513 in HepG2 cells (Table 52).

Table 52. Anti-HBV Activity and Cytotoxicity of TAF in HepG2 Cells Infected with HBV (A-H)

Drug	EC_{50} (nM)[a]	CC_{50} (nM)	SI[b]
TAF	86.6	> 44400	> 513

CC_{50} = concentration that resulted in 50% cytotoxicity; EC_{50} = concentration inhibiting viral replication by 50%;
SI = selectivity index; TAF = tenofovir alafenamide
a EC_{50} for TAF was mean of EC_{50} value for 11 wild-type clinical HBV isolates representing genotypes A to H, presented below.
b Ratio of CC_{50} to EC_{50}.
Source: PC-320-2003; PC-120-2007

2.1.3.9.1. Antiviral Activity of TAF Against HBV Clinical Isolates

The antiviral activity of TAF was assessed in HepG2 cells against a panel of 11 wild-type clinical HBV isolates representing genotypes A to H (m2.6.3, Section 1.3, PC-320-2003). Full-length genomes or pol/RT regions were amplified from treatment-naive patients infected with genotypes A to H, cloned into expression vectors, and transfected into HepG2 cells. After 7 days of treatment in the presence of TAF, HBV DNA intermediates were extracted and quantified by real-time polymerase chain reaction (PCR) for determination of in vitro susceptibility.

Overall, TAF showed potent antiviral activity against all HBV genotypes evaluated (Table 53). The concentration inhibiting viral replication by 50% (EC_{50}) values for the 11 isolates ranged from 34.7 to 134.4 nM, with an overall mean EC_{50} of 86.6 nM. Although genotypes D and H showed slight hypersensitivity to TAF, all other genotypes had similar TAF EC_{50} values compared with the control laboratory strain, pHY92.

Table 53. TAF Antiviral Activity Against Genotypes A to H Clinical HBV Isolates

Type	Genotype	Isolate ID	HBeAg Status	Cloned[a]	TAF	
					EC_{50} (nM)[b]	EC_{50} FC from Control[c]
HBV	A	001	Negative	Full-length	112.0	1.1
	B	002	Negative	Full-length	109.3	1.1
	C	003	Positive	Full-length	107.5	1.1
		004	Positive	Full-length	64.6	0.6
	D	005	Negative	Full-length	70.5	0.7
		006	Negative	Full-length	62.8	0.6
	E	007	Negative	Full-length	134.4	1.3
	F	008	Negative	pol/RT	92.5	0.9
	G	009	Negative	pol/RT	120.4	1.2
		010	Negative	pol/RT	43.8	0.4
	H	011	Negative	pol/RT	34.7	0.3
	Control (A)	pHY92	NA	Full-length	102.3	1.0

FC = fold change; HBeAg = HBV e antigen; NA = not available; TAF = tenofovir alafenamide
a Full-length genomes or pol/RT regions were amplified and cloned into an expression vector pHY106 or pRTAN (containing HBV genome of pHY92 except pol/RT), respectively, followed by transfection into HepG2 cells.
b Data represent the mean from a minimum of 2 independent experiments performed in quadruplicate.
c Fold change in mean EC_{50} value relative to the pHY92 control (genotype A).
Source: PC-320-2003

2.1.3.9.2. Inhibition of HBV Reverse Transcriptase Enzymatic Activity by the Active Metabolite of TAF

HBV is a member of the Hepadnaviridae family, while HIV-1 is a member of the Retroviridae family. Both HBV and HIV-1 replicate by reverse transcription requiring RNA-dependent DNA polymerase (RDDP), DNA-dependent DNA polymerase (DDDP), and ribonuclease H activities. Therefore, it is not surprising that both HBV and HIV-1 encode a RT enzyme with conserved homology {Toh 1983}. HBV RT has been interchangeably designated as polymerase, RT, or pol/RT, since it contains an additional N-terminal protein domain and spacer domain; the former of which is involved in protein-priming of viral DNA synthesis {Jones 2013}. In the interest of simplicity, the designation of HBV pol/RT will be used below in reference to viral pol/RT-based activities.

The effect of TFV-DP on the DDDP activity of HBV pol/RT was evaluated in an enzymatic assay using recombinant HBV pol/RT expressed and purified from baculovirus {Delaney 2006}. Polymerase activity of HBV pol/RT was inhibited by TFV-DP in a dose-dependent manner without a change in maximal upstroke velocity (V_{max}) (Figure 18). The K_i of DDDP inhibition by TFV-DP was determined to be 0.18 µM, which is 2.1-fold lower than the K_m of dATP (0.38 µM) {Xiong 1998}.

Figure 18. Inhibition of HBV pol/RT DNA-Dependent DNA Polymerase Activity by TFV-DP

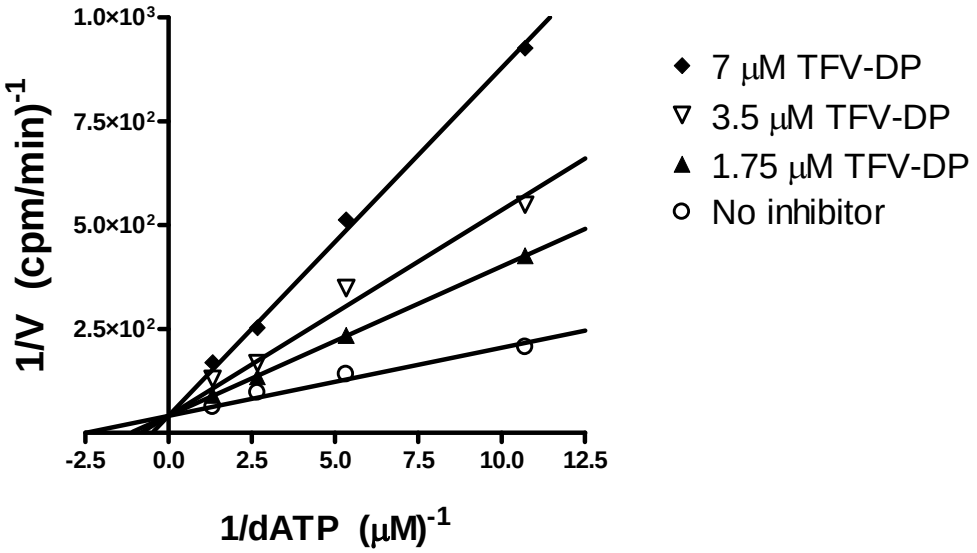

dATP = deoxyadenosine triphosphate; TFV-DP = tenofovir diphoshate; V = velocity
After incubation of HBV pol/RT with activated calf thymus DNA and dNTPs, inhibition of α-^{33}P-labeled dATP incorporation was measured in the presence of indicated concentrations of TFV-DP. Data are presented as a Lineweaver-Burk plot.
Source: {Delaney 2006}

These results showed that TFV-DP inhibits HBV pol/RT by binding competition with dATP into DNA, which caused premature termination of DNA synthesis upon its incorporation into the nascent DNA chain.

2.1.3.9.3. Activity of TAF Against Nucleos(t)ide-Resistant Mutants of HBV

Nucleos(t)ide-resistance RT inhibitor mutations in HBV have been defined for ADV {Hadziyannis 2006}, LAM {Lok 2003}, ETV {Tenney 2009}, and telbivudine (TBV) {Liaw 2009}, however, no detectable TDF resistance has been observed with up to 8 years of treatment {Corsa 2014}. TFV has been shown to exhibit potent inhibition of LAM-R, ETV-R, and TBV-R mutations in vitro. Against ADV-R mutations, TFV exhibits low-level reduced activity in vitro, yet is efficacious in the majority of ADV-experienced patients {van Bommel 2010}, {Qi 2007}, {Yang 2005}, {Patterson 2011}, {Berg 2014}.

To evaluate the antiviral activity of TAF against HBV containing NRTI-R mutation(s), a panel of 11 drug resistant mutants was created in a full-length HBV clinical isolate by site-directed mutagenesis (m2.6.3, Section 1.3, PC-320-2007). Constructs containing ADV-R (n = 5), LAM-R (n = 3), and/or ETV-R (n = 3) mutations were transfected into HepG2 cells and treated with TAF for 7 days in order to determine in vitro susceptibility.

Overall, TAF showed potent anti-HBV activity against all LAM-R (3 of 3) and ETV-R (3 of 3) recombinants and most ADV-R (4 of 5) recombinants, with mean change in EC_{50} values of < 2.0-fold compared with wild type (Table 54). One ADV-R recombinant (rtA181V + rtN236T), exhibited a low-level (3.7-fold) reduced susceptibility to TAF compared with wild type.

In terms of fold change compared with the wild-type isolate, susceptibility to TAF for this panel of recombinants was nearly identical to TFV with minor variability. As expected, all LAM-R and ETV-R recombinants exhibited significantly reduced susceptibility to LAM (> 48.8-fold) and ETV (> 28.6-fold), respectively.

2.1.3.9.4. In Vitro Anti-HBV Activity

Table 54. Antiviral Susceptibility of Recombinant HBV with Nucleos(t)ide-Resistant Mutations in Reverse Transcriptase

Type	RT Mutation(s)[a,b]	EC_{50} FC from WT Control[c,d]				
		TAF	TFV	AFV	LAM	ETV
WT	NA	1.0	1.0	1.0	1.0	1.0
ADV-R	rtA181T[e]	1.7	0.9	1.2	–	–
	rtA181T[f]	1.1	0.6	1.3	–	–
	rtA181V	1.2	1.0	1.2	–	–
	rtN236T	1.4	0.6	1.9	–	–
	rtA181V + rtN236T	3.7	2.8	2.7	–	–
LAM-R	rtM204I	1.6	1.8	–	> 48.8	–
	rtL180M + rtM204V	1.8	1.5	–	> 48.8	–
	rtV173L + rtL180M + rtM204V	0.9	1.6	–	> 48.8	–
ETV-R	rtL180M + rtM204V + rtT184G	1.7	1.2	–	–	> 28.6
	rtL180M + rtM204V + rtS202G	1.5	0.9	–	–	> 28.6
	rtL180M + rtM204V + rtM250V	1.2	1.5	–	–	> 28.6

AFV = adefovir; ETV = entecavir; FC = fold change; LAM = lamivudine; NA = not applicable; -R = resistant; RT = reverse transcriptase; TAF = tenofovir alafenamide; TFV = tenofovir; WT = wild-type; – = not tested

a RT domain-specific amino acid position numbering for HBV polymerase {Stuyver 2001}.
b Site-directed recombinants introduced into WT control (genotype D), followed by transfection into HepG2 cells.
c Fold change in mean EC_{50} value relative to WT control (genotype D). EC_{50} data averaged from at least 2 independent experiments performed in quadruplicate.
d Mean EC_{50} values against WT control for TAF, TFV, AFV, LAM, and ETV were 99.1 nM, 14.4 µM, 6.6 µM, 4.1 µM, and 17.5 nM, respectively.
e rtA181T mutation resulted in a W172* stop codon mutation in HBsAg.
f rtA181T mutation resulted in a W172L mutation in HBsAg.

Source: PC-320-2007; {Liu 2015}

2.1.3.9.5. HBV Resistance Selection Studies of TAF

Treatment of patients with chronic hepatitis B (CHB) with TDF has been shown to be effective in suppressing viral replication and in reducing inflammatory activity. For 2 Phase 3 clinical studies (GS-US-174-0102 and GS-US-174-0103), virologic analyses were performed to identify genotypic changes within HBV pol/RT from subject with detectable viral replication in the presence of TDF treatment. After more than 8 years of resistance surveillance, genotypic or phenotypic resistance to TDF has not been documented {Corsa 2014}.

Typically, the nonclinical resistance profile of TAF, TDF, or parent TFV would be studied in a series of dose-escalation resistance selection experiments in HBV-infected cells. The effect of increasing selective pressure on the wild-type HBV from TAF, TDF, or TFV would be assessed by analyzing the genotypic and phenotypic changes in the propagating virus over time. However, despite the advent of various model systems to characterize the HBV replication cycle, primary human hepatocytes retain susceptibility for infection for only a short time and hepatoma cell lines are not susceptible to infection due to lack of receptor expression {Zeisel 2015}. Therefore, in the absence of a robust tissue culture system that allows for sustained virus propagation, in vitro resistance selection against TAF has not been conducted.

2.1.3.9.6. TAF: In Vitro Efficacy Against Animal Models of HBV

The woodchuck hepatitis virus (WHV) in its natural host, the eastern woodchuck *Marmata monax*, is a frequently used model of HBV infection. While the in vivo efficacy of TAF in WHV-infected woodchucks has not yet been tested, the antiviral effect of oral administration of TDF has been assessed in this model against chronic WHV infection. TDF was evaluated in a short-term (4-week) placebo-controlled, dose-ranging study {Menne 2005}. Oral administration of TDF at 0.5, 1.5, and 5.0 mg/kg/day for 4 weeks reduced serum viral load significantly, resulting in 0.2 ($p < 0.01$), 1.1 ($p < 0.01$), and 1.5 $\log_{10}$ ($p < 0.05$) decreases, respectively, from the pretreatment levels. A dose of 15 mg/kg/day for 4 weeks reduced serum viral load by 1.2 $\log_{10}$ but was not considered statistically significant due to the degree of individual variation in the antiviral response.

In a separate long-term (48-week) study, the antiviral efficacy of oral administration of TDF, ADV, LAM, and FTC as well as the combinations of TDF or ADV with LAM and FTC at 15 mg/kg/day were evaluated in chronic WHV-infected woodchucks (m2.6.3, Section 1.3, PC-174-2004). At 12 weeks of treatment, the TDF-containing groups of TDF alone, LAM+TDF, and FTC+TDF had mean serum viral load reductions of 3.6, 3.7 and 4.2 $\log_{10}$ copies/mL, respectively. Between Weeks 12 and 24, varying degrees of viral rebound were observed across all drug treatment groups. At Week 48, the treatment groups of TDF alone, LAM+TDF, and FTC+TDF had mean serum viral load reductions of 2.9, 5.8, and 6.1 $\log_{10}$ copies/mL, respectively. In the entire 48-week dosing period, there was no evidence of toxicity in woodchucks treated with any of the drugs or drug combinations.

3. SECONDARY PHARMACODYNAMICS

The cytotoxicity, antiviral activity against other viruses, and studies on off-target effects are described in this section.

3.1. Secondary Pharmacodynamics

3.1.1. BIC

3.1.1.1. Cytotoxicity

The in vitro cytotoxicity of BIC was evaluated in multiple cell types of human origin including MT-2 and MT-4 T-lymphoblastoid cell lines, primary T-lymphocytes and macrophages, and in non-target cell lines and primary cells.

3.1.1.1.1. Cytotoxicity and Selectivity of BIC in T-Cell Lines

The cytotoxicity of BIC was evaluated in a 5-day cytopathic assay in uninfected MT-4 and MT-2 cell lines and exhibited CC_{50} values of 3.7 ± 0.1 µM and 10.3 ± 2.5 µM, respectively (Table 55) (m2.6.3, Section 1.1, PC-141-2032). When the antiviral activity of BIC is taken into account, these data indicate an HIV-1 selectivity (ie, CC_{50}/EC_{50} ratio) of ~1530 and ~6870 in MT-4 and MT-2 cells, respectively. BIC and DTG showed weak cytotoxicity (> 3 µM) and high selectivity (> 1500) in these cells lines.

Table 55. Cytotoxicity of BIC in T-Cell Lines

	MT-4 Cells[a]		MT-2 Cells[a]	
Compound	**CC_{50} (µM)**	**Selectivity[b]**	**CC_{50} (µM)**	**Selectivity[b]**
BIC	3.7 ± 0.1	1525	10.3 ± 2.5	6867
DTG	14.7 ± 1.9	9785	5.4 ± 0.2	3567

a CC_{50} values represent the mean ± SD of at least 4 independent measurements in triplicate.
b CC_{50}/EC_{50} ratio. Corresponding EC_{50} values are presented in Table 1.
Source: PC-141-2032.

3.1.1.1.2. Cytotoxicity and Selectivity of BIC in Primary T-Cells and Macrophages

To assess the cytotoxicity of BIC in the natural target cells for HIV-1 infection, cytotoxicity assays were performed in freshly isolated primary human CD4 T-cells and monocyte-derived macrophages (m2.6.3, Section 1.1, PC-141-2034). In these primary cells, cytotoxicity of BIC was less pronounced than in T-cell lines, translating into a larger HIV-1 selectivity (ie, CC_{50}/EC_{50} ratio) of 8,700-fold in CD4+ T lymphocytes and of 4,500-fold in macrophages (Table 56).

Table 56. Cytotoxicity of BIC in Primary Cells

Compound	CD4+ T Lymphocytes[a]		Monocyte-derived Macrophages[a]	
	CC_{50} (µM)	Selectivity[b]	CC_{50} (µM)	Selectivity[b]
BIC	13.0 ± 4.0	8,700	29.8 ± 7.7	4,500
DTG	52 ± 8.5	52,000	24.9 ± 1.2	8,000

a CC_{50} values represent the mean ± SD of 4 independent donors determined in triplicate.
b CC_{50}/EC_{50} ratio. Corresponding EC_{50} values are presented in Table 2.
Source: PC-141-2034

The cytotoxicity of BIC was also tested in fresh human PBMCs in the resting state and upon mitogen activation (m2.6.3, Section 1.1, PC-141-2034). The cytotoxicity of BIC in PBMCs was similar to that observed in primary CD4+ T cells and macrophages and did not significantly change upon the mitogenic activation of PBMCs (Table 57).

Table 57. Cytotoxicity of BIC in Resting and Mitogen-Activated PBMCs

Compound	CC_{50} (µM)[a]	
	Resting PBMCs	Activated PBMCs[b]
BIC	8.4 ± 1.9	5.7 ± 2.2
DTG	30.6 ± 10.0	23.9 ± 3.1

a CC_{50} values (mean ± SD) obtained from triplicate measurements in three independent donors over 6 days.
b Activated for two days with interleukin 2 and phytohemagglutinin prior to drug treatment.
Source: PC-141-2034

3.1.1.1.3. Cytotoxicity of BIC in Non-Target Cell Lines and Primary Cells

BIC was tested for cytotoxicity in 4 non-target human cell lines, including two hepatoma cell lines (Huh7 and HepG2), a prostate carcinoma cell line (PC3) and a normal embryonic lung fibroblast line (MRC5). In addition to these cell lines, the cytotoxicity of BIC was tested in primary human hepatocytes from two independent donors (m2.6.3, Section 1.4, PC-141-2042). BIC did not display any significant cytotoxicity against the four tested cell lines or the primary hepatocytes. CC_{50} values for BIC in the cell lines ranged from 34 to > 44 µM (Table 58). In primary human hepatocytes, BIC exhibited CC_{50} values of > 100 µM (Table 59). DTG exhibited a similar cytotoxicity profile in all the tested non-target human cell types. Puromycin was used as a positive control for cytotoxicity.

Table 58. Cytotoxicity of BIC in Non-Target Human Cell Lines

Compound	CC_{50} in Cell Lines (µM)[a]			
	Huh7 Human hepatoma	HepG2 Human hepatoma	PC3 Human prostate cancer	MRC5 Normal human fibroblasts
BIC	43.6	34.6	> 44	> 44
DTG	> 44	43.3	> 44	30.7
Puromycin	0.72	1.68	0.62	0.36

a CC_{50} values represent the mean of three independent measurements in triplicates.
Source: PC-141-2042.

Table 59. Cytotoxicity of BIC in Primary Human Hepatocytes

Compound	CC_{50} (µM)[a]	
	Donor 1	Donor 2
BIC	>100	>100
DTG	>100	>100
Puromycin	1.2	0.83

a CC_{50} values were obtained from 2 donors with each assay performed in duplicate.
Source: PC-141-2042.

3.1.1.2. Antiviral Activity of BIC Against Non-HIV Viruses

To assess whether BIC has any activity against viruses other than HIV, the compound was tested against hepatitis B and C viruses, influenza A virus, human rhinovirus (HRV), and RSV in cell-based assays (m2.6.3, Section 1.4, PC-141-2043).

BIC was tested in two HCV replicon cell lines containing either HCV genotype 1b or 2a replicons. BIC showed no inhibition of either genotype while 2-C-methyladenosine (2-CMeA), used as a positive control had expected antiviral activity consistent with previously reported data (Table 60). BIC was also tested for anti-HBV activity in the AD38 cell line, which replicates HBV. BIC did not inhibit the replication of HBV while the positive control compounds, FTC and TFV, showed antiviral activity (Table 60).

Table 60. Antiviral Activity of BIC Against Hepatitis Viruses

Compound[a]	HCV 1b Replicon Huh-7 cells[a]		HCV 2a Replicon Huh-7 cells[a]		HBV Production AD-38 cells[a]	
	EC_{50} (µM)	CC_{50} (µM)	EC_{50} (µM)	CC_{50} (µM)	EC_{50} (µM)[b]	CC_{50} (µM)
BIC	>44	>44	>44	>44	>50	>50
DTG	>44	>44	>44	>44	>50	>50
FTC	—	—	—	—	0.02	>50
TFV	—	—	—	—	0.36	>50
2-CMeA	0.112	42.2	0.301	>44	—	—

a Mean of 2 independent measurements in triplicate.
b Based on the production of extracellular HBV DNA.
Source: PC-141-2043.

BIC was also tested against four respiratory viruses including influenza viruses A and B, HRV, and RSV (Table 61). No selective antiviral activity was observed against influenza A or B for either BIC or DTG (CC_{50} values were lower than EC_{50} values). In contrast, the control compound 2'-fluoro-2'-deoxyguanosine (2'-FDG) had the expected level of antiviral activity against both influenza A and B. Neither BIC nor DTG showed any antiviral activity against HRV (tested against a mixture of three serotypes) or RSV type A. In contrast, control compounds rupintrivir and YM-53403 exhibited the expected antiviral activity against HRV and RSV, respectively.

Table 61. Antiviral Activity of BIC Against Respiratory Viruses

Compounds	Influenza NHBE Cells[a]			HRV[c] HI-HeLa Cells[a]		RSV HEp-2 Cells[d]	
	A/PC/1/73[b] EC_{50} (µM)	B/LEE/40[b] EC_{50} (µM)	CC_{50} (µM)	EC_{50} (µM)	CC_{50} (µM)	EC_{50} (µM)	CC_{50} (µM)
BIC	53.5	37.2	32.4	>50	>50	>50	31.7
DTG	12.8	15.1	8.3	>50	>50	>50	1.6
2'-FDG	6.0	14.0	>100	—	—	—	—
Rupintrivir	—	—	—	0.03	>10	—	—
YM-53403	—	—	—	—	—	0.35	>50

a Mean of a single triplicate measurement.
b A/PC/173 and B/LEE/40 represent influenza A and B strain respectively.
c HRV infection performed with an equal mixture of 3 rhinovirus strains containing HRV1A, HRV14, and HRV16.
d Mean of 2 independent measurements in quadruplicate.
Source: PC-141-2043.

3.1.1.3. Molecular Target Screen of BIC

A lead profiling screen (m2.6.3, Section 3.1, PC-141-2029) was conducted to evaluate the binding affinity of BIC (identified as GS-645383 in the report) to a diverse panel of 68 targets, including neuroreceptors, ion channels, and nuclear receptors. BIC showed no significant binding (>50%) at 10 µM, at approximately 290-fold of the estimated clinically efficacious free C_{max} of BIC (C_{max} = 13.7 µM; 0.25% free) when administered as B/F/TAF (50/200/25 mg). Inhibition of transporters, including OCT2 and MATE1, are discussed in m2.6.4, Section 7.1.4.

3.1.2. FTC

3.1.2.1. Cytotoxicity of FTC in Human Cells

The cytotoxicity of FTC has been evaluated extensively in vitro. In all the cell lines examined, cell growth was not affected at concentrations of FTC ≥ 100 µM. Results are shown in Table 62.

Table 62. Cytotoxicity of FTC in Comparison to 3TC and ZDV

Cells	CC_{50} (µM)		
	FTC	3TC	ZDV
MT-4	> 100[a], > 200[b]	> 100[a], > 33[b]	20[a], > 100[b]
PBMC	> 100[a]	> 100[a]	> 100[a]
CEM	> 100[a], > 100[b]	> 100[a], > 100[b]	14.3[a], > 6[b]
Vero	> 100[a]	> 100[a]	28.0[a]
IM9	> 100[b]	> 100[b]	70[b]
Molt 4	> 100[b]	> 100[b]	10[b]
HepG2 2.2.15	> 200[b], > 200[c]	> 200[b]	> 200[b]

3TC = lamivudine; FTC = emtricitabine; ZDV = zidovudine
a Data from reference: {Schinazi 1994}
b Data from reference: {Van Draanen 1994}
c Data from reference: {Furman 1992}

Because of the apparent correlation between toxicity to bone marrow progenitor cells in vitro and bone marrow suppression in vivo, human bone marrow progenitor colony-forming assays were performed. The concentration of FTC required to inhibit the formation of granulocyte-macrophage colonies by 50% (CC_{50}) was 300 ± 40 µM (n = 6). The CC_{50} for erythroid colonies was 220 ± 8 µM (n = 6).

The combination of TFV and FTC has also been studied in vitro for potential synergistic cellular toxicity in the MT-2 cell line (m2.6.3, Section 1.12, PC-164-2002). In combination studies of up to 5 µM FTC and 50 µM TFV, no effect on cell viability was observed using a XTT-based enzymatic assay. In all drug combinations, cell viability values were > 90% of controls that did not contain any drugs. Thus, there was no evidence of synergistic cellular toxicity for the combination of TFV with FTC in vitro. These results are in agreement with the high CC_{50} values for each individual drug (> 100 µM) and the overall high selectivity ratios for the individual drugs with reference to their anti-HIV-1 activities (> 100-fold).

3.1.2.1.1. In Vitro Cytotoxicity in Human Renal Proximal Tubule Epithelial Cells

The potential in vitro cytotoxicity of TFV alone or in combination with FTC (+COBI and EVG) was investigated in primary human renal proximal tubule epithelial cells (RPTECs) (m2.6.3, Section 1.6, PC-236-2012). Following a 5-day treatment, TFV was not cytotoxic to RPTECs from 2 independent donors at the highest concentrations tested (4000 µM) using either a cell viability or a lactate dehydrogenase release (LDH) readouts (Table 63). Tenofovir in combination with FTC (+COBI and EVG) did not affect the cytotoxicity of TFV in RPTECs when tested at concentrations corresponding to their respective peak plasma levels in HIV-infected patients treated with a clinical dose of each compound.

Table 63. Effect of COBI, FTC, and EVG on the Cytotoxicity of TFV in Human RPTECs

Compound	CC_{50} (µM)[a]	
	Cell Viability	LDH Release
TFV	> 4000	> 4000
COBI	26.2 ± 5.3	39.4 ± 0.8
EVG	13.7 ± 0.1	32.7 ± 0.1
FTC	> 100	> 100
TFV + COBI (2 µM)[b] + EVG (4.5 µM)[b] + FTC (8 µM)[b]	> 4000	> 4000
TFV + COBI (0.06 µM)[c] + EVG (1.2 µM)[c] + FTC (0.49 µM)[c]	> 4000	> 4000

LDH = lactate dehydrogenase; RPTECs = primary human renal proximal tubule epithelial cells
a The results represent mean ± SD from 4 independent experiments performed in RPTECs from 2 separate donors. CC_{50} values were determined in parallel from both cell viability (Cell Titer Glo) and from lactate dehydrogenase release readouts.
b The tested concentrations of COBI, EVG, and FTC correspond to peak plasma levels (C_{max}) in HIV-infected patients treated with a clinical dose of each compound.
c The tested concentrations of COBI, EVG, and FTC correspond to trough plasma levels (C_{min}) in HIV-infected patients treated with a clinical dose of each compound.
Source: PC-236-2012

3.1.2.1.2. In Vitro Cytotoxicity in Human Embryonic Kidney Cells Transiently Expressing Renal Transporters

The potential effect of FTC (+COBI and EVG) on the cytotoxicity of TFV was investigated in an in vitro model consisting of human embryonic kidney 293T cells co-expressing renal transporters organic anion transporter 1 (OAT1) and multidrug resistance-associated protein 4 (MRP4), which are known to mediate TFV active renal secretion (m2.6.3, Section 1.6, PC-236-2013). Tenofovir cytotoxicity was measured in these cells either alone or in combination with FTC (+COBI and EVG). Following a 4-day treatment, TFV showed minimal cytotoxicity in control cells that did not express the renal transporters (CC_{50} > 2000 µM) (Table 64). The cytotoxicity of TFV in cells expressing OAT1 was markedly increased due to its active intracellular accumulation (CC_{50} = 78.7 ± 1.3 µM). The OAT1-mediated cytotoxicity of TFV was reduced upon co-expression of MRP4 in the same cells due to increased efflux of the drug (CC_{50} = 299.5 ± 81.3 µM). Combination of TFV with either COBI alone or FTC (+COBI and EVG) at their pharmacologically relevant concentrations showed no significant change in the cytotoxicity of TFV in cells transiently expressing OAT1 alone, or OAT1 and MRP4 together.

Table 64. Effect of FTC (+COBI and EVG) on the Cytotoxicity of TFV in 293T Human Embryonic Kidney Cells Transiently Expressing Renal Transporters

Transient Gene Expression	Cytotoxic Effect, CC_{50} (µM)[a]			
	Puromycin	TFV	TFV + COBI (2.1 µM)[b]	TFV + COBI (2.1 µM)[b] + EVG (4.5 µM)[b] + FTC (8.2 µM)[b]
Negative Control	0.35 ± 0.02	> 2000	> 2000	> 2000
OAT1	0.21 ± 0.10	78.7 ± 1.3	68.3 ± 0.4	68.0 ± 4.1
OAT1 + MRP4	0.22 ± 0.06	299.5 ± 81.3	230.9 ± 82.6	228.8 ± 51.2

MRP4 = multidrug resistance protein 4; OAT1 = organic anion transporter 1
a The results represent mean ± SD from 3 independent experiments performed in transiently transfected 293T cells. CC_{50} values were determined from a cell viability (Cell Titer Glo) readout.
b The tested concentration of FTC, COBI, and EVG correspond to their respective peak plasma levels (C_{max}) in HIV-infected patients treated with a clinical dose of each compound.
Source: PC-236-2013

3.1.2.2. Inhibition of Cellular DNA Polymerases by FTC-TP

The inhibition of human HeLa cell DNA polymerases α, β, γ, and ε by FTC-TP was examined under steady-state conditions (m2.6.3, Section 1.2, TEZZ/93/0007) {Painter 1995}. Activated calf thymus DNA was used as the template for analysis of each enzyme. Under these conditions, FTC-TP was a weak inhibitor of each of the human DNA polymerases when compared with HIV-1 RT. Apparent K_i values were 6.0 µM for polymerase α; 17 µM for polymerase β; 6.0 µM for polymerase γ; and 150 µM for polymerase ε.

Inhibition of human DNA polymerase γ (Pol γ) is one of the proposed mechanisms for nucleoside analogue-derived toxicity. Therefore the potential for FTC-TP and 3TC 5'-triphosphate to serve as substrates for Pol γ was investigated using pre steady-state kinetics (m2.6.3, Section 1.2, TPI 9501). For dCTP (the natural substrate), FTC-TP, and 3TC 5'-triphosphate, the order of incorporation efficiency is dCTP (k_{pol}/K_d = 40 $\mu M^{-1}s^{-1}$) > 3TC 5'-triphosphate (k_{pol}/K_d = 0.014 $\mu M^{-1}s^{-1}$) > FTC-TP (k_{pol}/K_d = 0.0006 $\mu M^{-1}s^{-1}$). The low rate of incorporation and poor binding affinity of FTC-TP makes it the least favorable substrate for Pol γ in this analysis.

3.1.2.2.1. Evaluation of Mitochondrial Toxicity by FTC-TP

As a variety of clinical symptoms observed in patients with HIV treated with prolonged NRTI therapy may be linked to mitochondrial toxicity, the potential for mitochondrial toxicity of FTC was evaluated. HepG2 cells were incubated with FTC at concentrations ranging between 0.1 and 10 µM for 2 weeks (m2.6.3, Section 1.3, {Cui 1996}), and MT-2 cells were incubated with FTC at concentrations up to 100 µM for up to 8 weeks (m2.6.3, Section 1.5, TPI 11963). Under these conditions, FTC had no adverse effects on cell growth, mtDNA synthesis, or lactic acid production. In a separate study conducted in HepG2 cells exposed to concentrations of FTC ranging from 0.1 to 10 µM for 7 days, no effects on mitochondrial morphology were observed by transmission electron microscopy (m2.6.3, Section 1.5, 233 {Sommadossi 1996}).

The inhibition of mtDNA synthesis was also assessed in an in vitro cell culture assay using Molt-4 cells (a T-lymphoblast cell line). The ratio of mitochondrial to cellular DNA was determined after exposure of cells to clinically relevant concentrations of FTC (0.1, 1, 10, and 100 μM) (m2.6.3, Section 1.5, TGZZ/93/0016 and TGZZ/93/0023). The ratio of mtDNA to genomic DNA for Molt-4 cells treated with several nucleoside analogues is shown in (Table 65).

Treatment of Molt-4 cells with various concentrations of ddC resulted in a reduction of the mtDNA content of the cells. After 5 days of treatment with 0.05 μM ddC, there was an 80% reduction in the ratio of mitochondrial to cellular DNA; however, there was no apparent increase in doubling time of the treated cells (data not shown). At 0.5 μM ddC, there was a 92% reduction in the ratio of mitochondrial to cellular DNA.

Emtricitabine did not reduce the ratio of mitochondrial to cellular DNA when tested at concentrations of up to 100 μM after 7 days of continuous cell exposure.

Table 65. Ratio of Mitochondrial DNA to Cellular DNA in Molt-4 Cells

Compound	N	Concentration (μM)	Days	Mitochondrial DNA/Cellular DNA (Percent of Control)
Zalcitabine (ddC)	2	0.05	5	20 ± 10
		0.1	5	11 ± 8
		0.5	5	8 ± 1
		5.0	5[a]	ND
Emtricitabine (FTC)	2	0.1	7	104 ± 10
		1.0	7	121 ± 11
		10.0	7	98 ± 15
		100.0	7	123 ± 19
Zidovudine (ZDV)	1	0.5	9	130
		5.0	9	174
Fialuridine (FIAU)	2	0.1	7	82 ± 27
		0.5	7	89 ± 37
		5.0	2[a]	173 ± 78
Alovudine (FLT)	1	0.05	7	41
		0.1	7	17
		0.5	7	14
		5.0	5[a]	7
Stavudine (d4T)	1	0.5	9	113
		5.0	9	60

ND = not determined
a Cell death
b Standard deviation, n > 1
Source: TGZZ/93/0016 and TGZZ/93/0023

Thymidine analogues were also examined. After 7 days of treatment with 0.05 μM alovudine (FLT; 3'-dideoxy-3'-fluorothymidine), there was a 59% reduction in the ratio of mitochondrial to cellular DNA. After 9 days exposure to 5 μM d4T ((2R,5S)-1-(2,5-dihydro)-5-(hydroxymethyl)-2-furyl thymidine)), there was a 40% reduction in the ratio of mitochondrial to cellular DNA. In contrast, fialuridine (FIAU) caused no reduction in the ratio of mitochondrial to cellular DNA after 7 days exposure to 0.1 or 0.5 μM of drug; however, significant cell death was noted after exposure to 5 μM FIAU for 2 days. Zidovudine (3'-azido-3'-deoxythymidine, ZDV) at 0.5 or 5.0 μM caused no significant decrease in the ratio of mitochondrial to cellular DNA after 9 days exposure. It should be noted that cell death occurred at 5 μM ddC, FLT, and FIAU. Cell death was not noted in ZDV- or FTC-treated cells at concentrations up to 100 μM.

The lack of impact of FTC on mtDNA content and function is consistent with its very low affinity for DNA polymerase γ (Section 3.1.2.2).

3.1.2.3. Activity of FTC Against HBV

The in vitro anti-HBV activity of FTC has been studied extensively using the stably HBV-transfected cell line HepG2 2.2.15. In this system, FTC decreased levels of extracellular and intracellular HBV DNA in a dose-dependent manner. The EC_{50} values determined by various investigators using extracellular HBV DNA levels ranged from 0.01 to 0.04 μM. The FTC EC_{50} value based on intracellular DNA was somewhat higher, 0.16 μM, than the EC_{50} values based on extracellular DNA (Table 66) {Furman 1992}. In contrast to the situation with HIV, the EC_{50} values for FTC and 3TC are comparable against HBV.

Condreay and colleagues examined the effect of FTC on HBV replication in primary human hepatocytes {Condreay 1996}. Although EC_{50} values were not calculated, FTC at 2 μM completely inhibited the production of intracellular HBV DNA, even when added 24 hours after infection. The EC_{50} value calculated from inhibition of extracellular virus production is < 0.02 μM, a value that is comparable with that determined in HepG2 2.2.15 cells (Table 66).

Table 66. Anti-HBV Activity in HepG2 2.2.15 Cells of Compounds Approved and Under Development for HBV Infection

Compound	EC_{50} Values
FTC	0.01 ± 0.005 μM[a], 0.04 ± 0.006 μM[b]
β-L-Fd4C	< 0.1 μM[d]
Adefovir	0.03 ± 0.01 μg/mL[c]
Amdoxovir	13 ± 2.1 μg/mL[c]
Clevudine	0.1 ± 0.06 μg/mL[c]
Entecavir	0.004 μM[e]
L-dT	0.19 ± 0.09 μM[d]
L-dC	0.24 ± 0.08 μM[d]
3TC	0.008 ± 0.003 μM[a], 0.0016 ± 0.0005 μg/mL[c]
Lobucavir	0.1 ± 0.1 μg/mL[c]
Penciclovir	3.5 ± 0.2 μg/mL[c], 2.5 μM[d]
TFV	0.04 ± 0.02 μg/mL[c]

a Source: {Furman 1992}
b Source: {Schinazi 1994}
c Source: {Ma 1997}
d Source: {Shaw 1996}
e Source: {DeMan 2001}

Inhibition of HBV Reverse Transcriptase Enzymatic Activity by FTC-TP

The replication cycle of hepadnavirus includes the reverse transcription of an RNA template. This process is carried out by a polymerase that shares significant sequence homology with the RT of retroviruses, including HIV. Since all attempts to date to purify the human HBV DNA polymerase have been unsuccessful, examination of the effect of FTC-TP on HBV DNA polymerase was carried out using an endogenous polymerase assay. In this assay, intact virus particles are treated with 1% Nonidet-P40, a nonionic detergent that partially disrupts the virus particles and allows nucleotide 5′-triphosphate substrates to enter the virus particle so that DNA synthesis can occur. Davis and colleagues, using the endogenous polymerase assay, demonstrated that the HBV DNA polymerase could incorporate [α-^{32}P]FTC-TP into minus-strand DNA {Davis 1996}. Endogenous polymerase assays using HBV particles isolated from cell cultures treated with FTC-TP showed either reduced or no polymerase activity depending on the concentration of FTC-TP used. Furthermore, the particles produced in FTC-TP treated cells did not contain any detectable HBV plus strand DNA, which is consistent with the chain-terminating activity of incorporated FTC 5′-monophosphate. Taken together, the results demonstrate that FTC-TP serves as an alternative substrate inhibitor of the HBV DNA polymerase.

HBV Viral Resistance Selection Studies with FTC

Treatment of HBV-infected patients with 3TC has been shown to be effective in suppressing virus replication and in reducing inflammatory activity. However, resistance to this agent has been documented to be associated with mutations in the YMDD motif (amino acids 203 to 206) in domain C of the viral DNA polymerase, analogous to changes seen in the YMDD motif of HIV-1 RT. Inhibition assays performed using the hepatoma derived cell lines AD38 and AD79 {Cullen 1997}, which replicate wild-type and the M204V mutant HBV, respectively, confirmed that the HBV M204V mutation conferred resistance to FTC as well as to 3TC.

3.1.2.4. FTC: In Vivo Efficacy Against Viruses in Animal Models

The in vivo anti-hepatitis activity of FTC was first tested in a chimeric mouse model {Condreay 1994}. NIH bg-nu-xid mice were subcutaneously injected with suspensions of 10^7 HepG2 2.2.15 cells. Subcutaneous injection of these cells in mice resulted in the development of HBV-producing tumors in all animals. Hepatitis B virus could be detected in serum samples from the tumor-bearing mice using an immunoaffinity system linked to quantitative PCR. Beginning 1 week after injection, mice were orally dosed with 0.9, 3.5, 18.4, and 88.8 mg/kg/day FTC for 21 days. Comparison of tumor progression and human α-fetoprotein levels in control versus drug-dosed mice indicated that FTC did not have antitumor activity. However, FTC at the 18.4 and 88.8 mg/kg/day doses did significantly reduce circulating levels of HBV DNA. Examination of tumor extracts in these 2 dose groups revealed a marked reduction in intracellular levels of replicative HBV DNA intermediates, including double-stranded linear DNA.

Transgenic SCID Mice

Anti-HBV activity has also been reported for FTC in HBV transgenic SCID mice {Kamkolar 2002}. A group of 5 mice were treated with FTC at 100 mg/kg/day intraperitoneally for 6 days, and observed for an additional 6 days posttreatment. By Day 3 of treatment, 2 mice had undetectable HBV surface antigen (HBsAg), and an additional 2 mice cleared HBsAg on Day 5. The remaining mouse cleared HBsAg on Day 8. Hepatitis B virus DNA levels in blood were determined by semiquantitative PCR at Days 3, 5, 8, and 12. By Day 3 of treatment, PCR signals had dropped 10-fold in all of the mice. By Day 8, none of the mice had detectable HBV DNA levels by PCR. In contrast to 3TC, there were no signs of rebound in the levels of HBV DNA during the course of treatment.

Woodchuck Hepatitis Virus

The WHV in its natural host, the eastern woodchuck Marmata monax, is the most frequently used model of HBV infection. In an oral dosing study, 5 groups of chronically infected woodchucks were given FTC once daily at 1 of 5 doses (0.3, 1.0, 3.0, 10, or 30 mg/kg) for 4 weeks {Korba 2000}. At doses of 3.0 mg/kg and greater, FTC induced a statistically significant reduction in both serum viremia and replicative intermediates. The largest reduction in viremia, approximately 4.9 $\log_{10}$, and in replicative intermediates, approximately 80-fold, was seen at the 30-mg/kg dose. No significant effect on the levels of intrahepatic RNA, serum levels of WHV surface antigen (WHsAg), or the appearance of antibodies to WHsAg or WHV core

antigen in the serum were observed. Viremia returned to pretreatment levels within 1 to 2 weeks following the cessation of treatment at all doses. This rapid rebound is consistent with a lack of significant impact on levels of WHV closed-circular complementary DNA (cDNA).

Cullen and colleagues have studied the effect of FTC on WHV in naturally infected, wild-caught woodchucks {Cullen 1997}. Animals were dosed intraperitoneally at either 20 or 30 mg/kg twice daily for 4 weeks. Administration of the 20-mg/kg dose suppressed WHV DNA levels from 6- to 49-fold (average of 27-fold in the 6 animal groups). Serum DNA polymerase activity measured by the incorporation of [^{32}P]dCTP into WHV DNA was reduced in a similar fashion. A more profound effect was seen at the 30-mg/kg dose. Serum WHV DNA levels were reduced from 20- to 150-fold (average of 56-fold) in the 6 animal groups. Serum DNA polymerase activity was similarly reduced. Woodchuck hepatitis virus DNA levels in the liver (determined in biopsy specimens) were also reduced in all 6 of the animals in the 30-mg/kg treatment group. Reductions ranged from 68% to 98% of the pretreatment levels. The authors stated that while the level of replicative intermediates remained close to those seen pretreatment, the WHV genome was being shifted toward shorter fragments.

3.1.2.5. In Vitro Receptor Binding Potencies of FTC

The effects of FTC (named 524W91 in the report) on the specific binding of various radioactively labeled ligands were studied in 19 different receptor binding assays (m2.6.3, Section 1.5, TPZZ/93/0002). Tissues from Sprague Dawley rats were obtained in all but 2 assays. A heart preparation was obtained from beagle dogs for use as a calcium release channel-binding assay, and platelets which were isolated from New Zealand White rabbits were used for a platelet activating factor assay. Emtricitabine had no pharmacologically significant binding affinity to the receptors tested.

3.1.2.5.1. In Vitro Autonomic Pharmacology Effects on Peripheral Autonomic Receptors by FTC

A variety of isolated muscle preparations were used in vitro to assess effects of FTC on autonomic function and peripheral receptors (m2.6.3, Section 1.5, TPZZ/92/0055). Emtricitabine (0.1 µM or 1.0 µM) had little or no direct effect on various isolated muscle preparations and had no major inhibitory effects on the contractile responses to acetylcholine, norepinephrine, serotonin, isoproterenol, arachidonic acid, histamine, bradykinin, and angiotensin II.

3.1.3. TAF

3.1.3.1. Cytotoxicity in Human PBMCs and Cell Lines

The cytotoxicity profiles (CC_{50} values) of TAF, its stereoisomer GS-7339 (Figure 19), TDF, and TFV were investigated in resting and dividing human PBMCs following 5 days of continuous drug incubation (m2.6.3, Section 1.3, PC-120-2009). The maximum concentrations of drugs used were 100, 100, 50, and 2000 µM, for TAF, GS-7339, TDF, and TFV, respectively. Notably, TAF is only present at significant levels in the systemic circulation for less than 2 hours {Ruane 2013}; therefore TAF doses used in this in vitro study were supra-therapeutic in concentration and duration. CC_{50} values for TAF ranged from 6.8 µM in dividing PBMCs to 25.1 µM in

resting PBMCs (Table 67), leading to a high SI of > 1,900 in dividing PBMCs when compared with the EC_{50} value of 3.6 nM (m2.6.3, Section 1.3, PC-120-2004). The higher CC_{50} value obtained for GS-7339 compared with TAF indicates an even lower potential for cytotoxicity for the diastereomer and is supported by the limited conversion of the stereoisomer to TFV-DP {Lee 2005}. Overall, TAF showed a favorable toxicity profile in resting and dividing PBMCs.

Figure 19. Chemical Structures of the Diastereomers TAF and GS-7339

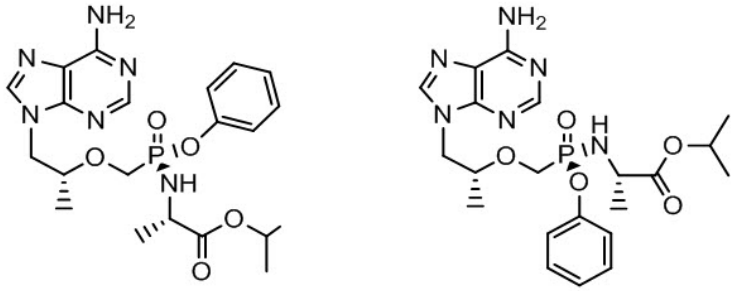

GS-7340 (TAF) GS-7339

Source: Report PC-120-2009

Table 67. In Vitro Cytotoxicity of TAF, GS-7339, TDF, and TFV in Resting and Dividing PBMCs

Class	Drug	Cytotoxicity CC_{50} (µM)[a]	
		Resting PBMCs	Dividing PBMCs
NtRTI	TAF	25.1 ± 11.5	6.8 ± 1.8
	GS-7339	> 124.6	> 186.2
	TDF	69.7 ± 22.1	19.6 ± 5.2
	TFV	> 2652	2150 ± 532

CC_{50} = drug concentration that results in a 50% reduction in cell viability; NtRTI = nucleotide reverse transcriptase inhibitor; PBMC = peripheral blood mononuclear cell; TAF = tenofovir alafenamide; TDF = tenofovir disoproxil fumarate; TFV = tenofovir

a Mean ± SD values from PBMCs isolated from up to 9 donors.

Source: PC-120-2009

The cytotoxicity profiles (CC_{50} values) of TAF, TDF, TFV, and a panel of clinically relevant antiretroviral inhibitors were also evaluated in 2 T-lymphoblastoid cell lines (MT-2 and MT-4) following 5 days of exposure (m2.6.3, Section 1.3, PC-120-2007). TAF had no observed cellular toxicity up to the highest tested compound concentration (53 µM) in the MT-2 cells. CC_{50} values for TAF ranged from 23.2 to > 53.0 µM in the 2 T-lymphoblastoid cell lines (Table 68). Based on observed CC_{50} and EC_{50} values, TAF exhibited SIs relative to antiviral activity of 1997 to > 3607 in T-lymphoblastoid cell lines, which was consistent with the results in PBMCs described above. Overall, TAF showed low cytotoxicity, and had a similar cytotoxicity profile in T-cell lines compared with other clinically relevant antiretroviral inhibitors.

The cytotoxicity profiles (CC_{50} values) of TAF, TDF, TFV, and a panel of clinically relevant antiretroviral inhibitors were also evaluated in a hepatic cell line (HepG2) following 5 days of exposure (PC-120-2007). The CC_{50} value for TAF was > 44.4 µM in the hepatic cell line (Table 68). TAF had no observed cellular toxicity up to the highest tested compound concentration (44.4 µM) in HepG2 cells. Overall, TAF had a similar cytotoxicity profile in hepatic cells compared with other clinically relevant antiretroviral inhibitors.

Table 68. In Vitro Cytotoxicity of TAF and other HIV Inhibitors in Human T-Lymphoblastoid and Hepatic Cell Lines

Class	Drug	Cytotoxicity CC_{50}, µM (MSD)[a]		
		Hepatic	T-Cell	
		HepG2	MT-2	MT-4
NtRTI	TAF	>44.4 (1)	>53.0 (1)	23.2 (1.13)
	TDF	>44.4 (1)	37.1 (1.02)	22.9 (1.04)
	TFV	>44.4 (1)	7605 (1.06)	6264 (1.13)
NRTI	FTC	>44.4 (1)	>53.0 (1)	>53.0 (1)
	3TC	>44.4 (1)	>53.0 (1)	>53.0 (1)
	ABC	>44.4 (1)	40.7 (1.02)	>53.0 (1)
	ZDV	>44.4 (1)	>53.0 (1)	>53.0 (1)
	ddI	>44.4 (1)	>53.0 (1)	>53.0 (1)
	ddC	>44.4 (1)	>53.0 (1)	>53.0 (1)
NNRTI	EFV	10.1 (1.05)	25.4 (1.03)	26.4 (1.04)
INSTI	RAL	>44.4 (1)	>53.0 (1)	>53.0 (1)
PI	ATV	>44.4 (1)	>53.0 (1)	>53.0 (1)
Control	PUR[b]	1.0 (1.12)	0.4 (1.05)	0.2 (1.06)

3TC = lamivudine; ABC = abacavir; ATV = atazanavir; CC_{50} = drug concentration that results in a 50% reduction in cell viability; ddC = zalcitabine; ddI = didanosine; DRV = darunavir; EFV = efavirenz; FTC = emtricitabine; INSTI = integrase strand transfer inhibitor; NNRTI = nonnucleoside reverse transcriptase inhibitor; NRTI = nucleoside reverse transcriptase inhibitor; NtRTI = nucleotide reverse transcriptase inhibitor; PI = protease inhibitor; RAL = raltegravir; TAF = tenofovir alafenamide; TDF = tenofovir disoproxil fumarate; TFV = tenofovir; ZDV = zidovudine

a All cells were treated for 5 days. Cytotoxicity CC_{50} values represent geometric of independent experiments (n=3) generated using 384-well assays. Multiplicative standard deviations (MSD) are shown in parenthesis.

b Puromycin (PUR) was used as a positive control in cytotoxicity assays.

Source: PC-120-2007

3.1.3.1.1. Hematopoietic Toxicity of TAF

The effects of TAF were investigated on human myeloid and erythroid progenitor cells using bone marrow from 3 human donors (m2.6.3, Section 1.6, PC-120-2016). Two TAF exposure conditions were evaluated: a continuous incubation for 14 days and a 12-hour pulse incubation with washout for 14 days. The continuous incubation was evaluated as a comparator (the standard procedure for these assays). The 12-hour pulse with washout was evaluated to better mimic the limited in vivo TAF plasma exposure (T_{max} = 38 minutes, $t_{1/2}$ = 25 minutes) at concentrations significantly above the mean TAF plasma C_{max} of 0.484 µM observed at steady

state in clinical studies {Ruane 2013}. The effects of continuous and 12-hour pulse incubation (in liquid media) with TAF on human erythroid and myeloid progenitor proliferation cultured in MethoCult™ 84434 media using 3 different prequalified frozen bone marrow lots were examined.

In the continuous incubation, the extrapolated IC_{50} was 3.3 µM for myeloid progenitor cell proliferation; the IC_{50} was > 3 µM for erythroid progenitor cell proliferation. Overall, TAF showed IC_{50} values in the continuous incubation in a range similar to other primary cells, such as activated PBMCs (IC_{50} = 6.8 µM; m2.6.3, Section 1.6, PC-120-2009). In the 12-hour pulse incubation exposure, the TAF IC_{50} was > 3 µM (the highest concentration tested) for erythroid and myeloid progenitor cell proliferation. Therefore, the IC_{50} values for TAF under continuous and pulsed exposure conditions were at least 7-fold higher than the clinical C_{max}, supporting a favorable profile in myeloid and erythroid progenitor cells.

Table 69. In Vitro Hematopoietic Toxicity of TAF in Comparison with 5-Fluorouracil

Bone Marrow Lot	Continuous Incubation				12-Hour Pulse Incubation			
	Erythroid IC_{50} (µM)		Myeloid IC_{50} (µM)		Erythroid IC_{50} (µM)		Myeloid IC_{50} (µM)	
	TAF	5-FU	TAF	5-FU	TAF	5-FU	TAF	5-FU
BM07B21195	> 3	3.20	3.30[ex]	3.97	> 3	20.34	> 3	51.41
BM10A33225	> 3	3.89	3.92[ex]	2.49	> 3	118.80[ex]	> 3	91.15
BM10AOF3062	> 3	4.09	>3	1.06	> 3	69.43	> 3	67.05

5-FU = 5-fluorouracil; ex = extrapolated value
Source: Report PC-120-2016

3.1.3.1.2. Hematopoietic Toxicity of TFV

The hematopoietic toxicity of TFV and 4 other NRTIs (ZDV, d4T, ddC, and 3TC) was evaluated in human $CD34^+$ bone marrow progenitor stem cells exposed to specific cytokines, which programmed their differentiation and expansion into the erythroid and myeloid lineages {Cihlar 2002}. The expansion of the 2 lineages in the presence of the tested drugs was determined with progenitor cells from 2 independent donors by immunofluorescence detection of lineage-specific cell surface markers. Irrespective of the donor, TFV, at concentrations as high as 200 µM, showed no significant effect on the expansion of the erythroid lineage from the progenitor stem cells as determined by the level of expression of glycophorin A (Table 70). Likewise, TFV showed only limited effects on the expansion of the myeloid lineage based on the expression of CD11b, with the inhibition being more pronounced in progenitor cells from donor 2 (CC_{50} of 85 µM). Likewise, 3TC exhibited only a weak cytotoxicity against both the erythroid and myeloid lineages, with a moderate degree of inhibition observed at a concentration of 200 µM. In contrast, ZDV and d4T produced notable suppression of the erythroid and myeloid lineage expansion. Zalcitabine caused by far the most severe suppression of both the erythroid and myeloid lineages with CC_{50} values ranging from < 0.06 to 0.38 µM.

Table 70. In Vitro Hematopoietic Toxicity of TFV in Comparison with Other NRTIs

Drug	Hematopoietic Toxicity – CC_{50} [µM][a]			
	Myeloid Lineage		Erythroid Lineage	
	Donor 1	Donor 2	Donor 1	Donor 2
TFV	> 200	85	> 200	> 200
ZDV	49	3.6	0.85	0.62
d4T	200	10.5	5.0	3.3
ddC	0.38	0.24	0.14	< 0.06
3TC	> 200	140	> 200	170

3TC = lamivudine; CC_{50} = drug concentration that results in a 50% reduction in cell viability; d4T = stavudine; ddC = zalcitabine; TFV = tenofovir; ZDV = zidovudine

a Concentration of each drug inhibiting production of the myeloid or erythroid lineage from progenitor stem cells by 50%. The results are from a single experiment performed in triplicate.

Source: {Cihlar 2002}

3.1.3.1.3. Renal Transporter-Dependent Cytotoxicity

The cytotoxicity of TAF and TFV was assessed in human HEK293T cells transiently expressing OAT1 and organic anion transporter 3 (OAT3) (m2.6.3, Section 1.6, PC-120-2018). Cells were incubated with serial dilutions of TFV or TAF for 4 days. TFV was more cytotoxic in OAT1- and OAT3-expressing cells compared with control transporter null cells (> 21- and > 3.6-fold change in CC_{50} values, respectively) (Table 71). Due to greater cellular permeability, the cytotoxicity of TAF was greater than TFV in control cells. However, there was little to no change in cytotoxicity associated with TAF in OAT1- and OAT3-expressing cells compared with control transporter null cells (0.5- to 3.5-fold change in CC_{50} values, respectively). The minor increase in CC_{50} value for TAF in OAT3-expressing cells compared with control cells was not associated with an increase in TAF intracellular levels, and similar changes in cytotoxicity were observed for puromycin and gemcitabine (other drugs that are not transported by OAT3). In addition, the SI (considering CC_{50} in renal HEK293 cells expressing OAT1 or OAT3 relative to EC_{50} in primary CD4+ T lymphocytes) for TAF (29,000 and 4270, respectively) was much higher than for TFV (14 and 82, respectively). Taken together, these results indicate that TAF does not interact with the renal transporters OAT1 or OAT3, and exhibits no OAT-dependent cytotoxicity in human epithelial kidney cells transiently expressing these transporters.

Table 71. In Vitro Cytotoxicity of TAF and TFV in the Presence and Absence of Organic Anion Transporters 1 and 3 in Human Epithelial Kidney Cells

Compound	CC_{50} (μM)[a] (Fold Change)[b]			HIV-1 EC_{50} (μM)[c]	Selectivity Index (OAT1)[d]	Selectivity Index (OAT3)[d]
	Control Cells	OAT1-Expressing Cells	OAT3-Expressing Cells			
TFV	> 2000 (1.0)	94 ± 71 (> 21.3)	553 ± 174 (> 3.6)	6.7 ± 2.2	14	82
TAF	163 ± 42 (1.0)	319 ± 56 (0.5)	47 ± 17 (3.5)	0.011 ± 0.003	29,000	4270

CC_{50} = drug concentration that results in a 50% reduction in cell viability; OAT = organic anion transporter; TAF = tenofovir alafenamide; TFV = tenofovir
a Data represent mean ± SD from 5 independent experiments performed in triplicate.
b Control CC_{50}/OAT CC_{50}
c EC_{50} values were calculated 3 days after infection of activated primary human CD4+ T lymphocytes with pseudotyped HIV-1 containing a luciferase reporter and incubation with serial dilutions of TFV or TAF.
d CC_{50}/EC_{50}
Source: Table modified from {Bam 2014b}; PC-120-2018

3.1.3.1.4. Renal Proximal Tubule Epithelial Cells

Effects of TFV have been studied in several in vitro models for renal proximal tubular toxicity and compared with those of cidofovir and adefovir in order to better understand the in vivo differences in nephrotoxicity observed between the 3 structurally related nucleotide analogs. In normal human RPTECs, TFV showed a negligible effect on cell growth with a CC_{50} of > 2,000 μM (Table 72). Moreover, TFV did not exhibit any marked effect on the long-term viability of quiescent RPTECs during a 25-day incubation (Table 72). In contrast, the half-life of quiescent RPTECs in the presence of cidofovir and adefovir was approximately 10 and 21 days, respectively (m2.6.3, Section 1.6, P4331-00037). In a separate study, TFV did not cause significant changes in cell viability in RPTECs after 22 days at concentrations up to 300 μM {Vidal 2006}.

Integrity of the proximal tubule epithelium is essential for maintaining the selective barrier between blood and urine. As shown in Table 72, TFV at concentrations as high as 3 mM did not significantly affect the in vitro integrity of the differentiated proximal tubule epithelium when assessed by measuring the transepithelial resistance after a 10-day drug incubation {Cihlar 2001}. By comparison, cidofovir and adefovir reduced the tubular epithelium integrity by 50% at 110 μM and 1.1 mM, respectively.

Human renal OAT1, a protein localized in the basolateral membrane of the renal proximal tubule epithelium, has been implicated in the etiology of cidofovir- and adefovir-associated nephrotoxicity {Ho 2000}. OAT1 has also been shown to induce the cytotoxicity of TFV by enhancing its intracellular accumulation in kidney cells. Unlike TFV, TAF does interact with and is not a substrate for OAT1 {Bam 2014b}.

Transport kinetics experiments revealed similar transport efficiency (calculated as V_{max}/K_m ratio) for cidofovir, adefovir, and TFV (Table 72) {Cihlar 2001} suggesting that a lack of interference with essential intracellular function(s) rather than a difference in renal transport is responsible for the improved nephrotoxicity profile of TFV.

Table 72. Profiles of TFV, Cidofovir, and Adefovir in In Vitro Models of Renal Proximal Tubular Toxicity

In vitro Assay	Tenofovir	Cidofovir	Adefovir
Inhibition of RPTECs growth; CC_{50} [μM][a]	> 2,000	260	495
Viability of RPTECs; $t_{1/2}$ [days][b]	> 25	9.7	21
Integrity of RPTEC epithelium; $CTER_{50}$[c] [μM]	> 3,000	110	1,100
Efficiency of human OAT1-mediated transport [V_{max}/K_m]	3.26	1.77	1.93

CC_{50} = drug concentration that results in a 50% reduction in cell viability; OAT1 = human organic anion transporter 1; RPTEC = renal proximal tubule epithelial cell
a CC_{50} was determined after 4 days incubation.
b In the presence of 500 μM drug.
c $CTER_{50}$, concentration reducing the transepithelial resistance of RPTEC monolayer cultured on microporous membrane by 50%. Epithelium integrity was evaluated after 10 days incubation.
Source: Report P4331-00037, {Cihlar 2001}

3.1.3.1.5. TAF Intracellular Metabolism in Primary Human Osteoblasts

Antiretrovirals, including TDF, have been associated with decreases in bone mineral density in clinical studies; therefore, the cytotoxic effect of clinically relevant TAF concentrations on PBMCs and primary osteoblasts was assessed in vitro (m2.6.3, Section 1.6, PC-120-2008). Drug loading studies with PBMCs determined that a 2-hour pulse and washout of 124 to 370 nM of TAF achieved intracellular TFV-DP levels comparable to those observed in vivo with a 25 mg dose of TAF. This dosing of TAF in vitro also aligned with the in vivo TAF plasma C_{max} of 484 nM. Comparable TFV-DP levels were achieved in primary osteoblasts with 3 days of daily 2-hour pulses at TAF concentrations similar to those used for PBMCs (100 to 400 nM).

No change in cell viability was observed in either primary osteoblasts or PBMCs. The mean TAF CC_{50} in primary osteoblasts with a 2-hour pulse and washout was > 500 μM, which is > 1033 times higher than the TAF plasma C_{max} (Table 73). In contrast, the cytotoxicity of 2 PIs, nelfinavir (NFV) and lopinavir (LPV), were 3.4 and 1.8 times higher than their respective C_{max} values (not adjusted for protein binding). In summary, primary osteoblasts were not preferentially loaded by TAF relative to PBMCs, and achieved comparable TFV-DP levels as PBMCs in vitro. Furthermore, there was no change in osteoblast or PBMC viability at clinically relevant TAF concentrations. In contrast, the CC_{50} values of the HIV-1 PIs NFV and LPV were only 3.4- and 1.8-fold higher than their respective C_{max} values (not taking into account plasma protein binding). Both of these PIs are documented to exhibit toxicity in cell lines and are associated with bone mineral density decreases in vivo {Callebaut 2011}, {Duvivier 2009}.

Table 73. In Vitro Cytotoxicity of TAF in Primary Osteoblasts

Clinical Data		Osteoblast In Vitro Assay Data				Ratio
Drug	**C_{max} (µM)**	**Drug**	**Treatment**	**N**	**CC_{50} (µM)[a]**	**CC_{50}/C_{max}**
TAF 25 mg QD	0.484 (TAF)[b]	TAF	2-hour pulse	5	>500	>1033
	0.05 (TFV)[b]	TFV	Continuous	4	>1000	>20000
TDF 300 mg QD	1 (TFV)[c]	TFV	Continuous	4	>1000	>1000
NFV 1250 mg BID	7 (NFV)[d]	NFV	Continuous	4	23.5 ± 4.5	3.4
LPV 800 mg QD[e]	18.7 (LPV)[f]	NFV	Continuous	4	33.5 ± 3.8	1.8

CC_{50} = drug concentration that results in a 50% reduction in cell viability; LPV = lopinavir; NFV = nelfinavir; TAF = tenofovir alafenamide; TDF = tenofovir disoproxil fumarate
a Mean ± SD
b {Ruane 2012}
c {Gilead Sciences Inc. 2013}
d {Agouron Pharmaceuticals Inc. 2013}
e Boosted with RTV 200 mg
f {Abbott 2013}
Source: PC-120-2008

3.1.3.2. Effect of TFV Diphosphate on Cellular DNA Polymerases

As described in Section 2.1.3.1, TAF is predominantly hydrolyzed to TFV by CatA cleavage in target lymphoid cells {Birkus 2008}, {Birkus 2007}, resulting in high intracellular levels of TFV-DP in vivo {Markowitz 2011}. The in vitro specificity of TFV-DP for viral polymerases relative to its interaction with mammalian DNA polymerases was determined.

Table 74 summarizes the inhibitory effects of TFV-DP on DNA synthesis catalyzed by the mammalian DNA polymerases α, β, and γ and by the rat DNA polymerases δ and ε {Cherrington 1995a}, {Kramata 1996}. The K_m for the natural substrate dATP is also shown. TFV-DP showed specificity for HIV-1 RT with K_i/K_m ratios 4- to 170-fold higher for mammalian DNA polymerases compared with HIV-1 RT. The K_i/K_m ratio was very high (85.3) for mtDNA polymerase γ, suggesting a low potential of TFV to interfere with the synthesis of mtDNA {Cherrington 1995a}. Additional studies have shown that 1 mM TFV-DP exhibited little effect on the in vitro replication of SV40 DNA indicating a significant specificity of TFV-DP toward the viral RT in comparison to the host DNA replication complex {Pisarev 1997}. Similar conclusions of strong specificity of TFV-DP toward HIV-1 RT have been made using pre-steady state enzyme kinetic experiments {Suo 1998}.

Table 74. Kinetic Inhibition Constants of TFV-DP Against DNA Polymerases α, β, γ, δ, and ε Versus HIV-1 Reverse Transcriptase

Enzyme	K_i (μM)	K_m dATP (μM)	K_i/K_m
Human DNA pol α	5.2	2.7	1.92
Human DNA pol β	81.7	5.6	14.6
Human DNA pol γ	59.5	0.7	85.3
Rat DNA pol δ/PCNA	7.1	0.7	10.2
Rat DNA pol ε	95.2	6.1	15.6
HIV-1 RT	0.21	0.42	0.50

DNA = deoxyribonucleic acid; PCNA = proliferating cell nuclear antigen; pol = polymerase; RT = reverse transcriptase
Data from references: {Cherrington 1995a}, {Kramata 1996}

In order to evaluate TFV-DP as a potential substrate for host polymerases, its incorporation efficiency into a DNA primer/template by human DNA polymerases α, β, and γ relative to the natural 2'-deoxynucleoside triphosphates (dNTPs) has been determined and compared with that of the triphosphates of other NRTIs {Patterson 2005}. TFV-DP showed similar or lower incorporation by DNA polymerases α and β compared with dideoxyadenosine triphosphate (ddATP; the active metabolite of ddI), dideoxycytidine triphosphate (ddCTP), 3TC-TP, and stavudine triphosphate (d4T-TP) (Table 75). Importantly, DNA pol γ incorporates TFV-DP into a DNA primer/template with a very low efficiency (0.06%) relative to the natural substrate. This observation confirms the conclusions from the inhibition studies above that TFV-DP has a low potential for host polymerase inhibition.

Table 75. Relative Efficiencies of Incorporation into DNA of TFV-DP and NRTI-Triphosphates by Human DNA Polymerases α, β, and γ

	Relative Efficiency of Incorporation (%)[a]		
dNTP Analog	Pol α	Pol β	Pol γ
TFV-DP	1.4	1.3	0.06
ddATP	0.25	80	20
ddCTP	0.1	125	25
3TC-TP	0.05	9.0	0.13
d4T-TP	6.3	142	8.0

dNTP = 2'-deoxynucleoside triphosphates
a Relative efficiency of incorporation (%) = $100 \times [V_{max}(\text{dNTP analog})/K_m(\text{dNTP analog})]/[V_{max}(\text{dNTP})/K_m(\text{dNTP})]$.
Source: {Cihlar 1997} .

3.1.3.2.1. Mitochondrial Toxicity

HIV-infected patients treated with NRTIs have exhibited a range of clinical side effects including myopathy, sensory neuropathy, lactic acidosis, and hepatic steatosis {Moyle 2000}, {Carr 2003}. It is believed that NRTI-induced mitochondrial toxicity plays a major role in these adverse symptoms. Many NRTIs, such as ddC, ddI, and d4T, can cause the depletion of mtDNA in cells due to the inhibition of mtDNA polymerase γ {Birkus 2002}, {Pan-Zhou 2000}. In contrast, previous studies have demonstrated a minimal effect of TFV on the mtDNA synthesis in vitro {Birkus 2002}, {Pan-Zhou 2000}.

3.1.3.2.2. Effect of TAF on Mitochondrial DNA Content

The potential for TAF to induce mtDNA depletion was evaluated in HepG2 (m2.6.3, Section 1.6, PC-120-2006), MT-2, and Jurkat T-cells {Stray 2017}. A quantitative real-time PCR assay was performed to measure the relative levels of mtDNA in cells treated with the drug. In this assay, cells treated with TAF (0.1, 0.3, or 1.0 µM for HepG2 cells and 0.37, 1.11, or 3.33 µM for MT-2 and Jurkat cells) for 10 days exhibited no significant reduction in mtDNA compared with untreated cells (Table 76). In contrast, cells treated with ddC (0.2, 2.0, or 20.0 µM for HepG2 and MT-2 cells, and 0.002, 0.02, and 0.2 µM for Jurkat cells) exhibited a dose-dependent decrease in mtDNA content. These data are consistent with the established lack of inhibition of the mtDNA polymerase γ by the active metabolite TFV-DP and suggest that TAF has a low potential for inhibiting mtDNA synthesis and inducing NRTI-related mitochondrial toxicities.

Table 76. Effect of TAF on Mitochondrial DNA Levels in HepG2, MT-2 and Jurkat Cells

Drug	Concentration (µM)	Relative Amount of mtDNA (% mtDNA)[a]	p-value compared with DMSO (Control)[b]
HepG2 Cells			
DMSO (control)	-	100.0 ± 15.3	-
TAF	0.1	86.4 ± 30.5	0.190
	0.3	88.1 ± 35.5	0.294
	1.0	94.6 ± 17.3	0.318
ddC	0.2	86.7 ± 24.2	0.127
	2.0	11.5 ± 6.2	< 0.0001
	20.0	6.6 ± 1.5	< 0.0001
MT-2 Cells			
DMSO (control)	-	102.4 ± 22.8	-
TAF	0.37	116.1 ± 11.2	0.355
	1.11	104.8 ± 4.5	0.862
	3.33	106.7 ± 15.9	0.770
ddC	0.2	94.3 ± 1.2	0.570
	2.0	41.7 ± 10.7	0.002
	20	19.4 ± 0.5	0.0002
Jurkat Cells			
DMSO (control)	-	101.2 ± 16.7	-
TAF	0.37	109.8 ± 12.4	0.434
	1.11	90.0 ± 6.0	0.295
	3.33	84.1 ± 5.7	0.121
ddC	0.002[c]	65.8 ± 6.7	0.087
	0.02	44.9 ± 4.6	0.013
	0.2	9.7 ± 1.3	< 0.0001

ddC = zalcitabine; DMSO = dimethylsulfoxide; mtDNA = mitochondrial DNA; TAF = tenofovir alafenamide
a Data represent the mean ± SD of 3 independent experiments performed in triplicate.
b Paired, 2-tailed Student's t-test.
c Jurkat cells exhibited heightened sensitivity to mtDNA depletion by ddC.
Source: Report PC-120-2006 and {Stray 2017}

3.1.3.2.3. Effect of TFV on Mitochondrial DNA Content

Hybridization analyses to quantify mtDNA and chromosomal DNA levels were performed to assess any relative impairment in mtDNA synthesis with TFV. In HepG2 cells following a 9-day treatment with TFV at concentrations ranging from 3 to 300 mM, no effect of TFV on the

synthesis of mtDNA was observed (Figure 20A). In contrast, ddC and ddI showed marked depletion of mtDNA in HepG2 cells. Stavudine and ZDV showed less pronounced effects, with a reduction of relative mtDNA content of 30% to 40% at 300 μM. Similar to TFV, 3TC and ABC did not significantly change the relative levels of mtDNA (Table 77; m2.6.3, Section 1.6, P1278-00042).

Treatment of skeletal muscle cells (SkMCs) with TFV and other NRTIs yielded very similar conclusions. Proliferating SkMCs did not show any decrease in mtDNA levels following a 9-day incubation with up to 300 μM of TFV (Figure 20B). Lamivudine, ABC, and ZDV also did not deplete mtDNA in these cells. Stavudine moderately reduced mtDNA, while ddC and ddI showed marked depletion of mtDNA in SkMCs. Similar effects of the tested drugs, including no depletion of mtDNA by TFV, were observed upon a 3-week treatment of quiescent nonproliferating SkMCs (Table 77; P1278-00042).

Figure 20. Effect of TFV and Other NRTIs on Mitochondrial DNA Content in Human Liver and Skeletal Muscle Cells

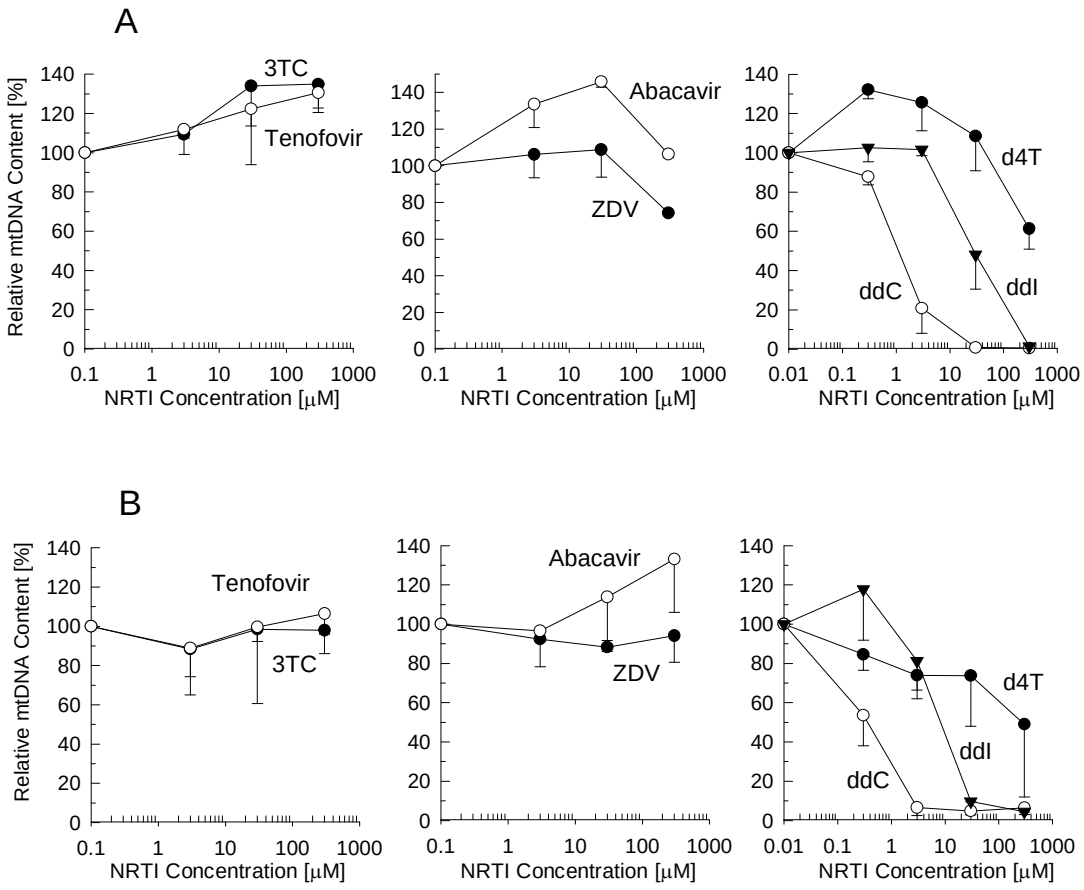

HepG2 human liver cells (A) and human skeletal muscle cells (B) were incubated with various drug concentrations for 9 days and DNA content was determined by hybridization analysis. Data are the means ± standard deviation from two independent experiments.
Source: Report P1278-00042

Effects of the drug on mtDNA in human RPTECs were also characterized. As shown in Table 77, no changes in relative mtDNA levels were observed following up to a 21-day treatment of differentiated RPTECs with TFV or ZDV. While d4T produced minor decrease in mtDNA content, ddC and ddI showed the most pronounced effects on mtDNA in RPTECs (Table 77; m2.6.3, Section 1.6, P1278-00042). In a separate study, levels of mtDNA or cytochrome c oxidase (COX) II mRNA were not affected by TFV treatment of RPTECs for 22 days at concentrations up to 300 μM {Vidal 2006}.

Table 77. Effect of TFV and Other NRTIs on Mitochondrial DNA Content in Differentiated Human Renal Proximal Tubular Epithelial Cells

Drug	Drug Concentration [μM]	Content of mtDNA [% of control][a]	
		12 days	21 days
TFV	300	118 ± 5.9	109 ± 9.2
ZDV	200	109 ± 3.0	104 ± 14.7
d4T	200	92.3 ± 13.9	77.0 ± 10.9
ddC	2	12.1 ± 1.1	5.1 ± 0.6
ddI	40	47.5 ± 5.3	25.7 ± 0.1

d4T = stavudine; ddC = zalcitabine; ddI = didanosine; mtDNA = mitochondrial DNA; TFV = tenofovir; ZDV = zidovudine
a Relative content of mtDNA in RPTECs after 12- and 21-day drug treatment given as mean ± standard deviation from a representative experiment performed in duplicates.
Source: P1278-00042

Overall, the relative effects of the drugs on mtDNA content were similar in all human cell types tested, and correlated well with the efficiencies of incorporation into DNA of the respective dNTP analogs by DNA polymerase γ determined in vitro (see Section 3.1.3.2).

Production of Lactic Acid

Lactic acid production is one of the widely used mitochondrial markers. Drug-related deficiencies in the mitochondrial oxidative phosphorylation system may induce a shift in the pyruvate/lactate ratio leading to increased production of lactic acid {Brinkman 1998}. As shown in Table 78, TFV does not increase the lactic acid production in HepG2 cells and SkMCs after 3- and 6-day incubations, respectively, relative to the untreated controls. Similarly, no effect was observed with 3TC. However, ZDV produced a concentration-dependent increase in the lactate production in both cell types tested (m2.6.3, Section 1.6, P1278-00042). Lactic acid production appears to be one of the few methods by which mitochondrial toxicity can be detected for ZDV in vitro. There were no measurable increases with TFV at concentrations up to 300 μM, and the likelihood of TFV causing clinical lactic acidosis is low.

Table 78. Effects of TFV and Other NRTIs on the In Vitro Production of Lactic Acid

Drug	Concentration (µM)	Lactic Acid Production (mg /10^6 cells)[a]	
		HepG2 cells[b]	SkMCs[b]
None	--	1.61 ± 0.25 (100)	7.53 ± 0.83 (100)
TFV	30	1.34 ± 0.18 (83)	7.23 ± 1.21 (96)
	300	1.62 ± 0.06 (101)	8.79 ± 1.97 (116)
ZDV	30	2.26 ± 0.04 (141)	10.39 ± 0.56 (138)
	300	3.32 ± 0.05 (207)	21.94 ± 4.04 (291)
3TC	30	1.92 ± 0.67 (119)	7.29 ± 1.47 (97)
	300	1.94 ± 0.14 (121)	8.13 ± 0.95 (108)

3TC = lamivudine; TFV = tenofovir; ZDV = zidovudine
a Extracellular lactate production given as a mean ± standard deviation from a representative experiment performed in duplicate. Data in parentheses represent percentage change from the no drug control.
b HepG2 cells and skeletal muscle cells (SkMCs) were incubated with drugs for 3 and 6 days, respectively.
Source: P1278-00042

3.1.3.2.4. Effect of TFV on Mitochondrial Protein Content and Intracellular Lipid Accumulation in a Hepatic Cell Line

The effects of TFV and other NRTIs on levels of mitochondrial proteins in HepG2 cells were also characterized by immunoblot analysis {Birkus 2002}. In particular, COX II and COX IV subunits of cytochrome *c* oxidase are encoded by mtDNA and nuclear DNA, respectively. Following a 9-day treatment with TFV at a concentration of 300 µM, no effect on cellular expression of the COX II and COX IV was observed. In contrast, a 9-day treatment with 30 µM ddC or 300 µM ddI inhibited the expression of COX II by > 90% and COX IV by 40-50%.

In a separate study, the effect of TFV on mitochondrial properties in HepG2 cells was evaluated (m2.6.3, Section 1.6, TX-104-2001). Following treatment for up to 25 days with TFV at concentrations of 1.2 µM and 12 µM, no effect on mtDNA content, COX II levels, lactate production, and lipid content was observed.

In vitro combination studies have been conducted in HepG2 cells to evaluate the potential mitochondrial toxicity of FTC and TFV (as well as other nucleosides) (m2.6.3, Section 1.6, TX-104-2001). HepG2 cells were exposed to FTC and TFV (as well as other nucleosides), either alone or in combination. HepG2 cells were treated for up to 25 days with concentrations of NRTIs equal to 1 and 10 times the maximal therapeutic plasma levels. Assay endpoints included cell growth, extracellular production of lactic acid, relative cellular content of mtDNA and mtDNA-encoded COX II, and intracellular lipid accumulation.

Emtricitabine and TFV alone or in combination with each other or other nucleosides generally had no time- or concentration-dependent effects on cytotoxicity (cell counts) or mitochondrial parameters in HepG2 liver cells. The dual combination of high-dose FTC + ZDV with or without TFV appeared to have greater cytotoxicity than the agents alone, but showed no increase in mitochondrial effects.

These studies confirmed that the potential of FTC and TFV to interfere with mitochondrial functions is low, whether administered alone or in combination with other licensed NRTIs.

3.1.3.3. TAF Activity Against Human Viruses

3.1.3.3.1. TAF: In Vivo Efficacy Against Retroviruses in an Animal Model

In a published study, the simian immunodeficiency virus (SIV) latent cell reservoir in SIV-infected pig-tailed macaques on a regimen of TFV and FTC was analyzed {Shen 2003}. Macaques were infected with SIV and showed primary viremia of 10^5 to 10^7 copies/mL at 2 weeks postinoculation (n = 4). At 50 days postinoculation, viral loads dropped to 10^3 to 10^5 copies/mL, and animals were either treated subcutaneously with TFV (20 mg/kg) and FTC (50 mg/kg) (n = 2) or were not given any drugs (n = 2). The treated macaques achieved SIV levels that were below the limit of detection (ie, < 100 copies/mL of viral RNA), whereas only 1 of the nontreated macaques showed a decrease in SIV RNA. Except for an isolated “blip” of detectable viremia, all treated animals remained close to or below the limit of detection for up to 6 months, suggesting that this regimen was effective against SIV in this macaque model. Given that viral load remained controlled in the treated animals, there was no evidence of resistance development through 6 months of dual therapy with TFV and FTC in this study.

A study was presented that explored preexposure chemoprophylaxis with ARVs as a strategy to prevent the transmission of HIV {Garcia-Lerma 2007}. All animals were subjected to 14 weekly rectal exposures with a low dose of SHIV (SIV/HIV chimeric virus). Three groups of 6 rhesus macaques were injected subcutaneously with TFV/FTC daily, at 2 hours before and 24 hours after the first virus exposure, or at 2 hours before first virus exposure only. Twenty-one control animals did not receive any ARV treatment. Twenty of the 21 control animals became infected after a median of 2.5 challenges. In contrast, all 6 animals treated with TFV/FTC daily or before and 24 hours after the first challenge were fully protected after 14 challenges. In the single-dose group, 1 of 6 animals was infected (data from 10 challenges were analyzed). In this animal model, the multiple-dose TFV/FTC combination provided a high level of protection against repeated virus challenges, whereas the single dose was highly effective, but not sufficient to fully protect against rectal transmission.

3.1.3.3.2. TAF: Antiviral Activity Against Non-HIV Viruses

The antiviral activity of TAF and TFV was assessed against a panel of 18 animal viruses, including ≥ 1 isolates of adenovirus, dengue type 2, influenza A, parainfluenza 3, RSV, coxsackie B virus, rhinovirus, herpes simplex virus (HSV) type 1 (HSV-1), HSV type 2 (HSV-2), human cytomegalovirus (HCMV), varicella zoster virus (VZV), vaccinia virus, HCV, HIV-1, and SIV (m2.6.3, Section 1.3, PC-120-2003). Virus and cells were mixed in the presence of the test compound (TAF or TFV) and incubated for 2 to 7 days, depending on the virus and

assay type, before antiviral effect (ie, cytoprotection) and cytotoxicity were assessed. Each virus was pretitered such that control wells exhibited 85% to 95% loss of cell viability due to virus replication. Therefore, antiviral effect was observed when compounds prevented virus replication.

As expected, both HIV-1 and SIV isolates were potently inhibited by TAF and TFV (Table 79). No antiviral activity was observed against 12 of the 14 remaining human viruses evaluated. TFV weakly inhibited the HSV-2 strain KW with an EC_{50} value of 146 µM, which is consistent with data previously published {Andrei 2011}. Similarly, TAF had an EC_{50} value of 424 nM for this viral isolate in MAGI R5 cells. Of note, initial experiments with HSV-2 strain KW in MRC-5 cells did not yield an EC_{50} value, probably due to a lack of TAF conversion to TFV in this cell type (data not shown). Overall, TAF and TFV activity against HSV-2 KW was 150- to 200-fold weaker than against HIV; weak activity was also observed for the HSV-2 strain MS strain (lab isolate). Finally, TAF had an EC_{50} of 843 nM against human parainfluenza. While the EC_{50} values against human parainfluenza indicate, at best, minimal TAF activity, cell growth inhibition was observed at the 1000 nM, indicating that the observed effect was likely due to cell inhibition. Neither TAF nor TFV exhibited cytotoxicity up to the high test concentrations of 1000 µM (TFV) or 1000 nM (TAF) used for these evaluations. Overall, the results indicate that TAF is a potent inhibitor of immunodeficiency retroviruses such as HIV and SIV and is a weak inhibitor of HSV-2. These results indicate that TAF is a highly specific antiviral agent with no relevant in vitro activity against the other tested human viral pathogens.

Table 79. TAF and TFV Antiviral Activity Against Human Viruses and SIV

Viruses	TAF (nM)		TFV (µM)		Positive Control
	EC_{50}	CC_{50}	EC_{50}	CC_{50}	
HIV-1_{NL4-3}	5.89	> 1000	2.30	> 100	ZDV
HIV-1_{BaL}	2.04	> 1000	1.05	> 100	ZDV
SIV_{mac239}	1.21	> 1000	0.73	> 1000	ZDV
SIV_{mac251}	0.51	> 1000	0.35	> 1000	ZDV
Adenovirus	> 1000	> 1000	> 1000	> 1000	RBV
Dengue Virus	> 1000	> 1000	> 1000	> 1000	RBV
HCV	> 1000	> 1000	> 1000	> 1000	rIFN-α
Coxsackie B Virus	> 1000	> 1000	> 1000	> 1000	enviroxime
Rhinovirus	> 1000	> 1000	> 1000	> 1000	enviroxime
Vaccinia	> 1000	> 1000	> 1000	> 1000	cidofovir
Influenza A	> 1000	> 1000	> 1000	> 1000	zanamivir, RBV
Human parainfluenza	843	> 1000[a]	> 1000[b]	> 1000[a]	enviroxime
RSV	> 1000	> 1000	> 1000	> 1000	RBV
VZV	> 1000	> 1000	> 1000	> 1000	acyclovir
HCMV	> 1000	> 1000	> 1000	> 1000	ganciclovir
HSV-1	> 1000	> 1000	> 1000[b]	> 1000	acyclovir
HSV-2_{KW}	424	> 1000	146	> 1000	acyclovir
HSV-2_{MS}	697	> 1000	278	> 1000	acyclovir

a Cell growth inhibition observed at the highest concentration.
b Viral inhibition observed at the highest concentration.
Source: PC-120-2003

3.1.3.4. In Vitro Receptor Binding Potencies of TDF and TFV

A primary screen was used to determine the effect of the major metabolite of TAF, TFV, and the other prodrug of TFV, TDF, on the inhibition or stimulation of binding in a series of 111 protein targets (neuroreceptors, ion channels, transporters, and nuclear receptors) (m2.6.3, Section 1.6, V2000020). The protein target was incubated in the presence of 10 µM TFV or TDF. The effect on the binding of the endogenous ligand was then determined. Responses of > 50% stimulation or inhibition were considered significant. There was no significant inhibition or stimulation of ligand binding to its protein target by either TFV or TDF. The results of this study demonstrate that neither TFV nor TDF significantly interacts with any of the 111 protein targets tested.

3.1.3.5. TAF metabolites/degradants

The cytotoxicity and antiviral activity of two TAF metabolites, M18 (GS-645552) and M28 (GS-652829) (Figure 17), was evaluated in two T-lymphoblastoid cell lines (MT-2 and MT-4) following 5 days of compound exposure (m2.6.3, Section 1.3, PC-120-2021). These metabolites are also degradants and the testing supported manufacturing activities. Both TAF metabolites had no cytotoxicity up to the highest tested concentration (57 µM). Both metabolites/degradants showed weak inhibition of HIV-1 replication with 1723 to 2630-fold lower inhibitory potency relative to TAF (EC_{50} values of 7.41 to 21.04 µM) for metabolite M28 and 121 to 130-fold lower inhibitor potency relative to TAF (EC_{50} values of 0.56 to 0.97 µM) for metabolite M18.

4. SAFETY PHARMACOLOGY

4.1. B/F/TAF

A comprehensive safety pharmacology program has been conducted for the 3 individual agents, BIC, FTC, and TAF. While the designs for these studies varied between the agents, the major organ systems were evaluated for BIC, FTC, and TAF individually. Bictegravir had no effect on vital organ systems in safety pharmacology studies. Neither FTC nor TAF had clinically relevant effects on vital organ systems in safety pharmacology studies. Although TAF showed some potential to prolong the PR interval in the 39-week dog study (m2.6.7, Section 7.3.5, TOX-120-002), no PR prolongation or any change in ECG results occurred in the cardiovascular safety pharmacology study or in the thorough QT study. Overall, the pharmacological assessment of BIC, FTC, and TAF supports the effective use of these 3 components of the B/F/TAF FDC together in combination therapy for HIV-1 disease. Additional safety pharmacology studies on the B/F/TAF combination are considered unwarranted.

4.2. BIC

To support the proposed clinical development plan, the nonclinical safety profile of BIC was characterized in studies evaluating the potential pharmacologic effects on specific organ systems. Study designs and parameters evaluated were consistent with accepted principles and practices as outlined in the International Council for Harmonisation (ICH), and United States (US) Food and Drug Administration (FDA) Center for Drug Evaluation and Research (CDER). All studies were conducted in accordance with US FDA Good Laboratory Practice (GLP).

The rat and monkey were selected for the in vivo investigations based on their suitable pharmacokinetic profiles and demonstration of comparable in vitro metabolic profiles to humans (m2.6.4, Section 5). The high dose in rats (300 mg/kg) was selected based on saturation of absorption (m2.6.4, Section 3.2.1.2) and the high dose in monkeys was selected based on the ICH recommended limit dose of 1000 mg/kg. As no gender-specific differences were observed in repeat dose rat (m2.6.7, Section 7.1.2, TX-141-2029) and repeat dose monkey (m2.6.7, Section 7.1.4, TX-141-2030) toxicity studies, use of only males in the CNS, respiratory and CV safety pharmacology studies was acceptable. Consistent with its intended administration in humans, studies were conducted by the oral route of administration. Oral formulations of the test material were prepared in 0.5% hydroxypropyl methylcellulose [Methocel K100 LV] and 0.1% Tween® 20 in reverse osmosis water (%w/w) for all in vivo studies.

4.2.1. Central Nervous System

Crl:WI(Han) rats (8 males/group) were administered a single dose of vehicle control article or 10, 30, 100, or 300 mg/kg BIC via oral gavage (m2.6.3, Section 1.7, PC-141-2047). Assessment of potential neurological effects was based on observations collected approximately 3, 7.5, 24 (Day 2), 48 (Day 3), 72 (Day 4), and 144 (Day 7) hours postdose using a modified Irwin battery of neurological assessments, including group home cage, hand-held, open-field, and elicited response observations. General measures of toxicity consisting of mortality, clinical observations, and body temperature were also recorded.

No BIC-related effects on mortality, clinical observations, body weights, body temperature, or any component of the modified Irwin battery of neurological assessments were observed up to Day 7 postdose. The no-observable-effect-level (NOEL) for neurological function for male rats is 300 mg/kg/day, the highest dose administered. Based on the Day 1 free C_{max} (141 µg/ml [males]; 0.01% free) in male rats of the 2-week repeat dose toxicity study (m2.6.7, Section 7.1.2, TX-141-2029), exposure in rats at the NOEL dose was approximately 0.92-fold the free BIC C_{max} concentration (C_{max} = 6.15 µg/mL; 0.25% free) following clinical administration of the B/F/TAF FDC.

4.2.2. Cardiovascular System

4.2.2.1. In Vitro

The in vitro effects of BIC on the hERG channel current (a surrogate for I_{Kr}, the rapidly activating delayed rectifier cardiac potassium current) was assessed at near-physiological temperature (m2.6.3, Section 4.1.1, PC-141-2049). The patch-clamp technique was used to measure the peak hERG tail current amplitude prior to and following exposure to vehicle [0.3% dimethylsulfoxide (DMSO) v/v in HEPES-buffered Physiological Salt Solution; HB-PS] or BIC. Terfenadine was used as a positive control at a submaximally effective concentration (60 nM) and confirmed the sensitivity of the test system to hERG inhibition.

BIC inhibited hERG current by (mean ± standard error of the mean [SEM]) 1.0 ± 0.4% at 0.8 µM (n = 3) and 10.3 ± 1.2% at 7.1 µM versus 0.8 ± 0.4% (n = 3) in control. Inhibition of hERG at 7.1 µM was statistically significant ($P < 0.05$) when compared to vehicle control values. Due to solubility limitations under conditions of the assay, the IC_{50} for the inhibitory effect of BIC on hERG potassium current was not calculated but was estimated to be greater than 7.1 µM, which is at least 200-fold above the free BIC C_{max} concentration (C_{max} = 13.7 µM; 0.25% free) following clinical administration of the B/F/TAF FDC.

4.2.2.2. In Vivo

Four conscious, telemetered male cynomolgus monkeys were administered a single dose of vehicle control article or 30, 100, or 1000 mg/kg BIC via oral gavage in a Latin square design (m2.6.3, Section 4.2.1, PC-141-2046). A washout period of 6 days occurred between each of the dosing days. Blood samples were collected from all animals predose and at 8 hours postdose during the collection of telemetry data. Cardiovascular parameters were continuously recorded for 90 minutes prior to dosing and through 75 hours after each dose. Cardiovascular parameters evaluated included heart rate, PR, QRS, RR, QT and QTc intervals, as well as systolic, diastolic and mean arterial pressures, and body temperature. Other parameters evaluated during the study included viability, clinical observations, food consumption, and body weight.

No BIC-related clinical observations, or effects on body weight, food consumption, or body temperature occurred, and no effects on ECG and hemodynamic parameters were observed up to 1000 mg/kg, the highest dose tested. Analysis of blood samples confirmed dose-related increases in exposure to BIC following dose administration. Based on the Day 1 free C_{max} (C_{max} = 109 µg/mL [males]; 0.31% free) in the 2-week repeat dose toxicity study (m2.6.7, Section 7.1.4,

TX-141-2030), exposure in male monkeys at the NOEL dose of 1000 mg/kg was at least 22-fold above the free BIC C_{max} concentration (C_{max} = 6.15 µg/mL; 0.25% free) following clinical administration of the B/F/TAF FDC.

4.2.3. Respiratory System

Crl:WI(Han) rats (8 males/group) were administered a single dose of vehicle control article or 10, 30, 100, or 300 mg/kg BIC via oral gavage (m2.6.3, Section 4.2.1, PC-141-2048). Assessment of respiratory function was based on analysis of tidal volume, respiration rate (breaths/minute), and minute volume. Plethysmography data were collected continuously for 2.5 hours 4 days prior to dosing (baseline), 2 hours through 8 hours after dosing, and for 2.5 hours beginning 22.5, 46.5, 70.5 and 142.5 hours after dosing (Day 2, 3, 4, and 7 postdose, respectively). Assessment of overall toxicity was based on mortality and clinical observations.

No BIC-related effects on respiratory function were observed. Based on these results, the NOEL for respiratory function in male rats is 300 mg/kg BIC, the highest dose administered. Based on the Day 1 free C_{max} (141 µg/ml [males]; 0.01% free) in male rats of the 2-week repeat dose toxicity study (m2.6.7, Section 7.1.2, TX-141-2029), exposure in rats at the NOEL dose was approximately 0.92-fold of the free BIC C_{max} concentration (C_{max} = 6.15 µg/mL; 0.25% free) following clinical administration of the B/F/TAF FDC.

4.3. FTC

4.3.1. Overt Pharmacodynamic Effects

In vivo studies on the CNS (mice and rats), CV system (rats and dogs), respiratory system (mice, rats and dogs), renal system (rats), and GI system (mice) were conducted. The studies were conducted prior to the implementation of ICH S7A (published in November 2000), but followed good scientific practices and established methods and protocols.

4.3.1.1. Mice

In a single-dose modified Irwin screen with toxicity observations, male ICR mice (10/dose) were given FTC orally at 0 (distilled water), 10, 30, or 100 mg/kg in a dose volume of 20 mL/kg, then observed for 7 days to collect data on behavioral effects (m2.6.3, Section 4.2.2, 477). Emtricitabine did not affect behavior at any dose. In a subsequent single-dose general pharmacology study, male CD-1 mice (4/dose) were given FTC orally at 0 (0.5% MC), 100, 250, 500, 750, or 1000 mg/kg, then observed for 7 days to collect data on body weight, rectal temperature, and behavior (m2.6.3, Section 4.2.2, TPZZ/93/0001). Emtricitabine did not affect body weight, rectal temperature, or behavior at any dose.

4.3.1.2. Rats

In a single-dose general pharmacology study, male CD (SD) rats (4/dose) were given FTC orally at 0 (0.9% saline), 250, 500, or 1000 mg/kg, then observed for 7 days to collect data on body weight, rectal temperature, and behavior (m2.6.3, Section 4.2.2, TPZZ/93/0001). Emtricitabine did not affect body weight, rectal temperature, or behavior at any dose. In a separate single-dose

study, male Wistar rats (5/dose) were given FTC orally at 0 (distilled water), 10, 30, or 100 mg/kg in a dose volume of 10 mL/kg (m2.6.3, Section 4.2.2, 477). Rectal temperature was measured before dosing at intervals up to 2 hours postdose. Again, FTC did not affect rectal temperature at any dose.

4.3.2. Central Nervous System

4.3.2.1. Mice

In a single-dose modified Irwin screen with toxicity observations, male ICR mice (10/dose) were given FTC orally at 0 (distilled water), 10, 30, or 100 mg/kg, then observed for 7 days to collect data on neurological and autonomic effects (m2.6.3, Section 4.2.2, 477). Emtricitabine did not produce neurological or autonomic effects at any dose. In a subsequent single-dose general pharmacology study, male CD-1 mice (4/dose) were given FTC orally at 0 (0.5% MC), 100, 250, 500, 750, or 1000 mg/kg, then observed for 7 days to collect data on reflexes (m2.6.3, Section 4.2.2, TPZZ/93/0001). Emtricitabine did not affect reflexes at any dose.

In a single-dose spontaneous locomotor activity study, male ICR mice (8/dose) were given FTC orally at 0 (distilled water), 10, 30, or 100 mg/kg. Spontaneous activity was recorded at 15-minute intervals for 2 hours postdose. Emtricitabine did not affect spontaneous locomotion at any dose.

In a single-dose motor coordination (rotorod) study, male ICR mice (10/dose) were given FTC orally at 0 (distilled water), 10, 30, or 100 mg/kg. Ability to remain on a rotating rod was evaluated at 0.5, 1, and 2 hours postdose. Emtricitabine did not affect motor coordination at any dose.

In a single-dose hexobarbital potentiation (sleeping time) study, male ICR mice (10/dose) were given FTC orally at 0 (distilled water), 10, 30, or 100 mg/kg, and then anesthetized with hexobarbital 1 hour later. Time to recovery from anesthesia (return of righting reflex) was measured. Emtricitabine did not affect duration of anesthesia at any dose.

In a single-dose anticonvulsant activity study, male ICR mice (10/dose) were given FTC orally at 0 (distilled water), 10, 30, or 100 mg/kg, then given a maximal electrical shock at 1 hour postdose. The occurrence of death or tonic/clonic convulsions was recorded. Emtricitabine did not affect mortality and had no anticonvulsant activity at any dose. In a second single-dose anticonvulsant activity study, male ICR mice (10/dose) were given FTC orally at 0, 10, 30, or 100 mg/kg, then given metrazole at 100 mg/kg at 1 hour postdose. The occurrence of death or tonic/clonic convulsions was recorded. Again, FTC did not affect mortality and had no anticonvulsant activity at any dose.

In a single-dose proconvulsant activity study, male ICR mice (10/dose) were given FTC orally at 0 (distilled water), 10, 30, or 100 mg/kg, then given a subthreshold electrical shock at 1 hour postdose. The occurrence of death or tonic/clonic convulsions was recorded. Emtricitabine did not affect mortality and had no proconvulsant activity at any dose. In a second single-dose proconvulsant activity study, male ICR mice (10/dose) were given FTC orally at 0 (distilled water), 10, 30, or 100 mg/kg, then given metrazole at 70 mg/kg at 1 hour postdose. The occurrence of death or tonic/clonic convulsions was recorded. Again, FTC did not affect mortality and had no proconvulsant activity at any dose.

In a single-dose analgesic activity study, male ICR mice (10/dose) were given FTC orally at 0 (distilled water), 10, 30, or 100 mg/kg. The time to tail-flick response to an uncomfortable heat stimulus was recorded before and 1 hour after dosing. Emtricitabine had no analgesic activity at any dose. In a second single-dose analgesic activity study, male ICR mice (10/dose) were given FTC orally at 0 (distilled water), 10, 30, or 100 mg/kg, then given phenylquinone at 2 mg/kg at 1 hour postdose. The number of writhes occurring during the next 10 minutes was recorded. Again, FTC had no analgesic activity at any dose. In a subsequent single-dose general pharmacology study, male CD-1 mice (4/dose) given FTC orally at 0 (0.5% MC), 100, 250, 500, 750, or 1000 mg/kg were evaluated for analgesia by the tail-flick test (m2.6.3, Section 4.2.2, TPZZ/93/0001). Once again, FTC had no analgesic activity at any dose.

4.3.2.2. Rats

In a single-dose general pharmacology study, male CD (SD) rats (4/dose) were given FTC orally at 0 (0.9% saline), 250, 500, or 1000 mg/kg, and then observed for 7 days to collect data on reflexes and analgesia (m2.6.3, Section 4.2.2, TPZZ/93/0001). Emtricitabine did not affect reflexes and had no analgesic activity at any dose.

In a single-dose conditioned avoidance response study, trained ovariectomized female Long-Evans rats (6/dose) were given FTC by intraperitoneal injection at 0 (0.5% MC), 30, or 100 mg/kg, then tested for their ability to respond to an audio-visual cue to avoid foot-shock. Emtricitabine did not affect conditioned avoidance response at any dose.

4.3.3. Cardiovascular System

4.3.3.1. Effects on Isolated Cardiac Muscle of Rat, Guinea Pig, and Cat

Emtricitabine was tested on different cardiac preparations to determine its effect on cardiac function in vitro (m2.6.3, Section 4.1.2, TPZZ/92/0056). Parameters measured following treatment with 1 μM FTC included: cardiac chronotropy (rat and guinea pig), cardiac inotrophy (cat and guinea pig), and the incidence of ventricular arrhythmias (rat). Results from these in vitro studies suggested that FTC was free of negative cardiac effects at 1 μM.

4.3.3.2. Rats

In a single-dose cardiovascular effects study, conscious male Wistar rats (5/dose) were given FTC orally at 0 (distilled water), 10, 30 or 100 mg/kg (m2.6.3, Section 4.2.2, 477). Heart rate and arterial blood pressure were measured before dosing and at 5, 30, and 60 minutes postdose. Emtricitabine did not affect heart rate or blood pressure at any dose. In a second single-dose cardiovascular effects study, conscious male CD (SD) rats (8/dose) were given FTC orally at 0 (0.5% MC) or 250 mg/kg (m2.6.3, Section 4.2.2, TPZZ/92/0057). Heart rate and blood pressure were measured at intervals for 4 hours postdose. Again, FTC did not affect heart rate or blood pressure.

4.3.3.3. Dogs

In a single-dose cardiovascular and respiratory effects study, 4 anesthetized male beagle dogs were given FTC intravenously (formulated in 5% dextrose in water) as consecutive bolus injections of 1.0, 2.5, 5, 10, and 20 mg/kg (cumulative dose = 38.5 mg/kg) over an hour, then monitored for 30 more minutes (m2.6.3, Section 4.2.2, TPZZ/92/0076). The average plasma concentration of FTC at 30 minutes postinfusion was 34.6 mg/mL. Heart rate, arterial blood pressure, and lead II ECG were measured at intervals, and blood pressure responses to norepinephrine, acetylcholine, carotid artery occlusion, and vagal nerve stimulation were evaluated 30 minutes after the last dose. Emtricitabine did not affect the ECG, cardiovascular function parameters, or blood pressure response to stimuli at any dose or time point.

4.3.4. Respiratory System

4.3.4.1. Mice

In a single-dose general pharmacology study, male CD-1 mice (4/dose) were given FTC orally at 0 (0.5% MC), 100, 250, 500, 750, or 1000 mg/kg, then observed for 7 days to collect data on respiratory rate (m2.6.3, Section 4.2.2, TPZZ/93/0001). Emtricitabine did not affect respiratory rate at any dose.

4.3.4.2. Rats

In a single-dose general pharmacology study, male CD (SD) rats (4/dose) were given FTC orally at 0 (0.9% saline), 250, 500, or 1000 mg/kg, and then observed for 7 days to collect data on respiratory rate. Emtricitabine did not affect respiratory rate at any dose (m2.6.3, Section 4.2.2, TPZZ/93/0001).

4.3.4.3. Dogs

In a single-dose cardiovascular and respiratory effects study, 4 anesthetized male beagle dogs were given FTC intravenously as consecutive bolus injections of 1, 2.5, 5, 10, and 20 mg/kg (cumulative dose = 38.5 mg/kg) over an hour, then monitored for 30 more minutes (m2.6.3, Section 4.2.2, TPZZ/92/0076). The average plasma concentration of FTC at 30 minutes postinfusion was 34.6 mg/mL. Respiratory rate and respiratory minute volume were measured at intervals. Emtricitabine did not affect respiratory function parameters at any dose or time point.

4.3.5. Renal System

In a single-dose renal function study, male Long Evans-derived rats (6/dose) were given FTC orally at 0 (distilled water), 10, 30, or 100 mg/kg and urine was collected for 6 hours postdose to measure pH, volume, and electrolyte concentrations (m2.6.3, Section 4.2.2, 477). Emtricitabine did not affect urine output, pH, or electrolyte excretion at any dose.

4.3.6. Gastrointestinal System

In a single-dose GI motility study, male ICR mice (10/dose) were given FTC orally at 0 (distilled water), 10, 30, or 100 mg/kg (m2.6.3, Section 4.2.2, 477), then given a charcoal suspension orally at 1 hour postdose and killed 15 minutes later to record intestinal transit of charcoal. Emtricitabine did not affect GI motility at any dose.

4.4. TAF

The safety pharmacology studies of TAF were conducted in accordance with GLP regulations. The in vitro hERG assay was also conducted in accordance with guidelines issues by the ICH.

In vivo safety pharmacology experiments were conducted using TAF as the monofumarate form (GS-7340-02) in 50 mM citric acid. In the in vitro hERG assay, TAF as GS-7340-03 was dissolved in DMSO and diluted with HEPES-buffered physiological saline to a final concentration of 0.3% DMSO.

4.4.1. Central Nervous System

The effect of TAF (as GS-7340-02) on the CNS was evaluated in male Sprague Dawley rats following administration of single oral doses of 0, 100, or 1000 mg/kg (80 or 800 mg free base equivalents [fbe]/kg) (m2.6.3, Section 4.2.3, R990188; CTBR 56518). The no-effect dose for a pharmacological effect on the CNS of the male Sprague Dawley rat was 1000 mg/kg.

4.4.2. Cardiovascular System

4.4.2.1. In Vitro

TAF (as GS-7340-03) was evaluated at concentrations of 1 and 10 µM (fbe), and hERG inhibition was not statistically significant ($p < 0.05$) when compared with vehicle control values. The IC_{50} for the inhibitory effect of TAF on hERG potassium current was estimated to be greater than 10 µM (m2.6.3, Section 4.1.3, PC-120-2005; ChanTest 111213.DPW).

4.4.2.2. In Vivo

Oral administration of TAF (as GS-7340-02) to conscious instrumented male beagle dogs at dose levels of 30 or 100 mg/kg (24 and 80 mg fbe/kg) did not induce pharmacologic effects on heart rate, systemic blood pressure, or ECGs (m2.6.3, Section 4.2.3, D2000006; CTBR 93205). Similarly, no pulse rate prolongation or any change in ECG results occurred in the thorough QT study (GS-US-120-0107). Although TAF showed some potential to prolong the PR interval in the 39-week dog study at 18/12 mg/kg/day, the slight change was associated with decreased weight gain, bone and renal toxicity, and significant decreases in T3 {Kienle 1994}, {Tribulova 2010}.

4.4.3. Gastrointestinal System

Administration of TAF (as GS-7340-02) to Sprague Dawley rats by oral gavage indicated that at 1000 mg/kg (800 mg fbe/kg), the rate of gastric emptying was reduced (m2.6.3, Section 4.2.3, R990187; CTBR 56519). At 100 mg/kg (80 mg fbe/kg), there was no clear effect on gastric emptying. The reduction in charcoal transit through the intestine at the 2-hour time point at 1000 mg/kg may have been due to reduced gastric emptying. A dose of 100 mg/kg was considered to have had no effect on gastric emptying or intestinal motility.

4.4.4. Renal System

The effect of TAF (as GS-7340-02) on the renal system was evaluated in male Sprague Dawley rats following administration of single oral doses of 0, 100, or 1000 mg/kg (80 or 800 mg fbe/kg) (m2.6.3, Section 4.2.3, R990186; CTBR 56520). Although urinary output of calcium was increased at 1000 mg/kg, this correlated with an increase in serum calcium concentration and indicated that the kidneys were functioning in order to reduce the serum calcium load. The no-effect dose for a pharmacological effect on the renal system of the male Sprague Dawley rat was 1000 mg/kg.

5. PHARMACODYNAMIC DRUG INTERACTIONS

5.1. B/F/TAF

The three-drug combination antiviral activity of BIC, FTC, and TAF was evaluated in 5-day cytopathic assays in MT-2 cells acutely infected with HIV-1. The antiviral effect of the three-drug combination was analyzed using the combination index method of the CalcuSyn software (Table 80). The triple combination of BIC + FTC + TAF showed synergy, with a mean combination index (CI) value of 0.60 ± 0.11 (n=3) (m2.6.3, Section 1.10, PC-380-2001). As a comparison, the triple combination of DTG + FTC + TAF was evaluated in parallel and also showed synergy (CI = 0.61 ± 0.23, n=3). The results for these two triple combinations (BIC + FTC + TAF and DTG + FTC + TAF) were not statistically different (t-test, p = 0.95). Previous control experiments showed FTC + FTC + FTC was additive (CI = 0.92 ± 0.06, n=3) and d4T + ZDV + ribavirin (RBV) was strongly antagonistic (CI > 5.9 ± 2.6, n = 3) {Kulkarni 2014}. There was no evidence of cytotoxicity observed in these triple combination experiments in cells exposed to these drugs in the absence of HIV-1 infection.

Table 80. B/F/TAF Triple Drug Antiviral Combination Index Values

Drug Combination	Combination Index ± SD[a]	Combination Result
BIC + FTC + TAF	0.60 ± 0.11	Synergy
DTG + FTC + TAF	0.61 ± 0.23	Synergy
FTC + FTC + FTC[b]	0.92 ± 0.06	Additive
d4T + ZDV + RBV[b]	>5.9 ± 2.6	Strong antagonism

d4T = stavudine; DTG = dolutegravir; FTC = emtricitabine; RBV = ribavirin; TAF = tenofovir alafenamide; ZDV = zidovudine; RBV = ribavirin

a Mean combination index (CI) and standard deviation calculated from n=3 experiments for both combinations. CI <1.1 = synergy; CI 0.9-1.1 additive; CI >1.1 antagonism

b Control experiments were performed previously and have been published {Kulkarni 2014}.

Source: PC-380-2001

5.2. BIC

5.2.1. Combination Studies of BIC with Other Antiretrovirals

To assess the antiviral activity of BIC in combination with clinically approved agents from other antiretroviral classes, BIC was tested in pair wise combinations with a panel of selected drugs including NRTIs, PIs and INSTIs. Specifically, the antiviral activity of BIC was evaluated in combination with five antiretroviral drugs including TAF, FTC, DRV, RAL, and EVG in a 5-day cytopathic assay using MT-2 cells acutely infected with HIV-1 (m2.6.3, Section 1.10, PC-141-2038). The effect of combining any two drugs was analyzed by the MacSynergy™ II software {Prichard 1990}, {Prichard 1993a}, {Prichard 1993b}.

Pair-wise combinations of BIC with nucleotide/nucleoside inhibitors of reverse transcriptase (TAF, FTC) or with the HIV PI (DRV) were highly synergistic (Table 81). When combined with other HIV-1 INSTIs (RAL and EVG), BIC showed additive anti-HIV activity. Similar

results were obtained when DTG was combined with the same panel of anti-HIV drugs. EVG + TAF, RBV + d4T, and BIC combined with itself were used as synergy, antagonism, and additivity controls, respectively.

Table 81. In Vitro Anti-HIV-1 Activity of BIC in Combination with Selected Antiretrovirals

Drug combination[b]	Synergy/Antagonism Volume[a]		Combination effect
	Type	Mean (nM^2.%)	
BIC + TAF	Synergy Antagonism	116 ± 27 -6.0 ± 5.8	Highly Synergistic
BIC + FTC	Synergy Antagonism	123 ± 56 -4.4 ± 6.7	Highly Synergistic
BIC + DRV	Synergy Antagonism	122 ± 41 -4.0 ± 10.4	Highly Synergistic
BIC + RAL	Synergy Antagonism	15.6 ± 15.2 -10 ± 6.9	Additive
BIC + EVG	Synergy Antagonism	13.0 ± 8.7 -6.0 ± 6.1	Additive
DTG + TAF	Synergy Antagonism	119 ± 48 -7.6 ± 8.7	Highly Synergistic
DTG + FTC	Synergy Antagonism	130 ± 56 -2.0 ± 8.8	Highly Synergistic
DTG + RAL	Synergy Antagonism	18.0 ± 15.2 -7.0 ± 11.5	Additive
DTG + EVG	Synergy Antagonism	13.0 ± 11.2 -4.0 ± 9.7	Additive
Control Combinations			
BIC + BIC	Synergy Antagonism	7.3 ± 10.3 -15.1 ± 10.1	Additive
EVG + TAF	Synergy Antagonism	120 ± 52 -5.7 ± 6.8	Highly Synergistic
RBV + d4T	Synergy Antagonism	9.7 ± 9.5 -146 ± 63	Highly Antagonistic

a The synergy/antagonism volumes represent the mean of at least 3 independent experiments performed in triplicates.
b EVG = elvitegravir, RBV = ribavirin, d4T = stavudine, DTG = dolutegravir, TAF = tenofovir alafenamide, FTC = emtricitabine, DRV = darunavir.
Source: PC-141-2038

5.3. FTC

5.3.1. Combination Studies of FTC with Other HIV Antiviral Drugs

The effect of combining FTC with other anti-HIV agents in the NRTI, NNRTI, and PI classes has been studied extensively using isobologram analysis. Results of 2-drug combination assays are presented in Table 82.

In all cases, in vitro combination studies with FTC and other anti-HIV agents resulted in additive to synergistic anti-HIV activity. No antagonism was observed under any of the reported conditions.

The combination antiviral activity of FTC with BIC and with TAF also showed synergy (m2.6.3, Section 1.10, PC-141-2038 and m2.6.3, Section 1.12, PC-120-2002).

Table 82. In Vitro Anti-HIV-1 Activity of FTC in Combination with Selected Antiretrovirals

Compounds	Class	Cell line	HIV Strain	Results
DLV	NNRTI	MT-2	LAI	Additive to Synergistic
EFV	NNRTI	MT-2	LAI	Additive to Synergistic
Emivirine	NNRTI	MT-2	LAI	Additive to Synergistic
NVP	NNRTI	MT-2	LAI	Additive to Synergistic
ABC	NRTI	MT-2	LAI	Additive to Synergistic
Adefovir	NRTI	MT-2	LAI	Additive to Synergistic
Amdoxovir	NRTI	MT-2	LAI	Additive to Synergistic
ddI	NRTI	MT-4	IIIB	Strongly Synergistic
ddI	NRTI	MT-2	IIIB	Additive
ddI	NRTI	MT-2	LAI	Additive to Synergistic
EVG	INSTI	MT-2	IIIB	Synergistic
3TC	NRTI	MT-2	LAI	Additive to Synergistic
RPV	NNRTI	MT-2	IIIB	Strongly Synergistic
d4T	NRTI	MT-2	IIIB	Additive
d4T	NRTI	MT-2	LAI	Additive to Synergistic
ddC	NRTI	MT-4	IIIB	Strongly Synergistic
ddC	NRTI	MT-2	IIIB	Additive
ZDV	NRTI	MT-4	IIIB	Strongly Synergistic
ZDV	NRTI	MT-2	IIIB	Additive
ZDV	NRTI	MT-2	LAI	Additive to Synergistic
APV	PI	MT-2	LAI	Additive to Synergistic
IDV	PI	MT-2	LAI	Additive to Synergistic
NFV	PI	MT-2	LAI	Additive to Synergistic
RTV	PI	MT-2	LAI	Additive to Synergistic

Source: 470, 10804, PC-183-2004, and PC-264-2001, {Painter 1995}, and {Bridges 1996}

5.4. TAF

5.4.1. In Vitro Anti-HIV-1 Activity of TAF in Combination with Selected Antiretrovirals

The anti-HIV-1 activity of TAF in combination with a broad panel of representatives from the major classes of approved anti-HIV agents (N[t]RTIs, NNRTIs, INSTIs, and PIs) was evaluated in HIV-1_{IIIB} infected MT-2 cells (m2.6.3, Section 1.12, PC-120-2002). This study was analyzed using the Prichard and Shipman: MacSynergy™ II software {Prichard 1990}, {Sanne 2003},

{Prichard 1993b}. Viral growth/inhibition was evaluated by measuring virus-induced cytopathic effects at the experimental endpoint. Combinations of ddI + RBV, d4T+RBV, and TAF + TAF were used as controls for synergy, antagonism, and additivity, respectively.

The combination of TAF with TFV resulted in an additive effect, as expected since both deliver TFV-DP to cells. TAF exhibited moderate to high synergistic effects (synergy volumes from 41 to 131 $\mu M^2\%$) when combined with any of the N(t)RTIs or NNRTIs (Table 83). The combination of TAF with INSTIs resulted in the highest level of synergy (synergy volumes of 116, 271, 205, and 179 $\mu M^2\%$ for BIC, EVG, RAL, and DTG, respectively). The combination of TAF with PIs resulted in moderate synergy (synergy volumes of 96 and 56 $\mu M^2\%$ for ATV and DRV, respectively). As expected, the combination of TAF with COBI, a PK enhancer coformulated with TAF in E/C/F/TAF and devoid of antiviral activity, resulted in an additive effect.

The synergy values observed for TAF with all the drugs tested were comparable with those of TFV performed in parallel (data not shown) and to values previously reported for TFV {Mulato 1997}. Importantly, none of the drug combinations containing TAF exhibited antagonistic antiviral effects.

Table 83. TAF Anti-HIV-1 Activity in Combination with Selected ARVs

Drug combination	Class	Volume ($\mu M^2\%$)		Net Effect
		Synergy[a]	Antagonism[a]	
TAF+TFV	NRTI	24	−14	Additive
TAF+FTC	NRTI	131	−9	Strong synergy
TAF+EFV	NNRTI	100	−7	Strong synergy
TAF+NVP	NNRTI	41	−14	Minor synergy
TAF+BIC	INSTI	116	-6.0	Strong synergy
TAF+EVG	INSTI	271	−9	Strong synergy
TAF+RAL	INSTI	205	−10	Strong synergy
TAF+DTG	INSTI	179	−10	Strong synergy
TAF+ATV	PI	96	−10	Moderate synergy
TAF+DRV	PI	56	−12	Moderate synergy
TAF+COBI	PK enhancer	17	−22	Additive
TAF+TAF	Control	20	−17	Additive
ddI+RBV	Control	302	−20	Strong synergy
d4T+RBV	Control	20	−340	Strong antagonism

a Data shown represent the mean from >3 independent experiments performed in triplicate. As defined by Prichard and colleagues {Prichard 1993a}, volumes of ≥ -25 to < 25 $\mu M^2\%$ indicate an additive effect; ≥ 25 to < 50 $\mu M^2\%$ indicate minor synergy; ≥ 50 to < 100 $\mu M^2\%$ indicate moderate synergy; ≥ 100 $\mu M^2\%$ indicates strong synergy, ≥ −50 to < −25 indicate minor antagonism, ≥ −100 to < −50 indicate moderate antagonism, and < −100 indicates strong antagonism.

Source: PC-120-2002 and PC-141-2038

5.4.1.1. Effect of Protease Inhibitors on Anti-HIV Activity of TAF

Since certain viral PIs have been shown to be potent inhibitors of CatA {Murakami 2010}, the effect of various PIs on the anti-HIV activity of TAF was evaluated in primary human $CD4^+$ T lymphocytes infected with VSV-G-pseudotyped $HIV\text{-}1_{NL4\text{-}3}$ containing a luciferase reporter gene (m2.6.3, Section 1.12, PC-120-2001; {Birkus 2012}). Antiviral activity of TAF (ie, protection from virus integration, EC_{50}) was measured after 3 days in the absence or presence of PIs, evaluated at their clinical C_{max} concentrations.

As shown in (Table 84), the antiviral potency of TAF, but not TDF, was significantly reduced 23.9- and 2.9-fold in the presence of telaprevir and boceprevir, respectively. In agreement with this data, both telaprevir and boceprevir were found to be potent inhibitors of CatA-mediated TAF activation in enzymatic assays. None of the other tested HIV PIs, host serine PIs, or the majority of HCV PIs affected the antiviral potency of TAF or TDF.

Overall, these data support the coadministration of the tested therapeutic PIs, with the exception of telaprevir or boceprevir, in combination with TAF, without negatively affecting its clinical pharmacology and intracellular conversion to parent TFV.

Table 84. Effect of COBI and Various Protease Inhibitors on the Anti-HIV Activity of TAF in Primary Human $CD4^+$ T Lymphocytes

Inhibitor Class	Drug	C_{max} (µM)	EC_{50} FC from TAF alone[a]	
			TAF[b]	TDF[b]
HIV PI	Darunavir	8.9	0.9	1.4
	Atazanavir	6.3	1.1	1.5
HCV PI	Telaprevir	5.2	23.9	1.6
	Boceprevir	3.3	2.9	1.3
	Simeprevir	13.3	1.1	1.7
CYP3A Inhibitor	COBI	2.2	0.9	1.8
Factor Xa Inhibitor	Apixaban	0.17	1.7	1.1
	Rivaroxaban	0.3	1.2	1.2
Thrombin Inhibitor	Argatroban	0.4	1.6	1.3
	Dabigatran	0.4	1.4	1.2
DPP4 Inhibitor	Sitagliptin	1.0	1.5	1.0

C_{max} = maximum observed concentration of drug; EC_{50} = concentration inhibiting viral replication by 50%; FC = fold change; PI = protease inhibitor; TAF = tenofovir alafenamide; TDF = tenofovir disoproxil fumarate.

a Mean fold change in TAF and TDF EC_{50} values from at least 4 donors performed in triplicate, expressed as a ratio of the activity in the presence versus the absence of protease inhibitor.

b EC_{50} value (TAF) = 5.6 nM; EC_{50} value (TDF) = 3.1 nM, determined from at least 4 donors assayed in triplicate.

Source: PC-120-2001

5.4.1.2. Effects of Protease Inhibitors of HIV and HCV, and Host Cell Proteases on Cathepsin A-mediated Activation of TAF

Because certain viral PIs have been shown to be potent inhibitors of CatA, the potential for drug-drug interactions between TAF and antiviral PIs was evaluated in biochemical assays using purified CatA (m2.6.3, Section 1.12, PC-120-2001, {Murakami 2010}). The HIV PIs DRV, ATV, LPV, and RTV did not inhibit CatA-mediated hydrolysis of TAF up to a concentration of 50 µM, well above the clinical C_{max} of each drug (Table 85). Similarly, HCV PIs TMC-435, BI-201355, MK-5172, GS-9256, and GS-9451 showed little-to-no inhibition of CatA, with IC_{50} values ranging from 25 to > 50 µM. On the other hand, both telaprevir and boceprevir, 2 covalent irreversible inhibitors of the HCV protease, were identified as potent inhibitors of CatA-mediated hydrolysis of TAF, with IC_{50} values of 0.3 and 0.2 µM, respectively. When adjusted for plasma binding, these IC_{50} values are 6- to 8-fold below the clinical maximum concentration (C_{max}) levels observed in patients.

In conclusion, the tested HIV PIs, host serine PIs, and the majority of HCV PIs exhibit minimal potential to interfere with the intracellular activation of TAF. These data support the co-administration of the tested therapeutic PIs, with the exception of telaprevir and boceprevir, in combination with TAF, without negatively affecting its clinical pharmacology and intracellular conversion to TFV.

Table 85. Effects of COBI, HIV-1 Protease Inhibitors, or HCV Protease Inhibitors on CatA-mediated Hydrolysis of TAF

Compound	IC_{50} ± SD (µM)[a]	C_{max} (µM)[b] Total Drug	C_{max} (µM)[c] Free Fraction
COBI or HIV-1 PIs			
DRV	> 50	8.9	1.6
ATV	> 50	6.3	0.7
LPV	> 50	15.2	0.3
RTV	> 50	1.3	0.02
COBI	> 50	2.2	0.2
HCV PIs			
Telaprevir	0.3 ± 0.17	5.2	1.5
Boceprevir	0.2 ± 0.02	3.3	1.3
TMC-435	> 50	13.3	< 0.002
BI-201335	25 ± 7	20	0.08
MK-5172	50	2.5	0.06
GS-9256	> 50	10.5	0.004
GS-9451	50	1.7	0.04

ATV = atazanavir; COBI = cobicistat; DRV = darunavir; HCV = hepatitis C virus; IC_{50} = 50% inhibitory concentration; LPV = lopinavir; PI = protease inhibitor; RTV = ritonavir; SD = standard deviation

a Data represent mean ± SD values from at least 2 independent experiments

b {Boffito 2008}, {Bristol-Myers Squibb Company 2011}, {Murphy 2001}, {Mathias 2010}, {Vertex Pharmaceuticals Incorporated 2011}, {Schering Corporation 2011}, {Manns 2011}, {Lawitz 2010}, {Goldwater 2010}, {Petry 2010}

c Concentration of free drug at C_{max} based on serum protein binding as determined by Gilead Sciences.

Source: Report PC-120-2001

5.4.1.3. Effect of the HCV NS5B Polymerase Inhibitor Sofosbuvir on the Anti-HIV Activity of TAF

The anti-HIV-1 activity of TAF in combination with the HCV nonstructural protein 5B (NS5B) polymerase inhibitor sofosbuvir (SOF) was evaluated in MT-2 cells (m2.6.3, Section 1.12, PC-120-2032). The anti-HIV-1 EC_{50} values of TAF were determined with and without SOF at concentrations spanning 0.5- to 2-fold C_{max} (0.64, 1.28, and 2.56 µM). Overall, no change was observed in the mean TAF EC_{50} value when evaluated in the presence of SOF (Table 86). These results suggested that, at the concentrations tested, SOF has no antagonistic effects on the anti-HIV activity of TAF.

Table 86. Effect of SOF on Anti-HIV Activity of TAF in MT-2 Cells

HCV Antiviral	Concentration (µM)	EC_{50} in nM (FC) from TAF Alone[a,b]
None	0	7.6 ± 1.5 (1.0)
SOF	0.64	8.3 ± 3.3 (1.1)
SOF	1.28	8.8 ± 3.0 (1.2)
SOF	2.56	7.0 ± 1.1 (0.9)

SOF = sofosbuvir; EC_{50} = concentration inhibiting viral replication by 50%; FC = fold change; NA = not applicable; TAF = tenofovir alafenamide

a Mean fold change in TAF EC_{50} values from at least 2 independent experiments performed in triplicate, expressed as a ratio of the activity in the presence and absence of SOF.

b Mean TAF EC_{50} value = 7.6 nM; determined from at least 3 independent experiments performed in triplicate.

c P-values compared mean TAF EC_{50} value in the presence versus the absence of SOF using a 2-tailed Student t-test, assuming equal variance.

Source: PC-141-2032

5.4.2. Metabolic Activation of TFV in Combination with Other Nucleos(t)ide Analogs

When combining NRTIs for HIV-1 and/or CHB treatment that share the same intracellular activation pathway, it is important to know their effect on intracellular phosphorylation as this may affect the antiviral activity and toxicity of a treatment regimen. While NRTIs within the same pathway are generally candidates for interaction, not all interactions result in decreased antiviral activity {Back 2005}.

The intracellular phosphorylation of TFV and FTC to their active metabolites, TFV-DP and FTC-TP, respectively, was investigated for potential antagonism (m2.6.3, Section 1.3, PC-164-2001). All forms of TFV, the free drug, the monophosphorylated form, and diphosphorylated form (ie, TFV, TFV-MP, and TFV-DP, respectively) were quantified in this analysis. The activated form of FTC (FTC-TP) was also measured. When 10 µM TFV was incubated alone in CEM cells, conversion to the active form, TFV-DP, was readily observed over the 24-hour time course (Table 87). Similarly, FTC-TP was also readily observed to form over the same time period when incubated alone (Table 88).

When TFV and FTC were incubated together (10 µM each), slightly higher levels of each respective active metabolite (TFV-DP and FTC-TP) were observed at 2 and 24 hours as compared with the NRTIs incubated alone in CEM cells (Figure 21, Table 87, and Table 88).

The slightly higher concentrations of active metabolites observed in the combination experiment may suggest slight enhancement of metabolism of both TFV and FTC; however, no difference in metabolite production was observed in cultured PBMCs {Borroto-Esdoa 2006}.

Table 87. Metabolism of 10 μM TFV Either Alone or in Combination with 10 μM FTC

Time	TFV Alone (pmol/million cells)[a]			TFV+FTC (pmol/million cells)[a]		
(h)	TFV	TFV-MP	TFV-DP	TFV	TFV-MP	TFV-DP
2	0.74 ± 0.31	0.02 ± 0.01	0.06 ± 0.01	0.50 ± 0.10	0.04 ± 0.01	0.09 ± 0.01
24	1.32 ± 0.48	0.54 ± 0.06	1.64 ± 0.08	0.97 ± 0.78	0.34 ± 0.03	2.24 ± 0.07

a Values determined by LC/MS/MS.
Source: PC-164-2001

Table 88. Metabolism of 10 μM FTC Either Alone or in Combination with 10 μM TFV

Time	FTC Alone (pmol/million cells)[a]	TFV+FTC (pmol/million cells)[a]
(h)	FTC-TP	FTC-TP
2	20.4 ± 0.5	22.0 ± 1.3
24	52.5 ± 11.3	71.6 ± 1.4

a Values determined by LC/MS/MS.
Source: PC-164-2001

Figure 21. Formation of the Active Metabolites of TFV and FTC

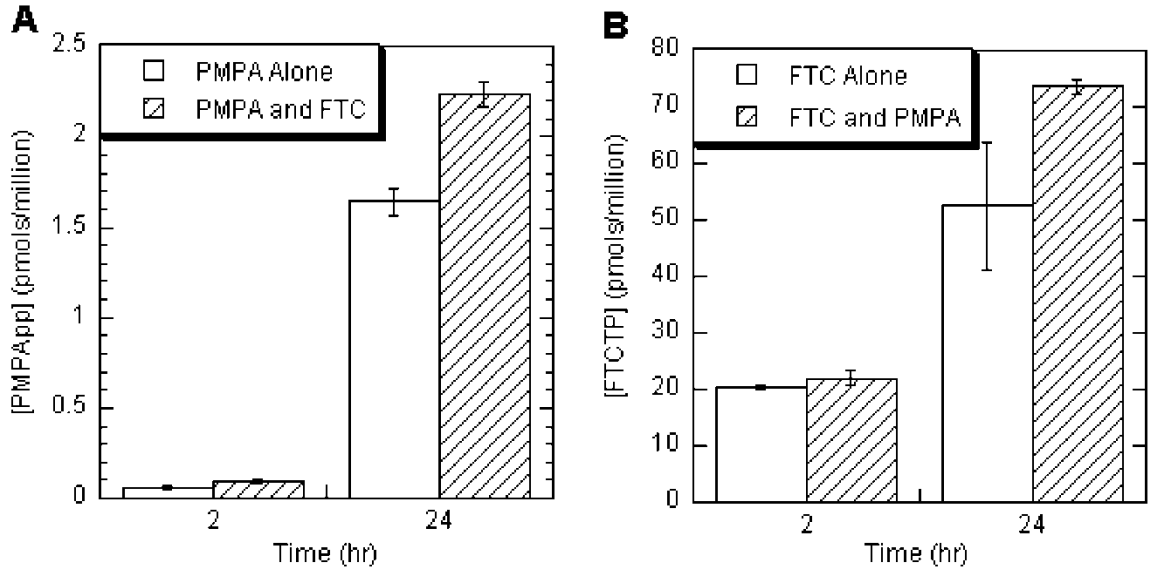

Concentrations of the active metabolites of TFV (A) and FTC (B), (TFV-DP and FTC-TP, respectively) formed after incubation of CEM-CCRF cells with 10 μM concentrations of NRTIs either alone or in combination.
PMPA = tenofovir
Source: PC-164-2001

Experiments were also carried out using TAF, which more efficiently delivers TFV, TFV-MP, and TFV-DP to cells, to determine if higher levels of TFV metabolites could affect the metabolism of FTC to FTC-TP (PC-164-2001). At these higher concentrations of TFV metabolites, no significant effect on the metabolism of FTC was observed with the combination as compared with the NRTI given alone. Additionally, no effects were seen on TAF metabolism with and without FTC.

These results demonstrate that the intracellular phosphorylation of both TFV and FTC to their respective activated metabolites (TFV-DP and FTC-TP) is not negatively affected by the simultaneous presence of the other NRTI. These results were observed using concentrations of drugs that are in excess of the plasma concentrations obtained in patients treated with these drugs (C_{max} values of 1 and 7 μM for TFV and FTC, respectively). A similar lack of an intracellular phosphorylation interaction has been described for TFV and ddI, 2 adenosine analogs that are known to have a higher degree of similarity in their phosphorylation pathways {Robbins 2003}. Taken together, these results show that, even at super physiological concentrations, there is little potential for a negative metabolic drug interaction at the level of phosphorylation between TFV and FTC and evidence for increased production of metabolites was detected in some cell lines.

The intracellular phosphorylation of TFV and ABC to their active metabolites, TFV-DP and CBV-TP, respectively, was investigated in T lymphoblastoid CEM cells for potential antagonism {Ray 2005}. Cells were incubated with TFV 10 μM and/or ABC 10 μM and the level of phosphorylated anabolites and natural pools of dATP and dGTP were determined by LC/MS/MS after 24 hours of incubation.

As shown in Table 89, levels of active metabolites produced from TFV and ABC after incubation with CEM cells showed no significant change upon introduction of the other NRTI. In addition, the pool sizes of competing natural substrates for TFV and ABC, dATP and dGTP, respectively, remained unchanged. Similar results were also observed in primary human PBMCs. Overall, these results indicate that there was no overlap between the anabolic routes of TFV and ABC and, thus, there is limited potential for drug interaction. These results are in agreement with combination results of TFV with ABC in PBMCs that showed additive anti-HIV activity {Ray 2005}.

Table 89. Metabolism of TFV 10 µM and/or ABC 10 µM Alone or in Combination and Their Effects on dATP and dGTP Pool Sizes in CEM Cells

Cell Type	Metabolite	Intracellular Concentration (pmol/10^6 cells)		
		TFV Alone	ABC Alone	TFV+ABC
CEM	TFV	1.42	NA	1.59
	TFV-MP	0.53	NA	0.47
	TFV-DP	1.49	NA	1.44
	CBV-TP	NA	0.12	0.18
	dATP[a]	40.3	40.3	41.7
	dGTP[a]	20.5	22.8	23.8

ABC = abacavir; CBV-TP = carbovir triphosphate; dATP = deoxyadenosine triphosphate; dGTP = deoxyguanosine triphosphate; NA = not applicable; TFV = tenofovir; TFV-MP = tenofovir monophosphate; TFV-DP = tenofovir diphosphate
a Intracellular concentrations of dATP and dGTP in untreated CEM cells were 42.7 and 23.7 pmol/10^6 cells, respectively. Following a 24-hour incubation with TFV 10 µM and/or ABC 10 µM, formation of phosphorylated anabolites and natural dATP and dGTP pools in CEM cells were determined by LC/MS/MS. Data were mean values from 4 independent experiments performed in duplicate.
Source: {Ray 2005}

TFV in combination with ddI does not affect the in vitro level of phosphorylated anabolites of either NRTI {Robbins 2003}, or alter the natural intracellular pools of 2′-deoxynucleoside triphosphates (dNTPs) {Vela 2005}. Additional in vitro studies showed that tenofovir monophosphate (TFV-MP) and TFV-DP can inhibit the phosphorolysis activity of purine nucleoside phosphorylase (PNP), which is involved in the metabolic degradation of ddI {Ray 2004}. Thus, the clinical observation of increased ddI plasma concentrations in treatment regimens containing TDF {Fulco 2003} appears to be due to inhibition of ddI degradation via inhibition of PNP by TFV.

The intracellular phosphorylation of TFV and ABC to their active metabolites, TFV-DP and CBV-TP, respectively, was investigated in vitro in CEM-SS cells for potential antagonism (m2.6.3, Section 1.3, PC-104-2008). The results demonstrate no difference in the intracellular phosphorylation of either compound when present in combination as compared with when given alone (Table 90 and Table 91). These in vitro results indicate that there is no overlap between the anabolic routes of these NRTIs and thus limited potential for a drug interaction. These results are in agreement with combination results that show additive anti-HIV activity of these compounds and a lack of antiviral antagonism.

Table 90. Metabolism of 10 μM TFV Either Alone or in Combination with 10 μM Abacavir

Time	TFV Alone (pmol/million cells)[a]			TFV+ABC (pmol/million cells)[a]		
(h)	TFV	TFV-MP	TFV-DP	TFV	TFV-MP	TFV-DP
2	1.27 ± 0.18	0.05 ± 0.01	0.17 ± 0.01	1.13 ± 0.03	0.05 ± 0.01	0.14 ± 0.02
24	1.71 ± 0.33	0.45 ± 0.02	1.54 ± 0.12	1.59 ± 0.14	0.41 ± 0.01	1.57 ± 0.04

a Values determined by LC/MS/MS.
Source: PC-104-2008

Table 91. Metabolism of 10 μM Abacavir Either Alone or in Combination with 10 μM TFV

Time	ABC Alone (pmol/million cells)[a]	ABC+TFV (pmol/million cells)[a]
(h)	CBV-TP[b]	CBV-TP[b]
2	0.03 ± 0.01	0.05 ± 0.02
24	0.17 ± 0.01	0.24 ± 0.03

a Values determined by LC/MS/MS.
b CBV-TP is the active anabolite of ABC.
Source: PC-104-2008

Coadministration of TDF and didanosine (ddI) has been clinically associated with increased plasma concentrations of ddI. In vitro studies showed that TFV-MP and TFV-DP can inhibit purine nucleoside phosphorylase (PNP), which is involved in the metabolic degradation of ddI {Ray 2004}. Thus, the clinical observation of increased ddI plasma concentrations appears to be due to inhibition of its degradation via inhibition of PNP by TFV.

In order to assess the potential effect of TFV on the natural pools of 2′-deoxynucleoside triphosphates (dNTPs) and ribonucleoside triphosphates (rNTPs), the T-cell line CEM-CCRF was treated with TFV, either alone or in combination with other NRTIs {Vela 2005}. There was no effect of TFV alone, or TFV plus ABC, ddI, or 3TC on either the intracellular dNTP or rNTP pool concentrations. The only tested NRTI that significantly altered dNTP pools was ZDV. Incubation of 10 μM ZDV, either alone or in combination with other NRTIs, increased dATP, dGTP, and thymidine triphosphate levels by up to 44%. In contrast to a control potent PNP inhibitor, TFV was unable to alter intracellular dNTP pools upon addition of exogenous 2′-deoxyguanosine. While inhibition of PNP-dependent ddI degradation is the most plausible mechanism for the drug interaction between ddI and TFV, TFV does not appear to be a potent enough inhibitor of PNP to cause changes in the other nucleotide pools.

5.4.3. TAF Activation in Primary Human Hepatocytes

The intracellular metabolism of TAF has been intensively studied in PBMCs and macrophages and the ester bond of TAF is known to be cleaved by lysosomal CatA {Birkus 2008}, {Birkus 2007}. To determine the enzymes involved in TAF activation in primary human hepatocytes, TAF hydrolase activity was assessed in cell extracts in the presence or absence of known CatA inhibitors (telaprevir and boceprevir), a CES1 inhibitor (BNPP), a cytochrome P450 enzyme 3A4 (CYP3A4) and P-glycoprotein (P-gp) inhibitor (COBI), or a combination of telaprevir and BNPP together (m2.6.3, Section 1.3, AD-120-2031, {Murakami 2015}).

BNPP inhibited metabolism of 0.5 µM TAF in a dose dependent manner with approximately 37, 30, or 66% inhibition observed at 2, 10, or 50 µM BNPP, respectively (Figure 22). Little or no effect on TFV-DP formation was observed with telaprevir, boceprevir, or cobicistat. While telaprevir alone caused little effect, greater inhibition was seen when telaprevir was added to BNPP than for BNPP alone at higher concentrations. For example, at concentrations of 10 µM and 50 µM of each inhibitor, inhibition of TFV-DP formation of approximately 84 and 95% inhibition, respectively, was observed. These results suggest that CES1 is the predominant enzyme activating TAF in primary human hepatocytes and that CatA also makes a minor contribution.

Figure 22. Effect of CES1, CatA, and CYP3A4 Inhibitors on Metabolism of 0.5 µM TAF to TFV-DP in Primary Human Hepatocytes

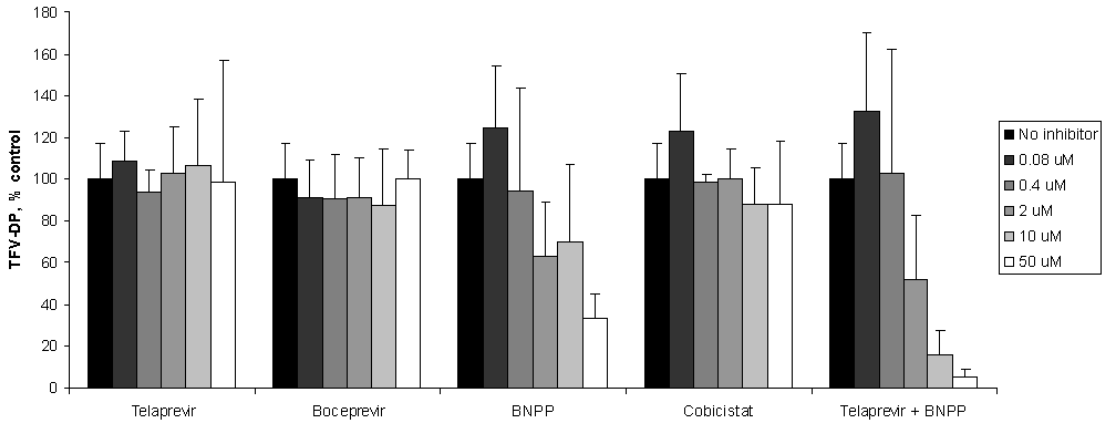

BNPP = bis-p-nitrophenyl phosphate; TFV-DP = tenofovir diphosphate
Primary human hepatocytes were continuously incubated with 0.5 µM TAF for 24 hours in the presence of increasing concentrations of inhibitors. Data represent mean ± SD values from 3 independent experiments in primary human hepatocytes from different donors in duplicate.
Source: Report AD-120-2031, {Murakami 2015}

5.4.3.1. Combination Study of TAF Anti-HBV Activity with Other Nucleos(t)ide Analogs

The anti-HBV activity of TFV in combination with other NRTIs was evaluated in AD38 cells, which express HBV under the control of a tetracycline-inducible promoter (m2.6.3, Section 1.12, PC-174-2006). Intracellular HBV DNA was quantified by real-time PCR after 4 days of drug treatment. Data analyses were based on both Bliss Independence (MacSynergy™ II software {Prichard 1990}, {Sanne 2003}, {Prichard 1993b}) and Loewe Additivity (Isobologram analysis) {Elion 1954} models.

The combination of TFV with 3TC, TBV, ETV, or adefovir (AFV) resulted in an additive antiviral effect by MacSynergy and Isobologram analyses (Table 92). Evaluation of the combination of TFV with FTC resulted in an additive effect by MacSynergy analysis and an additive to slightly synergistic effect by Isobologram analysis. No cytotoxic or antagonistic effects were observed with any of the drug combinations tested. These data are consistent with previous results obtained using a different HBV-expressing cell line where the combination of TFV with AFV demonstrated an additive effect {Delaney 2004}.

Table 92. TFV Anti-HBV Activity in Combination with NRTIs

Drug Combination	Class	MacSynergy Analysis[a]			Isobologram Analysis[b]	
		Volume ($\mu M^2\%$)				
		Synergy[a]	Antagonism[a]	Net Effect	D Value Range[c]	Net Effect
TFV+FTC	NRTI	6	−2	Additive	−0.25 to −0.12	Additive/Synergy
TFV+3TC	NRTI	7	−11	Additive	−0.17 to 0.12	Additive
TFV+ETV	NRTI	0	−10	Additive	0.036 to 0.24	Additive
TFV+TBV	NRTI	4	−9	Additive	0.066 to 0.047	Additive
TFV+AFV	NRTI	2	−14	Additive	−0.12	Additive

AFV = adefovir; ETV = entecavir; FTC = emtricitabine; LAM = lamivudine; TBV = telbivudine; TFV = tenofovir

a Mean synergy and antagonism volumes at 95% confidence interval ($\mu M^2\%$) from at least 3 independent experiments performed in triplicate. Net effect as defined by Prichard et al {Sanne 2003}, {Prichard 1990}. Synergy volumes of ≥ −25 to < 25 $\mu M^2\%$ indicated an additive effect; ≥ 25 to < 50 $\mu M^2\%$ indicated minor synergy; ≥ 50 to < 100 $\mu M^2\%$ indicated moderate synergy; ≥ 100 $\mu M^2\%$ indicated strong synergy. Antagonism volumes of ≥ −50 to < −25 indicated minor antagonism, ≥ −100 to < −50 indicated moderate antagonism, and < −100 indicated strong antagonism.

b D = deviation from additivity and was a result of statistical evaluation tested by a 1-tailed t test. D values between −0.2 and −0.1 were representative of a slight synergistic effect.

Source: PC-174-2006

5.4.3.2. Effect of Protease Inhibitors on Anti-HBV Activity of TAF

Since certain viral PIs have been shown to be potent inhibitors of CatA {Murakami 2010}, the effect of various PIs on the anti-HBV activity of TAF was evaluated in HepAD38 cells, which are stably transfected with HBV (m2.6.3, Section 1.12, PC-320-2004). All PIs were evaluated at their clinical C_{max} concentrations with the exception of simeprevir, which was evaluated at 25% C_{max} due to cytotoxicity at higher concentrations. After 4 days of drug treatment, intracellular HBV DNA was quantified by real-time PCR for determination of EC_{50} values.

Overall, no significant difference was observed in the mean TAF EC_{50} value when evaluated in the presence of any viral or host PI (Table 93). These results suggested that, at the concentrations tested, PIs have no antagonistic effects on the anti-HBV activity of TAF.

Table 93. Effect of COBI and Various Protease Inhibitors on the Anti-HBV Activity of TAF in HepAD38 Cells

Inhibitor Class	Drug	C_{max} (μM)	EC_{50} FC from TAF Alone[a,b]
HIV PI	Darunavir	8.9	0.9
HCV PI	Telaprevir	5.2	1.2
	Boceprevir	3.3	1.3
	Simeprevir	3.3[c]	0.7
CYP3A Inhibitor	COBI	2.2	0.9
Factor Xa Inhibitor	Apixaban	0.17	0.8
	Rivaroxaban	0.3	0.9
Thrombin Inhibitor	Argatroban	0.4	1.0
	Dabigatran	0.4	1.0
DPP4 Inhibitor	Sitagliptin	1.0	0.7

C_{max} = maximum observed concentration of drug; EC50 = concentration inhibiting viral replication by 50%; FC = fold change
a Mean fold change in TAF EC_{50} values from at least 2 independent experiments performed in quadruplicate, expressed as a ratio of the activity in the presence versus the absence of protease inhibitor.
b EC_{50} TAF value = 138.2 nM, determined from at least 2 independent experiments performed in quadruplicate.
c Simeprevir evaluated at 25% of clinical C_{max} due to reduced cell viability observed at C_{max}, which was consistent with previously observed cytotoxicity (CC_{50}) values {Lin 2009}.
Source: PC-320-2004

These results are different from those observed in the HIV-1 infected primary $CD4^+$ T cells, where TAF EC_{50} values increased 23.9- and 2.9-fold in the presence of telaprevir and boceprevir, respectively (Section 5.4.1.1). One possible explanation for this difference is that in hepatocytes, the initial step of TAF metabolism is hypothesized to be driven by a combination of CatA and CES1 (m2.6.3, Section 1.3, AD-120-2017; {Murakami 2015}), as opposed to CatA alone in PBMCs {Birkus 2007}, {Birkus 2008}.

In support of this hypothesis, the anti-HBV potency (EC_{50} value) of TAF in HepAD38 cells was further shown to be not significantly impacted by inhibition of CatA or CES1 alone, but only when both CatA and CES1 were inhibited by telaprevir and BNPP, respectively (Table 94). These results correlated with a significant reduction in TAF-derived metabolites (m2.6.3, Section 1.3, PC-320-2006), which was consistent with similar observations in primary human hepatocytes {Murakami 2015}.

Therefore, inhibition of CatA by telaprevir or boceprevir alone may not impact conversion of TAF to TFV-DP in HepAD38 cells, which express both CatA and CES1.

Table 94. Effect of Cathepsin A and/or Carboxylesterase 1 Inhibitors on Anti-HBV Activity of TAF in HepAD38 Cells

Target (Inhibitor Class)	Inhibitor	Concentration (µM)	EC_{50} FC from TAF Alone[a,b]	P-Value[c]
CatA (HCV PI)	Telaprevir	5.2	0.9	0.726
CES1 (NA)	BNPP	50	1.4	0.379
CatA (HCV PI) + CES1 (NA)	Telaprevir + BNPP	5.2 + 50	2.1	0.007

BNPP = bis-p-nitrophenyl phosphate; Cat A = cathepsin A, CES1 = carboxylesterase 1; EC_{50} = concentration inhibiting viral replication by 50%; FC = fold change; NA = not applicable; PI = protease inhibitor; TAF = tenofovir alafenamide

a Mean fold change in TAF EC_{50} values from at least 2 independent experiments performed in quadruplicate, expressed as a ratio of the activity in the presence and absence of inhibitor(s).

b Mean TAF EC_{50} value = 128.0 nM; determined from at least 2 independent experiments performed in quadruplicate.

c P-values compared mean TAF EC_{50} value in the presence versus the absence of inhibitor(s) using a 2-tailed Student t test, assuming equal variance.

Source: PC-320-2006

5.4.4. Effect of TAF on the Anti-HCV Activity of Antiviral Agents

The anti-HCV activity and cytotoxicity of HCV PIs in HCV genotype 1a Huh-7 replicon cells was evaluated after 3 days in the presence or absence of 1 µM TAF (m2.6.3, Section 1.12, PC-320-2001). In addition, the effect of TAF on other non-direct and direct-acting HCV antivirals was evaluated.

As shown in Table 95, TAF had no significant impact on the EC_{50} value of any HCV compound tested. Furthermore, CC_{50} values were not impacted by the presence of TAF. These results were consistent with the fact that HCV nonstructural protein 3 (NS3) PIs, telaprevir and boceprevir, are not dependent on CatA activity for their activity, and thus, are not impacted by TAF.

Table 95. Effect of TAF on the Anti-HCV Activity and Cytotoxicity of Direct and Nondirect-Acting Antivirals in HCV GT1a Replicon Cells

HCV Inhibitor Class (Target)	Compound[a]	Incubation with 1 µM TAF		
		EC_{50} (nM)	FC EC_{50} from Drug Alone[b]	CC_{50} (nM)
Nondirect-Acting Antivirals				
Not Applicable	interferon-α	3.7	1.3	> 122
	ribavirin	13836	1.0	> 1412320
Direct-Acting Antivirals				
PI (NS3)	telaprevir	1014	1.0	> 89600
	boceprevir	622	1.0	> 56750
	simeprevir	12.5	0.9	> 1080
NI (NS5B)	sofosbuvir	66.9	1.3	> 3400
NS5A	ledipasvir	0.05	0.8	> 2.5
	velpatasvir	0.01	0.9	> 1.1

CC_{50} = concentration inhibiting cell growth by 50%; EC_{50} = concentration inhibiting viral replication by 50%; FC = fold change; NI = nucleos(t)ide inhibitor; NS (3/4A/5A/5B) = nonstructural protein (3/4A/5A/5B); TAF = tenofovir alafenamide

a Mean EC_{50} values for interferon-α, ribavirin, telaprevir, boceprevir, simeprevir, sofosbuvir, ledipasvir, and velpatasvir were 2.8, 13929, 1054, 648, 13.5, 50.6, 0.06, and 0.011 nM, respectively.

b Mean fold change in drug EC_{50} values from at least 2 independent experiments performed in quadruplicate, expressed as a ratio of the activity in the presence versus the absence of TAF.

Source: PC-320-2001

6. DISCUSSION AND CONCLUSIONS

The INSTI BIC and the NRTIs FTC and TAF are potent and selective inhibitors of HIV-1 and HIV-2. All 3 drugs show potent ARV activity against diverse subtypes of HIV-1 in vitro. FTC and TAF are also potent inhibitors of HBV. Emtricitabine and TAF are phosphorylated intracellularly through nonoverlapping pathways, and in combination show no antagonism for the formation of their active metabolites. BIC does not require metabolic modification for activity. Two and 3 drug combinations of BIC, FTC, and TAF consistently show synergistic anti-HIV-1 activity in vitro and no evidence of toxicity.

The resistance profiles for the individual agents of BIC, FTC, and TAF have been well characterized. There is no cross-resistance between the NRTI and INSTI classes.

Nucleoside reverse transcriptase inhibitors carry a class labeling for mitochondrial toxicity; however, both FTC and TAF have shown a low potential for mitochondrial toxicity in long term toxicity studies and there was no evidence of toxicity to mitochondria in vitro and in vivo. Emtricitabine triphosphate and TFV-DP have high selectivities for HIV RT and are very weak inhibitors of mammalian DNA polymerases α, β, δ, and ε and mtDNA polymerase γ. However, as mitochondrial toxicity is not associated with INSTIs as a class, and as BIC is not anticipated to significantly increase the exposure of FTC or TFV, the potential for exacerbating mitochondrial toxicity is low.

Bictegravir, FTC, and TAF have no pharmacologically significant off-target binding affinity to the receptors tested. Bictegravir, FTC, and TAF have low in vitro cytotoxicity in a variety of human cell types. Bictegravir, FTC, and TAF had no or little effect on vital organ systems in safety pharmacology studies. Although TAF showed some potential to prolong the PR interval in the 39-week dog study, no findings were noted in the cardiovascular safety pharmacology study in dogs or in the thorough QT study.

There are no anticipated pharmacological interactions expected for the B/F/TAF FDC. Additional safety pharmacology studies on the B/F/TAF FDC are not warranted. The absence of nonclinical safety pharmacology studies with the combination is in accordance with the FDA Guidance for Industry, Nonclinical Safety Evaluation of Drug or Biologic Combinations, March 2006 and the Committee for Medicinal Products for Human Use (CHMP) Guideline on the Non-Clinical Development of Fixed Combinations of Medicinal Products (EMEA/CHMP/SWP/258498/2005, January 2008).

Overall, the pharmacodynamic and pharmacological assessment of BIC, FTC, and TAF supports the effective and safe use of these 3 agents together in combination therapy for HIV-1 disease.

7. REFERENCES

Abbott. KALETRA (lopinavir/ritonavir) Tablet, Film Coated for Oral use KALETRA (lopinavir/ritonavir) Solution for Oral use. US Prescribing Information. AbbVie LTD. North Chicago, IL. Revised January 2013:

Agouron Pharmaceuticals Inc. VIRACEPT® (nelfinavir mesylate) Tablets and Oral Powder. US Prescribing Information. La Jolla, CA. Revised May 2013. 2013:

Andrei G, Lisco A, Vanpouille C, Introini A, Balestra E, van den Oord J, et al. Topical Tenofovir, a Microbicide Effective against HIV, Inhibits Herpes Simplex Virus-2 Replication. Cell host & microbe 2011;10 (4):379-89.

Back DJ, Burger DM, Flexner CW, Gerber JG. The pharmacology of antiretroviral nucleoside and nucleotide reverse transcriptase inhibitors: implications for once-daily dosing. J Acquir Immune Defic Syndr 2005;39 Suppl 1:S1-23, quiz S4-5.

Balzarini J, Pelemans H, Esnouf R, De Clercq E. A novel mutation (F227L) arises in the reverse transcriptase of human immunodeficiency virus type 1 on dose-escalating treatment of HIV type 1-infected cell cultures with the nonnucleoside reverse transcriptase inhibitor thiocarboxanilide UC-781. AIDS Res Hum Retroviruses 1998;14 (3):255-60.

Bam RA, Birkus G, Babusis D, Cihlar T, Yant SR. Metabolism and antiretroviral activity of tenofovir alafenamide in CD4 T-cells and macrophages from demographically diverse donors. Antivir Ther 2014a:1-18.

Bam RA, Yant SR, Cihlar T. Tenofovir alafenamide is not a substrate for renal organic anion transporters (OATs) and does not exhibit OAT-dependent cytotoxicity. Antivir Ther 2014b:1-12.

Berg T, Zoulim F, Moeller B, Trinh H, Marcellin P, Chan S, et al. Long-term efficacy and safety of emtricitabine plus tenofovir DF vs. tenofovir DF monotherapy in adefovir-experienced chronic hepatitis B patients. J Hepatol 2014;60 (4):715-22.

Birkus G, Bam RA, Frey CR, Tsai L, Stray KM, Yant SR, et al. Intracellular Activation Pathways for GS-7340 and the Effect of Antiviral Protease Inhibitors [Poster J-115]. Presented at: 19th Conference on Retroviruses and Opportunistic Infections (CROI); 2012 March 5-8; Seattle, WA.

Birkus G, Hitchcock MJM, Cihlar T. Assessment of mitochondrial toxicity in human cells treated with tenofovir: comparison with other nucleoside reverse transcriptase inhibitors. Antimicrob Agents Chemother 2002;46 (3):716-23.

Birkus G, Kutty N, He GX, Mulato A, Lee W, McDermott M, et al. Activation of 9-[(R)-2-[[(S)-[[(S)-1-(Isopropoxycarbonyl)ethyl]amino] phenoxyphosphinyl]-methoxy]propyl]adenine (GS-7340) and other tenofovir phosphonoamidate prodrugs by human proteases. Mol Pharmacol 2008;74 (1):92-100.

Birkus G, Wang R, Liu XH, Kutty N, MacArthur H, Cihlar T, et al. Cathepsin A is the major hydrolase catalyzing the intracellular hydrolysis of the antiretroviral nucleotide phosphonoamidate prodrugs GS-7340 and GS-9131. Antimicrob Agents Chemother 2007;51 (2):543-50.

Bloor S, Kemp SD, Hertogs K, Alcorn T, Larder BA. Patterns of HIV drug resistance in routine clinical practice: a survey of almost 12000 samples from the USA in 1999. Antivir Ther 2000;5 (Suppl 3):132.

Boffito M, Miralles D, Hill A. Pharmacokinetics, efficacy, and safety of darunavir/ritonavir 800/100 mg once-daily in treatment-naive and -experienced patients. HIV Clin Trials 2008;9 (6):418-27.

Borroto-Esdoa K, Vela JE, Myrick F, Ray AS, Miller MD. In vitro evaluation of the anti-HIV activity and metabolic interactions of tenofovir and emtricitabine. Antivir Ther 2006;11 (3):377-84.

Brenner BG, Thomas R, Blanco JL, Ibanescu RI, Oliveira M, Mesplede T, et al. Development of a G118R mutation in HIV-1 integrase following a switch to dolutegravir monotherapy leading to cross-resistance to integrase inhibitors. J Antimicrob Chemother 2016;71:1948-53.

Bridges EG, Dutschman GE, Gullen EA, Cheng Y-C. Favorable interaction of β-L(-) nucleoside analogues with clinically approved anti-HIV nucleoside analogues for the treatment of human immunodeficiency virus. Biochem Pharmacol 1996;51 (6):731-6.

Brinkman K, Ter Hofstede HJ, Burger DM, Smeitink JAM, Koopmans PP. Adverse effects of reverse transcriptase inhibitors: mitochondrial toxicity as common pathway. AIDS 1998;12 (14):1735-44.

Bristol-Myers Squibb Company. Reyataz® (atazanavir sulfate) Capsules. US Prescribing Information. Princeton, NJ, USA. Revised February. 2011:

Brunelle MN, Lucifora J, Neyts J, Villet S, Holy A, Trepo C, et al. In Vitro Activity of 2,4-Diamino-6-[2-(Phosphonomethoxy)Ethoxy]-Pyrimidine against Multidrug-Resistant Hepatitis B Virus Mutants. Antimicrob Agents Chemother 2007;51 (6):2240-3.

Bukrinsky M, Sharova N, Stevenson M. Human immunodeficiency virus type 1 2-LTR circles reside in a nucleoprotein complex which is different from the preintegration complex. J Virol 1993;67 (11):6863-5.

Butler SL, Hansen MS, Bushman FD. A quantitative assay for HIV DNA integration in vivo. Nat Med 2001;7 (5):631-4.

Callebaut C, Stray K, Tsai L, Williams M, Yang ZY, Cannizzaro C, et al. In vitro characterization of GS-8374, a novel phosphonate-containing inhibitor of HIV-1 protease with a favorable resistance profile. Antimicrob Agents Chemother 2011;55 (4):1366-76.

Carr A. Toxicity of antiretroviral therapy and implications for drug development. Nat Rev Drug Discov 2003;2 (8):624-34.

Cavalcanti JS, Lanca AM, Ferreira JL, Eira M, Dantas DS, Brigido LF. In-vivo selection of the mutation F121Y in a patient failing raltegravir containing salvage regimen. Antiviral Res 2012;95:9-11.

Champoux JJ, Schultz SJ. Ribonuclease H: properties, substrate specificity and roles in retroviral reverse transcription. The FEBS journal 2009;276 (6):1506-16.

Cheng Y-C, Krishnan P, Chou KM, Liou JY, Lam W, Fu Q. The role of 3-phosphoglycerate kinase and AP endonuclease for the action of antiviral L-nucleoside against hepatitis B and human immunodeficiency virus [abstract]. Hep DART 2001; 2001 December 16-20; Maui, Hawaii. ELSEVIER. Abstract 030.

Cherrington JM, Allen SJW, Bischofberger N, Chen MS. Kinetic interaction of the diphosphates of 9-(2-phosphonylmethoxyethyl)adenine and other anti-HIV active purine congeners with HIV reverse transcriptase and human DNA polymerases α, β, and γ. Antivir Chem Chemother 1995a;6 (4):217-21.

Cherrington JM, Allen SJW, McKee BH, Chen MS. Kinetic analysis of the interaction between the diphosphate of (*S*)-1-(3- hydroxy-2-phosphonylmethoxypropyl)cytosine, ddCTP, AZTTP, and FIAUTP with human DNA polymerases β and γ. Biochem Pharmacol 1994;48 (10):1986-8.

Cherrington JM, Mulato AS, Fuller MD, Chen MS. In vitro selection and characterization of HIV-1 viral isolates with reduced sensitivity to PMEA. 4th International HIV Resistance Conference; 1995b Jul; Sardinia, Italy.

Cihlar T, Birkus G, Greenwalt DE, Hitchcock MJM. Tenofovir exhibits low cytotoxicity in various human cell types: comparison with other nucleoside reverse transcriptase inhibitors. Antiviral Res 2002;54 (1):37-45.

Cihlar T, Chen MS. Incorporation of selected nucleoside phosphonates and anti-human immunodeficiency virus nucleotide analogues into DNA by human DNA polymerases α, β and γ. Antivir Chem Chemother 1997;8 (3):187-95.

Cihlar T, Ho ES, Lin DC, Mulato AS. Human renal organic anion transporter 1 (hOAT1) and its role in the nephrotoxicity of antiviral nucleotide analogs. Nucleosides Nucleotides Nucleic Acids 2001;20 (4-7):641-8.

Condreay LD, Condreay JP, Jansen RW, Paff MT, Averett DR. (-)-cis-5-fluoro-1-[2-(hydroxymethyl)-1,3-oxathiolan-5-yl]cytosine (524W91) inhibits hepatitis B virus replication in primary human hepatocytes. Antimicrob Agents Chemother 1996;40 (2):520-3.

Condreay LD, Jansen RW, Powdrill TF, Johnson LC, Selleseth DW, Paff MT, et al. Evaluation of the potent anti-hepatitis B virus agent (-) cis-5-fluoro-1-[2-(hydroxymethyl)-1,3-oxathiolan-5-yl]cytosine in a novel in vivo model. Antimicrob Agents Chemother 1994;38 (3):616-9.

Corsa A, Liu Y, Flaherty JF, Marcellin P, Miller M, Kitrinos KM. No Detectable Resistance to Tenofovir Disoproxil Fumarate (TDF) in HBeAg+ and HBeAg- Patients With Chronic Hepatitis B (CHB) After Eight Years of Treatment [Poster 1707]. The 65th Annual Meeting of the American Association for the Study of Liver Diseases: The Liver Meeting (AASLD); 2014 November 7-11; Boston MA United States.

Cui L, Schinazi RF, Gosselin G, Imbach J-L, Chu CK, Rando RF, et al. Effect of beta-enantiomeric and racemic nucleoside analogues on mitochondrial functions in HepG2 cells. Biochem Pharmacol 1996;52 (10):1577-84.

Cullen JM, Smith SL, Davis MG, Dunn SE, Botteron C, A C, et al. In vivo antiviral activity and pharmacokinetics of (-)-cis-5-fluoro-1-[2-(hydroxymethyl)-1,3-oxathiolan-5-yl]cytosine in woodchuck hepatitis virus-infected woodchucks. Antimicrob Agents Chemother 1997;41:2076-82.

Damond F, Collin G, Matheron S, Peytavin G, Campa P, Delarue S, et al. Letter. In vitro phenotypic susceptibility to nucleoside reverse transcriptase inhibitors of HIV-2 isolates with the Q151M mutation in the reverse transcriptase gene. Antivir Ther 2005;10 (7):861-5.

Davis MG, Wilson JE, VanDraanen NA, Miller WH, Freeman GA, Daluge, et al. DNA polymerase activity of hepatitis B virus particles: differential inhibition by L-enantiomers of nucleotide analogs. Antiviral Res 1996;30 (2-3):133-45.

De Antoni A, Foli A, Lisziewicz J, Lori F. Mutations in the *pol* gene of human immunodeficiency virus type 1 in infected patients receiving didanosine and hydroxyurea combination therapy. J Infect Dis 1997;176:899-903.

Delaney WE, IV, Ray AS, Yang H, Qi X, Xiong S, Zhu Y, et al. Intracellular metabolism and in vitro activity of tenofovir against hepatitis B virus. Antimicrob Agents Chemother 2006;50 (7):2471-7.

Delaney WE, IV, Yang H, Miller MD, Gibbs CS, Xiong S. Combinations of adefovir with nucleoside analogs produce additive antiviral effects against hepatitis B virus in vitro. Antimicrob Agents Chemother 2004;48 (10):3702-10.

DeMan RA, Wolters LMM, Nevens F, Chua D, Sherman M, Lai, Cing L, Gadana A, et al. Safety and Efficacy of Oral Entecavir Given for 28 Days in Patients With Chronic Hepatitis B Virus Infection. Hepatology 2001;34 (3):578-82.

Deval J, White KL, Miller MD, Parkin NT, Courcambeck J, Halfon P, et al. Mechanistic basis for reduced viral and enzymatic fitness of HIV-1 reverse transcriptase containing both K65R and M184V mutations. J Biol Chem 2004;279 (1):509-16.

Duvivier C, Kolta S, Assoumou L, Ghosn J, Rozenberg S, Murphy RL, et al. Greater decrease in bone mineral density with protease inhibitor regimens compared with nonnucleoside reverse transcriptase inhibitor regimens in HIV-1 infected naive patients. AIDS 2009;27 (7):817-24.

Eisenberg EJ, He G-X, Lee WA. Metabolism of GS-7340, a novel phenyl monophosphoramidate intracellular prodrug of PMPA, in blood. Nucleosides Nucleotides Nucleic Acids 2001;20 (4-7):1091-8.

Elion GB, Singer S, Hitchings GH. Antagonists of nucleic acid derivatives. VIII. Synergism in combinations of biochemically related antimetabolites. J Biol Chem 1954;208 (2):477-88.

Feng JY, Myrick FT, Margot NA, Mulamba GB, Rimsky L, Borroto-Esoda K, et al. Virologic and enzymatic studies revealing the mechanism of K65R- and Q151m-associated HIV-1 drug resistance towards emtricitabine and lamivudine. Nucleosides Nucleotides Nucleic Acids 2006;25 (1):89-107.

Feng JY, Shi J, Schinazi RF, Anderson KS. Mechanistic studies show that (-)-FTC-TP is a better inhibitor of HIV-1 reverse transcriptase than 3TC-TP. FASEB J 1999;13 (12):1511-7.

Frankel FA, Invernizzi CF, Oliveira M, Wainberg MA. Diminished efficiency of HIV-1 reverse transcriptase containing the K65R and M184V drug resistance mutations. AIDS 2007;21 (6):665-75.

Fulco PP, Kirian MA. Effect of tenofovir on didanosine absorption in patients with HIV. Ann Pharmacother 2003;37 (9):1325-8.

Furman PA, Davis M, Liotta DC, Paff M, Frick LW, Nelson DJ, et al. The anti-hepatitis B virus activities, cytotoxicities, and anabolic profiles of the (-) and (+) enantiomers of cis-5-fluoro-1-[2-(hydroxymethyl)-1,3-oxathiolan-5-yl]cytosine. Antimicrob Agents Chemother 1992;36 (12):2686-92.

Furman PA, Wilson JE, Reardon JE, Painter GR. The effect of absolute configuration on the anti-HIV and anti-HBV activity of nucleoside analogues. Antivir Chem Chemother 1995;6 (6):345-55.

Garcia-Lerma JG, MacInnes H, Bennett D, Reid P, Nidtha S, Weinstock H, et al. A novel genetic pathway of human immunodeficiency virus type 1 resistance to stavudine mediated by the K65R mutation. J Virol 2003;77 (10):5685-93.

Garcia-Lerma JG, Otten R, Cong M-e, Jackson E, Janssen R, Folks T, et al. Intermittent antiretroviral prophylaxis with tenofovir and emtricitabine protects macaques against repeated rectal SHIV exposures [abstract 85]. 16th International HIV Drug Resistance Workshop; 2007 June 12-16; Bridgetown, Barbados.

Geretti AM, Armenia D, Ceccherini-Silberstein F. Emerging patterns and implications of HIV-1 integrase inhibitor resistance. Curr Opin Infect Dis 2012;25 (6):677-86.

Gilead Sciences Inc. VIREAD® (tenofovir disoproxil fumarate) tablets, for oral use VIREAD® (tenofovir disoproxil fumarate) powder, for oral use. U.S. Prescribing Information. Foster City, CA. Revised October 2013:

Goldwater R, DeMicco M, Zong J, Chittick G, Yuen G, West S, et al. Safety, pharmacokinetics and antiviral activity of single oral doses of the HCV NS3 protease inhibitor GS-9256 [Poster Abstract 824]. 61st Annual Meeting of the American Association for the Study of Liver Diseases (AASLD); 2010 October 29th - November 2nd; Boston, MA.

Gu Z, Fletcher RS, Arts EJ, Wainberg MA, Parniak MA. The K65R mutant reverse transcriptase of HIV-1 cross-resistant to 2',3'-dideoxycytidine, 2',3'-dideoxy-3'-thiacytidine, and 2',3'-dideoxyinosine shows reduced sensitivity to specific dideoxynucleoside triphosphate inhibitors in vitro. J Biol Chem 1994a;269 (45):28118-22.

Gu Z, Gao Q, Fang H, Salomon H, Parniak MA, Goldberg E, et al. Identification of a mutation of codon 65 in the IKKK motif of reverse transcriptase that encodes human immunodeficiency virus resistance to 2',3'-dideoxycytidine and 2',3'-dideoxy-3'-thiacytidine. Antimicrob Agents Chemother 1994b;38 (2):275-81.

Hadziyannis SJ, Tassopoulos NC, Heathcote EJ, Chang TT, Kitis G, Rizzetto M, et al. Long-term Therapy With Adefovir Dipivoxil for HBeAg-Negative Chronic Hepatitis B for up to 5 Years. Gastroenterology 2006;131 (6):1743-51.

Harrigan PR, Miller MD, McKenna P, Brumme ZL, Larder BA. Phenotypic susceptibilities to tenofovir in a large panel of clinically derived human immunodeficiency virus type 1 isolates. Antimicrob Agents Chemother 2002;46 (4):1067-72.

Heijtink RA, Kruining J, de Wilde GA, Balzarini J, De Clercq E, Schalm SW. Inhibitory effects of acyclic nucleoside phosphonates on human hepatitis B virus and duck hepatitis B virus infections in tissue culture. Antimicrob Agents Chemother 1994;38 (9):2180-2.

Henry M, Tourres C, Colson P, Ravaux I, Poizot-Martin I, Tamalet C. Coexistence of the K65R/L74V and/or K65R/T215Y mutations on the same HIV-1 genome. J Clin Virol 2006;37 (3):227-30.

Hertogs K, Bloor S, De Vroey V, Van Den Eynde C, Dehertogh P, Van Cauwenberge A, et al. A novel human immunodeficiency virus type 1 reverse transcriptase mutational pattern confers phenotypic lamivudine resistance in the absence of mutation 184V. Antimicrob Agents and Chemother 2000;44 (3):568-73.

Hightower KE, Wang R, Deanda F, Johns BA, Weaver K, Shen Y, et al. Dolutegravir (S/GSK1349572) exhibits significantly slower dissociation than raltegravir and elvitegravir from wild-type and integrase inhibitor-resistant HIV-1 integrase-DNA complexes. Antimicrob Agents Chemother 2011;55 (10):4552-9.

Hill J. In vitro synergy studies of FTC in combination with MKC 442, AZT, Nelfinavir (NELF), Nevirapine (NEV) against HIV. Triangle Pharmaceuticals, Inc. Report No. Doc #470. July 31, 1997.

Ho ES, Lin DC, Mendel DB, Cihlar T. Cytotoxicity of antiviral nucleotides adefovir and cidofovir is induced by the expression of human renal organic anion transporter 1. J Am Soc Nephrol 2000;11 (3):383-93.

Jeong LS, Schinazi RF, Beach JW, Kim HO, Nampalli S, Shanmuganathan K, et al. Asymmetric synthesis and biological evaluation of beta-L-(2R,5S)- and alpha-L-(2R,5R)-1,3-oxathiolane-pyrimidine and -purine nucleosides as potential anti-HIV agents. J Med Chem 1993;36 (2):181-95.

Jones G, Ledford RM, Yu F, Chen X, Miller MD, Tsiang M, et al. In vitro resistance profile of HIV-1 mutants selected by the HIV-1 integrase inhibitor, GS-9137 (JTK-303) [poster number 627]. 14th Conference on Retroviruses and Opportunistic Infections; 2007 February 25-28; Los Angeles, Calif, USA.

Jones SA, Hu J. Hepatitis B virus reverse transcriptase: diverse functions as classical and emerging targets for antiviral intervention. Emerging microbes & infections 2013;2 (9):1-9.

Kagan RM, Lee TS, Ross L, Lloyd RM, Jr., Lewinski MA, Potts SJ. Molecular basis of antagonism between K70E and K65R tenofovir-associated mutations in HIV-1 reverse transcriptase. Antiviral Res 2007;75 (3):210-8.

Kalayjian RC, Landay A, Pollard RB, Taub DD, Gross BH, Francis IR, et al. Age-related immune dysfunction in health and in human immunodeficiency virus (HIV) disease: association of age and HIV infection with naive CD8+ cell depletion, reduced expression of CD28 on CD8+ cells, and reduced thymic volumes. J Infect Dis 2003;187 (12):1924-33.

Kamkolar M, Clayton MM, Zhang SM, Black PL, Schinazi RF, Feitelson MA. Novel therapeutics for hepatitis B and C: Evaluation of therapies for hepatitis B virus in the HBV transgenic SCID mouse model. In: Schinazi RF, Rice CM, Sommadossi JP, eds. Frontiers in Viral Hepatitis. Netherlands: Elsevier Science; 2002: 211-22.

Kienle RD, Bruyette D, Pion PD. Effects of thyroid hormone and thyroid dysfunction on the cardiovascular system. Vet Clin North Am Small Anim Pract 1994;24 (3):495-507.

Kobayashi M, Nakahara K, Seki T, Miki S, Kawauchi S, Suyama A, et al. Selection of diverse and clinically relevant integrase inhibitor-resistant human immunodeficiency virus type 1 mutants. Antiviral Res 2008;doi:10.1016/j.antiviral.2008.06012.

Kobayashi M, Yoshinaga T, Seki T, Wakasa-Morimoto C, Brown KW, Ferris R, et al. In Vitro antiretroviral properties of S/GSK1349572, a next-generation HIV integrase inhibitor. Antimicrob Agents Chemother 2011;55 (2):813-21.

Korba BE, Schinazi RF, Cote P, Tennant B, Gerin JL. Effect of oral administration of emtricitabine on woodchuck hepatitis virus replication in chronically infected woodchucks. Antimicrob Agents Chemother 2000;44 (6):1757-60.

Kramata P, Birkus G, Otmar M, Votruba I, Holy A. Structural features of acyclic nucleotide analogs conferring inhibitory effects on cellular replicative DNA polymerases. Collection Symposium Series (Holy A and Tocik Z, eds), Institute of Organic Chemistry and Biochemistry, Academy of Sciences of Czech Republic, Prague, Czech Republic 1996;1:188-91.

Kramata P, Downey KM, Paborsky LR. Incorporation and excision of 9-(2-phosphonylmethoxyethyl)guanine (PMEG) by DNA polymerase delta and epsilon in vitro. J Biol Chem 1998;273 (34):21966-71.

Kulkarni R, Hluhanich R, McColl DM, Miller MD, White KL. The combined anti-HIV-1 activities of emtricitabine and tenofovir plus the integrase inhibitor elvitegravir or raltegravir show high levels of synergy in vitro. Antimicrob Agents Chemother 2014;58 (10):6145-50.

Lacombe K, Ollivet A, Gozlan J, Durantel S, Tran N, Girard PM, et al. A novel hepatitis B virus mutation with resistance to adefovir but not to tenofovir in an HIV-hepatitis B virus-co-infected patient. AIDS 2006;20 (17):2229-31.

Lada O, Benhamou Y, Cahour A, Katlama C, Poynard T, Thibault V. In vitro susceptibility of lamivudine-resistant hepatitis B virus to adefovir and tenofovir. Antivir Ther 2004;9 (3):353-63.

Lataillade M, Chiarella J, Kozal MJ. Natural polymorphism of the HIV-1 integrase gene and mutations associated with integrase inhibitor resistance. Antivir Ther 2007;12 (4):563-70.

Lawitz E, Hill JB, Marbury T, Rodriguez-Torres M, DeMicco M, Quesada J, et al. Three-day, dose-ranging study of the HCV NS3 protease inhibitor GS-9451 [Poster Abstract 820]. 61st Annual Meeting of the American Association for the Study of Liver Diseases (AASLD); 2010 October 29th - November 2nd; Boston, MA.

Ledford RM, Vela JE, Ray AS, Callebaut C, Miller MD, McColl DJ. The long intracellular half-life of tenofovir diphosphate correlates with persistent inhibition of HIV-1 replication in vitro [poster number 60]. 19th International Conference on Antiviral Research (ICAR); 2006 May 7-11; San Juan, Puerto Rico.

Lee WA, He G-X, Eisenberg E, Cihlar T, Swaminathan S, Mulato A, et al. Selective intracellular activation of a novel prodrug of the human immunodeficiency virus reverse transcriptase inhibitor tenofovir leads to preferential distribution and accumulation in lymphatic tissue. Antimicrob Agents Chemother 2005;49 (5):1898-906.

Liaw YF, Gane E, Leung N, Zeuzem S, Wang Y, Lai CL, et al. 2-Year GLOBE trial results: telbivudine Is superior to lamivudine in patients with chronic hepatitis B. Gastroenterology 2009;136 (2):486-95.

Lin TI, Lenz O, Fanning G, Verbinnen T, Delouvroy F, Scholliers A, et al. In vitro activity and preclinical profile of TMC435350, a potent hepatitis C virus protease inhibitor. Antimicrob Agents Chemother 2009;53 (4):1377-85.

Liu Y, Kitrinos K, Babusis D, Ray A, Miller MD, Callebaut C. Lack of Effect of Tenofovir Alafenamide (TAF) on Primary Osteoblasts In Vitro at Clinically Relevant Drug Concentrations [Poster H-664]. 53rd Interscience Conference on Antimicrobial Agents and Chemotherapy (ICAAC); 2013 September 10-13; Denver, CO,.

Liu Y, Mitchell B, Dinh P, Miller MD, Kitrinos KM. Antiviral Activity of Tenofovir Alafenamide Against Drug-Resistant HBV Isolates In Vitro [Poster 2021]. American Association for the Study of Liver Diseases (AASLD); 2015 13-17 November; San Francisco, CA.

Lok ASF, Lai C-L, Leung N, Yao G-B, Cui Z-Y, Schiff ER, et al. Long-term safety of lamivudine treatment in patients with chronic hepatitis B. Gastroenterology 2003;125 (6):1714-22.

Ly JK, Margot NA, MacArthur H, Hung M, Miller MD, White KL. The balance between NRTI discrimination and excision drives the susceptibility of HIV-1 RT mutants K65R, M184V and K65R+M184V. Antivir Chem Chemother 2008;18 (6):307-16.

Ma TW, Lin J, Newton M, Cheng YC, Chu CK. Synthesis and anti-hepatitis B virus activity of 9-(2-deoxy-2-fluoro-β-L-arabinofuranosyl)purine nucleosides. J Med Chem 1997;40 (17):2750-4.

Malet I, Fourati S, Charpentier C, Morand-Joubert L, Armenia D, Wirden M, et al. The HIV-1 integrase G118R mutation confers raltegravir resistance to the CRF02_AG HIV-1 subtype. J Antimicrob Chemother 2011.

Malet I, Gimferrer Arriaga L, Artese A, Costa G, Parrotta L, Alcaro S, et al. New raltegravir resistance pathways induce broad cross-resistance to all currently used integrase inhibitors. J Antimicrob Chemother 2014;69 (8):2118-22.

Manns MP, Bourliere M, Benhamou Y, Pol S, Bonacini M, Trepo C, et al. Potency, safety, and pharmacokinetics of the NS3/4A protease inhibitor BI201335 in patients with chronic HCV genotype-1 infection. J Hepatol 2011;54 (6):1114-22.

Marchand B, White KL, Ly JK, Margot NA, Wang R, McDermott M, et al. Effects of the translocation status of human immunodeficiency virus type 1 reverse transcriptase on the efficiency of excision of tenofovir. Antimicrob Agents Chemother 2007;51 (8):2911-9.

Margot NA, Hluhanich RM, Jones GS, Andreatta KN, Tsiang M, McColl DJ, et al. In vitro resistance selections using elvitegravir, raltegravir, and two metabolites of elvitegravir M1 and M4. Antiviral Res 2012;93 (2):288-96.

Margot NA, Lu B, Cheng A, Miller MD. Resistance development over 144 weeks in treatment-naive patients receiving tenofovir disoproxil fumarate or stavudine with lamivudine and efavirenz in Study 903. HIV Med 2006a;7 (7):442-50.

Margot NA, Waters JM, Miller MD. In Vitro Human Immunodeficiency Virus Type 1 Resistance Selections with Combinations of Tenofovir and Emtricitabine or Abacavir and Lamivudine. Antimicrob Agents Chemother 2006b;50 (12):4087-95.

Markowitz M, Zolopa A, Ruane P, Squires K, Zhong L, Kearney BP, et al. GS-7340 Demonstrates Greater Declines in HIV-1 RNA than Tenofovir Disoproxil Fumarate During 14 Days of Monotherapy in HIV-1 Infected Subjects [Oral Presentaton / Paper 152LB]. 18th Conference on Retroviruses and Opportunistic Infections (CROI); 2011 February 27 - March 2; Boston, MA.

Mathez D, Schinazi RF, Liotta DC, Leibowitch J. Infectious amplification of wild-type human immunodeficiency virus from patients' lymphocytes and modulation by reverse transcriptase inhibitors in vitro. Antimicrob Agents Chemother 1993;37 (10):2206-11.

Mathias AA, German P, Murray BP, Wei L, Jain A, West S, et al. Pharmacokinetics and pharmacodynamics of GS-9350: a novel pharmacokinetic enhancer without anti-HIV activity. Clin Pharmacol Ther 2010;87 (3):322-9.

McColl DJ, Chappey C, Parkin NT, Miller MD. Prevalence, genotypic associations and phenotypic characterization of K65R, L74V and other HIV-1 RT resistance mutations in a commercial database. Antivir Ther 2008;13:189-97.

McColl DJ, Chen X. Strand transfer inhibitors of HIV-1 integrase: bringing IN a new era of antiretroviral therapy. Antiviral Res 2010;85 (1):101-18.

Menne S, Cote PJ, Korba BE, Butler SD, George AL, Tochkov IA, et al. Antiviral effect of oral administration of tenofovir disoproxil fumarate in woodchucks with chronic woodchuck hepatitis virus infection. Antimicrob Agents Chemother 2005;49 (7):2720-8.

Mesplede T, Quashie PK, Wainberg MA. Resistance to HIV integrase inhibitors. Curr Opin HIV AIDS 2012;7 (5):401-8.

Meyer PR, Matsuura SE, So AG, Scott WA. Unblocking of chain-terminated primer by HIV-1 reverse transcriptase through a nucleotide-dependent mechanism. Proc Natl Acad Sci USA 1998;95 (23):13471-6.

Miller MD, Anton KE, Mulato AS, Lamy PD, Cherrington JM. Human immunodeficiency virus type 1 expressing the lamivudine-associated M184V mutation in reverse transcriptase shows increased susceptibility to adefovir and decreased replication capability in vitro. J Infect Dis 1999;179 (1):92-100.

Miller MD, Margot N, Lu B, Zhong L, Chen S-S, Cheng A, et al. Genotypic and phenotypic predictors of the magnitude of response to tenofovir disoproxil fumarate treatment in antiretroviral-experienced patients. J Infect Dis 2004;189 (5):837-46.

Miller MD, Margot NA, Lamy PD, Fuller MD, Anton KE, Mulato AS, et al. Adefovir and tenofovir susceptibilities of HIV-1 after 24 to 48 weeks of adefovir dipivoxil therapy: genotypic and phenotypic analyses of study GS-96-408. J Acquir Immune Defic Syndr Hum Retrovirol 2001;27 (5):450-8.

Miller MD, White KL, Petropoulos CJ, Parkin NT. Decreased replication capacity of HIV-1 clinical isolates containing K65R or M184V RT mutations [poster]. 10th Conference on Retroviruses and Opportunistic Infections; 2003 February 10-14; Boston, Mass, USA. Poster Number 616.

Min S, Song I, Borland J, Chen S, Lou Y, Fujiwara T, et al. Pharmacokinetics and safety of S/GSK1349572, a next-generation HIV integrase inhibitor, in healthy volunteers. Antimicrob Agents Chemother 2010;54 (1):254-8.

Moyle G. Clinical manifestations and management of antiretroviral nucleoside analog-related mitochondrial toxicity. Clin Ther 2000;22 (8):911-36.

Mulato AS, Cherrington JM. Anti-HIV activity of adefovir (PMEA) and PMPA in combination with antiretroviral compounds: in vitro analyses. Antiviral Res 1997;36 (2):91-7.

Mulato AS, Lamy PD, Miller MD, Li W-X, Anton KE, Hellmann NS, et al. Genotypic and phenotypic characterization of human immunodeficiency virus type 1 variants isolated from AIDS patients after prolonged adefovir dipivoxil therapy. Antimicrob Agents Chemother 1998;42 (7):1620-8.

Murakami E, Babusis D, Wang T, Park Y, Lepist EI, Hao J, et al. Efficient Hepatic Delivery of Tenofovir by Prodrug Tenofovir Alafenamide in Nonclinical Studies Supports Low-Dose Treatment of Hepatitis B Virus [Abstract]. HepDART: Frontiers in Drug Development for Viral Hepatitis; 2013 December 8-12; Big Island, HI.

Murakami E, Tolstykh T, Bao H, Niu C, Steuer HM, Bao D, et al. Mechanism of activation of PSI-7851 and its diastereoisomer PSI-7977. J Biol Chem 2010;285 (45):34337-47.

Murakami E, Wang T, Park Y, Hao J, Lepist EI, Babusis D, et al. Implications of Efficient Hepatic Delivery by Tenofovir Alafenamide (GS-7340) for Hepatitis B Virus Therapy [Accepted Manuscript]. Antimicrob Agents Chemother 2015;59 (6):3563-9.

Murphy RL, Brun S, Hicks C, Eron JJ, Gulick R, King M, et al. ABT-378/ritonavir plus stavudine and lamivudine for the treatment of antiretroviral-naive adults with HIV. AIDS 2001;15 (1):F1-F9.

Naeger LK, Margot NA, Miller MD. Tenofovir is Less Susceptible to Pyrophosphorolysis and Nucleotide-Dependent Chain-Terminator Removal than Zidovudine or Stavudine. XIV International Roundtable on Nucleosides, Nucelotides, and Their Biological Applications; 2000 Sep 10-14; San Francisco, Calif.

Paff MT, Averett DR, Prus KL, Miller WH, Nelson DJ. Intracellular metabolism of (-)- and (+)-cis-5-fluoro-1-[2-(hydroxymethyl)-1,3-oxathiolan-5-yl]cytosine in HepG2 derivative 2.2.15 (subclone P5A) cells. Antimicrob Agents Chemother 1994;38 (6):1230-8.

Painter G, St. Clair MH, Chingm S, Noblin J, Wang L, Furman PA. 524W91. Anti-HIV, Anti-Hepatitis B Virus. Drugs of the Future 1995;20 (8):761-5.

Palmer S, Margot N, Gilbert H, Shaw N, Buckheit R, Jr, Miller M. Tenofovir, adefovir, and zidovudine susceptibilities of primary human immunodeficiency virus type 1 isolates with non-B subtypes or nucleoside resistance. AIDS Res Hum Retroviruses 2001;17 (12):1167-73.

Pan-Zhou X-R, Cui L, Zhou X-J, Sommadossi J-P, Darley-Usmar VM. Differential effects of antiretroviral nucleoside analogs on mitochondrial function in HepG2 cells. Antimicrob Agents Chemother 2000;44 (3):496-503.

Parikh UM, Bacheler L, Koontz D, Mellors JW. The K65R mutation in human immunodeficiency virus type 1 reverse transcriptase exhibits bidirectional phenotypic antagonism with thymidine analog mutations. J Virol 2006a;80 (10):4971-7.

Parikh UM, Barnas DC, Faruki H, Mellors JW. Antagonism between the HIV-1 reverse-transcriptase mutation K65R and thymidine-analogue mutations at the genomic level. J Infect Dis 2006b;194 (5):651-60.

Parikh UM, Zelina S, Sluis-Cremer N, Mellors JW. Molecular mechanisms of bidirectional antagonism between K65R and thymidine analog mutations in HIV-1 reverse transcriptase. AIDS 2007;21 (11):1405-14.

Patterson SJ, George J, Strasser SI, Lee AU, Sievert W, Nicoll AJ, et al. Tenofovir disoproxil fumarate rescue therapy following failure of both lamivudine and adefovir dipivoxil in chronic hepatitis B. Gut 2011;60:247-54.

Patterson TF, Boucher HW, Herbrecht R, Denning DW, Lortholary O, Ribaud P, et al. Strategy of following voriconazole versus amphotericin B therapy with other licensed antifungal therapy for primary treatment of invasive aspergillosis: impact of other therapies on outcome. Clin Infect Dis 2005;41 (10):1448-52.

Perez-Bercoff D, Wurtzer S, Compain S, Benech H, Clavel F. Human immunodeficiency virus type 1: resistance to nucleoside analogues and replicative capacity in primary human macrophages. J Virol 2007;81 (9):4540-50.

Petropoulos CJ, Parkin NT, Limoli KL, Lie YS, Wrin T, Huang W, et al. A novel phenotypic drug susceptibility assay for human immunodeficiency virus type 1. Antimicrob Agents Chemother 2000;44:920-8.

Petry A, Brainard DM, Van Dyck K, Nachbar R, De Lepeleire I, Caro L, et al. Safety and antiviral activity of MK-5172, a novel HCV NS3/4a protease inhibitor with potent activity against known resistance mutants, in genotype 1 and 3 hcv-infected patients [Poster Abstract]. Presented at: 61st Annual Meeting of the American Association for the Study of Liver Diseases (AASLD); 2010; Boston, MA.

Pisarev VM, Lee S-H, Connelly MC, Fridland A. Intracellular metabolism and action of acyclic nucleoside phoshonates on DNA replication. Mol Pharmacol 1997;52 (1):63-8.

Pluymers W, Neamati N, Pannecouque C, Fikkert V, Marchand C, Burke TR, Jr., et al. Viral entry as the primary target for the anti-HIV activity of chicoric acid and its tetra-acetyl esters. Mol Pharmacol 2000;58 (3):641-8.

Pommier Y, Pilon A, Bajaj K, Mazumder A, Neamati N. HIV-1 integrase as a target for antiviral drugs. Antivir Chem Chemother 1997;8 (6):463-83.

Pozniak A, Mingrone H, Shuldyakov A, Brites C, Andrade-Villanueva JF, Hagins D, et al. Dolutegravir (DTG) Versus Raltegravir (RAL) in ART-Experienced, Integrase-Naive Subjects: 24 Week Interim Results From SAILING (ING111762) [Poster 179LB]. 20th Conference on Retroviruses and Opportunistic Infections; 2013 March 3-6; Atlanta, GA.

Prichard MN, Aseltine KR, Shipman C, Jr. MacSynergy™ II, Version 1.0. University of Michigan, Ann Arbor, Michigan, 1993a:

Prichard MN, Prichard LE, Shipman C, Jr. Strategic design and three-dimensional analysis of antiviral drug combinations. Antimicrob Agents Chemother 1993b;37 (3):540-5.

Prichard MN, Shipman C, Jr. A three-dimensional model to analyze drug-drug interactions. Antiviral Res 1990;14 (4-5):181-205.

Qi X, Xiong S, Yang H, Miller M, Delaney WE, IV. In vitro susceptibility of adefovir-associated hepatitis B virus polymerase mutations to other antiviral agents. Antivir Ther 2007;12 (3):355-62.

Quashie PK, Mesplede T, Han YS, Oliveira M, Singhroy DN, Fujiwara T, et al. Characterization of the R263K mutation in HIV-1 integrase that confers low-level resistance to the second-generation integrase strand transfer inhibitor dolutegravir. J Virol 2012;86 (5):2696-705.

Quashie PK, Mesplede T, Han YS, Veres T, Osman N, Hassounah S, et al. Biochemical analysis of the role of G118R-linked dolutegravir drug resistance substitutions in HIV-1 integrase. Antimicrob Agents Chemother 2013a;57 (12):6223-35.

Quashie PK, Mesplede T, Wainberg MA. Evolution of HIV integrase resistance mutations. Curr Opin Infect Dis 2013b;26 (1):43-9.

Ray A, Olson L, Fridland A. Role of purine nucleoside phosphorylase in drug interactions between 2',3'-dideoxyinosine and allopurinol, ganciclovir or tenofovir. Antimicrob Agents Chemother 2004;48 (4):1089-95.

Ray AS, Myrick F, Vela JE, Olson LY, Eisenberg EJ, Borroto-Esoda K, et al. Lack of a metabolic and antiviral drug interaction between tenofovir, abacavir and lamivudine. Antivir Ther 2005;10 (3):451-7.

Rimsky LT. In vitro synergy studies with FTC and other anti-HIV compounds. Triangle Pharmaceuticals, Inc. Report No. Doc #10804. January 12, 2001.

Robbins BL, Greenhaw JJ, Connelly MC, Fridland A. Metabolic pathways for activation of the antiviral agent 9-(2-phosphonylmethoxyethyl)adenine in human lymphoid cells. Antimicrob Agents Chemother 1995;39 (10):2304-8.

Robbins BL, Srinivas RV, Kim C, Bischofberger N, Fridland A. Anti-human immunodeficiency virus activity and cellular metabolism of a potential prodrug of the acyclic nucleoside phosphonate 9-*R*-(2-phosphonomethoxypropyl)adenine (PMPA), Bis(isopropyloxymethylcarbonyl) PMPA. Antimicrob Agents Chemother 1998;42 (3):612-7.

Robbins BL, Wilcox CK, Fridland A, Rodman JH. Metabolism of tenofovir and didanosine in quiescent or stimulated human peripheral blood mononuclear cells. Pharmacotherapy 2003;23 (6):695-701.

Ross L, Parkin N, Chappey C, Fisher R, St Clair M, Bates M, et al. Phenotypic impact of HIV reverse transcriptase M184I/V mutations in combination with single thymidine analog mutations on nucleoside reverse transcriptase inhibitor resistance. AIDS 2004;18 (12):1691-6.

Ruane P, DeJesus E, Berger D, Markowitz M, Bredeek UF, Callebaut C, et al. GS-7340 25 mg and 40 mg Demonstrate Greater Antiviral Activity Compared with TDF 300 mg in a 10-Day Monotherapy Study of HIV-1 Infected Patients [Presentation]. 19th Conference on Retroviruses and Opportunistic Infections (CROI); 2012 March 7th; Seattle, WA.

Ruane PJ, Dejesus E, Berger D, Markowitz M, Bredeek UF, Callebaut C, et al. Antiviral Activity, Safety, and Pharmacokinetics/Pharmacodynamics of Tenofovir Alafenamide as 10-Day Monotherapy in HIV-1-Positive Adults. J Acquir Immune Defic Syndr 2013;63 (4):449-55.

Sanne I, Piliero P, Squires K, Thiry A, Schnittman S, AI424-007 Clinical Trial Group. Results of a phase 2 clinical trial at 48 weeks (AI424-007): a dose-ranging, safety, and efficacy comparative trial of atazanavir at three doses in combination with didanosine and stavudine in antiretroviral-naive subjects. Journal of Acquired Immune Deficiency Syndromes 2003;32 (1):18-29.

Schering Corporation. Victrelis® (boceprevir) Capsules. US Prescribing Information. Whitehouse Station, NJ, USA. Revised May. 2011:

Schinazi RF, Gosselin G, Faraj A, Korba BE, Liotta DC, Chu CK, et al. Pure nucleoside enantiomers of beta-2',3'-dideoxycytidine analogs are selective inhibitors of hepatitis B virus in vitro. Antimicrob Agents Chemother 1994;38 (9):2172-4.

Schinazi RF, Lloyd RM, Jr, Nguyen M-HH, Cannon DL, McMillan A, Ilksoy N, et al. Characterization of human immunodeficiency viruses resistant to oxathiolane-cytosine nucleosides. Antimicrob Agents Chemother 1993;37 (4):875-81.

Schinazi RF, McMillan A, Cannon D, Mathis R, Lloyd RM, Peck A, et al. Selective inhibition of human immunodeficiency viruses by racemates and enantiomers of cis-5-fluoro-1-[2-(hydroxymethyl)-1,3-oxathiolan-5-yl]cytosine. Antimicrob Agents Chemother 1992;36 (11):2423-31.

Shaw T, Mok S, Locarnini S. Inhibition of hepatitis B virus DNA polymerase by enantiomers of penciclovir triphosphate and metabolic basis for selective inhibition of HBV replication by penciclovir. Hepatology 1996;24 (5):996-1002.

Shen A, Zink MC, Mankowski JL, Chadwick K, Margolick JB, Carruth LM, et al. Resting $CD4^+$ T lymphocytes but not thymocytes provide a latent viral reservoir in a simian immunodeficiency virus-*Macaca nemestrina* model of human immunodeficiency virus type 1-infected patients on highly active antiretroviral therapy. J Virol 2003;77 (8):4938-49.

Shewach DS, Liotta DC, Schinazi RF. Affinity of the antiviral enantiomers of oxathiolane cytosine nucleosides for human 2'-deoxycytidine kinase. Biochem Pharmacol 1993;45 (7):1540-3.

Shimura K, Kodama E, Sakagami Y, Matsuzaki Y, Watanabe W, Yamataka K, et al. Broad antiretroviral activity and resistance profile of the novel human immunodeficiency virus integrase inhibitor elvitegravir (JTK-303/GS-9137). J Virol 2008;82 (2):764-74.

Shirasaka T, Kavlick MF, Ueno T, Gao W-Y, Kojima E, Alcaide ML, et al. Emergence of human immunodeficiency virus type 1 variants with resistance to multiple dideoxynucleosides in patients receiving therapy with dideoxynucleosides. Proc Natl Acad Sci USA 1995;92 (6):2398-402.

Sluis-Cremer N, Sheen CW, Zelina S, Torres PS, Parikh UM, Mellors JW. Molecular mechanism by which the K70E mutation in human immunodeficiency virus type 1 reverse transcriptase confers resistance to nucleoside reverse transcriptase inhibitors. Antimicrob Agents Chemother 2007;51 (1):48-53.

Sommadossi J-P. Data from clonogenic assays CFU-GM and BFU-E and mitochondrial assays for TP0001 and TP0004 as compared to AZT. Triangle Pharmaceuticals, Inc. Report No. 233. October 15, 1996.

Srinivas RV, Fridland A. Antiviral activities of 9-*R*-2-phosphonomethoxypropyl adenine (PMPA) and bis(isopropyloxymethylcarbonyl)PMPA against various drug-resistant human immunodeficiency virus strains. Antimicrob Agents Chemother 1998;42 (6):1484-7.

Stray KM, Park Y, Babusis D, Callebaut C, Cihlar T, Ray AS, et al. Tenofovir alafenamide (TAF) does not deplete mitochondrial DNA in human T-cell lines at intracellular concentrations exceeding clinically relevant drug exposures. Antiviral Res 2017;140:116-20.

Stuyver LJ, Locarnini SA, Lok A, Richman DD, Carman WF, Dienstag JL, et al. Nomenclature for antiviral-resistant human hepatitis B virus mutations in the polymerase region. Hepatology 2001;33 (3):751-7.

Suo Z, Johnson KA. Selective inhibition of HIV-1 reverse transcriptase by an antiviral inhibitor, (R)-9-(2-Phosphonylmethoxypropyl)adenine. J Biol Chem 1998;273 (42):27250-8.

Svarovskaia ES, Feng JY, Margot NA, Myrick F, Goodman D, Ly JK, et al. The A62V and S68G Mutations in HIV-1 Reverse Transcriptase Partially Restore the Replication Defect Associated With the K65R Mutation. J Acquir Immune Defic Syndr 2008;48 (4):428-36.

Tenney DJ, Rose RE, Baldick CJ, Pokornowski KA, Eggers BJ, Fang J, et al. Long-term monitoring shows hepatitis B virus resistance to entecavir in nucleoside-naive patients is rare through 5 years of therapy. Hepatology 2009;49 (5):1503-14.

Thomas M, Brady L. HIV integrase: a target for AIDS therapeutics. Trends Biotechnol 1997;15 (5):167-72.

Tisdale M, Alnadaf T, Cousens D. Combination of mutations in human immunodeficiency virus type 1 reverse transcriptase required for resistance to the carbocyclic nucleoside 1592U89. Antimicrob Agents Chemother 1997;41 (5):1094-8.

Tisdale M, Kemp SD, Parry NR, Larder BA. Rapid in vitro selection of human immunodeficiency virus type 1 resistant to 3'-thiacytidine inhibitors due to a mutation in the YMDD region of reverse transcriptase. Proc Natl Acad Sci USA 1993;90 (12):5653-6.

Toh H, Hayashida H, Miyata T. Sequence homology between retroviral reverse transcriptase and putative polymerases of hepatitis B virus and cauliflower mosaic virus. Nature 1983;305:827-9.

Tribulova N, Knezl V, Shainberg A, Seki S, Soukup T. Thyroid hormones and cardiac arrhythmias. Vascular pharmacology 2010;52 (3-4):102-12.

Ussery MA, Wood OL, Kunder SC, Bacho MA, Broud DD, Vona SF, et al. Antiviral activity of six novel compounds [(-)-FTC, (+/-)-FTC, D-DAPD, D-D4FC, CS-92 and CS-87) in the HIV-infected HuPBMC SCID mouse model [abstract]. Antivir Ther 1998;3 (Suppl 1):7-8. Abstract 9.

van Bommel F, de Man RA, Wedemeyer H, Deterding K, Petersen J, Buggisch P, et al. Long-term efficacy of tenofovir monotherapy for hepatitis B virus-monoinfected patients after failure of nucleoside/nucleotide analogues. Hepatology 2010;51 (1):73-80.

Van Draanen NA, Tisdale M, Parry NR, Jansen R, Dornsife RE, Tuttle JV, et al. Influence of stereochemistry on antiviral activities and resistance profiles of dideoxycytidine nucleosides. Antimicrob Agents Chemother 1994;38 (4):868-71.

Vela JE, Miller MD, Rhodes GR, Ray AS. Effect of tenofovir in combination with other anti-HIV NRTIs on intracellular nucleotide pools [poster number H-1901]. 45th Interscience Conference on Antimicrobial Agents and Chemotherapy; 2005 December 16-19; Washington, DC, USA.

Vertex Pharmaceuticals Incorporated. INCIVEK™ (telaprevir) Film Coated Tablets. US Prescribing Information. Cambridge, MA. May 2011:

Vidal F, Domingo JC, Guallar J, Saumoy M, Cordobilla B, Sanchez de la Rosa R, et al. In vitro cytotoxicity and mitochondrial toxicity of tenofovir alone and in combination with other antiretrovirals in human renal proximal tubule cells. Antimicrob Agents Chemother 2006;50 (11):3824-32.

Wainberg MA, Miller MD, Quan Y, Salomon H, Mulato AS, Lamy PD, et al. In vitro selection and characterization of HIV-1 with reduced susceptibility to PMPA. Antivir Ther 1999;4 (2):87-94.

White K, Niedziela-Majka A, Novikov N, Miller M, Tsiang M. The Integrase Strand Transfer Inhibitor Bictegravir has a Long Integrase/DNA Dissociation Half-life [Poster P025]. HIV Glasgow; 2016 23-26 October; Glasgow, United Kingdom.

White KL, Chen JM, Feng JY, Margot NA, Ly JK, Ray AS, et al. The K65R reverse transcriptase mutation in HIV-1 reverses the excision phenotype of zidovudine resistance mutations. Antivir Ther 2006;11:155-63.

White KL, Chen JM, Margot NA, Wrin T, Petropoulos CJ, Naeger LK, et al. Molecular mechanisms of resistance to tenofovir by HIV-1 RT containing a diserine insertion after residue 69 and multiple thymidine analog-associated mutations [abstract]. 12th International HIV Drug Resistance Workshop; 2003 June 10-14; Los Cabos, Mexico. Abstract 33.

White KL, Chen JM, Margot NA, Wrin T, Petropoulos CJ, Naeger LK, et al. Molecular mechanisms of tenofovir resistance conferred by human immunodeficiency virus type 1 reverse transcriptase containing a diserine insertion after residue 69 and multiple thymidine analog-associated mutations. Antimicrob Agents Chemother 2004;48 (3):992-1003.

White KL, Margot NA, Ly JK, Chen JM, Ray AS, Pavelko M, et al. A combination of decreased NRTI incorporation and decreased excision determines the resistance profile of HIV-1 K65R RT. AIDS 2005;19 (16):1751-60.

White KL, Margot NA, Wrin T, Petropoulos CJ, Miller MD, Naeger LK. Molecular mechanisms of resistance to human immunodeficiency virus type 1 with reverse transcriptase mutations K65R and K65R+M184V and their effects on enzyme function and viral replication capacity. Antimicrob Agents Chemother 2002;46 (11):3437-46.

Wilson JE, Aulabaugh A, Caligan B, McPherson S, Wakefield JK, Jablonski S, et al. Human immunodeficiency virus type-1 reverse transcriptase. Contribution of Met-184 to binding of nucleoside 5'-triphosphate. J Biol Chem 1996;271 (23):13656-62.

Wilson JE, Martin JL, Borroto-Esoda K, Hopkins S, Painter G, Liotta DC, et al. The 5'-triphosphates of the (-) and (+) enantiomers of cis-5-fluoro-1-[2-(hydroxymethyl)-1,3-oxathiolane-5-yl]cytosine equally inhibit human immunodeficiency virus type 1 reverse transcriptase. Antimicrob Agents Chemother 1993;37 (8):1720-2.

Winston A, Mandalia S, Pillay D, Gazzard B, Pozniak A. The prevalence and determinants of the K65R mutation in HIV-1 reverse transcriptase in tenofovir-naive patients. AIDS 2002;16 (15):2087-9.

Wolf K, Walter H, Beerenwinkel N, Keulen W, Kaiser R, Hoffmann D, et al. Tenofovir resistance and resensitization. Antimicrob Agents Chemother 2003;47 (11):3478-84.

Xiong X, Flores C, Yang H, Toole JJ, Gibbs CS. Mutations in hepatitis B DNA polymerase associated with resistance to lamivudine do not confer resistance to adefovir in vitro. Hepatology 1998;28 (6):1669-73.

Yang H, Qi X, Sabogal A, Miller M, Xiong S, Delaney WE, IV. Cross-resistance testing of next-generation nucleoside and nucleotide analogues against lamivudine-resistant HBV. Antivir Ther 2005;10 (5):625-33.

Yang J, Shi D, Yang D, Song X, Yan B. Interleukin-6 alters the cellular responsiveness to clopidogrel, irinotecan, and oseltamivir by suppressing the expression of carboxylesterases HCE1 and HCE2. Mol Pharmacol 2007;72 (3):686-94.

Ying C, De Clercq E, Neyts J. Lamivudine, adefovir and tenofovir exhibit long-lasting anti-hepatitis B virus activity in cell culture. J Viral Hepat 2000;7 (1):79-83.

Yokota T, Konno K, Shigeta S, Holý A, Balzarini J, De Clercq E. Inhibitory effects of acyclic nucleoside phosphonate analogues of hepatitis B virus DNA synthesis in HB611 cells. Antivir Chem Chemother 1994;5 (2):57-63.

Zeisel MB, Lucifora J, Mason WS, Sureau C, Beck J, Levrero M, et al. Towards an HBV cure: state-of-the-art and unresolved questions-report of the ANRS workshop on HBV cure. Gut 2015;64 (8):1314-26.

Zhang D, Caliendo AM, Eron JJ, DeVore KM, Kaplan JC, Hirsch MS, et al. Resistance to 2',3'-dideoxycytidine conferred by a mutation in codon 65 of the human immunodeficiency virus type 1 reverse transcriptase. Antimicrob Agents Chemother 1994;38 (2):282-7.

SECTION 2.6.3—PHARMACOLOGY TABULATED SUMMARY

BICTEGRAVIR/EMTRICITABINE/TENOFOVIR ALAFENAMIDE

Gilead Sciences

[redacted] **20**[redacted]

CONFIDENTIAL AND PROPRIETARY INFORMATION

TABLE OF CONTENTS

1. PHARMACOLOGY OVERVIEW

1.1. Primary Pharmacodynamics of BIC

Test Article: BIC

Type of Study/Description	GLP[a]	Test System	Method of Administration	Testing Facility	Gilead Study No.
BIC Primary Pharmacodynamics					
Antiviral Activity and Selectivity of GS-9883 in T-Cell Lines	No	Human Lymphoblastoid T-cell lines MT-2 and MT-4, HIV-1 IIIb virus	In Vitro	Gilead Sciences, Inc., Foster City, CA, USA.	PC-141-2032
Effect of Human Serum and Serum Components on the Antiviral Activity of GS-9883	No	Human Lymphoblastoid T-cell line MT-2, HIV-1 IIIb virus, recombinant HIV-1 virus LAI-RLuc containing Renilla luciferase reporter gene	In Vitro	Gilead Sciences, Inc., Foster City, CA, USA.	PC-141-2033
Antiviral Activity and Cytotoxicity of GS-9883 in Primary $CD4^+$ T Lymphocytes and Monocyte-Derived Macrophages	No	Human CD4+ T-lymphocytes, human monocyte derived macrophages, human PBMCs, HIV-1 BaL virus	In Vitro	Gilead Sciences, Inc., Foster City, CA, USA.	PC-141-2034
Antiviral Activity of GS-9883 against HIV Clinical Isolates	No	Human PBMCs, HIV of various subtypes and HIV-2	In Vitro	[redacted] USA.	PC-141-2035
Antiviral Activity of BIC against HIV-1 O and N	No	Human PBMCs, HIV-1 O and N	In Vitro	[redacted] USA.	PC-141-2057
Inhibition of HIV-1 Integrase Strand Transfer and 3'Processing Activities by GS-9883	No	Purified recombinant HIV-1 integrase expressed and isolated from E. coli, synthetic oligonucleotide strand transfer and 3'processing substrates	In Vitro	Gilead Sciences, Inc., Foster City, CA, USA.	PC-141-2036
Association and Dissociation of BIC with HIV-1 IN/DNA Complexes	No	Scintillation proximity assay	In Vitro	Gilead Sciences, Inc., Foster City, CA, USA.	PC-141-2058
Inhibition of HIV-1 Integration in MT-2 Cells by GS-9883	No	Human lymphoblastoid T-cell lines MT-2 and SupT1, SODk1 2G cell line producer of pseudotyped single cycle HIV-1 particles, HIV-1 IIIb virus, oligonucleotide primers and probes for qPCR	In Vitro	Gilead Sciences, Inc., Foster City, CA, USA.	PC-141-2037
Effect of Increasing Multiplicity of Infection of the Antiviral Activity of BIC	No	HIV-1 strain IIIb and Human lymphoblastoid T-cell line MT-2 Cells	In Vitro	Gilead Sciences, Inc., Foster City, CA, USA.	PC-141-2054

Test Article: BIC

Type of Study/Description	GLP[a]	Test System	Method of Administration	Testing Facility	Gilead Study No.
Activity of GS-9883 against Drug-Resistant HIV-1 Mutant Variants	No	Human lymphoblastoid T-cell line MT-2, HIV-1 IIIb virus, HIV-1 HXB2 virus and HXB2 virus variants containing various site-directed mutations associated with NRTI, NNRTI and PI resistance	In Vitro	Gilead Sciences, Inc., Foster City, CA, USA.	PC-141-2039
Activity of GS-9883 Against INSTI-resistant Mutants of HIV-1	No	Human lymphoblastoid T-cell line MT-2, HIV-1 HXB2 virus and HXB2 virus variants containing various site-directed mutations associated with INSTI resistance	In Vitro	Gilead Sciences, Inc., Foster City, CA, USA.	PC-141-2040
Antiviral Activity of GS-9883 against HIV-1 Clinical Isolate Clones with Integrase Strand Transfer Inhibitor Mutations	No	Human embryonic kidney 293 cells, HIV-1 NL4-3 and patient-derived resistance test vectors	In Vitro	[redacted] USA	PC-141-2050
Antiviral Activity of GS-9883 against HIV-1 Isolates with Integrase Strand Transfer Inhibitor Mutations	No	Human embryonic kidney 293 cells, HIV-1 NL4-3 and patient-derived resistance test vectors	In Vitro	[redacted] USA	PC-141-2051
Antiviral Activity of GS-9883 against HIV-1 Site-Directed Mutant with Integrase Strand Transfer Inhibitor Mutations	No	Human embryonic kidney 293 cells, HIV-1 NL4-3 and patient-derived resistance test vectors	In Vitro	[redacted] USA	PC-141-2055
Viral Resistance Selection Studies with BIC	No	Human lymphoblastoid T-cell line MT-2, HIV-1 IIIb virus, inhibitor-selected HIV-1 IIIb variants	In Vitro	Gilead Sciences, Inc., Foster City, CA, USA.	PC-141-2041
Viral Resistance Selection Studies with BIC	No	Human lymphoblastoid T-cell line MT-2, HIV-1 IIIb virus, inhibitor-selected HIV-1 IIIb variants	In Vitro	Gilead Sciences, Inc., Foster City, CA, USA.	PC-141-2052
Viral Resistance Selection Studies with BIC	No	Human lymphoblastoid T-cell line MT-2, HIV-1 strain xxLAI, inhibitor-selected HIV-1 xxLAI varaints	In Vitro	Gilead Sciences, Inc., Foster City, CA, USA.	PC-141-2056

BIC = bictegravir (GS-9883); DNA = deoxyribonucleic acid; GLP = Good laboratory practice; GS-9883 = bictegravir; HIV = human immunodeficiency virus; PBMC = peripheral blood mononuclear cell; qPCR = quantitative polymerase chain reaction

a An entry of "Yes" indicates that the study includes a GLP compliance statement.

1.2. Primary Pharmacodynamics of FTC

Test Article: FTC

Type of Study/Description	Test System	Method of Administration	Testing Facility	Study No and Reference
FTC Primary Pharmacodynamics				
Phosphorylation of FTC	Calf thymus deoxycytidine kinase	In vitro	[redacted] USA	TESF/91/0014
Phosphorylation of FTC	Calf thymus deoxycytidine kinase	In vitro	[redacted] USA	TESF/92/0002
Phosphorylation of FTC	dCMP kinase and nucleoside monophosphate kinase	In vitro	[redacted] USA	TEIT/92/0005
Phosphorylation of FTC	Nucleoside monophosphate kinase and nuclear diphosphate kinase	In vitro	[redacted] USA	TGZZ/93/0025
Inhibition of HIV-1 reverse transcriptase	Endogenous RT assay Chain-termination substrate assays Purified HIV-1 reverse transcriptase enzyme assay	In vitro	Division of Virology, Burroughs Wellcome Co. Research Triangle Park, NC	Antimicrob Agents Chemother 1993;37:1270–2 {Wilson 1993}
Inhibition of HIV-1 reverse transcriptase	Pre–steady-state kinetic analysis of HIV-1 reverse transcriptase	In vitro	Gilead Sciences, Inc., USA	FASEB J 1999;13:1511-7 {Feng 1999}
Antiviral activity vs HIV-1 and HIV-2	Human PBMCs and various T cell lines	In vitro	Veterans Affairs Medical Center, Decatur, Georgia	Antimicrob Agents Chemother 1992;36:2423–31 {Schinazi 1992}
Antiviral activity vs HIV-1	Human PBMCs, human T-cell lines MT-2 and CEM	In vitro	Gilead Sciences, Inc., USA	TPI 462 v2
Antiviral activity against various subtypes of HIV-1	Human PBMCs	In vitro	Gilead Sciences, Inc., USA	TPI 10498 v2

Test Article: FTC

Type of Study/Description	Test System	Method of Administration	Testing Facility	Study No and Reference
Antiviral activity against various subtypes of HIV-1	HeLa cells	In vitro	Gilead Sciences, Inc., USA	TPI 11419 v2
MAGI-LU assay validation 1: Inhibitory effect of FTC on HIV-1 xxLAI viral infection is independent of MOI of the infecting virus	MAGI cells	In vitro	Gilead Sciences, Inc., USA	10518 v2
Effect of MOI on inhibition of HIV-1 replication by FTC	Human PBMCs	In vitro	Gilead Sciences, Inc., USA	11773
DXG, FTC, and ZDV: Time of addition	MAGI cells	In vitro	Gilead Sciences, Inc., USA	10247
Effect of human serum on the antiviral activity of FTC assessed in CEM cells infected with the LAI strain of HIV-1	CEM cells	In vitro	Gilead Sciences, Inc., USA	463
Selection of FTC resistant virus	Human T-cell lines, MT-4 cells	In vitro	Burroughs Wellcome Co., Research Triangle Park, NC 27709 USA	Proc Natl Acad Sci USA 1993;90:5653–5656 {Tisdale 1993}
Selection of FTC resistant virus	Human PBMCs	In vitro	Emory University, Atlanta, GA, USA	Antimicrob Agents Chemother 1993;37:875–881 {Schinazi 1993}
Antiviral activity vs nucleoside reverse transcriptase inhibitor-resistant recombinant HIV-1 clinical isolates	MT-4 cells	In vitro	[redacted] Belgium	TPI 11148
Activity against drug-resistant HIV-1 with K65R mutation	Recombinant mutant enzymes and viruses in MT-2 cells	In vitro	Gilead Sciences, Inc., USA	TPI 15883
Virologic and enzymatic studies revealing the mechanism of K65R- and Q151M-associated HIV-1 drug resistance towards FTC and lamivudine (3TC)	MT-2 cells and in vitro	In vitro	Gilead Sciences, Inc., USA	Nucleosides, Nucleotides, and Nucleic Acids 2006;25:89–107 {Feng 2006}
Metabolism of FTC	$HepG_2$ 2.2.15 (P5A) cells	In vitro	[redacted] USA	TEZA/92/0062

Test Article: FTC

Type of Study/Description	Test System	Method of Administration	Testing Facility	Study No and Reference
Metabolism of FTC	CEM T-lymphoblast cells	In vitro	[redacted] USA	TEZA/92/0103
Metabolism of FTC in hepatitis B infected cells	HepG2 (humanhepatocellular carcinoma) cells	In vitro	[redacted] USA	TEZA/92/0111
Effect of FTC on human DNA polymerase	HeLa S3 cells and purified human polymerases α, β, γ, and ε	In vitro	[redacted] USA	TEZZ/93/0007
Effect of FTC on human polymerase γ	Human polymerase γ	In vitro	Gilead Sciences, Inc., USA	TPI 9501
Effect of orally administered FTC and lamivudine in the HuPBMC-SCID mouse model of HIV-1 infection	HuPBMC-SCID mouse model of HIV-1 infection	Oral	Gilead Sciences, Inc., USA	TPI 11985
Antiviral activity of FTC in vivo	HuPBMC-SCID mouse model of HIV-1 infection	Intraperitoneal (IP)	Emory University, Atlanta, GA, USA	2nd International Workshop on HIV Drug Resistance and Treatment Strategies, 1998, Lake Maggiore, Italy, Abstract 9 {Ussery 1998}

dCMP = deoxycytidine monophosphate; DNA = deoxyribonucleic acid; DXG = 9-(β-D-1,3-dioxolan-4-yl)guanine (metabolite of prodrug amdoxovir); FTC = emtricitabine; GLP = Good laboratory practice; HIV = human immunodeficiency virus; MOI = multiplicity of infection; PBMC = peripheral blood mononuclear cell; qPCR = quantitative polymerase chain reaction; ZDV = zidovudine

1.3. Primary Pharmacodynamics of TAF

Studies supporting the primary pharmacodynamics of TAF are presented in this table and are inclusive of studies that utilized TAF, TDF, TFV, or FTC/TDF.

Test Article: TAF, TDF, TFV, FTC/TDF

Type of Study/Description	GLP[a]	Test System	Method of Administration	Testing Facility	Gilead Study No.
TAF Primary Pharmacodynamics					
Drug Combination Studies with TAF	No	MT-2 cells	In Vitro	Gilead Sciences Foster City, CA USA	PC-120-2002
Antiviral Activity of TAF and TFV Against a Panel of Animal Viruses	No	In Vitro	In Vitro	Gilead Sciences Foster City, CA USA	PC-120-2003
Profiling of TAF Antiviral Activity Against HIV-1 and HIV-2 Clinical Isolates in Primary Cells	No	Primary Cells	In Vitro	Gilead Sciences Foster City, CA USA	PC-120-2004
Cytotoxicity Assay with TAF	No	MT-2, MT-4, and HepG2 cells	In Vitro	Gilead Sciences Foster City, CA USA	PC-120-2007
Cytotoxic Effect of TAF on PBMCs	No	PBMCs	In Vitro	Gilead Sciences Foster City, CA USA	PC-120-2009
TAF In Vitro Resistance Selection Studies with Wild-Type HIV-1 Isolates	No	MT-2 cells	In Vitro	Gilead Sciences Foster City, CA USA	PC-120-2011
TAF In Vitro Resistance Selection Studies with TDF-Resistant HIV-1 Isolates	No	MT-2 cells	In Vitro	Gilead Sciences Foster City, CA USA	PC-120-2012
In Vitro Evaluation of TAF Resistance Barrier	No	MT-2 cells	In Vitro	Gilead Sciences Foster City, CA USA	PC-120-2013
In Vitro Resistance Profile of TAF Against Patient-Derived Recombinant HIV-1 Isolates	No	Recombinant HIV-1 Clinical Isolates	In Vitro	[redacted] USA	PC-120-2014
Comparison of TAF Resistance Profile in Multiple In Vitro Assays	No	In Vitro	In Vitro	Gilead Sciences Foster City, CA USA	PC-120-2015

Test Article: TAF, TDF, TFV, FTC/TDF

Type of Study/Description	GLP[a]	Test System	Method of Administration	Testing Facility	Gilead Study No.
Effect of TAF on CatA Hydrolase Activity and TAF Antiretroviral Activity	No	Purified CatA, primary CD4+, T-lymphocytes, MDMs	In Vitro	Gilead Sciences Foster City, CA USA	PC-120-2017 Antiviral Therapy, 2014;10.3851/IMP2767 {Bam 2014a}
Antiviral Activity and Cytotoxicity of TAF Metabolites	No	MT-2 and MT-4 cells	In Vitro	Gilead Sciences Foster City, CA USA	PC-120-2021
Mechanism of action (activation of tenofovir via phosphorylation)	No	Human T lymphoid cells (CEMss, CEMss^{r-1})	In vitro	St Jude Children's Hospital and University of Tennessee, Memphis, TN, USA	Antimicrob Agents Chemother 1995 Oct;39(10):2304–8 {Kalayjian 2003}
Antiviral activity of PMPA vs prodrugs of PMPA against wild-type HIV_{IIIB} and evaluation of cytotoxicity	No	Human resting/activated PBMCs and T lymphocyte (MT-2) cells	In vitro	St Jude Children's Hospital and University of Tennessee, Memphis, TN, USA	Antimicrob Agents Chemother 1998 Mar;42(3):612–7 {Robbins 1998}
Mechanism of action (intracellular metabolism): In vitro phosphorylation of tenofovir and abacavir	No	CEM-CCRF cells	In vitro	Gilead Sciences, Inc., USA	PC-104-2008
Mechanism of action (intracellular metabolism): Role of purine nucleoside phosphorylase in drug interactions between 2′,3′-dideoxyinosine and allopurinol, ganciclovir, or tenofovir	No	CEM-CCRF cells and activated PBMCs	In vitro	Gilead Sciences, Inc., USA	Antimicrob Agents Chemother 2004;48(4):1089–95 {Ray 2004}
Mechanism of action (intracellular metabolism): Effect of tenofovir in combination with other anti-HIV nucleoside reverse transcriptase inhibitors (NRTIs) on intracellular nucleotide pools	No	CEM-CRFF cells	In vitro	Gilead Sciences, Inc., USA	45th Interscience Conference on Antimicrobial Agents and Chemotherapy, Poster H-1901 {Vela 2005}
Mechanism of action (intracellular metabolism in vitro following in vivo dosing)	No	PBMCs Macaque monkeys	In vitro In vivo, subcutaneous (SC)	[redacted] USA	P2001025

Test Article: TAF, TDF, TFV, FTC/TDF

Type of Study/Description	GLP[a]	Test System	Method of Administration	Testing Facility	Gilead Study No.
Inhibitory effects of tenofovir & TDF on human HIV_{IIIB} RT and human DNA polymerases	No	HIV_{IIIB} RT, human DNA polymerase (α, β, γ)	In vitro	Gilead Sciences, Inc., USA	Antiviral Chemistry and Chemotherapy 1995;6(4):217–21 {Cherrington 1995}
Structural features of acyclic nucleotide analogs conferring inhibitory effects on cellular replicative DNA polymerases	No	In vitro	In vitro	Gilead Sciences Inc., USA	Institute of Organic Chemistry and Biochemistry, Academy of Sciences of Czech Republic 1996;1:188–91 {Kramata 1996}
Incorporation into DNA by DNA polymerase	No	Primer template DNA, DNA polymerases (α, β, γ)	In vitro	Gilead Sciences, Inc., USA	Antiviral Chemistry and Chemother 1997 May;8(3): 187–95 {Cihlar 1997}
Antiviral activity of tenofovir vs HIV-1 non-B subtypes (A, C, D, E, F, G, O) and HIV-1 isolates with nucleoside-associated resistance	No	PBMCs	In vitro	Gilead Sciences, Inc., USA and Southern Research Institute, Frederick, MD, USA	AIDS Res Hum Retroviruses 2001;17:1167–73 {Palmer 2001}
Antiviral activity and resistance properties vs wild type HIV_{IIIB}	No	MT-2 cells	In vitro	McGill University AIDS Center, Montreal, Canada	Antiviral Therapy 1999;4(2):87–94 {Wainberg 1999}
Selection of resistant virus with subtype C HIV-1	No	Cord blood mononuclear cells	In vitro	McGill University AIDS Center, Montreal, Canada	AIDS 2006;20(9):F9–F13 {Brenner 2006}
Antiviral activity vs HIV-1 expressing the K70E mutation	No	Clinical isolates from AIDS patients treated with adefovir dipivoxil long-term therapy	In vitro	Gilead Sciences, Inc., USA	Antimicrob Agents Chemother 1998 Jul;42(7):1620–8 {Mulato 1998}
Molecular mechanism by which the K70E mutation in HIV-1 reverse transcriptase confers resistance to NRTIs	No	In vitro	In vitro	University of Pittsburgh, School of Medicine, Pittsburgh, PA, USA	Antimicrob Agents Chemother 2007;51:48–53 {Sluis-Cremer 2007}
HIV-1: resistance to nucleoside analogues and replication capacity in primary human macrophages	No	Primary human macrophages	In vitro	Hôpital Bichat-Claude Bermard, Paris, France	J. Virol 2007;81:4540–4550 {Perez-Bercoff 2007}

Test Article: TAF, TDF, TFV, FTC/TDF

Type of Study/Description	GLP[a]	Test System	Method of Administration	Testing Facility	Gilead Study No.
A combination of decreased NRTI incorporation and decreased excision determines the resistance profile of HIV-1 K65R RT	No	MT-2 cells, RT enzyme assay	In vitro	Gilead Sciences Inc., USA	AIDS 2005;19:1751–1760 {White 2005}
Effects of the translocation status of HIV-1 reverse transcriptase on the efficiency of excision of tenofovir	No	RT enzyme assay	In vitro	McGill University, Montreal, Quebec, Canada and Gilead Sciences Inc., USA	Antimicrob Agents Chemother 2007;51:2911–2919 {Marchand 2007}
The K65R reverse transcriptase mutation in HIV-1 reverses the excision phenotype of ZDV resistance mutations	No	MT-2 cells, RT enzyme assay	In vitro	Gilead Sciences Inc., USA	Antiviral Ther 2006; 11:155–163 {White 2006}
Antagonism between the HIV-1 reverse transcriptase mutation K65R and TAMs at the genomic level	No	In vitro	In vitro	University of Pittsburgh, School of Medicine, Pittsburgh, PA, USA	J Infec Dis 2006,194:651–660 {Parikh 2006b}
Molecular mechanisms of bidirectional antagonism between K65R and TAMs in HIV-1 RT	No	In vitro	In vitro	University of Pittsburgh, School of Medicine, Pittsburgh, PA, USA	AIDS 2007;21:1405–1414 {Parikh 2007}
The K65R mutation in HIV-1 reverse transcriptase exhibits bidirectional phenotypic antagonism with TAMs	No	In vitro	In vitro	University of Pittsburgh, School of Medicine, Pittsburgh, PA, USA	J Virol 2006,80:4971–4977 {Parikh 2006a}
Coexistence of the K65R/L74V and/or K65R/T215Y mutations on the same HIV-1 genome	No	In vitro	In vitro	Timone Hospital and CNRS UMR 6020, France	J Clin Virol 2006;37:227–230 {Henry 2006}
The A62V and S68G mutations in HIV-1 reverse transcriptase partially restore the replication defect associated with the K65R mutation	No	MT-2 cells, RT enzyme assay	In vitro	Gilead Sciences Inc., USA	J Acquir Immune Defic Syndr 2008;48:428–436 {Svarovskaia 2008}
Diminished efficiency of HIV-1 reverse transcriptase containing the K65R and M184V drug resistance mutations	No	In vitro	In vitro	McGill AIDS Centre, Montreal, Quebec, Canada	AIDS 2007;21:665–675 {Frankel 2007}

Test Article: TAF, TDF, TFV, FTC/TDF

Type of Study/Description	GLP[a]	Test System	Method of Administration	Testing Facility	Gilead Study No.
The balance between NRTI discrimination and excision drives the susceptibility of HIV-1 RT mutant K65R, M184V, and K65R+M184V	No	MT-2 cells, RT enzyme assay	In vitro	Gilead Sciences Inc., USA	Antivir Chem Chemother 2008;18:307–316 {Ly 2008}
Molecular basis of antagonism between K70E and K65R tenofovir-associated mutations in HIV-1 reverse transcriptase	No	In vitro	In vitro	Quest Diagnostics Nichols Institute, USA; Glaxo SmithKline USA; University of Minnesota, MN, USA; and Research Think Tank Inc., USA	Antivir Res 2007;75:210–218 {Kagan 2007}
Mechanistic basis for reduced viral and enzymatic fitness of HIV-1 reverse transcriptase containing both K65R and M184V mutations	No	In vitro	In vitro	Université Aix-Marseille, France and Gilead Sciences Inc., USA	J Biol Chem 2004; 279:509–516 {Deval 2004}
Antiviral activity vs drug resistant HIV variants	No	Clinical isolates of drug resistant HIV-1 variants, MT-2 cells	In vitro	St Jude Children's Hospital and University of Tennessee, Memphis, TN, USA	Antimicrob Agents. Chemother 1998;42:1484–7 {Srinivas 1998}
Patterns of HIV resistance of clinical isolates from Study GS-96-408	No	MT-2 cells	In vitro	Gilead Sciences, Inc., USA	JAIDS 2001;27:450–8 {Miller 2001}
Antiviral activity vs HIV-1 variants from clinical isolates	No	MOLT-4 cells, PBMCS, and H9 cells	In vitro	National Cancer Institute, Bethesda, MD, USA	Proc Natl Acad Sci USA 1995;92:2398–2402 {Shirasaka 1995}
Unblocking of chain-terminated primer by HIV-1 reverse transcriptase	No	In vitro	In vitro	University of Miami, Miami, FL, USA	Proc Natl Acad Sci 1998 Nov;95(23):13471–6 {Meyer 1998}
Unblocking of chain-terminated primer by HIV-1 reverse transcriptase	No	In vitro	In vitro	Gilead Sciences, Inc., USA	XIV International Roundtable on Nucleosides, Nucleotides and their Biological Applications; 2000; San Francisco, CA {Naeger 2000}

Test Article: TAF, TDF, TFV, FTC/TDF

Type of Study/Description	GLP[a]	Test System	Method of Administration	Testing Facility	Gilead Study No.
Antiviral activity and replication capability vs HIV-1 expressing the 3TC-associated M184V mutation	No	MT-2 cells and PBMCs	In vitro	Gilead Sciences, Inc., USA	J Infect Dis 1999 Jan; 179(1):92–100 {Miller 1999}
Effects of K65R mutation on HIV-1 replication capacity	No	293T cells	In vitro	[redacted] USA	PC-104-2004
Antiviral activity vs wild-type and drug-resistant HIV-1	No	MT-4 cells	In vitro	Virco NV, Mechelen, Belgium and Gilead Sciences, Inc., USA	Antimicrob Agents Chemother 2002 Apr;46(4):1067–72. {Harrigan 2002}
Protein binding of cidofovir, cyclic HPMPC, PMEA, and PMPA in human plasma and serum	No	In vitro	In vitro	Gilead Sciences, Inc., USA	P0504-00039.1
Phosphorylation of tenofovir and FTC	No	CEM CRFF cells	In vitro	Gilead Sciences, Inc., USA	PC-164-2001
Selection of resistant HIV-1 with combinations of tenofovir and FTC	No	MT-2 cells	In vitro	Gilead Sciences, Inc., USA	PC-164-2005
Antiviral activity of the combination of tenofovir and FTC	No	SIV-infected rhesus monkeys	SC	John Hopkins University, Baltimore, MA, USA	Journal of Virology 2003; 77:4938–4949 {Shen 2003}
Intermittent antiretroviral prophylaxis with tenofovir and FTC protects macaques against repeated rectal SHIV exposures	No	SHIV-challenged rhesus monkeys	SC	Centers for Disease Control and Prevention, Atlanta, GA, USA; Emory University, Decatur, GA, USA	16th International HIV Resistance Workshop, 2007, Barbados, Abstract 85 {Garcia-Lerma 2007}
In Vitro Assessment of GS-7340 as a Substrate for Human OATP1B1 and OATP1B3	No	CHO cells	In vitro	Gilead Sciences Foster City, CA, USA	AD-120-2022
In Vitro Activation of GS-1278, GS-4331 and GS-7340 in Primary Human Hepatocytes	No	Primary human hepatocytes	In vitro	Gilead Sciences Foster City, CA, USA	AD-120-2017
Lack of TAF Cytotoxic Effect on Primary Osteoblasts at Clinically Relevant Drug Concentrations	No	In vitro	In vitro	Gilead Sciences Foster City, CA, USA	PC-120-2008

Test Article: TAF, TDF, TFV, FTC/TDF

Type of Study/Description	GLP[a]	Test System	Method of Administration	Testing Facility	Gilead Study No.
Tenofovir Alafenamide Loading in Primary Human $CD4^+$ T Cell Subsets	No	Primary human CD4+T cells	In vitro	Gilead Sciences Foster City, CA, USA	PC-120-2023
Selective Intracellular Activation of a Novel Prodrug of the Human Immunodeficiency Virus Reverse Transcriptase Inhibitor Tenofovir Leads to Preferential Distribution and Accumulation in Lymphatic Tissue	No	Dog	Oral	Gilead Sciences Foster City, CA, USA	Antimicrob Agents Chemother 2005;49(5):1898-1906 {Lee 2005}
A Single Dose Pharmacokinetic Bioavailability Study of GS-7430-02 in Rhesus Monkeys	No	Rhesus monkey	Oral	[redacted] USA (In-life phase) [redacted] Canada (Analysis)	P2000087
Plasma and Liver Pharmacokinetics of Tenofovir Alafenamide (TAF) Following Single Oral Administration in Male Beagle Dogs	No	Dog	Oral	[redacted] USA (In-life phase) Gilead Sciences Foster City, CA, USA (Analysis)	AD-120-2034
Plasma and Liver Pharmacokinetics of Tenofovir Alafenamide (GS-7340) Following 7-Day Oral Administration in Male Beagle Dogs	No	Dog	Oral	[redacted] USA (In-life phase) Gilead Sciences Foster City, CA, USA (Analysis)	AD-120-2033
Tenofovir Alafenamide Demonstrates Broad Cross-Genotype Activity Against Wild-type HBV Clinical Isolates In Vitro	No	HepG2 cells	In vitro	Gilead Sciences Foster City, CA, USA	PC-320-2003

Test Article: TAF, TDF, TFV, FTC/TDF

Type of Study/Description	GLP[a]	Test System	Method of Administration	Testing Facility	Gilead Study No.
Cytotoxicity Profile of Tenofovir Alafenamide (GS-7340)	No	MT-2, MT-4, and HepG2 cells	In vitro	Gilead Sciences Foster City, CA, USA	PC-120-2007
Antiviral Activity of TAF Against Drug-Resistant HBV Isolates	No	HepG2 cells	In vitro	Gilead Sciences Foster City, CA, USA	PC-320-2007
Effect of Cathepsin A, Carboxylesterase 1, CYP3A4 on Primary Human Hepatocytes	No	Primary human hepatocytes	In vitro	Gilead Sciences, Inc., Foster City, CA USA	AD-120-2031
Effect of TAF on CatA-mediated Activation and Antiretroviral Activity	No	Purified CatA and primary CD4+ T lymphocytes	In vitro	Gilead Sciences, Inc., Foster City, CA USA	PC-120-2001
CatA and CES1 Expression and Enzymatic Activation of TAF in HepG2 and HepAD38 Cells	No	HepG2 and HepAD38 cells	In vitro	Gilead Sciences, Inc., Foster City, CA USA	PC-320-2006
Intracellular Metabolism and In Vitro Activity of Tenofovir Against Hepatitis B Virus	No	HBV reverse transcriptase	In vitro	Gilead Sciences Foster City, CA, USA	Antimicrob Agents Chemother 2006;50(7):2471-2477 {Delaney 2006}
Antiviral activity vs human HBV	No	Human hepatoblastoma cell line (HB611)	In vitro	Rational Drug Design Laboratories, Fukushima, Japan	Antiviral Chemistry and Chemother 1994;5(2):57–63. {Yokota 1994}
Antiviral activity vs 3TC-resistant human HBV	No	HepG2 cells	In vitro	Gilead Sciences, Inc., USA	Antiviral Therapy 2005;10:625–33 {Yang 2005}
Antiviral activity vs wild type and 3TC-resistant human HBV	No	HepG2, HepAD38, and HepAD79 cells	In vitro	Gilead Sciences, Inc., USA	Antiviral Research 2002; 54: 37-45 {Cihlar 2002} P4331-00038
Antiviral activity against HBV with the rtA194T mutation	No	HepG2 cells	In vitro	Gilead Sciences, Inc., USA	PC-104-2012
Antiviral activity against HBV with entecavir-associated resistance mutations	No	HepG2 cells	In vitro	[redacted] Australia	PC-174-2003

Test Article: TAF, TDF, TFV, FTC/TDF

Type of Study/Description	GLP[a]	Test System	Method of Administration	Testing Facility	Gilead Study No.
Lamivudine, Adefovir, and Tenofovir Exhibit Long-Lasting Anti-Hepatitis B Virus Activity in Cell Culture	No	HepG2 2.2.15 cells	In vitro	Rega Institute for Medical Research Leuven, Belgium	J Viral Hep 2000;7:79-83 {Ying 2000}
Anti-Human Immunodeficiency Virus Activity and Cellular Metabolism of a Potential Prodrug of the Acyclic Nucleoside Phosphonate 9-*R*-(2-Phosphonomethoxypropyl) adenine (PMPA), Bis(isopropyloxymethylcarbonyl) PMPA	No	Human resting/activated PBMCs and T lymphocyte (MT-2) cells	In vitro	St Jude Children's Hospital and University of Tennessee Memphis, TN, USA	Antimicrob Agents Chemother 1998;42(3):612–617 {Robbins 1998}
The Long Intracellular Half-Life of Tenofovir Diphosphate Correlates with Persistent Inhibition of HIV-1 Replication In Vitro	No	In vitro	In vitro	Gilead Sciences Foster City, CA, USA	19th International Conference on Antiviral Research; 2006; San Juan Puerto Rico {Ledford 2006}
Mechanism of Action (Intracellular Metabolism In Vitro Following In Vivo Dosing)	No	PBMCs Macaque monkeys	In vitro In vivo, subcutaneous (SC)	[redacted] USA	P2001025
Mutations in Hepatitis B DNA Polymerase Associated with Resistance to Lamivudine Do Not Confer Resistance to Adefovir In Vitro	No	In vitro	In vitro	Gilead Sciences Foster City, CA, USA	Hepatology 1998; 28(6):1669-1673 {Xiong 1998}
Inhibitory Effects of Tenofovir & TDF on Human HIV_{IIIB} RT and Human DNA Polymerases	No	HIV_{IIIB} RT, human DNA polymerase (α, β, γ)	In vitro	Gilead Sciences Foster City, CA, USA	Antiviral Chemistry and Chemotherapy 1995;6(4):217–221 {Cherrington 1995}
Protein Binding of Cidofovir, Cyclic HPMPC, PMEA, and PMPA in Human Plasma and Serum	No	In vitro	In Vitro	Gilead Sciences Foster City, CA, USA	P0504-00039.1

Test Article: TAF, TDF, TFV, FTC/TDF

Type of Study/Description	GLP[a]	Test System	Method of Administration	Testing Facility	Gilead Study No.
Antiviral Effect of Oral Administration of Tenofovir Disoproxil Fumarate in Woodchucks with Chronic Woodchuck Hepatitis Virus Infection	No	Woodchucks	Oral	College of Veterinary Medicine, Cornell University Ithaca, NY, USA	Antimicrob Agents Chemother 2005;49(7):2720-2728 {Menne 2005}
A 48 Week Dosing Study of Adefovir Dipivoxil (ADV), Tenofovir Disoproxil Fumarate (TDF), Emtricitabine (FTC), and Lamivudine (3TC), Alone and in Combination, Using the Woodcheck Model of Hepatitis B Virus Infection	No	Woodchucks	Oral	[redacted] USA	PC-174-2004
No Detectable Resistance to Tenofovir Disoproxil Fumarate (TDF) in HBeAg+ and HBeAg- Patients With Chronic Hepatitis B (CHB) After Eight Years of Treatment	No	In vitro	In vitro	Gilead Sciences Foster City, CA, USA	The 65th Annual Meeting of the American Association for the Study of Liver Diseases; 2014; Boston MA United States. Poster 1707 {Corsa 2014}

3TC = lamivudine; ADV = adefovir dipivoxil; CatA = cathepsin A; CES1 = carboxylesterase 1; CHB = Chronic hepatitis B; CYP3A4 = Cytochrome P450 3A4; DNA = deoxyribonucleic acid; FTC = emtricitabine; GLP = Good Laboratory Practice; HBeAg = hepatitis B e antigen; HBV = Hepatitis B virus; HIV = human immunodeficiency virus; HPMPC = (S)-9-[3-hydroxy-2-(phosphonomethoxy)propyl]-2,6-diaminopurine (Cidofovir); OATP1B1 = organic anion transporting polypeptide 1B1; OATP1B3 = organic anion transporting polypeptide 1B3; PBMC = peripheral blood mononuclear cell; PMEA = adefovir, 9-(2-phosphonylmethoxyethyl)adenine (adefovir); PMPA = tenofovir, 9-R-2-Phosphonomethoxypropyl adenine; RT = reverse transcriptase; SHIV = simian/human immunodeficiency virus; TAF = tenofovir alafenamide; TAMs = thymidine analogue mutations; TDF = tenofovir disoproxil fumarate; TFV = tenofovir; ZDV = zidovudine

a An entry of "Yes" indicates that the study includes a GLP compliance statement.

1.4. Secondary Pharmacodynamics of BIC

Test Article: BIC

Type of Study/Description	GLP[a]	Test System	Method of Administration	Testing Facility	Gilead Study No.
Secondary Pharmacodynamics					
Cytotoxicity of GS-9883 in Non-Target Cell Lines and Primary Cells	No	Human hepatoma cell lines (Huh7 and HepG2), human prostate carcinoma cell line (PC3), normal human embryonic lung fibroblast line (MRC5) and primary human hepatocytes	In Vitro	Gilead Sciences, Inc., Foster City, CA, USA.	PC-141-2042
Antiviral Activity of GS-9883 against Non-HIV Viruses	No	Chronically HBV infected AD38 cells, Huh 7-Lunet derived stable HCV replicon cell lines containing either HCV1b replicon or HCV2a replicon, H1-HeLa cells infected with human rhinoviruses (HRV1A, HRV14, HRV16), normal human bronchial/ tracheal epithelial cells (NHBE) infected with Influenza A virus (A/Port Chalmers/1/73) or Influenza B virus (B/LEE/40), Hep-2 Cells infected with RSV	In Vitro	Gilead Sciences, Inc., Foster City, CA, USA.	PC-141-2043
Molecular Target Screen of GS-9883	No	Human, rabbit, rat, hamster, and mouse receptors	In vitro	[redacted] Taiwan, [redacted]	PC-141-2029 ([redacted] AB19482)

BIC = bictegravir (GS-9883); GS-9883 = bictegravir; HIV = human immunodeficiency virus

1.5. Secondary Pharmacodynamics of FTC

Test Article: FTC

Type of Study/Description	GLP[a]	Test System	Method of Administration	Testing Facility	Study No.
Antiviral activity vs human hepatitis B virus (HBV), Cytotoxicity	No	Human hepatoma cell line HepG2.2.15	In vitro	Emory University, Atlanta, GA, USA	Antimicrob Agents Chemother 1994;38:2172–2174 {Schinazi 1994}
Antiviral activity vs human hepatitis B virus (HBV)	No	Human hepatoma cell line HepG2.2.15	In vitro	Yale University, New Haven, CT, USA	{Ma 1997}
Antiviral activity vs human hepatitis B virus (HBV)	No	Human hepatoma cell line HepG2.2.15	In vitro	Victorian Infectious Diseases Reference Laboratory, Fairfield Hospital, Victoria, Australia	{Shaw 1996}
Antiviral activity vs human hepatitis B virus (HBV)	No	Primary human hepatocytes	In vitro	Burroughs Wellcome Co., Research Triangle Park, NC 27709 USA	{Condreay 1996}
Antiviral activity vs human HBV, Cytotoxicity	No	Human hepatoma cell line HepG2.2.15	In vitro	Burroughs Wellcome Co., Research Triangle Park, NC 27709 USA	Antimicrob Agents Chemother 1992;36:2686–2692 {Furman 1992}
Effect on HBV replication in vivo	No	Mouse	Oral	Burroughs Wellcome Co., Research Triangle Park, NC 27709 USA	Antimicrob Agents Chemother 1994;38:616–619 {Condreay 1994}
Effect on HBV replication in vivo	No	In vitro	In vitro	Glaxo Wellcome, Research Triangle Park, NC, USA	{Davis 1996}
Effect on HBV replication in vivo	No	SCID mouse	IP	Thomas Jefferson University, PA, USA	Frontiers in Viral Hepatitis 2002. Elsevier Science, Printed in the Netherlands {Kamkolar 2002}
Effect on HBV replication in vivo	No	Woodchuck	Oral	Georgetown University, MA, USA	Antimicrob Agents Chemother 2000;44:1757–1760 {Kamkolar 2002}

Test Article: FTC

Type of Study/Description	GLP[a]	Test System	Method of Administration	Testing Facility	Study No.
Effect on HBV replication in vivo	No	Woodchuck	IP	Glaxo Wellcome, Research Triangle Park, NC, USA	Antimicrob Agents Chemother 1997;41:2076–2082 {Cullen 1997}
Cytotoxicity assay	No	Molt-4 cells	In vitro	Department of Pharmacology, School of Medicine, University of North Carolina, Chapel Hill, NC, USA	J Biol Chem 264:11934–7 {Wilson 1993}
In Vitro Receptor Binding Potencies of FTC	No	In vitro binding assay	In vitro	[redacted] USA	TPZZ/93/0002
In Vitro Autonomic Pharmacology Cholinergic (Muscarinic) Activity Alpha-adrenoceptor Activity Beta-adrenoceptor Activity Serotonin Receptor Activity	No	 Guinea pig ileum Rabbit aortic strips Guinea pig trachea and atria Rat fundus strips	In vitro	[redacted] USA	TPZZ/92/0055
Antiviral Activity vs. Human Hepatitis B Virus (HBV), Cytotoxicity	No	Human hepatoma cell line HepG2.2.15	In vitro	Emory University, Atlanta, GA, USA	Antimicrob Agents Chemother. 1994; 38:2172-2174 {Schinazi 1994}
Antiviral Activity vs. Human HBV, Cytotoxicity	No	Human hepatoma cell line HepG2.2.15	In vitro	Burroughs Wellcome Co., Research Triangle Park, NC 27709 USA	Antimicrob Agents Chemother. 1992; 36:2686-2692 {Furman 1992}
Cytotoxicity Assay	No	MT-4, CEM, IM9, Molt-4, and HepG2.2.15 cells	In vitro	Burroughs Wellcome Co., Research Triangle Park, NC 27709 USA	Antimicrob Agents Chemother. 1994; 38:868-871 {Van Draanen 1994}
Mitochondrial Toxicity	No	Human hepatoma cell line HepG2	In vitro	University of Alabama, Birmingham, USA	Biochem. Pharmacol. 1996; 52:1577-1584 {Cui 1996}

Test Article: FTC

Type of Study/Description	GLP[a]	Test System	Method of Administration	Testing Facility	Study No.
An In Vitro Evaluation of the Effects on Cell Growth and Mitochondrial Functions in the MT2 Cell Line after Long Term Exposure to Antiviral Xenobiotics	No	Human T cell line, MT-2 cells	In vitro	Gilead Sciences, Inc., Foster City, CA USA	TPI 11963
Data from Clonogenic Assays CFU-GM and BFU-E and Mitochondrial Assays for TP0001 and TP0004 as Compared to AZT	No	Human bone marrow progenitor cells	In vitro	Gilead Sciences, Inc. USA	233 {Sommadossi 1996}
Effect of FTC on Mitochondrial DNA	No	Molt-4 cell culture assay	In vitro	[redacted] USA	TGZZ/93/0016
Effect of FTC on Mitochondrial DNA	No	Molt-4 cell culture assay	In vitro	[redacted] USA	TGZZ/93/0023

AZT = zidovudine; BFU-E = burst forming unit-erythroid; CFU-GM = colony forming unit granulocyte, monocyte; FTC = emtricitabine, GLP = Good laboratory practice; HBV = hepatitis B virus; HIV = human immunodeficiency virus
a An entry of "Yes" indicates that the study includes a GLP compliance statement.

1.6. Secondary Pharmacodynamics of TAF

Studies supporting the secondary pharmacodynamics of TAF are presented in this table and are inclusive of studies that utilized TAF, TDF, TFV, or FTC/TDF.

Test Article: TFV, TAF

Type of Study/Description	GLP[a]	Test System	Method of Administration	Testing Facility	Study No.
Binding Screen to Neuroreceptors, Ion Channels, Transporters, Nuclear Receptors	No	Protein targets	In vitro	[redacted] Taiwan	V2000020
Cytotoxic Effect of TAF on PBMCs	No	PBMCs	In vitro	Gilead Sciences, Inc., Foster City, CA USA	PC-120-2009
Cytotoxicity Assay with TAF	No	MT-2, MT-4, and HepG2 cells	In vitro	Gilead Sciences, Inc., Foster City, CA USA	PC-120-2007
Cytotoxicity Assay with TFV	No	HepG2, human skeletal muscle cells (SKMC), human renal proximal tubule epithelial cells (RPTECs)	In vitro	Gilead Sciences, Inc., Foster City, CA USA	Antiviral Research 2002; 54: 37-45 {Cihlar 2002} P4331-00037
Cytotoxicity Assay with TFV	No	RPTECs	In vitro	Hospital Universitari de Tarragona, Tarragona, Spain	Antimicrob. Agents Chemother., 2006;50 (11):3824-32 {Vidal 2006}
Effects of TAF on Hematopoietic Progenitors	No	Erythroid and myeloid progenitors	In vitro	[redacted] Canada	PC-120-2016 GLD06A
Cytotoxicity Assay with TAF	No	HEK293T cells expressing renal OAT1 and OAT3 transporters and primary human CD4+ T lymphocytes	In vitro	Gilead Sciences, Inc., Foster City, CA USA	PC-120-2018 Antiviral Therapy, 2014; 10.3851/IMP2770 {Bam 2014b}
Cytotoxic Effect of TAF on Primary Osteoblasts	No	PBMCs and human proliferating osteoblast cells	In vitro	Gilead Sciences, Inc., Foster City, CA USA	PC-120-2008
Antiviral Activity and Cytotoxicity of TAF Metabolites	No	MT-2 and MT-4 cells	In vitro	Gilead Sciences, Inc., Foster City, CA USA	PC-120-2021
Mitochondrial Toxicity with TFV	No	HepG2, SKMC, RPTECs	In vitro	Gilead Sciences, Inc., Foster City, CA USA	P1278-00042 Antimicrob Agents Chemother 2002; 45: 716-723 {Birkus 2002}

Test Article: TFV, TAF

Type of Study/Description	GLP[a]	Test System	Method of Administration	Testing Facility	Study No.
Effect of TAF on Mitochondrial DNA	No	HepG2 cells	In vitro	Gilead Sciences, Inc., Foster City, CA USA	PC-120-2006 {Stray 2017}
Antiviral activity vs human HBV and duck HBV	No	Human hepatoma cell line HepG2, primary duck hepatocytes	In vitro	Erasmus University Rotterdam, Holland, Catholic University, Leuven Belgium	Antimicrob Agents Chemother 1994 Sep;38(9):2180–2 {Heijtink 1994}
Interaction of antiviral nucleoside phosphonates (adefovir, cidofovir, tenofovir) with renal organic anion and cation transporters)	No	Xenopus laevis oocytes expressing hOAT1, hOAT2, or hOAT3	In vitro	[redacted] USA	PC-103-2001
Effect of HIV Protease Inhibitors and Other Therapeutics on the Transport of Tenofovir by Human Renal Organic Anion Transporter Type 1 (hOAT 1)	No	Chinese hamster ovary cells expressing hOAT1	In vitro	Gilead Sciences, Inc., Foster City, CA USA	PC-104-2010
Effect of HIV Protease Inhibitors on the transport of Tenofovir by human Renal Organic Anion Transporter Type 3 (hOAT3)	No	BHK cells (Baby hamster kidney) expressing hOAT3	In vitro	Gilead Sciences, Inc., Foster City, CA USA	PC-104-2011
Lack of a Contribution from MRP1 in Tubular Re-absorption of Tenofovir	No	Madin-Darby canine kidney cells	In vitro	Gilead Sciences, Inc., Foster City, CA USA	PC-104-2014
Mitochondrial Toxicity of Necleos(t)ide RT Inhibitors	No	HepG2 cells	In vitro	[redacted] Germany	TX-104-2001
Cytotoxicity Assay with TFV alone and in combination with COBI or EVG+COBI+FTC	No	RPTECs	In vitro	Gilead Sciences, Inc., Foster City, CA USA	PC-236-2012

Test Article: TFV, TAF

Type of Study/Description	GLP[a]	Test System	Method of Administration	Testing Facility	Study No.
Cytotoxicity Assay with TFV alone and in combination with COBI or EVG+COBI+FTC	No	Human embryonic kidney 293T cells transiently expressing OAT1 and MRP4 transporters	In vitro	Gilead Sciences, Inc., Foster City, CA USA	PC-236-2013
Resistance Development Over 144 Weeks in Treatment-Naive Patients Receiving Tenofovir Disoproxil Fumarate or Stavudine with Lamivudine and Efavirenz in Study 903	No	In vitro	In vitro	Gilead Sciences Foster City, CA, USA	HIV Med 2006;7(7):442-450 {Margot 2006}

CatA = cathepsin A; COBI = cobicistat; DNA = deoxyribonucleic acid; EVG = elvitegravir; FTC = emtricitabine; GLP = Good Laboratory Practice; HBV = hepatitis B virus; hOAT 1 = human renal organic anion transporter type 1; hOAT 3 = human renal organic anion transporter type 3; MRP1 = multi-drug resistance associated protein 1; MRP4 = multidrug resistance protein 4; OAT = organic anion transporter; PBMC = peripheral blood mononuclear cell; RPTECs = renal proximal tubule epithelial cells; SKMC = skeletal muscle cells; TAF = tenofovir alafenamide; TFV = tenofovir
a An entry of "Yes" indicates that the study includes a GLP compliance statement.

1.7. Safety Pharmacology of BIC

Test Article: BIC

Type of Study/Description	GLP[a]	Test System	Method of Administration	Testing Facility	Gilead (CRO) Study No.
In Vitro					
In Vitro Effect of GS-9883 on the hERG Channel	Yes	Human embryonic kidney cells (HEK293)	In vitro	[redacted] USA	PC-141-2049 ([redacted] 131024.DPW)
In Vivo					
Effect of GS-9883 on the Central Nervous System of Rats	Yes	Rat/Crl:WI(Han)	Oral gavage	[redacted] USA	PC-141-2047 ([redacted] 8292938)
Effect of GS-9883 on the Respiratory System of Rats	Yes	Rat/Crl:WI(Han)	Oral gavage	[redacted] USA	PC-141-2048 ([redacted] 8292939)
Effect of GS-9883 on the Cardiovascular System of the Monkey	Yes	Monkey/Cynomolgus	Oral gavage	[redacted] USA	PC-141-2046 ([redacted] 8292937)

GS-9883 = bictegravir; hERG = human ether-a-go-go related gene

1.8. Safety Pharmacology of FTC

Test Article: FTC

Type of Study/Description	GLP[a]	Test System	Method of Administration	Testing Facility	Study No.
In Vitro					
Isolated Guinea Pig Ileum	No	Guinea Pig, Duncan Hartley	In Vitro	[redacted]	477
Isolated Cardiac Muscle Isolated Perfused Rat Heart Electrically Driven Papillary and Atrial Muscle of the Cat Spontaneously-beating Guinea Pig Paired Atria	No	Rat heart Cat papillary and atrial muscle strips Guinea pig paired atria	In Vitro	[redacted] USA	TPZZ/92/0056
In Vivo					
General High Dose Pharmacology Testing Results for FTC					
Modified Irwin Screen	No	Mouse, ICR	Oral	[redacted] Taiwan	477
CNS - Spontaneous Locomotor Activity	No	Mouse, ICR	Oral		
CNS – Motor Incoordination (Roto-rod Test)	No	Mouse, ICR	Oral		
CNS – Hexobarbital Potentiation (Sleeping Time)	No	Mouse, ICR	Oral		
CNS – Anticonvulsant Activity (Maximal Electroshock)	No	Mouse, ICR	Oral		
CNS - Anticonvulsant Activity (Metrazole)	No	Mouse, ICR	Oral		
CNS – Proconvulsant Activity (Electroshock)	No	Mouse, ICR	Oral		
CNS – Proconvulsant Activity (Metrazole)	No	Mouse, ICR	Oral		

Test Article: FTC

Type of Study/Description	GLP[a]	Test System	Method of Administration	Testing Facility	Study No.
CNS - Analgesic Activity (Tail Flick)	No	Mouse, ICR	Oral	[redacted] Taiwan	477
CNS – Analgesic Activity (Phenylquinone Writhing)	No	Mouse, ICR	Oral		
CNS – Body Temperature	No	Rat, Wistar	Oral		
Cardiovascular Function	No	Rat Wistar	Oral		
Renal Function	No	Rat, Long Evans	Oral		
Gastrointestinal Motility	No	Mouse, ICR	Oral		
Overt Pharmacological Effects	No	Mouse, CD-1 Rat, CD (Sprague Dawley)	Oral gavage	[redacted] USA	TPZZ/93/0001
Conditioned Avoidance Response	No	Rat, Long Evans	Intraperitoneal	[redacted] USA	TPZZ/93/0119
Systolic Blood Pressure and Heart Rate	No	Conscious Normotensive Rat, CD (Sprague Dawley)	Oral	[redacted] USA	TPZZ/92/0057
Cardiovascular, Respiratory and Autonomic Function					
Cardiovascular and Respiratory Effects in Spontaneously Breathing Dogs Anesthetized with Allobarbital-Urethane	No	Anesthetized Dogs, Beagle	Intravenous	[redacted] USA	TPZZ/92/0076
Effects on the Changes in Mean Arterial Blood Pressure Induced by Norepinephrine, Carotid Occlusion, Acetylcholine and Vagal Nerve Stimulation in the Anesthetized Dog	No	Anesthetized Dogs, Beagle	Intravenous		

CNS = central nervous system; FTC = emtricitabine; GLP = Good Laboratory Practice
a An entry of "Yes" indicates that the study includes a GLP compliance statement.

1.9. Safety Pharmacology of TAF

Test Article: TAF

Type of Study/Description	GLP[a]	Test System	Method of Administration	Testing Facility	Gilead (CRO) Study No.
In Vitro					
Cardiovascular (hERG Inhibition)	Yes	Human embryonic kidney cells (HEK293)	In vitro	[redacted]	PC-120-2005 ([redacted]111213.DPW)
In Vivo					
Cardiovascular	Yes	Conscious male beagle dog	Oral gavage	[redacted] Canada	D2000006 ([redacted] 93205)
CNS	Yes	Male Sprague Dawley rat	Oral gavage	[redacted] Canada	R990188 ([redacted]56518)
Gastrointestinal	Yes	Male Sprague Dawley rat	Oral gavage	[redacted] Canada	R990187 ([redacted]56519)
Renal	Yes	Male Sprague Dawley rat	Oral gavage	[redacted] Canada	R990186 ([redacted]56520)

CNS = central nervous system; CRO = contract research organization; GLP = Good Laboratory Practice; hERG = human ether-a-go-go related gene
a An entry of "Yes" indicates that the study includes a GLP compliance statement.

1.10. Pharmacodynamic Drug Interactions of BIC

Test Article: BIC

Type of Study/Description	GLP[a]	Test System	Method of Administration	Testing Facility	Gilead Study No.
Pharmacodynamic Drug Interactions					
In vitro Antiviral Activity of GS-9883 in Combination with Other Anti-retroviral Agents	No	Human lymphoblastoid T-cell line MT-2, HIV-1 IIIb virus	In Vitro	Gilead Sciences, Inc., Foster City, CA, USA.	PC-141-2038
Three-Drug Combination Study of the Antiviral Activity of BIC, FTC and TAF	No	Human lymphoblastoid T-cell line MT-2, HIV-1 IIIb virus	In Vitro	Gilead Sciences, Inc., Foster City, CA, USA.	PC-380-2001

BIC = bictegravir; FTC = emtricitabine; GLP = Good Laboratory Practice; GS-9883 = bictegravir; HIV = human immunodeficiency virus; TAF = tenofovir alafenamide

1.11. Pharmacodynamic Drug Interactions of FTC

Type of Study/Description	Test System	Method of Administration	Testing Facility	Study No and Reference
FTC Pharmacodynamic Drug Interactions				
Antiviral activity in combination with other antiretroviral drugs	MT 2 cells	In vitro	Gilead Sciences, Inc., USA	470
In vitro synergy studies with FTC and other anti-HIV compounds.	MT 2 cells	In vitro	Gilead Sciences, Inc., USA	10804

FTC = emtricitabine; HIV = human immunodeficiency virus

1.12. Pharmacodynamic Drug Interactions of TAF

Studies supporting the pharmacodynamic drug interaction of TAF are presented in this table and are inclusive of studies that utilized TAF, TDF, TFV, or FTC/TDF.

Type of Study/Description	Test System	Method of Administration	Testing Facility	Study No and Reference
TAF Pharmacodynamic Drug Interactions				
Effect of Inhibitors of HIV, HCV, and Host Cell Proteases on Cathepsin A-mediated Activation and Antiretroviral Activity of Tenofovir Alafenamide	Purified CatA and primary CD4+ T-lymphocytes	In vitro	Gilead Sciences, Inc., USA	PC-120-2001
Antiviral activity in combination with other antiretroviral drugs	MT-2 cells	In vitro	Gilead Sciences, Inc., USA	PC-183-2004
Antiviral activity in combination with other antiretroviral drugs	MT-2 cells	In vitro	Gilead Sciences, Inc., USA	PC-104-2005
Antiviral activity in combination with other antiretroviral drugs	MT-2 cells	In vitro	Gilead Sciences, Inc., USA	PC-104-2006
Antiviral activity in combination with other antiretroviral drugs	MT-2 cells	In vitro	Gilead Sciences, Inc., USA	PC-164-2002
Antiviral HIV-1 dual drug combination study of FTC, RPV, and TFV	MT-2 cells	In Vitro	Gilead Sciences, Inc., USA	PC-264-2001
Effect of Protease Inhibitors on the Anti-HBV Activity of Tenofovir Alafenamide	HepAD38 cells	In vitro	Gilead Sciences Foster City, CA, USA	PC-320-2004
CatA and CES1 Expression and Enzymatic Activation of TAF in HepG2 and HepAD38 Cells	In vitro	In vitro	Gilead Sciences Foster City, CA, USA	PC-320-2006
Tenofovir Alafenamide Antiviral Activity in Combination with Antiretroviral Agents	MT-2 cells	In vitro	Gilead Sciences Foster City, CA, USA	PC-120-2002
Effect of Tenofovir Alafenamide on the Activity of HCV Inhibitors	Huh-7 cells	In vitro	Gilead Sciences Foster City, CA, USA	PC-320-2001

Type of Study/Description	Test System	Method of Administration	Testing Facility	Study No and Reference
Effect of Sofosbuvir on the HIV-1 Antiviral Activity of TAF	MT-2 cells	In vitro	Gilead Sciences Foster City, CA, USA	PC-120-2032
Lack of a Metabolic and Antiviral Drug Interaction Between Tenofovir, Abacavir and Lamivudine	CCRF-CEM cells and PBMCs	In vitro	Gilead Sciences Foster City, CA, USA	Antivir Ther 2005;10(3): 451-457 {Ray 2005}
Metabolism of Tenofovir and Didanosine in Quiescent or Stimulated Human Peripheral Blood Mononuclear Cells	PBMCs	In vitro	St Jude Children's Research Hospital Memphis, TN, USA	Pharmacotherapy 2003; 23(6):695-701 {Robbins 2003}
Mechanism of Action (Intracellular Metabolism): Effect of Tenofovir in Combination with Other Anti-HIV Nucleoside Reverse Transcriptase Inhibitors (NRTIs) on Intracellular Nucleotide Pools	CEM-CRFF cells	In vitro	Gilead Sciences Foster City, CA, USA	45th Interscience Conference on Antimicrobial Agents and Chemotherapy, Poster H-1901 {Vela 2005}
Mechanism of Action (Intracellular Metabolism): Role of Purine Nucleoside Phosphorylase in Drug Interactions Between 2′,3′-dideoxyinosine and Allopurinol, Ganciclovir, or Tenofovir	CEM-CCRF cells and activated PBMCs	In vitro	Gilead Sciences Foster City, CA, USA	Antimicrob Agents Chemother 2004;48(4):1089–1095 {Ray 2004}
Anti-HBV Activity of TFV in Combination with Nucleoside Analogues	AD38 cell line	In vitro	Gilead Sciences Foster City, CA, USA	PC-174-2006
Combinations of Adefovir with Nucleoside Analogs Produce Additive Antiviral Effects Against Hepatitis B Virus In Vitro	HepG2 cells	In vitro	Gilead Sciences Foster City, CA, USA	Antimicrob Agents Chemother 2004;48(10):3702-3710 {Delaney 2004}
Anti-HIV Activity of Adefovir (PMEA) and PMPA in Combination with Antiretroviral Compounds: In Vitro Analyses	MT2 cells	In vitro	Gilead Sciences Foster City, CA, USA	Antiviral Res 1997;36(2):91-97 {Mulato 1997}

CatA = cathepsin A; CES1 = carboxylesterase 1; FTC = emtricitabine; HBV = hepatitis B virus; HCV = hepatitis C virus; HIV = human immunodeficiency virus; PBMC = peripheral blood mononuclear cell; PMEA = adefovir, 9-(2-phosphonylmethoxyethyl)adenine (adefovir); PMPA = tenofovir, 9-R-2-Phosphonomethoxypropyl adenine; TAF = tenofovir alafenamide; TFV = tenofovir

2. PRIMARY PHARMACODYNAMICS

2.1. BIC

Studies of the primary pharmacodynamics of BIC are presented in Section 1.1.

2.2. FTC

Studies of the primary pharmacodynamics of FTC are presented in Section 1.2.

2.3. TAF

Studies of the primary pharmacodynamics of TAF are presented in Section 1.3.

3. SECONDARY PHARMCODYNAMICS

3.1. BIC

Test Article: BIC

Systems Evaluated	Method of Administration	Concentration (µM)[b]	Noteworthy Findings	GLP[a]	Gilead (CRO) Study Number
Molecular target screen	In Vitro	10	No significant binding at 10 µM	No	PC-141-2029 ([redacted]AB19482)

GLP = Good Laboratory Practice
a An entry of "Yes" indicates that the study includes a GLP compliance statement.
b Free concentration

3.2. FTC

Studies of the secondary pharmacodynamics of FTC are listed in Section 1.5.

3.3. TAF

Studies of the secondary pharmacodynamics of TAF are listed in Section 1.6.

4. SAFETY PHARMACOLOGY

4.1. In Vitro Studies

4.1.1. BIC

Test Article: BIC

Organ Systems Evaluated	Species/Strain	Method of Administration	Concentration (µM)[a]	Number per Group	Noteworthy Findings	GLP[b]	Gilead (CRO) Study Number
Cardiovascular (hERG Inhibition)	Human embryonic kidney cells (HEK293)	In Vitro	0.8, 7.1	3 per dose	10.3 ± 1.2% at 7.1 µM; IC_{50} > 7.1 µM	Yes	PC-141-2049 ([redacted]131024.DPW)

BIC = bictegravir; CRO = contract research organization; GLP = Good laboratory practice; hERG = human ether-a-go-go-related gene
a Free concentration
b An entry of "Yes" indicates that the study includes a GLP compliance statement.

4.1.2. FTC

Test Article: FTC

Organ Systems Evaluated	Species/Strain	Method of Administration	Dose (µM or M)	Number per Group	Noteworthy Findings	GLP[a]	Study No.
Contractile Responses	Isolated Guinea Pig Ileum	In Vitro	10, 30, 100 µM	6 ileum strips per group	FTC did not elicit any significant agonist effect upon guinea pig ilea or alter contractile responses induced by acetylcholine, histamine or $BaCl_2$	No	477
Isolated Perfused Rat Heart	Rat heart	In Vitro	10^{-4} M	—	Perfusion of isolated rat hearts at 10^{4} M produced decreases in heart rate of 5 ± 4% that were similar to that of control hearts (6 ± 5% decrease). The incidence of ventricular premature extrasystoles in FTC-treated hearts was no greater than that observed in control hearts. No ventricular tachycardia or fibrillation occurred in hearts treated with FTC or vehicle control.	No	TPZZ/92/0056
Electrically Driven Papillary and Atrial Muscle of the Cat	Cat papillary and atrial muscle strips	In Vitro	10^{-4} M	7 muscle strips	Minor positive inotropism (12 ± 6% increase in developed tension) was observed on papillary muscle preparations (n = 7) after incubation for 30 minutes with FTC. Negligible positive inotropism (2 ± 3% increase in developed tension) occurred on cat atrial preparations (n = 5) following a 30 minute incubation. The maximum following rate at which atrial muscle would follow electrical stimulation was not affected by FTC.	No	TPZZ/92/0056
Spontaneously-beating Guinea Pig Paired Atria	Guinea pig paired atria	In Vitro	10^{-4} M	—	Fifteen-minute incubation with FTC produced no direct chronotropic or inotropic effects on spontaneously-beating guinea-pig atria.	No	TPZZ/92/0056

FTC = emtricitabine; GLP = Good laboratory practice
a An entry of "Yes" indicates that the study includes a GLP compliance statement.

4.1.3. TAF

Test Article: TAF (GS-7340-03)

Organ Systems Evaluated	Species/Strain	Method of Administration	Dose (µM)	Number per Concentration	Noteworthy Findings	GLP[a]	Gilead (CRO) Study Number
Cardiovascular (hERG Inhibition)	Human embryonic kidney cells (HEK293)	In vitro	0, 1, and 10µM	3 replicates	No significant inhibition IC_{50} > 10 µM	Yes	PC-120-2005 ([redacted]111213.DPW)

CRO = contract research organization; GLP = Good laboratory practice; hERG = human ether-a-go-go related gene; TAF = tenofovir alafenamide
a An entry of "Yes" indicates that the study includes a GLP compliance statement.

4.2. In Vivo Studies

4.2.1. BIC

Test Article: BIC

Organ Systems Evaluated	Species/Strain	Method of Administration	Dose[a] (mg/kg)	Gender and n per Group	Noteworthy Findings	GLP[b]	Gilead (CRO) Study Number
Central Nervous System	Rat/Crl:WI(Han)	Oral Gavage	0[c], 10, 30, 100, 300 (NOEL)	8 Males/Group	None	Yes	PC-141-2047 ([redacted]8292938)
Respiratory System	Rat/Crl:WI(Han)	Oral Gavage	0[c], 10, 30, 100, 300 (NOEL)	8 Males/Group	None	Yes	PC-141-2048 ([redacted]8292939)
Cardiovascular System	Monkey/Cynomolgus	Oral Gavage	0[c], 30, 100, 1000 (NOEL)	4 Males (Latin Square Design)	None	Yes	PC-141-2046 ([redacted]8292937)

BIC = bictegravir; CRO = contract research organization; GLP = Good laboratory practices; NOEL = no observed effect level
a Single dose
b An entry of "Yes" indicates that the study includes a GLP compliance statement.
c Vehicle control article was 0.5% (w/w) hydroxypropyl methylcellulose (Methocel K100 LV) and 0.1% (w/w) Tween® 20 in reverse osmosis water.

4.2.2. FTC

Test Article: FTC

Organ Systems Evaluated	Species/Strain	Method of Administration	Dose (mg/kg)	Gender and n per Group	Noteworthy Findings	GLP[a]	Study No.
Modified Irwin Screen	Mouse/ICR	Oral	10, 30, 100	10 Males/Group	FTC did not cause any noteworthy findings on behavioral, autonomic, or neurological signs in animals at all doses.	No	477
CNS – Spontaneous Locomotor Activity	Mouse/ICR	Oral	10, 30, 100	8 Males/Group	FTC had no significant effect on spontaneous locomotor activity.	No	477
CNS – Motor Incoordination (Roto-rod Test)	Mouse/ICR	Oral	10, 30, 100	10 Males/Group	FTC had no significant effect on motor incoordination.	No	477
CNS – Hexobarbital Potentiation (Sleeping Time)	Mouse/ICR	Oral	10, 30, 100	10 Males/Group	FTC had no significant prolongation of hexobarbital sleeping time.	No	477
CNS – Anticonvulsant Activity (Maximal Electroshock)	Mouse/ICR	Oral	10, 30, 100	10 Males/Group	FTC had no significant effect on the number of animals experiencing clonic/tonic convulsions and mortality.	No	477
CNS – Anticonvulsant Activity (Metrazole)	Mouse/ICR	Oral	10, 30, 100	10 Males/Group	FTC had no significant effect on the number of animals experiencing clonic/tonic convulsions and mortality.	No	477
CNS – Proconvulsant Activity (Electroshock)	Mouse/ICR	Oral	10, 30, 100	10 Males/Group	FTC had no significant effect on the incidence of clonic/tonic convulsions and mortality.	No	477
CNS – Proconvulsant Activity (Metrazole)	Mouse/ICR	Oral	10, 30, 100	10 Males/Group	FTC had no significant effect on the incidence of clonic/tonic convulsions and mortality.	No	477
CNS –Analgesic Activity (Tail Flick)	Mouse/ICR	Oral	10, 30, 100	10 Males/Group	FTC caused no significant increase in latency of the tail flick response.	No	477

Test Article: FTC

Organ Systems Evaluated	Species/Strain	Method of Administration	Dose (mg/kg)	Gender and n per Group	Noteworthy Findings	GLP[a]	Study No.
CNS – Analgesic Activity (Phenylquinone Writhing)	Mouse/ICR	Oral	10, 30, 100	10 Males/Group	No significant attenuation of PQ-inducing writhing was observed after all tested doses.	No	477
CNS – Body Temperature	Rat/Wistar	Oral	10, 30, 100	10 Males/Group	FTC did not cause any significant change in body temperature.	No	477
General Pharmacology	Mouse/CD-1	Oral	100, 250, 500, 750, 1000	4 Males/Group	No effects on body weight, rectal temperature, behavior, reflexes, or respiration rate, and had no analgesic activity.	No	TPZZ/93/0001
General Pharmacology	Rat/CD (Sprague Dawley)	Oral	250, 500, 1000	4 Males/Group	Rats exhibited no visible effects. Minimal respiratory rate effects were only noted at 750 mg/kg (21% decrease) and in the control animals (29% increase). Behavioral reflexes were unaffected at doses up to 1000 mg/kg.	No	TPZZ/93/0001
Conditioned Avoidance Response	Rat/ Long Evans	Intraperitoneal	30, 100	6 Females/Group	Control days – avoided shock on 95 ± 2 trials (mean ± SEM). Vehicle – avoided shock on 96 ± 1 trials. Emtricitabine 30 or 100 mg/kg – avoided shock 97 ± 1 and 94 ± 2 trials, respectively. In neither control, vehicle, nor the drug conditions did the rats fail to escape shock on the trials in which they failed to avoid. After 100 mg/kg, inter-trial crosses declined significantly (to 42 ± 12) but inter-trial crosses also declined significantly after vehicle injection (to 34 ± 8), an injection effect that has been seen before.	No	TPZZ/93/0119

Test Article: FTC

Organ Systems Evaluated	Species/Strain	Method of Administration	Dose (mg/kg)	Gender and n per Group	Noteworthy Findings	GLP[a]	Study No.
Cardiovascular Function	Rat/Wistar	Oral	5, 10, 50	5 Males/Group	No significant effect on mean arterial blood pressure and heart rate was found.	No	477
Systolic Blood Pressure and Heart Rate	Conscious Normotensive Rat/CD (SD)	Oral	250	8 Males/Group	No statistically significant differences in systolic blood pressure or heart rate were found.	No	TPZZ/92/0057
Cardiovascular, Respiratory and Autonomic Function	Anesthetized Dogs/Beagle	Intravenous	Total cumulative dose 38.5	4 Males/Group	No statistically significant changes in mean arterial blood pressure or heart rate. No drug-related arrhythmias were observed in the Lead II electrocardiogram. There were no decreases in respiratory parameters. Increases in respiratory rate of up to 3.8 breaths/minute and minute volume of up to 0.5 l/minute were seen 10 minutes after dosing FTC; however, they were not statistically significant. The average plasma level of 2 FTC-treated dogs 30 minutes following the last dose was 140 mM. This represents 93-fold the anticipated anti-HIV/HBV IC_{50} values *in vitro* at a minimum.	No	TPZZ/92/0076
Renal Function	Rat/ Long Evans	Oral	10, 30, 100	6 Males/Group	FTC failed to cause any significant change in urine volume output, electrolyte excretion or pH values.	No	477
Gastrointestinal Motility	Mouse/ICR	Oral	10, 30, 100	10 Males/Group	No significant change in GI motility was observed.	No	477

CNS = central nervous system; FTC = emtricitabine; GI = gastrointestinal; GLP = Good laboratory practices; HBV = hepatitis B virus; HIV = human immunodeficiency virus; IC_{50} = 50% inhibitory concentration
a An entry of "Yes" indicates that the study includes a GLP compliance statement.

4.2.3. TAF

Test Article: TAF (GS-7340-02)

Organ Systems Evaluated	Species/Strain	Method of Administration	Dose (mg/kg)	Gender and n per Group	Noteworthy Findings	GLP[a]	Gilead (CRO) Study Number
Cardiovascular	Dog/Beagle	Oral gavage	30, 100 (NOEL)	3 Males/group	None	Yes	D2000006 ([redacted]93205)
CNS	Rat/Sprague Dawley CD (Crl: CD®(SD)BR)	Oral gavage	0, 100, 1000 (NOEL)	10 Males/group	None	Yes	R990188 ([redacted]56518)
Gastrointestinal	Rat/Sprague Dawley CD (Crl: CD®(SD)BR)	Oral gavage	0, 100 (NOEL), 1000	9 Males/group	At 1000 mg/kg, the rate of gastric emptying was reduced.	Yes	R990187 ([redacted]56519)
Renal	Rat/Sprague Dawley CD (Crl: CD®(SD)BR)	Oral gavage	0, 100, 1000 (NOEL)	10 Males/group	None	Yes	R990186 ([redacted]56520)

CNS = central nervous system; CRO = contract research organization; GLP = Good laboratory practice; GS-7340-02 = tenofovir alafenamide as the monofumarate form (1:1 ratio of GS-7340 to fumarate); NOEL = no-observed-effect level

a An entry of "Yes" indicates that the study includes a GLP compliance statement.

5. PHARMACODYNAMIC DRUG INTERACTIONS

5.1. BIC

Studies of the pharmacodynamic drug interactions of BIC are presented in Section 1.10.

5.2. FTC

Studies of the pharmacodynamic drug interactions of FTC are presented in Section 1.11.

5.3. TAF

Studies of the pharmacodynamic drug interactions of TDF are presented in Section 1.12.

6. REFERENCES

Bam RA, Birkus G, Babusis D, Cihlar T, Yant SR. Metabolism and antiretroviral activity of tenofovir alafenamide in CD4 T-cells and macrophages from demographically diverse donors. Antivir Ther 2014a:1-18.

Bam RA, Yant SR, Cihlar T. Tenofovir alafenamide is not a substrate for renal organic anion transporters (OATs) and does not exhibit OAT-dependent cytotoxicity. Antivir Ther 2014b:1-12.

Birkus G, Hitchcock MJM, Cihlar T. Assessment of mitochondrial toxicity in human cells treated with tenofovir: comparison with other nucleoside reverse transcriptase inhibitors. Antimicrob Agents Chemother 2002;46 (3):716-23.

Brenner BG, Oliveira M, Doualla-Bell F, Moisi DD, Ntemgwa M, Frankel F, et al. HIV-1 subtype C viruses rapidly develop K65R resistance to tenofovir in cell culture. AIDS 2006;20 (9):F9-F13.

Cherrington JM, Allen SJW, Bischofberger N, Chen MS. Kinetic interaction of the diphosphates of 9-(2-phosphonylmethoxyethyl)adenine and other anti-HIV active purine congeners with HIV reverse transcriptase and human DNA polymerases α, β, and γ. Antivir Chem Chemother 1995;6 (4):217-21.

Cihlar T, Birkus G, Greenwalt DE, Hitchcock MJM. Tenofovir exhibits low cytotoxicity in various human cell types: comparison with other nucleoside reverse transcriptase inhibitors. Antiviral Res 2002;54 (1):37-45.

Cihlar T, Chen MS. Incorporation of selected nucleoside phosphonates and anti-human immunodeficiency virus nucleotide analogues into DNA by human DNA polymerases α, β and γ. Antivir Chem Chemother 1997;8 (3):187-95.

Condreay LD, Condreay JP, Jansen RW, Paff MT, Averett DR. (-)-cis-5-fluoro-1-[2-(hydroxymethyl)-1,3-oxathiolan-5-yl]cytosine (524W91) inhibits hepatitis B virus replication in primary human hepatocytes. Antimicrob Agents Chemother 1996;40 (2):520-3.

Condreay LD, Jansen RW, Powdrill TF, Johnson LC, Selleseth DW, Paff MT, et al. Evaluation of the potent anti-hepatitis B virus agent (-) cis-5-fluoro-1-[2-(hydroxymethyl)-1,3-oxathiolan-5-yl]cytosine in a novel in vivo model. Antimicrob Agents Chemother 1994;38 (3):616-9.

Corsa A, Liu Y, Flaherty JF, Marcellin P, Miller M, Kitrinos KM. No Detectable Resistance to Tenofovir Disoproxil Fumarate (TDF) in HBeAg+ and HBeAg- Patients With Chronic Hepatitis B (CHB) After Eight Years of Treatment [Poster 1707]. The 65th Annual Meeting of the American Association for the Study of Liver Diseases: The Liver Meeting (AASLD); 2014 November 7-11; Boston MA United States.

Cui L, Schinazi RF, Gosselin G, Imbach J-L, Chu CK, Rando RF, et al. Effect of beta-enantiomeric and racemic nucleoside analogues on mitochondrial functions in HepG2 cells. Biochem Pharmacol 1996;52 (10):1577-84.

Cullen JM, Smith SL, Davis MG, Dunn SE, Botteron C, A C, et al. In vivo antiviral activity and pharmacokinetics of (-)-cis-5-fluoro-1-[2-(hydroxymethyl)-1,3-oxathiolan-5-yl]cytosine in woodchuck hepatitis virus-infected woodchucks. Antimicrob Agents Chemother 1997;41:2076-82.

Davis MG, Wilson JE, VanDraanen NA, Miller WH, Freeman GA, Daluge, et al. DNA polymerase activity of hepatitis B virus particles: differential inhibition by L-enantiomers of nucleotide analogs. Antiviral Res 1996;30 (2-3):133-45.

Delaney WE, IV, Ray AS, Yang H, Qi X, Xiong S, Zhu Y, et al. Intracellular metabolism and in vitro activity of tenofovir against hepatitis B virus. Antimicrob Agents Chemother 2006;50 (7):2471-7.

Delaney WE, IV, Yang H, Miller MD, Gibbs CS, Xiong S. Combinations of adefovir with nucleoside analogs produce additive antiviral effects against hepatitis B virus in vitro. Antimicrob Agents Chemother 2004;48 (10):3702-10.

Deval J, White KL, Miller MD, Parkin NT, Courcambeck J, Halfon P, et al. Mechanistic basis for reduced viral and enzymatic fitness of HIV-1 reverse transcriptase containing both K65R and M184V mutations. J Biol Chem 2004;279 (1):509-16.

Feng JY, Myrick FT, Margot NA, Mulamba GB, Rimsky L, Borroto-Esoda K, et al. Virologic and enzymatic studies revealing the mechanism of K65R- and Q151m-associated HIV-1 drug resistance towards emtricitabine and lamivudine. Nucleosides Nucleotides Nucleic Acids 2006;25 (1):89-107.

Feng JY, Shi J, Schinazi RF, Anderson KS. Mechanistic studies show that (-)-FTC-TP is a better inhibitor of HIV-1 reverse transcriptase than 3TC-TP. FASEB J 1999;13 (12):1511-7.

Frankel FA, Invernizzi CF, Oliveira M, Wainberg MA. Diminished efficiency of HIV-1 reverse transcriptase containing the K65R and M184V drug resistance mutations. AIDS 2007;21 (6):665-75.

Furman PA, Davis M, Liotta DC, Paff M, Frick LW, Nelson DJ, et al. The anti-hepatitis B virus activities, cytotoxicities, and anabolic profiles of the (-) and (+) enantiomers of cis-5-fluoro-1-[2-(hydroxymethyl)-1,3-oxathiolan-5-yl]cytosine. Antimicrob Agents Chemother 1992;36 (12):2686-92.

Garcia-Lerma JG, Otten R, Cong M-e, Jackson E, Janssen R, Folks T, et al. Intermittent antiretroviral prophylaxis with tenofovir and emtricitabine protects macaques against repeated rectal SHIV exposures [abstract 85]. 16th International HIV Drug Resistance Workshop; 2007 June 12-16; Bridgetown, Barbados.

Harrigan PR, Miller MD, McKenna P, Brumme ZL, Larder BA. Phenotypic susceptibilities to tenofovir in a large panel of clinically derived human immunodeficiency virus type 1 isolates. Antimicrob Agents Chemother 2002;46 (4):1067-72.

Heijtink RA, Kruining J, de Wilde GA, Balzarini J, De Clercq E, Schalm SW. Inhibitory effects of acyclic nucleoside phosphonates on human hepatitis B virus and duck hepatitis B virus infections in tissue culture. Antimicrob Agents Chemother 1994;38 (9):2180-2.

Henry M, Tourres C, Colson P, Ravaux I, Poizot-Martin I, Tamalet C. Coexistence of the K65R/L74V and/or K65R/T215Y mutations on the same HIV-1 genome. J Clin Virol 2006;37 (3):227-30.

Kagan RM, Lee TS, Ross L, Lloyd RM, Jr., Lewinski MA, Potts SJ. Molecular basis of antagonism between K70E and K65R tenofovir-associated mutations in HIV-1 reverse transcriptase. Antiviral Res 2007;75 (3):210-8.

Kalayjian RC, Landay A, Pollard RB, Taub DD, Gross BH, Francis IR, et al. Age-related immune dysfunction in health and in human immunodeficiency virus (HIV) disease: association of age and HIV infection with naive CD8+ cell depletion, reduced expression of CD28 on CD8+ cells, and reduced thymic volumes. J Infect Dis 2003;187 (12):1924-33.

Kamkolar M, Clayton MM, Zhang SM, Black PL, Schinazi RF, Feitelson MA. Novel therapeutics for hepatitis B and C: Evaluation of therapies for hepatitis B virus in the HBV transgenic SCID mouse model. In: Schinazi RF, Rice CM, Sommadossi JP, eds. Frontiers in Viral Hepatitis. Netherlands: Elsevier Science; 2002: 211-22.

Kramata P, Birkus G, Otmar M, Votruba I, Holy A. Structural features of acyclic nucleotide analogs conferring inhibitory effects on cellular replicative DNA polymerases. Collection Symposium Series (Holy A and Tocik Z, eds), Institute of Organic Chemistry and Biochemistry, Academy of Sciences of Czech Republic, Prague, Czech Republic 1996;1:188-91.

Ledford RM, Vela JE, Ray AS, Callebaut C, Miller MD, McColl DJ. The long intracellular half-life of tenofovir diphosphate correlates with persistent inhibition of HIV-1 replication in vitro [poster number 60]. 19th International Conference on Antiviral Research (ICAR); 2006 May 7-11; San Juan, Puerto Rico.

Lee WA, He G-X, Eisenberg E, Cihlar T, Swaminathan S, Mulato A, et al. Selective intracellular activation of a novel prodrug of the human immunodeficiency virus reverse transcriptase inhibitor tenofovir leads to preferential distribution and accumulation in lymphatic tissue. Antimicrob Agents Chemother 2005;49 (5):1898-906.

Ly JK, Margot NA, MacArthur H, Hung M, Miller MD, White KL. The balance between NRTI discrimination and excision drives the susceptibility of HIV-1 RT mutants K65R, M184V and K65R+M184V. Antivir Chem Chemother 2008;18 (6):307-16.

Ma TW, Lin J, Newton M, Cheng YC, Chu CK. Synthesis and anti-hepatitis B virus activity of 9-(2-deoxy-2-fluoro-β-L-arabinofuranosyl)purine nucleosides. J Med Chem 1997;40 (17):2750-4.

Marchand B, White KL, Ly JK, Margot NA, Wang R, McDermott M, et al. Effects of the translocation status of human immunodeficiency virus type 1 reverse transcriptase on the efficiency of excision of tenofovir. Antimicrob Agents Chemother 2007;51 (8):2911-9.

Margot NA, Lu B, Cheng A, Miller MD. Resistance development over 144 weeks in treatment-naive patients receiving tenofovir disoproxil fumarate or stavudine with lamivudine and efavirenz in Study 903. HIV Med 2006;7 (7):442-50.

Menne S, Cote PJ, Korba BE, Butler SD, George AL, Tochkov IA, et al. Antiviral effect of oral administration of tenofovir disoproxil fumarate in woodchucks with chronic woodchuck hepatitis virus infection. Antimicrob Agents Chemother 2005;49 (7):2720-8.

Meyer PR, Matsuura SE, So AG, Scott WA. Unblocking of chain-terminated primer by HIV-1 reverse transcriptase through a nucleotide-dependent mechanism. Proc Natl Acad Sci USA 1998;95 (23):13471-6.

Miller MD, Anton KE, Mulato AS, Lamy PD, Cherrington JM. Human immunodeficiency virus type 1 expressing the lamivudine-associated M184V mutation in reverse transcriptase shows increased susceptibility to adefovir and decreased replication capability in vitro. J Infect Dis 1999;179 (1):92-100.

Miller MD, Margot NA, Lamy PD, Fuller MD, Anton KE, Mulato AS, et al. Adefovir and tenofovir susceptibilities of HIV-1 after 24 to 48 weeks of adefovir dipivoxil therapy: genotypic and phenotypic analyses of study GS-96-408. J Acquir Immune Defic Syndr Hum Retrovirol 2001;27 (5):450-8.

Mulato AS, Cherrington JM. Anti-HIV activity of adefovir (PMEA) and PMPA in combination with antiretroviral compounds: in vitro analyses. Antiviral Res 1997;36 (2):91-7.

Mulato AS, Lamy PD, Miller MD, Li W-X, Anton KE, Hellmann NS, et al. Genotypic and phenotypic characterization of human immunodeficiency virus type 1 variants isolated from AIDS patients after prolonged adefovir dipivoxil therapy. Antimicrob Agents Chemother 1998;42 (7):1620-8.

Naeger LK, Margot NA, Miller MD. Tenofovir is Less Susceptible to Pyrophosphorolysis and Nucleotide-Dependent Chain-Terminator Removal than Zidovudine or Stavudine. XIV International Roundtable on Nucleosides, Nucelotides, and Their Biological Applications; 2000 Sep 10-14; San Francisco, Calif.

Palmer S, Margot N, Gilbert H, Shaw N, Buckheit R, Jr, Miller M. Tenofovir, adefovir, and zidovudine susceptibilities of primary human immunodeficiency virus type 1 isolates with non-B subtypes or nucleoside resistance. AIDS Res Hum Retroviruses 2001;17 (12):1167-73.

Parikh UM, Bacheler L, Koontz D, Mellors JW. The K65R mutation in human immunodeficiency virus type 1 reverse transcriptase exhibits bidirectional phenotypic antagonism with thymidine analog mutations. J Virol 2006a;80 (10):4971-7.

Parikh UM, Barnas DC, Faruki H, Mellors JW. Antagonism between the HIV-1 reverse-transcriptase mutation K65R and thymidine-analogue mutations at the genomic level. J Infect Dis 2006b;194 (5):651-60.

Parikh UM, Zelina S, Sluis-Cremer N, Mellors JW. Molecular mechanisms of bidirectional antagonism between K65R and thymidine analog mutations in HIV-1 reverse transcriptase. AIDS 2007;21 (11):1405-14.

Perez-Bercoff D, Wurtzer S, Compain S, Benech H, Clavel F. Human immunodeficiency virus type 1: resistance to nucleoside analogues and replicative capacity in primary human macrophages. J Virol 2007;81 (9):4540-50.

Ray A, Olson L, Fridland A. Role of purine nucleoside phosphorylase in drug interactions between 2',3'-dideoxyinosine and allopurinol, ganciclovir or tenofovir. Antimicrob Agents Chemother 2004;48 (4):1089-95.

Ray AS, Myrick F, Vela JE, Olson LY, Eisenberg EJ, Borroto-Esoda K, et al. Lack of a metabolic and antiviral drug interaction between tenofovir, abacavir and lamivudine. Antivir Ther 2005;10 (3):451-7.

Robbins BL, Srinivas RV, Kim C, Bischofberger N, Fridland A. Anti-human immunodeficiency virus activity and cellular metabolism of a potential prodrug of the acyclic nucleoside phosphonate 9-*R*-(2-phosphonomethoxypropyl)adenine (PMPA), Bis(isopropyloxymethylcarbonyl) PMPA. Antimicrob Agents Chemother 1998;42 (3):612-7.

Robbins BL, Wilcox CK, Fridland A, Rodman JH. Metabolism of tenofovir and didanosine in quiescent or stimulated human peripheral blood mononuclear cells. Pharmacotherapy 2003;23 (6):695-701.

Schinazi RF, Gosselin G, Faraj A, Korba BE, Liotta DC, Chu CK, et al. Pure nucleoside enantiomers of beta-2',3'-dideoxycytidine analogs are selective inhibitors of hepatitis B virus in vitro. Antimicrob Agents Chemother 1994;38 (9):2172-4.

Schinazi RF, Lloyd RM, Jr, Nguyen M-HH, Cannon DL, McMillan A, Ilksoy N, et al. Characterization of human immunodeficiency viruses resistant to oxathiolane-cytosine nucleosides. Antimicrob Agents Chemother 1993;37 (4):875-81.

Schinazi RF, McMillan A, Cannon D, Mathis R, Lloyd RM, Peck A, et al. Selective inhibition of human immunodeficiency viruses by racemates and enantiomers of cis-5-fluoro-1-[2-(hydroxymethyl)-1,3-oxathiolan-5-yl]cytosine. Antimicrob Agents Chemother 1992;36 (11):2423-31.

Shaw T, Mok S, Locarnini S. Inhibition of hepatitis B virus DNA polymerase by enantiomers of penciclovir triphosphate and metabolic basis for selective inhibition of HBV replication by penciclovir. Hepatology 1996;24 (5):996-1002.

Shen A, Zink MC, Mankowski JL, Chadwick K, Margolick JB, Carruth LM, et al. Resting $CD4^+$ T lymphocytes but not thymocytes provide a latent viral reservoir in a simian immunodeficiency virus-*Macaca nemestrina* model of human immunodeficiency virus type 1-infected patients on highly active antiretroviral therapy. J Virol 2003;77 (8):4938-49.

Shirasaka T, Kavlick MF, Ueno T, Gao W-Y, Kojima E, Alcaide ML, et al. Emergence of human immunodeficiency virus type 1 variants with resistance to multiple dideoxynucleosides in patients receiving therapy with dideoxynucleosides. Proc Natl Acad Sci USA 1995;92 (6):2398-402.

Sluis-Cremer N, Sheen CW, Zelina S, Torres PS, Parikh UM, Mellors JW. Molecular mechanism by which the K70E mutation in human immunodeficiency virus type 1 reverse transcriptase confers resistance to nucleoside reverse transcriptase inhibitors. Antimicrob Agents Chemother 2007;51 (1):48-53.

Sommadossi J-P. Data from clonogenic assays CFU-GM and BFU-E and mitochondrial assays for TP0001 and TP0004 as compared to AZT. Triangle Pharmaceuticals, Inc. Report No. 233. October 15, 1996.

Srinivas RV, Fridland A. Antiviral activities of 9-*R*-2-phosphonomethoxypropyl adenine (PMPA) and bis(isopropyloxymethylcarbonyl)PMPA against various drug-resistant human immunodeficiency virus strains. Antimicrob Agents Chemother 1998;42 (6):1484-7.

Stray KM, Park Y, Babusis D, Callebaut C, Cihlar T, Ray AS, et al. Tenofovir alafenamide (TAF) does not deplete mitochondrial DNA in human T-cell lines at intracellular concentrations exceeding clinically relevant drug exposures. Antiviral Res 2017;140:116-20.

Svarovskaia ES, Feng JY, Margot NA, Myrick F, Goodman D, Ly JK, et al. The A62V and S68G Mutations in HIV-1 Reverse Transcriptase Partially Restore the Replication Defect Associated With the K65R Mutation. J Acquir Immune Defic Syndr 2008;48 (4):428-36.

Tisdale M, Kemp SD, Parry NR, Larder BA. Rapid in vitro selection of human immunodeficiency virus type 1 resistant to 3'-thiacytidine inhibitors due to a mutation in the YMDD region of reverse transcriptase. Proc Natl Acad Sci USA 1993;90 (12):5653-6.

Ussery MA, Wood OL, Kunder SC, Bacho MA, Broud DD, Vona SF, et al. Antiviral activity of six novel compounds [(-)-FTC, (+/-)-FTC, D-DAPD, D-D4FC, CS-92 and CS-87) in the HIV-infected HuPBMC SCID mouse model [abstract]. Antivir Ther 1998;3 (Suppl 1):7-8. Abstract 9.

Van Draanen NA, Tisdale M, Parry NR, Jansen R, Dornsife RE, Tuttle JV, et al. Influence of stereochemistry on antiviral activities and resistance profiles of dideoxycytidine nucleosides. Antimicrob Agents Chemother 1994;38 (4):868-71.

Vela JE, Miller MD, Rhodes GR, Ray AS. Effect of tenofovir in combination with other anti-HIV NRTIs on intracellular nucleotide pools [poster number H-1901]. 45th Interscience Conference on Antimicrobial Agents and Chemotherapy; 2005 December 16-19; Washington, DC, USA.

Vidal F, Domingo JC, Guallar J, Saumoy M, Cordobilla B, Sanchez de la Rosa R, et al. In vitro cytotoxicity and mitochondrial toxicity of tenofovir alone and in combination with other antiretrovirals in human renal proximal tubule cells. Antimicrob Agents Chemother 2006;50 (11):3824-32.

Wainberg MA, Miller MD, Quan Y, Salomon H, Mulato AS, Lamy PD, et al. In vitro selection and characterization of HIV-1 with reduced susceptibility to PMPA. Antivir Ther 1999;4 (2):87-94.

White KL, Chen JM, Feng JY, Margot NA, Ly JK, Ray AS, et al. The K65R reverse transcriptase mutation in HIV-1 reverses the excision phenotype of zidovudine resistance mutations. Antivir Ther 2006;11:155-63.

White KL, Margot NA, Ly JK, Chen JM, Ray AS, Pavelko M, et al. A combination of decreased NRTI incorporation and decreased excision determines the resistance profile of HIV-1 K65R RT. AIDS 2005;19 (16):1751-60.

Wilson JE, Martin JL, Borroto-Esoda K, Hopkins S, Painter G, Liotta DC, et al. The 5'-triphosphates of the (-) and (+) enantiomers of cis-5-fluoro-1-[2-(hydroxymethyl)-1,3-oxathiolane-5-yl]cytosine equally inhibit human immunodeficiency virus type 1 reverse transcriptase. Antimicrob Agents Chemother 1993;37 (8):1720-2.

Xiong X, Flores C, Yang H, Toole JJ, Gibbs CS. Mutations in hepatitis B DNA polymerase associated with resistance to lamivudine do not confer resistance to adefovir in vitro. Hepatology 1998;28 (6):1669-73.

Yang H, Qi X, Sabogal A, Miller M, Xiong S, Delaney WE, IV. Cross-resistance testing of next-generation nucleoside and nucleotide analogues against lamivudine-resistant HBV. Antivir Ther 2005;10 (5):625-33.

Ying C, De Clercq E, Neyts J. Lamivudine, adefovir and tenofovir exhibit long-lasting anti-hepatitis B virus activity in cell culture. J Viral Hepat 2000;7 (1):79-83.

Yokota T, Konno K, Shigeta S, Holý A, Balzarini J, De Clercq E. Inhibitory effects of acyclic nucleoside phosphonate analogues of hepatitis B virus DNA synthesis in HB611 cells. Antivir Chem Chemother 1994;5 (2):57-63.